Cerebellar Impact on Thalamocortical Networks in Epilepsy

Oscar Eelkman Rooda

Colofon

The research described in this thesis was performed at the Department of Neuroscience, Erasmus Medical Center Rotterdam and the Gladstone Institute of Neurological Disease, San Francisco.

The research in this thesis was financially supported by the Netherlands Organisation for Scientific Research (NWO-VIDI grant #016.121.346) and internal grant program of the Erasmus Medical Center (mRace).

ISBN: 978-94-6299-899-5

Lay-out: Nikki Vermeulen - Ridderprint BV
Printing: Ridderprint BV - www.ridderprint.nl

Cerebellar Impact on Thalamocortical Networks in Epilepsy

Cerebellaire impact op thalamocorticale netwerken

Proefschrift

ter verkrijging van de graad van doctor aan de
Erasmus Universiteit Rotterdam
op gezag van de rector magnificus

prof.dr. H.A.P. Pols

en volgens besluit van het College voor Promoties.

De openbare verdediging zal plaatsvinden op

Woensdag 28 maart 2018
om 13.30 uur

door

Oscar Hubert Jan Eelkman Rooda
geboren op 03 oktober 1988
te Rotterdam

Erasmus University Rotterdam

Promotiecommissie

Promotoren:	Prof. Dr. C.I. De Zeeuw
	Prof. Dr. C.M.F. Dirven
Overige leden:	Prof. Dr. P.A.E. Sillevis Smitt
	Dr. C.P.J. de Kock
	Dr. M. Schonewille
Copromotor:	Prof. Dr. F.E. Hoebeek

Een beetje zeiler wordt niet
bang van harde tegenwind

Contents

Preface

The communication between cerebellum and cerebrum in non-motor forms of neurological disease is poorly understood. One of these diseases is epilepsy and still lacks understanding and control. Epileptic attacks typically originate in thalamocortical pathways, which are influenced by cerebellar output. This output is particularly known during various forms of motor behavior and coordination, but has also been implicated in (daily) cognitive functioning. This thesis primarily focuses on how cerebellar output contributes to thalamocortical communication and the potential therapeutic benefits of manipulation of cerebellar output in disease. I used epileptic mouse models and their wild type littermates which are well characterized and perfectly suited to study cerebellar impact on (epileptic) processes in a preclinical setting. To do so I have made use of multiple techniques, including optogenetics, (single-unit) electrophysiology, neuro-anatomical tracing and imaging, both in freely moving and head-fixed animals. Overlooking all the results I do believe my thesis fuels further research of cerebellar impact on thalamocortical networks but also revealed new questions and (pre)clinical possibilities.

Oscar Eelkman Rooda

1

A general introduction

1.1 Epilepsy – a disease once sacred

One of the major goals of fundamental brain research is to elucidate how groups of neurons communicate to generate behavior. To understand this we perform research in animals such as worms, flies, fish, mice and monkeys which in some cases is supported by computer simulations. We do so because our understanding of basic neurophysiology of a healthy brain is an important limiting factor when understanding mechanisms underlying neurological disorders and developing effective therapies for them. Epilepsy is one of these and is estimated to affect 1% of the population with 30% of patients having untreatable seizures despite optimal antiepileptic drugs [1]. It's a disease which is actually already known for at least 3000 years. One of the oldest accounts is a Babylonian tablet in the British Museum of London which describes one of the first reports with spectacular observations. This 'epilepsy tablet', which dates back to ~1000 B.C., describes features of epileptic attacks what we would recognize today as tonic-clonic, absence, Jacksonian, complex partial and even gelastic attacks of epilepsy [2]. The Babylonians considered epilepsy rightfully as abnormal, but described it as the result of demons in the body where each type of seizure was represented by a particular demon.

A different opinion about the cause of epilepsy other than a paranormal intrusion of the body was offered by the Greeks with the publication of 'on the Sacred Disease' (putatively written by one of the 'Fathers of Medicine'; Hippocrates), who regarded epilepsy as a physical disorder due to natural causes. It took however many centuries before the primitive concepts of making observations were replaced by rational and scientific notions, i.e., alike modern-day common practice in life science and medicine.

The start of this 'era' is probably best exemplified by the notifications and reports of John Hughlings Jackson (1835-1911). Widely recognized as one of the modern founding fathers regarding epilepsy research. One of the reasons for this is that he and his colleagues recognized the outcome of experiments being a matter of perspective and thus makes reporting and defining an essential task to do for any researcher. Furthermore is his 'founding father status' in part because of how remarkably accurate he was in his theories about epilepsy in a time where electroencephalographic recordings did not even exist.

1.2 Hughlings Jackson's; ahead of his time

Modern sophisticated neuro-diagnostic tools such as electroencephalic recordings and brain imaging were not available late 19th century. It was however the individual effort of many people who were responsible for the advance of knowledge in neurology. Under far from ideal circumstances people such as Nissl, Alzheimer, Golgi and Cajal performed

and achieved remarkable progress in the field of neurology and neuroanatomy. Regarding epilepsy there were many people who significantly contributed to the organized way of gaining knowledge about how to treat this disease.

Late summer 1909 there was a congress in Budapest attended by a few neurologists and physicians in the rising field of neurosurgery where the International League Against Epilepsy (ILAE) was launched. By that time Harvey Cushing was already pioneering in electrical stimulation during brain surgery since he just published a report in *Brain* (a journal founded by Hughlings Jackson starting with a lecture about the diagnosis of epilepsy, **Figure 1**) about electrical stimulation of the postcentral cortex evoking sensory responses and auras of focal attacks [3].

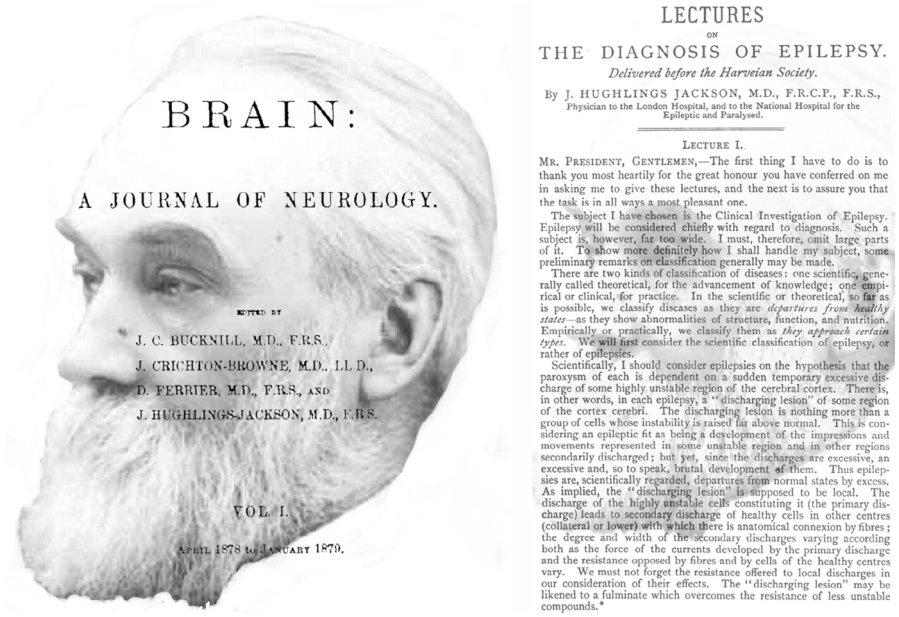

BRAIN:

A JOURNAL OF NEUROLOGY.

EDITED BY

J. C. BUCKNILL, M.D., F.R.S.,
J. CRICHTON-BROWNE, M.D., LL.D.,
D. FERRIER, M.D., F.R.S., AND
J. HUGHLINGS-JACKSON, M.D., F.R.S.

VOL. I.

APRIL 1878 to JANUARY 1879.

LECTURES
ON
THE DIAGNOSIS OF EPILEPSY.
Delivered before the Harveian Society.

By J. HUGHLINGS JACKSON, M.D., F.R.C.P., F.R.S.,
Physician to the London Hospital, and to the National Hospital for the Epileptic and Paralysed.

LECTURE I.

MR. PRESIDENT, GENTLEMEN,—The first thing I have to do is to thank you most heartily for the great honour you have conferred on me in asking me to give these lectures, and the next is to assure you that the task is in all ways a most pleasant one.

The subject I have chosen is the Clinical Investigation of Epilepsy. Epilepsy will be considered chiefly with regard to diagnosis. Such a subject is, however, far too wide. I must, therefore, omit large parts of it. To show more definitely how I shall handle my subject, some preliminary remarks on classification generally may be made.

There are two kinds of classification of diseases: one scientific, generally called theoretical, for the advancement of knowledge; one empirical or clinical, for practice. In the scientific or theoretical, so far as is possible, we classify diseases as they are *departures from healthy states*—as they show abnormalities of structure, function, and nutrition. Empirically or practically, we classify them as *they approach certain types*. We will first consider the scientific classification of epilepsy, or rather of epilepsies.

Scientifically, I should consider epilepsies on the hypothesis that the paroxysm of each is dependent on a sudden temporary excessive discharge of some highly unstable region of the cerebral cortex. There is, in other words, in each epilepsy, a "discharging lesion" of some region of the cortex cerebri. The discharging lesion is nothing more than a group of cells whose instability is raised far above normal. This is considering an epileptic fit as being a development of the impressions and movements represented in some unstable region and in other regions secondarily discharged; but yet, since the discharges are excessive, an excessive and, so to speak, brutal development of them. Thus epilepsies are, scientifically regarded, departures from normal states by excess. As implied, the "discharging lesion" is supposed to be local. The discharge of the highly unstable cells constituting it (the primary discharge) leads to secondary discharge of healthy cells in other centres (collateral or lower) with which there is anatomical connexion by fibres; the degree and width of the secondary discharges varying according both as the force of the currents developed by the primary discharge and the resistance opposed by fibres and by cells of the healthy centres vary. We must not forget the resistance offered to local discharges in our consideration of their effects. The "discharging lesion" may be likened to a fulminate which overcomes the resistance of less unstable compounds.*

Figure 1. First issue of *Brain* and its founding editor Hughlings Jackson (1835-1911).

Harvey Cushing and his colleagues (Sir Victor Horsley and later on Wilder Penfield) were among the first to use electrical stimulation to elicit electrical activity in the brain and monitor the behavioral readout.

Although Cushing is in many aspect a very important pioneering neurosurgeon in the 20th century it was Hughlings Jackson who laid the foundation for how we try to understand epilepsy nowadays.

In a series of landmark papers Hughlings Jackson published his observations on convulsions and seizures saying that there was an unstoppable force causing a sudden and temporary loss of nerve tissue function which was the underlying cause of epilepsy [4]. A short while longer he proceeded by saying that that 'this nerve-tissue should be considered as more unstable, over-ready and excitable; there is discharge too soon; its Time is shortened' [5] which were remarkable observations for that time. These clinical observations were enough for Hughlings Jackson to inform his colleague neurosurgeon dr. Horsley that it was probably a 'cortical irritation' causing focal attacks of epilepsy and he suggested to perform a craniotomy and remove it [6, 7]. Whether or not that was the last time for a neurologist to convince a neurosurgeon so easy to perform a procedure remains unclear. Nevertheless it was the beginning of a time where Horsley performed surgery on many patients with an encouraging result; his patients survived [8]. It is remarkable how the combination of local anesthesia and intraoperative cortical stimulation aiming for reproduction of a seizure was the essential of epilepsy surgery performed in a time when neuromodulation by electrical stimulation was at its infancy. It forms however the fundamentals by how we perform awake cranial surgery nowadays.

Not only was Hughlings Jackson a remarkable clinician, he also proved himself capable of fundamental research. He performed several experiments together with Charles E. Beevor observing thumb and finger responses in monkeys after electrical cerebral cortex stimulations. Parallel to this, Hughlings Jackson's colleague and former student, David Ferrier, started to experimentally proof the observations made by Hughlings Jackson. It was this combination which supported Hughlings Jackson in his observations and recommendations to perform surgeries on patients. The close translational collaboration between experimenters/students (Ferrier and Beevor), neurosurgeon (Horsley) and neurologist (Hughlings Jackson) still serves today as a crucial bench to bedside model for modern day epilepsy research and translational neuroscience in general.

1.3 Electrical stimulation – why and how?

Horsley and colleagues were using electrical stimulation knowing that the brain functions by electrical signals and that stimulation can evoke normal responses (like the thumb movements mentioned earlier) and abnormal responses (like the auras of focal attacks reported by Cushing). Probably they didn't foresee that precise and standardized electrical stimulation came on the rise a few decades later as a treatment for abnormal responses. The use of precise localization is nowadays called functional stereotactic surgery and many patients cannot benefit neuromodulation treatment without the landmark paper

introducing this. That moment is marked a few years after the first publications from Horsley and Cushing when neurologist dr. Spiegel and neurosurgeon dr. Wycis reported in the cross-discipline journal Science the creation of a stereotactic apparatus and its use in humans to perform ablative procedures [9].

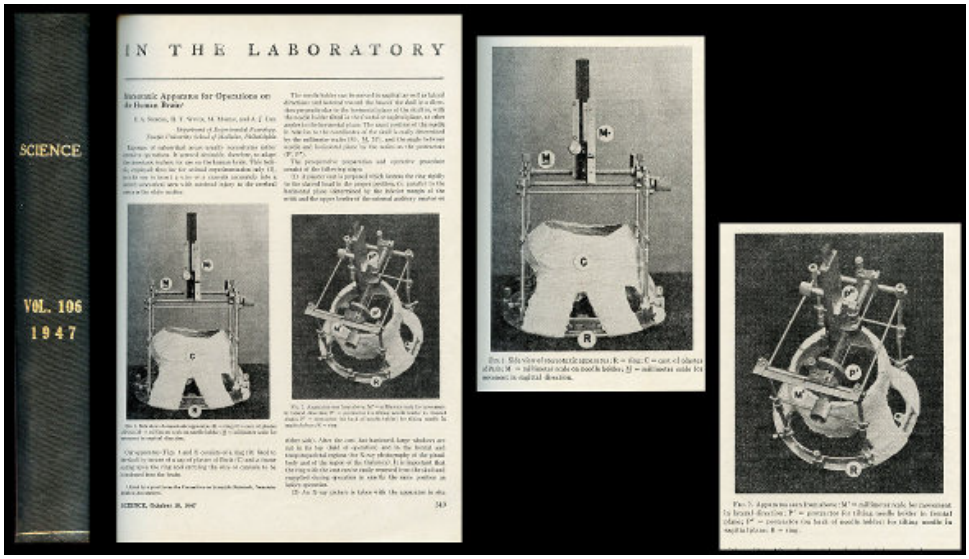

Figure 2. Image of the first publication of a stereotaxic apparatus for implantation of electrodes in the human brain in Science.

Many people fail to recognize this original publication as aiming to refine the rough methods used for performing e.g. lobotomies in psychiatric patients by replacing it for stereotactic procedures. Instead many think it is designed for treating movement disorders such as M. Huntington and Parkinson.

The fact that neuromodulation was indicated for treating psychiatric disorders and the pioneering work of Horsley, Cushing, Penfield and others in the identification of epileptic foci using electrical stimulation made it easy to hypothesize that these foci could be treated with the technique of electrode implantation and intermittent stimulation [10]. Subsequently therapeutic chronic stimulation in thalamus and cerebellum was introduced for patients having refractory epilepsy [11-13]. Over the years many trials have been performed with inconsistent results in the beginning. This was arguably due to unprecise localization methods and limited knowledge about physiology, mechanism of action and anatomy connections (**Chapter 3** of this thesis focuses further on these issues). Recently more and stronger evidence in larger studies came available indicating that neuromodulation

of thalamus or cortex can be an additional treatment for epilepsy patients since seizure reduction up to 68% has been reported after 5 years of follow-up [14, 15]. Fact remains that nowadays epilepsy is still an invalidating disease that leaves many patients without any adequate treatment options. This and proceeding knowledge are one of the reasons that my thesis (re)focuses on the question if cerebellar output can function as a remote site to control epilepsy. To understand this it is important to know the differences between normal and abnormal brain functioning.

1.4 Do oscillations occur in normal brain activity?

A lot of essential brain functions such as memory consolidation, navigation and sleep are based upon synchronized, rhythmic firing among smaller or larger neuronal cell populations; i.e. oscillations [16]. Neural oscillations can be seen as the rhythmic glowing of an army of fireflies where every firefly represents a brain cell. Different groups of fireflies and their frequency of lighting represent different oscillatory frequencies. Another example would be that neural oscillations can be seen as the many different ripples in a pool of water after a stone bouncing in.

Pioneering work on oscillations was published by Vladimir Práwdicz-Neminski from the Kiev University. His 1912 publication of an 'elektrocerebrogramm' in dogs pioneered recording electrical brain activity. He also identified two different rhythms what he referred to as 'waves of the first and second order', nowadays better known as alpha and beta waves. Práwdicz-Neminski was very likely not the first with his recordings (Richard Caton recorded already in 1875 electrical potentials of rabbit and monkeys) and a little later Hans Berger followed publishing an 'elektrenkephalogramm' recording in humans which subsequently changed into the English version 'Electroencephalogram' or EEG [17]. The first discovered and best-known frequency band is alpha activity (8 – 13 Hz); prominent during relaxed wakefulness or the awake resting-state in the absence of sensory inputs. Other frequency bands are delta (1 – 4 Hz), theta (4 – 8 Hz), beta (13 – 30 Hz) and gamma (30 – 70 Hz) (as reviewed by [18] (**Figure 3**).

All frequency bands have their specific properties and relations to brain functioning. Delta band frequencies are classically known to occur during deep sleep and appears to be controlled by cerebral cortex in the absence of sensory input. Theta frequency is important for working memory and emotional arousal and arises from cortical GABAergic interneurons impacting corticothalamic connectivity. Beta frequency is prominent during vigilance and attention and gamma frequency highlights feature integration involved in perception.

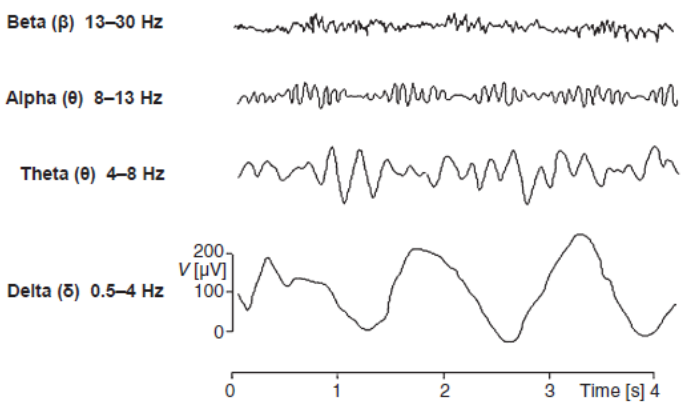

Figure 3. Main oscillation frequencies in EEG. (Constant 2012 et al.)

All of these frequency bands can be considered as global network processes and thus hard to attribute to one specific brain region. Cerebral cortices affect their downstream connective hubs such as thalamus, basal ganglia and others with these rhythms. These structures give feedback in return which can modify the main cerebral oscillation frequencies. To exemplify how natural oscillations enable different brain activity patterns I will explain this by using two recognizable brain activities; i.e. sleep and memory processes. Although the exact mechanism is far from elucidated in general it is likely that different stages of sleep coordinate the (re-)activation and distribution of other brain-region dependent memories [19]. Slow-wave sleep (using oscillatory frequencies < 1 Hz) are thought to re-activate memory traces of events whereas REM sleep (characterized by theta (4 – 8 Hz) oscillations) is thought to contribute to consolidation of these memory traces. This indicates that different brain oscillations have their own function in activating and synergizing different brain regions to accomplish their specific goals. Taken together, specific brain functions need different oscillatory patterns to establish a temporal and spatial relation with a well-defined event. More specific this means that establishing memory will likely fail or be significantly hampered if sleep patterns are lacking.

1.5 Sleep and epilepsy are(n't) the same

Not all oscillations are necessarily good oscillations. Numerous pathological oscillations are known to form the basis of neurological disorders. One of them is Alzheimer's disease (AD) which is associated with different than normal slow-wave activity in neocortex, thalamus and hippocampus [20]. Other examples are traumatic brain injury and epilepsy.

A common misconception about epilepsy is that seizures occur due to short-circuited brain activity. A more accurate description is that seizures are typically due to run-away excitation of brain network activity. I will now introduce how these conditions come about and will utilize the commonalities between oscillations in the healthy brain during sleep stages and in the epileptic brain during seizures. Using this frame-of-reference I hope to enhance the general understanding of the impact of cerebellar stimulations on generalized seizures.

Both sleep and epilepsy arise predominantly in networks where the thalamus forms a critical structure for generating normal and abnormal oscillations. *Thalamos* is the Greek word for innermost room or sleeping chamber which was used in the Archaic Greek house as a room connecting (in)directly the many other chambers and passages. Prior to modern neuroscience it was thought that thalamus acted as a reservoir where vital spirits were stored. Nowadays thalamus is generally recognized as the coordinating center for the flow of information between the senses and cerebral cortices, although recent findings expand this functionality extensively [21-23]. The reciprocal connectivity between the thalamus and cerebral cortex is crucial to generate flow of oscillations that encode, for instance, sensorimotor integration patterns that are essential for daily functioning. Feedforward and feedback connections within and between the thalamic and cortical areas ultimately lead to a dynamic regulation of oscillatory patterns that may synchronize distant thalamocortical networks. The amount of synchrony in groups of cells in the thalamic network seems to be crucial in determining whether normal or pathological oscillations occur. Normal synchronous oscillations occur, as explained earlier, during various behavioral states, e.g. sleep, but hypersynchronous discharges are associated with generalized epilepsy. Both normal and abnormal oscillations can be detected using EEG recordings (see **Figure 4**). An example rhythm that reflects normal activity of ensembles of thalamocortical cells are so-called sleep spindles whereas the pathological variant are Spike-Wave Discharges (SWDs). Although significantly different a close correlation can be found between sleep-spindles and SWDs (Fig. 4). One of the arguments for this is that we can assume that the circuit used for generating spindles is comparable with the circuit that generates absence seizures. Prominent in this is the finding that thalamic activity was in phase with the timing of spike-wave discharges in patients with absence epilepsy [24]. This was confirmed when thalamus and cortex were found firing together during spindles [25].

Moreover the generation of a pattern of sleep spindles or SWDs seems to critically depend on the amount of cells recruited to participate in the spindle sequences or SWDs [26-29].

Furthermore similar features such as being intermittent, lasting a few seconds and present throughout the cortex are soft arguments that absence seizures and spindles use the same circuit. Finally and most important is the proof that there is no need for rewiring

the thalamic circuit to initiate spike-wave discharges. This was shown many times when infusing GABAa receptor antagonists in thalamic slices changed spindle-oscillations in epileptiform oscillations [30-32].

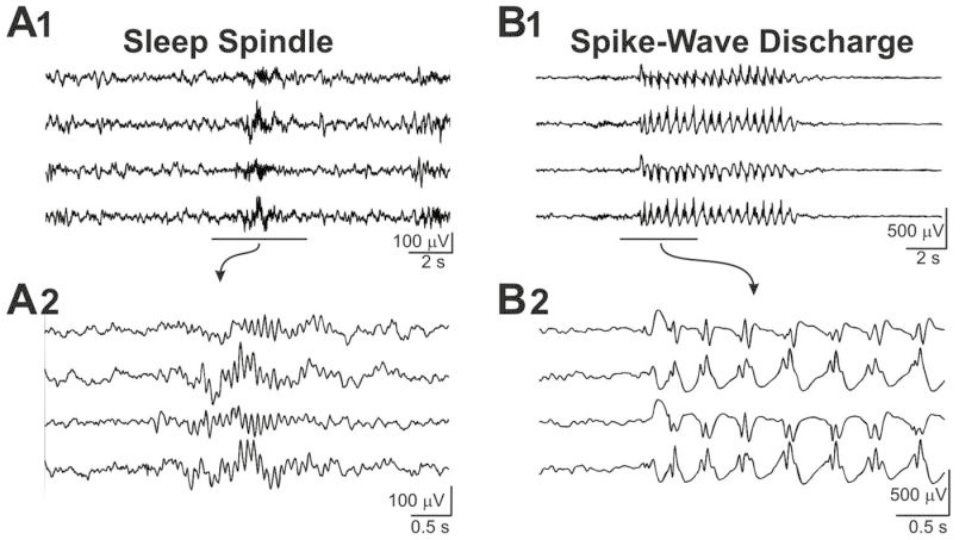

Figure 4. Cortical LFP recordings showing sleep and epileptic signals. (Beenhakker 2009)

Although the circuit might be the same it is far from clear what initiates such oscillations. Several groups suggested that cortical activity is responsible based in part on the observation that cortical cells start oscillating before cerebral EEG recordings follow [33-35]. And indeed terminating cortical 'foci' activity using lidocaine reduced the occurrence of SWDs. However, unpublished observations from our groups' cerebellar nuclei recordings also did show oscillatory firing prior to subsequent spike-wave discharges and upgrading its activity using gabazine completely abolished spike-wave discharge occurrence (**this thesis**).
Furthermore it was shown that the start of absence epilepsy in a genetic mouse mutant, i.e. *tottering,* coincided with impaired feedforward thalamocortical inhibition onto layer IV neurons [36]. While this can still be seen as the problem residing in the cortex another group revealed for several absence epilepsy animal models that compromised GABA uptake directly in the thalamus because of aberrant GABA transporter GAT-1 functioning resulted in both behavior and ECoG correlates of absence seizures [37]. And who else, if not Hughlings Jackson, reported about a patient exhibiting epilepsy when having cerebellar pathology [38]. This shows that the question if cerebral cortex is the main initiator of epileptic oscillations remains a very open one and is not for sure to be answered with a yes.

And if or not the cortex is the focus another interesting questions in the past and future of treating epilepsy is how to intervene in epileptic networks to regain control.

1.4 The thalamus as a hub between cerebellum and cerebrum

To know how to intervene in epileptic networks it is essential to know how thalamic neurons generate (spindle) oscillations (**Figure 5**). In the thalamus this occurs because a thalamic subdivision, i.e. reticular thalamus (RT), directs inhibitory feedback to another subdivision, i.e. dorsal thalamus relay nuclei (TRN).

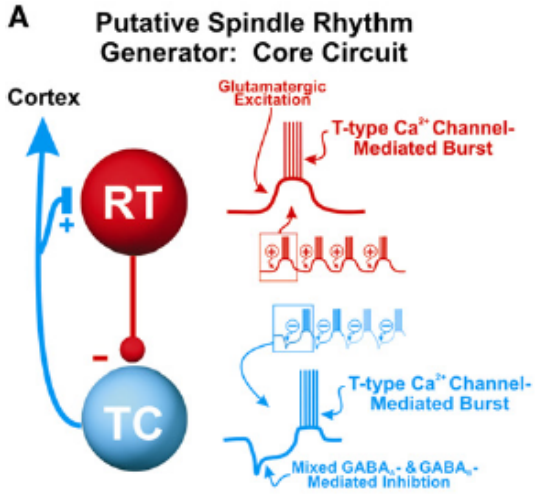

Figure 5. Schematic representation of thalamocortical interaction (Beenhakker 2009).

These relay nuclei receive excitatory and inhibitory input from other subcortical nuclei and send (at least in rodents) excitatory feedforward and feedback information to reticular thalamus and cerebral cortex. One of these subcortical nuclei is the cerebellum which influences TRN neurons with excitatory input. This mechanism is further introduced and explained in Box 3 in **Chapter 2.**

In principle, this back and forth excitation and inhibition between RT and TRN is the fundamental circuitry of a very important oscillation generator in the brain and provides support for the 'waxing and waning experience' most often seen in oscillations.

Over the years several brain targets for intervention in pathological oscillations underlying refractory epilepsy have been proposed [39]. Question remains if the cerebellum is well-positioned for intervention using its excitatory output predominantly on TRN neurons.

Therefore **Chapter 2** introduces the cerebellum as a potential candidate and serves as a kick-off for the rest of this thesis focusing on the question whether cerebellum can function as a remote control site to control thalamocortical (pathological) oscillations.

1.6 Aims of this dissertation

The aim of this thesis is to further elucidate neural mechanisms underlying the role of the cerebellum in generalized epilepsy and more specifically if the cerebellum can be used as a remote control site to influence thalamocortical networks in health and during epilepsy.
Following an introduction on electrical brain stimulation in general and fundamental brain processes at first I aimed to provide an overview in **Chapter 2** of commonly used stimulation targets. In this context we implemented cerebellar studies and propose several new stimulation strategies to maximize impact on thalamocortical networks.
This chapter raised the question which (optogenetic) research tools were best to study effects of directly impacting cerebellar neurons and its long ranging projections to downstream targets (**Chapter 3**).
After these introductory chapters we first aimed to question in **Chapter 4** to what extent modulation of simple and specifically complex spike activity (crucial identifiers of Purkinje cell activity; the sole output of cerebellar cortex) is related to Generalized Spike-and-Wave Discharges occurring in awake *tottering* mice and what this tells us about the involvement of the inferior olive. After identifying the upstream firing activity related to the occurrence of GSWDs I continue by investigating the role of Cerebellar Nuclei in two different generalized absence epilepsy models and if (optogenetic) short- and (pharmacologic) long-term modulation of firing activity can impact the occurrence of epileptic attacks (**Chapter 5**).
How and to what extent cerebellum can impact thalamic nuclei remains largely unknown. Therefore we aimed to elucidate this with an *in vitro* study (**Chapter 6**) in wildtype animals by demonstrating the effect of cerebellothalamic synapses.
Next we investigated what effect synchronizing cerebellar output has on thalamic nuclei in an in vivo mouse model of absence epilepsy. Using the results of this chapter we come to a candidate mechanism underlying cerebellum reestablishing control in thalamocortical networks (**Chapter 7**).
Finally I analyze if cerebellum is capable of stopping generalized epilepsy in another much more severe generalized epilepsy mouse model, i.e. Dravet mouse (**Chapter 8**).

2

Controlling cerebellar output to treat refractory epilepsy

Trends in Neurosciences 2015:
L. Kros, O.H.J. Eelkman Rooda, C.I. De Zeeuw, and F.E. Hoebeek

Generalized epilepsy is characterized by recurrent seizures caused by oscillatory neuronal firing throughout thalamo-cortical networks. Current therapeutic approaches often intervene at the level of the thalamus or cerebral cortex to ameliorate seizures. Here, we review the therapeutic potential of cerebellar stimulation. The cerebellum forms a prominent ascending input to the thalamus and, whereas stimulation of the foliated cerebellar cortex exerts inconsistent results, stimulation of the centrally located cerebellar nuclei reliably stops generalized seizures in experimental models. Stimulation of this area indicates that the period of stimulation with respect to the phase of the oscillations in thalamo-cortical networks can optimize its effect, opening up the possibility of developing on-demand DBS treatments.

2.1 Neurostimulation for drug-resistant epilepsy

Epilepsy, defined as the occurrence of recurrent, unprovoked seizures, is one of the most common neurological disorders, affecting approximately 65 million people worldwide [40, 41]. The disorder can have devastating effects on one's life, not only directly due to the clinical effects, which may include injury and hospitalization, but also due to socio-economic effects such as social isolation, stigmatization, educational difficulties and unemployment. These various consequences of epilepsy result in a high comorbidity with psychiatric disorders and an increased suicide rate [42]. Anti-epileptic drugs (AEDs), which induce considerable side-effects, provide a decrease in seizure occurrence of more than 50% in ~70% of epilepsy patients [1, 41-43]. In the remaining 30% of patients the next line of treatment is often invasive. If the focus (or foci) of the seizures can be localized, and if the tissue involved is accessible and non-eloquent (**Glossary**), patients can be treated by neurosurgical resection [44]. If patients cannot be operated upon or show refractory epilepsy following resection, they are potential candidates for neurostimulation, which comprises ~30% of the medication-resistant cases.

Selecting the optimal stimulation target to treat these severely affected patients is a challenging task. However, the current surge of data from various clinical trials on the impact of vagal nerve stimulation (VNS) and deep brain stimulation (DBS) in the thalamus or epileptic focus reveals that for various types of drug-resistant epilepsies specific neurostimulation paradigms have therapeutic value (**Box 1**). Moreover, recent experimental evidence indicates that neurostimulation of the cerebellum can have potential therapeutic benefits [45, 46]. In contrast to the cerebellar cortex, which has been probed for treatment of epilepsy since the dawn of deep brain stimulation (DBS) [47], the cerebellar nuclei (CN) have rarely been targeted for seizure control in epilepsy patients [48, 49]. However, the CN are in a key position to affect a wide range of thalamic nuclei (**Box 2**) and can therefore, in our opinion, be of potential therapeutic interest for the treatment of particular types of epilepsy. Here, we will address why the CN should be targeted and how the impact of the CN on thalamo-cortical networks should be studied in experimental epilepsy models. We aim to provoke a re-evaluation of the potential use of cerebellar neurostimulation to stop epileptic seizures. Given the outcome of this evaluation we propose that single pulse stimulation of CN should be considered for novel closed-loop approaches that refine on-demand seizure control.

Box 1. Common neurostimulation treatment in the clinic

-Vagal nerve stimulation

Regardless of the type of seizures, the first line of neurostimulation treatment for refractory epilepsy [50] is vagal nerve stimulation (VNS). A meta-analysis on the results of VNS in thousands of epilepsy patients revealed that on average 50% of patients showed a 51% reduction in seizure frequency, with the important side notes that generalized seizures are more effectively treated than focal seizures and that very few patients will become seizure-free following VNS treatment [50]. The mechanisms underlying the therapeutic effect of VNS have only recently been described to rely at least partially on the prevention of hyper-synchronized neuronal activity (**Box 2**) [51-53].

-DBS for partial seizures

Apart from VNS various other neurostimulation trials have been conducted to treat refractory epilepsy of various types [39]. The SANTE study aimed to treat frontal and temporal lobe partial seizures in patients with drug-resistant epilepsy by stimulating the anterior nucleus of the thalamus (ANT) [54]. High-frequency stimulation effectively lowered seizure frequency by ≥50% in 43% of patients during the first year and by 69% in 68% of patients in the fifth year of stimulation [15]. These results indicate that continuous, i.e. non-responsive, ANT stimulation, is to some extent effective in treating patients with an epileptic focus in the frontal and temporal lobes.

In addition to this open-loop approach, responsive neurostimulation has also been tested in patients with refractory partial seizures. Patients enrolled in the 'Neuropace' study received a patient-tailored electrical stimulation in the epileptic focus upon the onset of epileptogenic activity patterns in frontal or temporal lobe [55]. The recently published findings revealed a stable level of seizure reduction up to 66% [56]. Together these data indicate that partial seizures originating from the frontal or temporal lobe may be adequately treated using responsive focal stimulation and continuous stimulation of the interconnected anterior thalamus nucleus.

-Thalamic DBS for primarily generalized seizures

Another form of refractory epilepsy is primarily generalized epilepsy. Neurostimulation treatment for these types of seizures requires a structure that projects to wide areas of the cerebral cortex. The centromedian (CM) thalamus region projects diffusely to agranular layers of cerebral cortices as well as to subcortical structures [57-59]. A recent single-blinded study on the effects of high frequency CM stimulation reported that all six patients of generalized epilepsies showed a reduced occurrence of seizures [60], which was in line with earlier findings of the Velasco group on dozens of patients [61-65].

Box 2. Anatomy of the cerebello-thalamo-cortical tract

The robust anatomical connectivity between cerebellum and thalamocortical networks has given substantial impetus to the general interest in cerebellar stimulation in epilepsy. Due to the anatomical accessibility of the cerebellar cortex, and the purely inhibitory nature of its sole output neuron, the Purkinje cell, this structure was initially stimulated in various experimental setting [39]. Nonetheless, owing to the complex foliation of the cerebellar cortex and its division in functional zones (i.e., 'zebrin bands') [79], the impact of stimulation on the activity of CN neurons is presumably highly variable (**Online Table S1**). One particularly relevant aspect of this pathway is that Purkinje cells' action potential firing seems determined by their anatomical location: higher firing frequencies have been recorded in zebrin-negative bands and lower frequencies in zebrin-positive bands [80]. Although the impact of these differences on the activity of CN neurons, which form the final output of the cerebellum, remains to be elucidated, cerebellar cortical stimulation has profound effects on the firing patterns of CN neurons mediated by perisomatic inhibitory axon terminals [81-83].

Axons of CN neurons form the superior cerebellar peduncle (brachium conjunctivum) and project to a variety of brain regions, including several pre-motor nuclei in the mesodiencephalic junction, inferior olive, thalamus, superior colliculus and zona Incerta [84-89]. The cerebellar axons that innervate the primary 'relay', secondary 'associative' and intralaminar nuclei of the thalamus form mainly large diameter, excitatory terminals on proximal dendrites that are believed to provide a potent excitatory input [86, 89-92]. In the figure panel we provide an overview of the cerebello-thalamo-cortical connectivity for the rodent thalamus. It should be noted that for the human and primate brain the cerebello-thalamic connectivity has been mostly studied for the laterally-located dentate nucleus, with a particular focus on axons innervating the nuclei analogous to the rodent ventrolateral thalamus [79, 87, 93]. However, because the CN in other mammalian species have been shown to connect to many thalamic nuclei other than the ventrolateral complex, we assume that the CN also provide dense projections throughout the thalamic complex in the primate brain. Thalamic connectivity with cortical areas as well as interspecies differences are reviewed in detail elsewhere [86, 94].

2.2 Cerebellar stimulation – the cortex

From the first half of the 20th century, electrophysiological recordings have revealed that in addition to the thalamus and cerebral cortex the cerebellum also shows oscillatory neuronal activity during generalized epileptic seizures (**Box 3 and 4**). Following the work of Moruzzi in the 1940s on the regulatory effect of cerebellar stimulation on clonic motor behavior [66], several studies were undertaken to investigate the potential use of stimulation of the cerebellum to stop epileptic seizures of various kinds in rats, cats and monkeys, yielding mainly positive results (as reviewed by [67]). Subsequent studies on electrical stimulation

of the cerebellum in epileptic patients indicated that stimulation of the cerebellar cortex could effectively stop psychomotor, generalized tonic-clonic, myoclonic, partial or focal seizures (**Online Table 1 in supplement**) [47, 68-75]. Yet, two out of three subsequent and independently conducted double-blind studies on the effects of cerebellar cortical stimulation in epilepsy patients reported a much more limited and inconsistent effect, shifting the general opinion away from cerebellar cortex stimulation [76-78]. In these studies, the efficacy of stimulation treatment appeared to depend on many factors, such as: the location and size of cerebellar cortical stimulation sites and the type and severity of seizures involved.

There are several reasons that could underlie the variable and inconsistent effects of cerebellar cortex stimulation on epileptic seizures. First, the overall density and complexity of the deeply penetrating foliation of the cerebellar cortex and the pronounced convergence of the inhibitory Purkinje cell projections to CN neurons complicates the entrainment of CN firing by cortical stimulation (**Figure 1**) [83, 95]. These limits prevent effective reduction of oscillatory firing in the cerebello-thalamo-cortical networks (**Box 3**).

Second, responses in the CN to partially synchronized Purkinje cell input is also variable, in that not all types of CN neurons show a post-inhibitory rebound in membrane potential and/or action potential firing [105, 107-111]. Third, the distribution of synaptic afferents is likely to differ for individual types of neurons [112]. Fourth, because the patients included in these early cerebellar cortex stimulation trials suffered from various types of seizures involving dedicated parts of their brains, the gross positioning may have been suboptimal for seizure intervention (**Online Table 1 in supplement**). Together, these factors may have induced variability in the effects of chronic stimulation of the cerebellar cortical stimulation on the seizure frequency, which had been reported previously in a range of experimental animal models [113]. However, it was recently shown that optogenetic stimulation of parvalbumin-expressing Purkinje cells and interneurons in the cerebellar cortex were effective in shortening the pharmacologically induced temporal lobe seizures [45]. Moreover, stimulating vermal, but not the lateral, cerebellum was effective in decreasing seizure frequency, which may be related to the pronounced connectivity of the vermal cerebellum with the temporal lobe [45, 114]. Although this study did not report the estimated number of optogenetically-modulated Purkinje cell or CN neurons, the applied light intensities [115] modulated a sufficiently large portion of cerebellar neurons to shorten temporal lobe seizures.

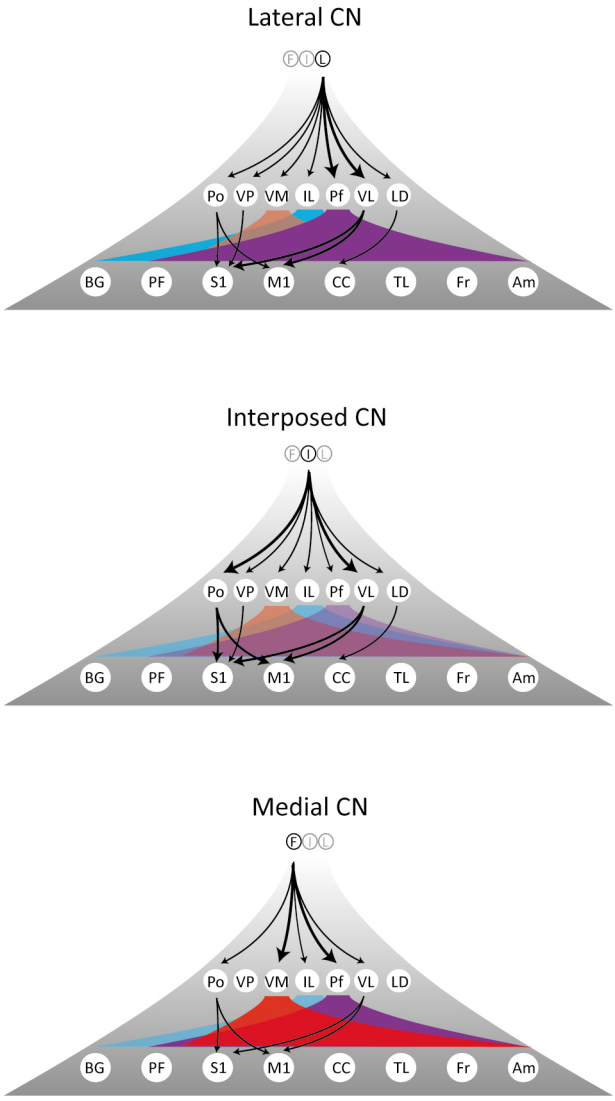

Figure 1. Rodent cerebellar projections to dorsal thalamus and connected cortical regions

Note that thickness of the arrows indicate the putative strength of the indicated cerebellar connections to thalamic nuclei. Thickness of the arrows and transparency of the shaded areas indicate the putative strength of cerebellar impact on thalamocortical connections. VM, IL and PF project particularly diffuse to cortical areas and are therefore represented differently (shaded areas) than the more focused projections from Po, VP, VL and LD (arrows).

LD = Lateral dorsal thalamic nucleus, VP = Ventral posterior thalamic nucleus, VL = Ventral lateral thalamic nucleus, Po = Posterior thalamic nuclear complex, Pf = Parafascicular thalamic nucleus, VM = Ventral medial thalamic nucleus, IL, intralaminar thalamic nuclei (i.e., centromedian, centrolateral and mediodorsal), Am = Amygdala, PF = Prefrontal cortex, S1 = Primary somatosensory cortex, M1 = Primary motor cortex, CC = Cingulate cortex, Fr = Frontal cortex.

Box 3. Pathophysiology in cerebello-thalamo-cortical tract during generalized epilepsy seizures

Although it is widely recognized that various brain structures are involved in generalized epilepsy, the role of thalamocortical networks in its pathogenesis has been studied in particular detail [96, 97]. During generalized seizures thalamic and cortical neurons show repetitive, synchronous action potential firing (and pausing), which can be recorded as generalized spike-and-wave discharges (GSWDs – see **Glossary**) in the electro-encephalogram (EEG) and electrocorticogram (ECoG) [96, 98, 99]. This particular firing pattern is caused by the local interplay between excitatory and inhibitory neurons; upon inhibition I_h-current and $Ca_V3.1$-channels are activated, which depolarize the membrane and subsequently evoke bursts of action potentials [29, 99]. Moreover, both thalamocortical relay neurons and corticothalamic neurons potently drive action potential firing in the inhibitory reticular thalamic nucleus neurons, which in turn are particularly tuned to transmit bursts of action potential firing [100], thereby facilitating the oscillatory network activity that underlies GSWDs [97]. Also, the interconnected cerebellar neurons show epilepsy-related activity changes, which are most likely caused by enhanced excitatory collateral input from pontine and olivary nuclei that relay oscillatory firing patterns from the cerebral cortex (see also **Box 2**) [90, 101]. In fact, experimental studies show that epileptic seizures are generally accompanied by oscillatory action potential firing in the sole output neurons of the cerebellar cortex (i.e. Purkinje cells) as well as CN neurons [45, 46, 102-104]. These principle neurons are susceptible to oscillatory activity, as they, like thalamic and cerebral cortical neurons, encompass I_H- and/or $Ca_V3.1$- and $Ca_V3.3$-channels that activate upon inhibitory input, supporting burst firing [81]. In principle, these ion conductances could also start epileptic oscillatory activity, which might occur in the sparse cases of cerebellar epileptogenesis (**Box 4**). At the very least these conductances allow CN projection neurons to transmit the oscillatory spiking patterns to downstream targets, i.e., thalamic relay neurons [82, 91, 92, 105, 106]. Stimulating CN neurons, which have an exclusively glutamatergic impact on thalamic neurons, should in principle be effective in preventing hyperpolarization of the thalamic membrane potentials and thereby prevent the aforementioned burst-firing [29, 100]. A similar mechanism to prevent too high levels of thalamic hyperpolarization have been the aim of various pharmacological interventions (e.g. [37]).

2.3 Cerebellar stimulation – The CN

Electrical stimulation of the fastigial, interposed and/or dentate nucleus as well as that of the *brachium conjunctivum* (superior cerebellar peduncle) (**Box 2**) has been reported to shorten and reduce the occurrence of seizures in various epilepsy seizures. For instance, both cobalt- and electrically-evoked generalized and hippocampal seizures in cats were effectively stopped using low (20-40 Hz) and high (200-400 Hz) stimulation of the interposed and dentate nuclei [116, 117]. However, other studies on the impact of CN stimulation

in comparable chemically- and electrically induced epilepsy models showed limited or no positive effects [113, 118]. A recent study showed that CN stimulation is effective in stopping generalized spike and wave discharges (GSWDs; see **Glossary**) in genetic mouse models of absence epilepsy (**Figure 2)**. Increasing the neuronal activity in the interposed nuclei in particular, was highly effective in stopping GSWDs, stopping up to 100% of positive responses even following unilateral stimulation [46]. One of the potential causes for the difference in efficacy between this recent study and previous ones is the use of optogenetic stimulation. Yet, this seems a rather unlikely source of the sharp difference between the findings, since optogenetic stimulation in the cerebellum and various other regions has been a validated approach to modulate neuronal spiking during epileptic seizures, just as electrical stimulation [45, 115, 126]. Unlike in the situation of cerebellar cortex stimulation, it is unlikely that inadequate entrainment of CN action potential firing evoked the variable effects in stopping seizures (**Figure 1**), since the volume of the stimulated CN is limited: even in the adult human brain the cerebellar dentate nucleus has a rather limited volume of ~400 mm^3, while the emboliformis, globose and fastigial nucleus each cover at most ~50 mm^3 [127, 128]. Moreover, electrically stimulating the dentate nucleus in epilepsy patients was reported highly effective [48, 49, 129]. Therefore we argue that the variability in efficacy of stopping epileptic seizures is most likely due to inadequate modulation of CN neuronal spiking or a mismatch between the stimulated region and the type of seizures.

Based upon the anatomical connections between the individual CN and the thalamic subnuclei and interconnected cortical networks, electrical stimulation of CN should in principle be effective to reach vast areas of the cerebrum (**Box 2**). Indeed, stimulating medial CN that project more densely to the limbic system, appears more effective in stopping temporal lobe seizures [45], whereas manipulation of the more laterally located CN was most effective in manipulating the occurrence of GSWDs in genetic mouse models of absence epilepsy [46]. These findings corroborate earlier studies on the differential impact of electrical stimulation of the lateral and medial cerebellum on various types of epilepsy seizure occurrence (as reviewed by [67]). Thereby these results advocate the application of CN stimulation in a subnucleus specific manner to investigate the differential impact on thalamo-cortical networks.

Box 4: Cerebellar epileptogenesis

Apart from thalamic and cerebral cortical foci, epilepsy can also arise from other neuronal structures [119]. Among these is the cerebellum, which has been linked to focal and generalized seizures as early as the 17th century (reviewed by [120]). The general scientific interest in cerebellar involvement in epilepsy was initiated by John Hughling Jackson's description of a 5 year old boy, who experienced 'tetanus-like' seizures and was found to have a tumor in the cerebellar vermis [121]. Ever since, many case reports have shown that cerebellar tumors or lesions can indeed result in various types of epileptic seizures, including generalized seizures, which disappear after complete resection of the affected region (as reviewed by [122]). Still, it remains to be elucidated whether pathophysiological cerebellar activity by itself can be sufficient to cause epileptic seizures.

Few experimental reports exist on cerebellar epileptogenesis. It has been shown that using the well-described *L7/Pcp2-Cre* mouse line, which is generally used for Purkinje cell specific gene manipulations but also reveals extra-cerebellar *Cre*-expression, the conditional deletion of the *Cacna1a* gene, which codes for the pore-forming subunit of $Ca_V2.1$ calcium channels, resulted in the occurrence of GSWDs [123]. More recently, it was also reported that the *Cacna1a* ablation from cerebellar granule cells using the *Gabra6-Cre* mouse line evoked spontaneously occurring GSWDs [124]. These data implicate abnormal cerebellar output induces secondary changes in the activity of thalamic relay neurons and their cortical targets; thus provoking oscillations in thalamo-cortical networks. Given that the deletion of *Cacna1a* from the majority, but not all, cerebellar granule cells did not evoke increased levels of irregular cerebellar action potential firing, nor ataxic motor behavior nor other gross pathologies like epilepsy [125], it could be that particular aspects of the cerebellar activity patterns provide protective effects against epilepsy. Future studies should further denote under which conditions aberrant cerebellar output can protect from or induce hyper-synchronous thalamo-cortical activity.

2.4 Correlations between epilepsy and cerebellar atrophy: implications for neurostimulation

Even before the advent of volumetric brain imaging, patients with generalized seizures due to mesial temporal lobe epilepsy were found to have cerebellar pathology upon postmortem examination (reviewed by [130]). In general, patients with chronic epilepsy retain the gross morphology of their cerebellar cortex and nuclei, but the total volume of their cerebellum as well as the density of their main cortical output neuron, i.e. the Purkinje cell, eventually decreases [131]. Moreover, the degree of cerebellar atrophy can often be correlated to the number and intensity of seizures [130]. Together, these associations raise questions regarding the extent to which co-occurrence of epilepsy and cerebellar atrophy reflect a common cause and/or cerebellar atrophy facilitates epileptic seizures.

In principle, both causal conditions may occur. On the on hand, there are many possible genetic mutations that can cause both epilepsy and cerebellar atrophy independent from one another. For example, mutations in the *CACNA1A*-gene and *NPC (Niemann-Pick disease type C)* gene, which are known to cause Familial Hemiplegic Migraine type 1 and Niemann-Pick disease, respectively, directly affect expression profiles in various types of neurons in both the cerebral cortex and cerebellum and these in turn are probably directly capable of inducing epileptic seizures and cerebellar atrophy, respectively [132, 133]. In addition the genetic aberrations that cause progressive myoclonic epilepsies, such as Unverricht-Lundborg (*CSTB*-gene) and LaFora disease (*EPM2A*-gene) are also known to directly cause cerebellar atrophy [134, 135]. Yet it is also known that cerebellar atrophy in turn may also facilitate epileptogenesis, in that structural impairment of the cerebellum facilitates a relapse of generalized seizures following neurosurgical resection of the temporal lobules [136] (see also **Box 4**). Moreover, pharmacological silencing of CN activity in rat and mouse models of epilepsy results in a pronounced increase in seizure occurrence [46, 137], just as the surgical removal of the interposed and lateral CN reduces the threshold for secondarily generalized seizures induced by amygdaloid kindling (**Glossary**) [138].

When studying the cause and consequence of epilepsy and cerebellar atrophy in patients, one should note that anti-epileptic drugs such as phenytoin [139] and benzodiazepine derivatives [140] can compromise cerebellar anatomy in the long-run; thus even though such drugs may reduce the seizures in the initial stage of the treatment, when permanently applied they may damage the cerebellum and thereby worsen the level of epilepsy. Indeed, the iconic epilepsy patient Henry Molaison ('patient H.M.'), who was treated for many years with phenytoin before he was subjected to a bilateral hippocampal resection, also suffered from a severe cerebellar atrophy [141, 142] and probably even from white matter lesions that affected the cerebellar output to thalamo-cortical networks [143-145].

Given the complex interactions between epilepsy and cerebellar pathology over the course of the disease, it is critical to assess the integrity of the cerebellar output to the thalamo-cortical networks before implementing DBS. Clearly, cerebellar stimulation will be relatively ineffective in patients with lesions in their superior cerebellar peduncle. However, despite the considerable size of the cerebello-thalamo-cortical tract (**Box 2**), until recently it was not possible to adequately assess its complex pathology in a clinical setting [93]. Only since the development of dedicated magnetic resonance imaging (MRI) sequences that allow accurate diffusion tensor imaging (DTI; **Glossary**) is it possible to non-invasively and quantitatively evaluate the anatomy of the cerebello-thalamo-cortical tract in epileptic patients [87]. In principle DTI can also be used to position stimulus electrodes in grey and/or white matter structures [146, 147].

2.5 Optimizing paradigms for cerebellar stimulation

In addition to tailoring the placement of DBS electrodes to the patho-anatomical characteristics of cerebello-thalamo-cortical tracts, the potential impact of DBS on epilepsy can also be optimized by applying dedicated stimulation paradigms that are adjusted in the temporal domain. The parameters that should be taken into consideration in this respect include the frequency, regularity, synchronicity, duration and phase of stimulation (**Figure 2**).

2.5.1 Low vs high frequency

DBS can be used to activate neuronal structures, but also to inactivate structures [148]. Injecting negative current in the neuropil depolarizes membranes and thereby evokes action potentials in neurons or passing axons, inducing release of neurotransmitters at axonal terminals. High-frequency stimulation (typically ≥130 Hz) may deplete neurotransmitters from terminals and thereby temporarily 'silence' the stimulated neurons, whereas low-frequency stimulation continuously evokes enhanced activity according to the stimulated pattern [148]. Although this differentiation appears rather clear cut, several issues prevent a straightforward setting of stimulus frequency.

First, different types of neurons are endogenously active at widely ranging frequencies. Therefore, it is of utmost importance to consider the experimental evidence available for the stimulation target. For example, the CN contain a heterogeneous, partially interconnected population of neurons, which fire at a wide range of firing frequencies in awake behaving animals [46, 81, 105, 112, 149]. Given this variation and connectivity, DBS at a particular frequency may continuously activate one particular type of neuron, while temporarily silencing another one, and thereby exert its downstream effects quite differently from those at other frequencies.

Second, neurotransmitter release from specific cell types is tuned to particular frequencies of the stimulated cells and to properties of the downstream targets. For example, the cerebellar input to thalamic nuclei has been described to be of a 'driver' type, which typically indicates that neurotransmitter release evoked by high frequency stimulation is subject to paired-pulse depression [150]. Thus, if CN cells are stimulated at a frequency that far exceeds their endogenous firing frequency, their transmission onto thalamic neurons may be dampened. In line with this notion, clinical studies report that stimulation below 100 Hz can be highly effective in treating epilepsy [48, 49] or tremor [148, 151].

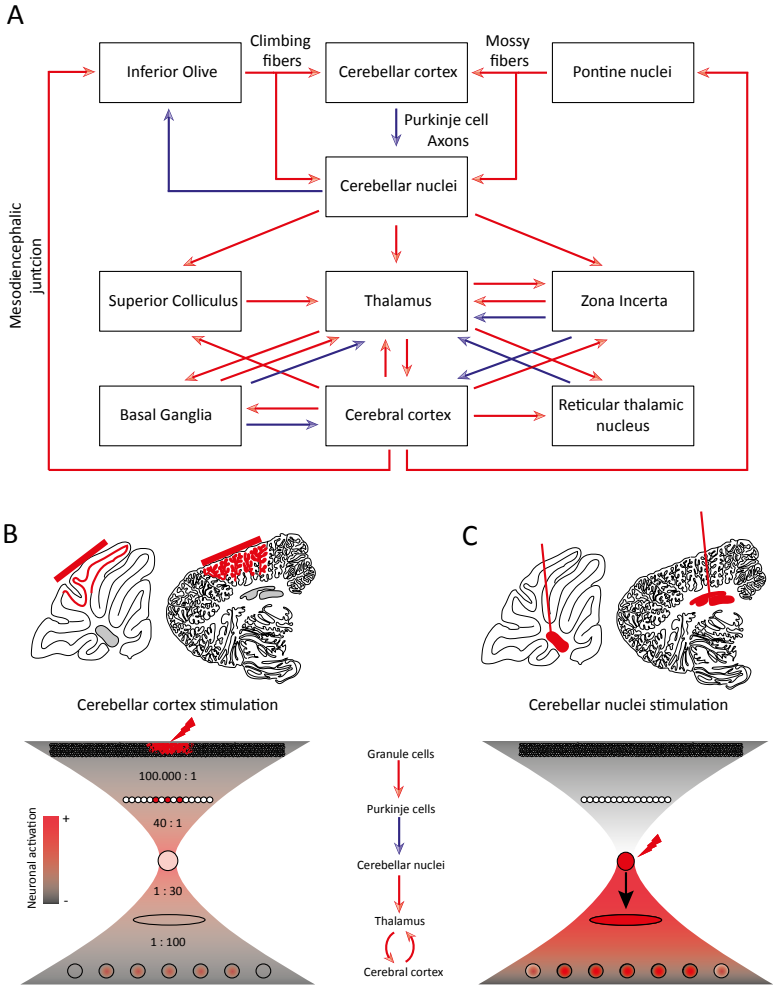

Figure 2. Cerebellar stimulation and the impact on thalamo-cortical networks.

(a) Schematic representation of epilepsy-relevant afferent and efferent cerebellar projections. Red arrows represent excitatory projections and blue arrows represent inhibitory connections. (b) (Top panel) Sagittal view of the mouse (left) and human (right) vermal cerebellum. The thin outlines indicate the cerebellar surface and the thicker lines indicate the Purkinje cell layer. The grey volumes embedded within the cortex represent the medial cerebellar nuclei ('fastigial nuclei'). Red rectangular shapes above the cerebellum represent electrical stimulation electrodes (e.g. [78]) and the red lines within the cerebellum indicate the area activated by this stimulation. (Bottom panel) Schematic representation of the convergence and divergence of the cerebello-thalamo-cortical tract: Purkinje cells receive a strongly convergent input from granule cells [129] and subsequently provide a converging input to the cerebellar nuclei [83]. The cerebellar nuclei project divergently to the thalamic nuclei (see also **Box 2**) [84], each of which can innervate numerous cortical neurons [86]. The red lightning bolt represents the site and extent of cerebellar cortical stimulation and the red color indicates the stimulus-evoked increase in neuronal action potential firing. (c) As in B but for cerebellar nuclei stimulation. Note that due to the degree of convergence and divergence of their respective afferent and efferent projections, direct stimulation of the cerebellar nuclei can alter the neuronal action potential firing in larger thalamocortical areas as opposed to cerebellar cortical stimulation.

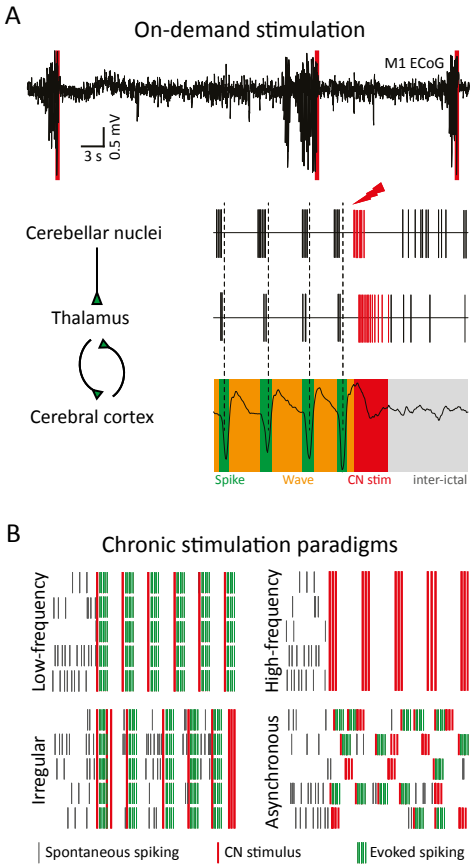

Figure 3. Cerebellar stimulation to stop epilepsy.

(a) (Top panel) On-demand stimulation effectively stops spontaneously occurring GSWDs as shown by primary motor cortex (M1) ECoG recordings from awake *C3H/HeOuJ* mice [8]. Vertical red lines indicate the optogenetic stimulations. (Bottom panels) Schematic representation of the CN, thalamic and cortical activity patterns during an absence seizure that is stopped by increasing the neuronal action potential firing in CN during the 'wave' phase of the GSWD, i.e., the phase during which most CN, thalamic and cortical neurons remain silent [46, 99]. (b) Schematic representation of chronic stimulation paradigms and their putative effect on CN action potential firing. When delivered by a conventional lead that contains a single contact point, the stimulation pulses ('CN stimulus' - red bold lines) delivered at low frequency (top left) are likely to entrain the local neuronal spiking ('evoked spiking' - green lines) synchronously; a change from spontaneous spiking ('spontaneous spiking' – dark lines). In contrast, high frequency stimulation is likely to stop action potential firing [148]. Also irregular stimulus patterns are likely to evoke arbitrary levels of synchronicity when applied through the conventional stimulus leads. Yet, by using novel stimulation leads equipped with tens of contact points [151, 156] it should be feasible to randomize the neuronal firing patterns and thereby mimic interictal neuronal firing.

2.5.2 Irregular vs regular

So far, electrical stimulation paradigms designed to treat epilepsy are of a regular pattern. However, several *in vivo* studies in awake animals have indicated that dentate neurons do not show a regular firing pattern, but instead reveal an irregular firing pattern, reflecting the integration of intrinsic pacemaking activity with inhibitory and excitatory synaptic inputs [81-83]. Using a conventional stimulation electrode, regular stimulation patterns at frequencies known to drive activity are likely to induce a regular firing pattern in all neurons within reach of the current field generated by the electrode lead. Inducing regular firing patterns for extended periods of time may exert artificial long-term effects on synaptic transmission in the downstream nuclei (e.g., [81]). To address this issue, a different stimulus pattern may be considered resembling the endogenous, i.e., irregular, neuronal firing pattern. A recent experimental study in the field of neuro-rehabilitation on the impact of irregular CN stimulus patterns on stroke-affected cerebral cortex reported increased recovery rates compared to regular stimulation patterns [152]. Irregular stimulation patterns are currently also under consideration for patients with Parkinson's disease and essential tremor [153]. Using this approach, the stimulation paradigms may be utilized to mimic CN interictal firing patterns and thereby better control epileptic seizures.

2.5.3 Synchronous vs asynchronous

Both the anatomy of the cerebellar cortex and its axonal afferents promote synchronous action potential firing in cortical Purkinje cells [154], which potently evokes well timed-spiking in CN (**Box 2**) [81-83, 155]. These bouts of synchronous cerebellar activity can be evoked readily by both sensory and motor inputs [81]. During epileptic absence seizures and temporal lobe seizures cerebellar firing is phase-locked to oscillations in thalamocortical networks [45, 46, 104]. The putative hyper-synchronization of the cerebellar output during epileptic seizures is therefore likely to corroborate the synchronization of neuronal firing in thalamic nuclei (**Box 2** and **Figure 1**). Thus, supported by an optimal convergence - divergence ratio of its inputs and outputs, the CN appear to be suitable locus to provide an intervention stopping the hyper-synchronized neuronal activity in thalamocortical networks. The question is to what extent these intervening signals themselves should be synchronized or not. On one hand, asynchronous signals may gradually impose a desynchronizing effect, but on the other, synchronized bursts of activity out of phase with the hyper-synchronized neuronal activity in the thalamocortical networks may provide an initial boost to break the rhythm. Currently, several novel electrode designs are being tested that allow the generation of variable current density at multiple, individual contact

points [151, 156], which in principle should allow differential regulation of the level of asynchronous and synchronous stimulation in the CN.

2.5.4 On-demand vs chronic

Regardless of the spatiotemporal pattern, electrical stimulation can be applied for shorter or longer durations and with or without a particular phase relation to periodic biological or pathological events (like a seizure episode). Currently, most clinical stimulation paradigms are applied chronically for long periods of time or intermittently in a semi-chronic fashion. For diseases with a chronic effect, like Parkinsonism and essential tremor, continuous stimulation paradigms appear most suitable [151]. However, the episodic nature of epilepsy, with intense but relatively short periods of aberrant thalamocortical activity, may call for a more dynamic, on-demand, approach (**Glossary**) [157, 158]. Applying electrical stimulation only when the seizure occurs requires an optimal design of the stimulation paradigms to counteract the pathological activity patterns. Such a tailored stimulus approach has recently been successfully applied in studies of rodent models of generalized or spontaneous epilepsy [45, 46, 126, 159, 160] and of patients with temporal lobe epilepsy [56]; indeed, these studies showed that seizure-triggered single-pulse stimulation delivered shortly after onset is highly effective in stopping the spike and wave discharges. Moreover, with this on-demand approach, the moment of stimulation can be adjusted to the intrinsic phase of the seizures, allowing a highly precise level of temporal control. Recent analysis of varying the moment of stimulation with respect to the phase of the spike and wave discharges has indicated that increases in the excitatory input of CN neurons to thalamic neurons are most likely to stop seizures when they are initiated during the hyperpolarization phase (i.e. wave) of thalamo-cortical networks (**Figure 2**) [46]. Although further refinement of the exact phase between the onset of the single pulse stimulus and network oscillations is warranted [161, 162], these benefits of on-demand DBS further advocate the parallel avenue of closed-loop applications in which both the duration and phase of the stimulus are reproducibly controlled at a high temporal resolution based on the input of the EEG signals.

2.6 Concluding remarks and future directions

Following the initial studies on the therapeutic use of cerebellar stimulation to stop epilepsy, several decades of cerebellar research have substantially improved our understanding of cerebellar information processing. Future neurobiological experiments should aim to utilize the latest advancements in optogenetic tools or electrode design to apply stimulus

paradigms tailored to endogenous, local activity patterns [151, 153]. Due to the rapidly increasing understanding of the pathophysiological mechanisms underlying various types of epilepsies [97] it may soon become clear which particular DBS paradigms are optimal for treatment of the various types of drug-resistant epilepsies (see also **Box 1**). The anatomical and electrophysiological characteristics of the cerebello-thalamo-cortical tract provide sufficient possibilities to stop GSWD episodes in animal models of absence seizures [46]. Future research should elucidate whether the CN stimulation is also effective in stopping convulsive seizures characterized by the phasic occurrence of GSWDs, like generalized tonic-clonic seizures [163].

3

A guide to *in vivo* optogenetic applications for cerebellar studies

Accepted as Chapter for Book 'Neuromethods':

O.H.J. Eelkman Rooda and F.E. Hoebeek

The mammalian cerebellum consists of a superficial cortex and centrally located output nuclei, which together with brainstem nuclei are organized in a modular fashion. Regardless of the function, these cerebellar modules consist of the same cell types and their connectivity has been unraveled to some detail using electrical stimulation experiments. To unravel the highest level of detail, cell-specific stimulation experiments are warranted, which cannot be accomplished using electrical stimulation. To reach this unprecedented level of specificity optogenetic applications are now being implemented in cerebellar studies. Due to the extensive knowledge about cell-specific markers in both the cerebellar cortex and the cerebellar nuclei, optogenetics can be applied cell-specifically. Ideally the anatomical and electrophysiological characteristics of the cerebellum can be utilized for designing future optogenetic studies. In this chapter we review the opportunities and pitfalls for optogenetic studies in the cerebellum. We provide insights into the technical issues at hand and which solutions are currently available.

3.1 Introduction: Shining light on cerebellar optogenetics

Since the beginning of electrical stimulation also the cerebellum has been probed for functional relevance. Early work from Morruzzi in the 1940-1950s indicated that motor responses and body posture could be precisely adapted by electrical stimulation of defined parts of the cerebellar surface [66]. It didn't take long before researchers started to evaluate the power of cerebellar stimulation when it comes to limiting brain perturbations, e.g. stopping epilepsy. Although the anti-epileptic effects of cerebellar stimulation were extensively probed in experimental animals and confirmed in initial clinical trials, subsequent double-blind studies revealed that the exact location of stimulation was affecting the efficacy (reviewed in[164]). The spatial precision of cerebellar stimulation has been of great importance for gaining insight in cerebellar functioning. Anatomical tracing studies in the late 1900s revealed that specific regions of the cerebellar cortex form functional modules together with downstream cerebellar nuclei and the inferior olive nuclei in the ventral brainstem [165, 166]. Especially in the cerebellar cortex this anatomical differentiation has been shown to be very precise and results in the need of neuromodulation techniques with high spatial resolution. Although novel electrode designs brought new options for neuromodulation on a micro-scale the recent development of optogenetics launched a new era of investigating brain functioning. Apart from the option of applying neurostimulation to a specific type of neuron rather than a volume of brain tissue, many light-sensitive ion channels have been described, which not only allow researchers to excite neurons, but also to inhibit their action potential firing (extensively reviewed in [167] and other literature). Alike for other brain areas also for cerebellar research optogenetics provide numerous opportunities. This chapter combines reports of optogenetic applications in the cerebellar field with a technical guideline for questioning cerebellar interactions with up- and downstream targets using optogenetics.

3.2 Optogenetic approaches in the Cerebellar Cortex

The foliated cerebellar cortex (CC) consists of 3 readily distinguishable layers of gray matter and a core of white matter, the latter of which is a combination of afferent mossy fibres and climbing fibres and efferent Purkinje cell axons. Adjacent to the white matter is the cytological diverse granular layer, which contains numerous granule cells, Golgi cells, Lugaro cells and unipolar brush cells. Distal to the granular layer a monolayer of Purkinje cells separates granule cells from the molecular layer, which contains molecular layer interneurons, i.e., stellate and basket cells. This outer layer also contains the dendritic trees of Purkinje cells and Golgi cells as well as the granule cell axons. In principle each of the cell-

types can be targeted using optogenetic tools (**Figure 1**), which would have been impossible using electrical stimulation techniques (juxta-cellular stimulation of single neurons is not discussed in this chapter, but could be used to increase action potential firing in a single neuron [168]). The increasing knowledge of anatomical connections of cortical neurons and their concurrent activity [169-171] enables one to control the activity in functionally distinctive modules or microzones using specific (sub-) populations of cerebellar neurons [154].

3.2.1 How to induce opsin expression

A common method to accomplish cell-specific expression of light-sensitive channels is the Cre-LoxP system, which is based upon the expression of Cre recombinase and its capacity to cause DNA synapsis and site-specific recombination of DNA strands at genetically engineered loxP sites [172].

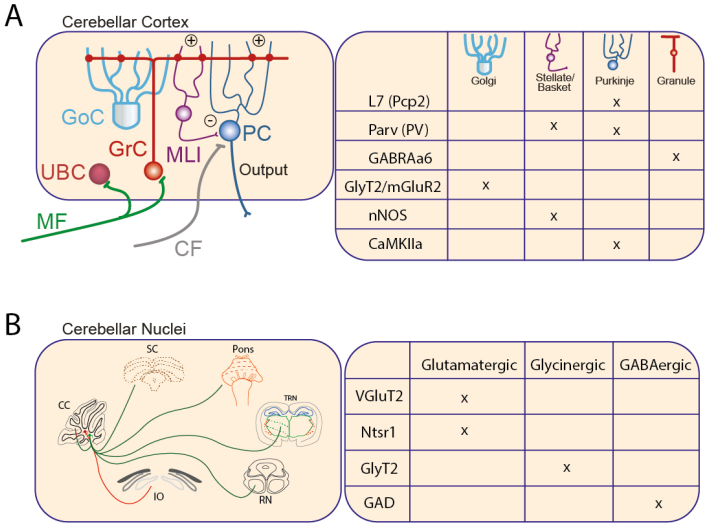

	Golgi	Stellate/ Basket	Purkinje	Granule
L7 (Pcp2)			x	
Parv (PV)		x	x	
GABRAa6				x
GlyT2/mGluR2	x			
nNOS		x		
CaMKIIa			x	

	Glutamatergic	Glycinergic	GABAergic
VGluT2	x		
Ntsr1	x		
GlyT2		x	
GAD			x

Figure 1. Circuitry and cell-specific promotors of cerebellar neurons.

(A) (left) Schematic and simplified illustration of cerebellocortical circuitry. (right) Table with promotors identifying promotors for different cortical cells. (B) (left) Schematic and simplified illustration of cerebellar nuclei output and its downstream targets. (right) Table with promotors identifying promotors for different CN neurons. Apart from the listed promotors, several non-selective promotors like synapsin or CAG have been utilized in the cerebellum. See main text for references and examples (mGluR2 is specific for a subset of Golgi cells [261]. UBC = unipolar brush cell; GrC = granule cell; GoC = Golgi cell; MLI = molecular layer interneuron; PC = Purkinje cell; MF = mossy fiber; CF = climbing fiber; CC = cerebellar cortex; SC = superior colliculus; TRN = thalamic relay nuclei; RN = red nucleus; IO = inferior olive; L7-PCP2 = L7 Purkinje cell protein 2; Parv = parvalbumine; GABRA6 = alpha6-subunit of GABAA-receptor; GlyT2 = glycine transporter type 2; nNOS = neuronal nitric oxide synthase; and CaMKIIa = calcium-calmodulin-activated kinase type II alpha.

For optogenetics constructs the transgene can be preceded by a LoxP-flanked stop cassette and thus will only be expressed if the cell expresses Cre-recombinase. This commonly used strategy can be applied for instance, by cross-breeding a Cre-mouse line [173] (**Figure 1**) and any of the AI-mouse lines [174, 175]. Of these, the AI-27 or AI-32 mouse lines result in cell-specific expression of the channelrhodopsin 2-construct (ChR2), which encodes for light-sensitive ion-channels that mediate neuronal depolarization [167], combined with a red- or yellow-fluorescent protein construct, respectively. To drive ChR2-expression in Purkinje cells the most commonly used approach is to cross-breed with a transgenic mouse line in which the L7 (Purkinje cell protein 2) promotor for Purkinje-cell specific transgene expression [176], which is linked to Cre-recombinase [177] and thereby can be used for Purkinje cell-specific mutations (reviewed by [81]). For instance, L7Cre*Ai32 mutant mice show Purkinje cell specific ChR2-expression and can be identified by their YFP-positive identity (**Figure 2A**) [178]. Of note is that in several recent studies the specificity of the L7/Pcp2-Cre mouse lines has been questioned [123, 171] and warrants a detailed evaluation of the expression. To avoid the potential a-specific expression of Cre-lines, one option is to induce ChR2-transfection using *in utero* electroporation [179]. To direct the transfection specifically to cerebellar neurons, one option is to inject ChR2-encoding constructs into the 4th ventricle and electroporate the cerebellar progenitor cells in the rhombic lip or the subventricular zone near the 4th ventricle during embryonic days 10.5 and 12.5 [180] (**Figure 2B**). Novel electrode designs should warrant acceptable success ratios [181] and numerous constructs that can be used for excitatory or inhibitory optogenetics [175] should provide ample options for cerebellar optogenetics. One consideration is that the transfection rates of *in utero* electroporation typically fall short of those reached by cross-breeding transgenic mouse lines – a difference that can also be advantageous if mosaic but cell-specific expression is the goal. Another option is to transfect the cerebellum by cerebrospinal fluid injections, which results in mosaic expression throughout the whole CNS [182, 183].

To reach a more spatially restricted expression of opsins, often viral vectors are used. From the pre-optogenetics era of gene therapy it is known that various vectors can be used to transfect cerebellar cell types. Apart from Lenti-viral backbones (see for instance refs [184-186]), cerebellar tissue can be transfected using adeno-associated viral (AAV) vectors [187-189] (**Figure 2C**). As has been shown in other parts of the CNS [190], the various AAV-serotypes can lead to widely varying transfection efficiency rates and even serotype-specific tropism. Apart from the serotypes, also the promotors can be utilized to tune the transfection in cerebellar tissue. In case the location of transfection rather than the cell-type specificity is most important, human synapsin (hSyn) is commonly used and results

in neuron-specific staining. Another commonly used promotor is ubiquitous CMV and chicken-β-actin fused to CMV enhancer (CAG). When packaged in an AAV1-vector the CAG promotor showed an elevated specificity for Purkinje cells [187]. Another commonly used promotor is parvalbumine, which is endogenously expressed in Purkinje, stellate and basket cells [191-193]. Apart from these generally used promotors, cerebellar scientists have also been exploring the use of cell-specific markers. For cerebellar granule cells, the α6 subunit of the GABA-A receptors (GABRα6) is a selective marker [194].

Kim and colleagues produced an AAV1-GABRα6-GFP vector, which indeed resulted in selective expression of GFP molecules in granule cells [195]. In the same study, also an AAV1-vector was produced that packaged the αCaMKII-promotor, which is selective for Purkinje cells in the cerebellar cortex. Finally, the Augustine lab and collaborators generated a transgenic mouse in which ChR2 is expressed under a neuronal nitric oxide synthase promotor, which resulted in selective expression in molecular layer interneurons [193, 196, 197]. These results indicate that the viral constructs can be readily tuned to drive cell-specific transfection in the cerebellar cortex. Another approach to reach cell-specific expression is by injecting a transgenic mouse that expresses Cre-recombinase in a cell-specific manner with a viral vector that encodes the opsin-construct preceded by a floxed Stop codon (**Figure 2C**) (see for instance refs [111, 198]).

As has been pointed out previously [199], using the extensive knowledge of the anatomical connections within the cerebellum can help to study the functional connectivity of identified cell types. Great care needs to be taken that the volume, location and spread of the viral particles is restricted. Viral vectors can be injected using iontophoresis (see ref [200] for a functional protocol), although it is more common to use air-pressure. Pressure injections can be performed using injection systems that can be purchased from various vendors, or can easily be manufactured using an injection syringe, a piece of tubing and a glass injection pipette. Important for pressure injections is that the speed and volume are tightly controlled. Typically, the speed of injection is <50 nl/min and the volume for intracerebellar injections below 200 nl. Another measure taken to limit the spread of the viral vectors beyond the injected area is to leave the injection pipette in place for several minutes before retracting. To reach a stable opsin expression level, experiments are typically started after >3 weeks of incubation time, although the latency until stable levels have been reached could vary per serotype and promotor [190].

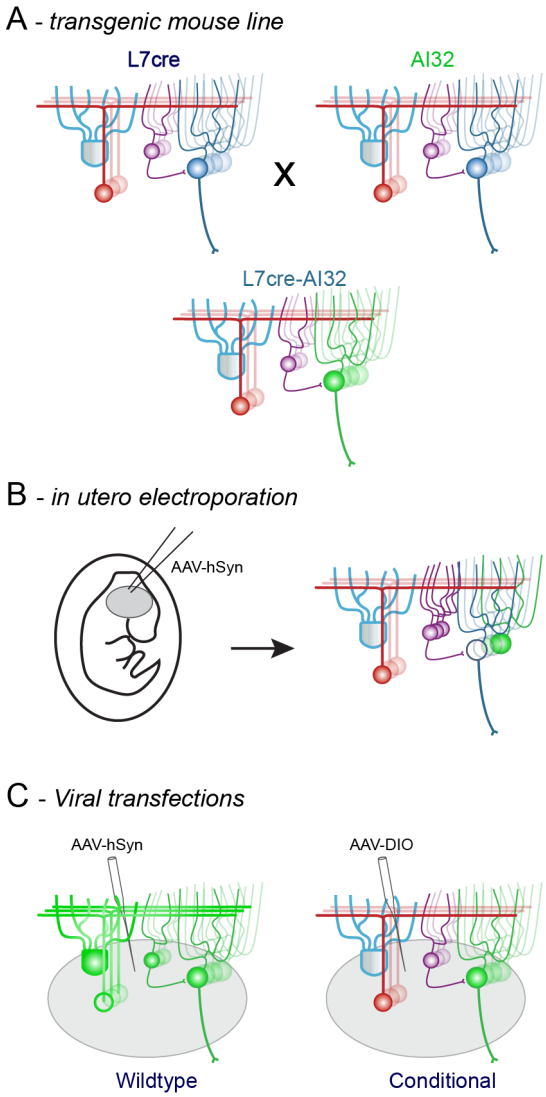

Figure 2. Transfection techniques for (non)specific expression.

(A) Cell-specific expression of ChR2 using a Purkinje cell-specific Cre-mouse line (L7cre) and a transgenic mouse in which the ChR2-construct and the fluorescent reporter are preceded by a floxed stop codon (AI32). Crossbreeding of these two lines results in Purkinje cell-specific expression of ChR2 throughout the whole cerebellum. (B) *In utero* electroporation using a-specific promotors like hSyn can still result in a cell-specific transfection due to the spatial and temporal specificity of the viral presence. (C) (left) Viral expression using a-specific promotors will result in opsin expressing in multiple cell types. (right) injecting a L7Cre mouse that expresses Cre-recombinase Purkinje cells only with a viral vector that encodes the opsin-construct preceded by a floxed Stop codon will result in Purkinje cell specific expression of ChR2, but only in the injected region.

3.2.2 Combining light and recording in the cerebellar cortex

Once the cerebellar tissue expresses opsins, the next step is to apply light to the brain. The intensity of light needed ranges between opsins, but for the commonly used variants of ChR2 1-5 mW/mm^2 is typically sufficient to evoke action potential firing [167, 201]. Although some experimental studies on ChR2-stimulation in the cerebellum aimed to record the spread of light in tissue and its effects on Purkinje cell action potential firing [115, 202] it is not clear whether the foliation and mixture of grey and white matter layers in the cerebellar cortex affect the spread of light. Although simplified calculation tools are readily available to the scientific community [203] these do not take into account that light attenuation coefficients [204] and other important characteristics vary widely in the brain [205]. Recently developed predictive models like the OptogenSIM platform by Liu et al [205] provide the scientific community with readily accessible tools for more realistic estimations of how far the light of particular wavelengths will travel. This could be particularly informative for experiments that report the physiological and behavioral responses following optical stimulation of the cerebellum with large (200-400 μm diameter) optic fibers (Figure 3A).

To limit the spread of light, small-diameter optic fibers (< 100 μm diameter) can be purchased from several vendors. Another option is to strip optic fibers and pull them to sharp-tip using heating and grinding (see for instance ref [193]). Once the diameter is sufficiently limited, they can be attached directly to recording electrodes to apply optical stimulation directly to the recorded area (Figure 3B). One important consideration for local optical stimulation is the fact that local optical stimulation causes stimulus artefacts evoked by photoelectrochemical effects that were first described by the French physicist Becquerel in 1839 and are considered as the main mechanism of stimulus artefact for conventional metal electrodes [206-208]. It is produced by photonic excitation of electrons at the electrode valence band that absorbs the photon energy; subsequently an electric potential is generated because these excited electrons leave their orbit [206, 208]. There are several ways to deal with this artefact. One of them is to place the recording electrode at a distance from the light source (Figure 3B) although this might not always be an option when recording and stimulating close to each other.

If possible another solution would be to switch to low energy photons (green light instead of blue) which in combination with decreasing light intensity to such levels that the amplitude of the artefact falls below the background noise might be a more reasonable solution. However opsins require a minimum light intensity to be activated so a more ideal solution would be an artefact free recording method. Several groups tried to eliminate

the photoelectric artefact by developing fully transparent electrodes with increasing manufacturing complexity [209-211]. The use of tin-doped indium-oxide and graphene as material does not seem favorable for (chronic) *in vivo* applications since indium tin oxide oxidizes over time and thereby alters the biocompatibility [212]. Still, a straightforward solution is to use the classic liquid filled glass pipettes and insert an optic fiber into the taper (Figure 3C,D). By placing a Pt or Ag/AgCl recording electrode at the back of the pipette, i.e. far from the light source, the charged ions move through the liquid instead of through the conduction band of the brain. This custom-made 'optrode' returns high quality single cell recordings virtually free of photoelectric artefacts. Note that this fiber-in-glass approach is not suited for chronic applications since the glass pipettes is very thin, fragile and are subject to increasing tip resistances over time that limit the recording quality.

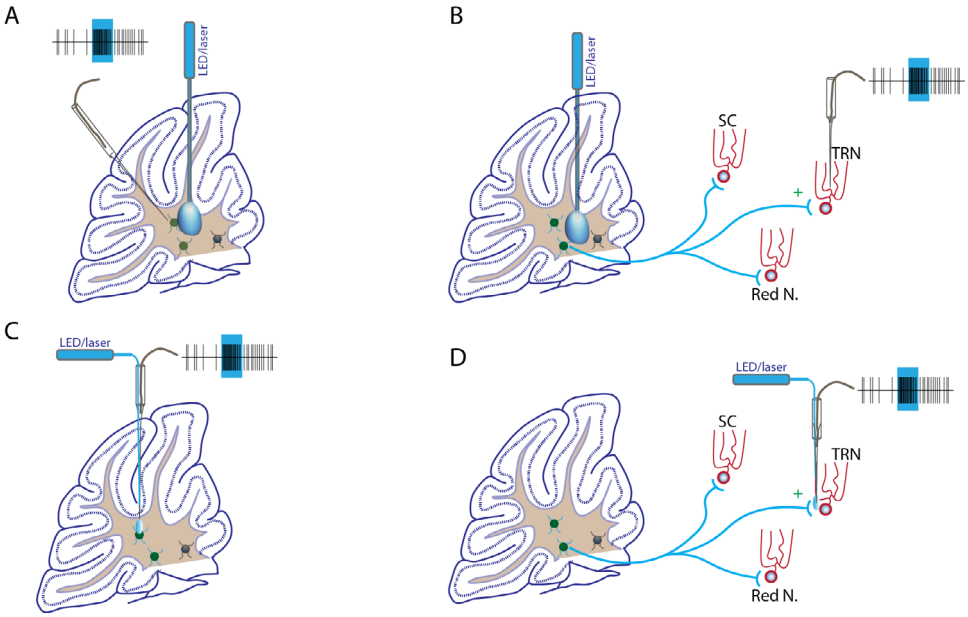

Figure 3. Stimulation and recording methods.

(A) Schematic for recording CN neurons (left top, schematic trace in which black vertical lines represent action potentials and the blue box the time of optical stimulation of ChR2) using a glass pipette (transparent tube including a wire) with a separate optic fiber (vertical blue probe) for light delivery. (B) Schematic for recording downstream targets with light delivery in CN. Note that this will also activate other pathways which might cause network effects. (C) Schematic for combined recording and light delivery through glass pipette. (D) Schematic for combined recording and light delivery at CN terminals in downstream nuclei to isolate the specific effect of cerebellar output on downstream targets without initiating network effect. SC = superior colliculus; TRN = thalamic relay nuclei; and Red N = red nucleus.

3.2.3 Optical stimulation – upper and lower limits

Ideally, optogenetics experiments are designed to encompass a recording electrode at the stimulation site. In this way the experimenters can tune their optical stimulation paradigm to the intended neuromodulation. Several landmark papers scrutinized the kinetics of opsin constructs and the neuronal responses [201, 213-218], which clearly indicate that optical stimulation cannot only be too low, but also too high. In the case of ChR2 over-stimulation would result in a decrease rather than in increase of action potential firing. Such an inhibitory effect is typically mediated by a 'depolarization block' caused by ChR2-mediated depolarization that inactivates sodium channels and subsequently inhibits action potential firing [219]. Obviously, such effects may lead to false assumptions, for instance, when correlating 'prolonged action potential generation' to a behavioral readout, while in fact the action potential firing was only initially elevated and then silenced. In a similar fashion the use of inhibitory opsins should be carefully considered. For instance, it was recently shown that when using chloride-conducting channelrhodopsins the expected inhibition of neurotransmitter release was effectively reversed [220]. To prevent previously mentioned over-activation artefacts, the maximum pulse length and the power should be critically considered. It is possible to prevent over-activation effects by implementing a duty cycle. This will limit the amount of light exposure but can also dramatically change the output compared to a continuous pulse of light. It is easy to recognize that a 200 ms long 50 Hz train of short (3 ms) light pulses (17 ms pause) and a 200 ms long continuous light pulse will have a completely different effect on the opsin-expressing neuron as well as on its downstream targets [219].

Sustained activation of any type of rhodopsin by light can also lead to heat induction. Heating depends on many properties such as power of light, duration and the wavelength, but also on (and not limited to) intrinsic brain properties, temperature loss (due to skull removal), blood flow etc. Commonly used light power densities for optical stimulation have been reported to marginally increase local temperatures near the stimulation site, leading to enhanced activity of neurons [221-223]. Recently it has been shown that prolonged light introduction of 10 mW can lead to temperature increases ranging between 1°C to 4°C across a large volume of tissue, which resulted in directly increased firing rates by up to 40% [224]. Another important issue is the diameter of optic fiber. It has been shown that the core peak temperature change for 62 μm fibers with the same light output (10 mW) is several °C higher compared to a 200 μm diameter fiber [224]. To control for the impact of such heating effects on neuronal firing and thereby on the study results, it is of upmost importance to include a set of control experiments in which the same optical stimulation is

applied in ChR2-negative animals. In case prolonged activation of the opsins is an absolute necessity a potential solution could be to use step-function opsins, which require only short light-pulse to activate long-lasting increases in action potential firing [167, 225].

3.2.4 Mediating Purkinje cell activity using opsins

It is of great importance to select the type of opsin and the optical stimulation paradigm that match the electrophysiological characteristics of the target cells. One of the main reasons for this is that opsins are membrane bound and thus the membrane surface area is linearly related to the number of light-sensitive ion channels that can be incorporated. For instance, granule cells, which are the smallest cerebellar neurons, can fit less opsin-channels than the larger Purkinje cells. The impact of activating light-sensitive ion channels is also related to the membrane properties – granule cells have a ~10-fold higher membrane resistance then Purkinje cells [125] and thus, the activation of a certain number of ion channels has a bigger impact on the membrane potential of granule cells than on Purkinje cells. Apart from the passive membrane properties it is likely that also the intracellular constellation has an impact on the neuronal response to opsin activation. For instance, Purkinje cells typically do not express voltage-gated sodium channels in their dendritic tree; activation of a high density of sodium-permeable ion-channels, i.e., ChR2-channels, in this membrane may induce pathophysiological processes. Indeed, in our hands the use of high density light stimulation on freshly prepared *in* vitro slices containing Purkinje cells expressing ChR2(H134R) can induce excitotoxicity (unpublished observation, F.E.H.).

Purkinje cells endogenously fire two types of action potentials (simple and complex spikes), which come about because of a delicately organized interaction between dendritic and somatic characteristics [226, 227], and thus the use of optogenetics directly in Purkinje cells to manipulate action potential firing is precarious. The available data on direct manipulation of Purkinje cell activity [45, 111, 171, 178, 185, 186, 197, 228], which has been achieved using a myriad of opsins, should be evaluated critically. First and foremost, Purkinje cells are characterized by an intrinsic pacemaking activity [229] that can easily be disrupted by, for instance, abnormal levels of excitatory inputs [230, 231], and result in abnormal firing patterns. Moreover, opsins' actions may depend on the viral vector used: Jackman and colleagues recently showed that when ChR2(H134R) is expressed by AAV1, 5, or 8 serotypes, repetitive stimulation resulted artificially in paired-pulse depression, whereas this was not the case when the same construct was encoded by AAV9 or by crossbreeding of mutant mouse lines [232]. Another important consideration for selecting suitable optogenetic constructs is the fluorescent tag that is typically coupled to the opsin.

Asrican and colleagues identified differences in light-evoked currents when tagging ChR2 with various fluorescent tags. Most notably, Purkinje cells that expressed ChR2-mCherry showed intracellular protein aggregates and the membrane potential did not respond to optical stimulation whereas Purkinje cells transfected with ChR2-YFP showed membrane-bound expression and responded with depolarizing currents upon optical stimulation [191] (but see refs [198, 220] for mCherry-containing constructs without aggregates). These findings underline the importance of selecting the optimal optogenetics construct and inclusion of controls for the efficacy of optical stimulation.

Most of the studies that allow critical evaluation of optogenetics concern activating opsins, i.e., ChR2 and correlates. Yet, a critical evaluation of the impact of inhibitory opsins, i.e. proton pumps [233], chloride channels [213, 234, 235] and light-gated chloride pumps [236, 237], is equally important. For the most widely used Halorhodopsin (eNpHR3.0) and Archaerhodopsin (eArch3.0) it was shown that short illumination (millisecond range) of axonal terminals attenuates synaptic transmission, albeit that eArch3.0 is a more potent inhibitor than eNphR3.0. Notably, such pulsed inhibition also resulted in potent rebound responses [220], which obviously is of importance for the interpretation of any readout. For longer inhibition (minute range) the use of eArch3.0 resulted in counterintuitively elevated presynaptic calcium concentrations and hence increased spontaneous neurotransmitter release [220]. For future investigations that require long-term inhibition of neuronal firing rates, other options include chemogenetic approaches that utilize G-protein-coupled receptors that can be selectively activated by designer drugs (e.g., excitatory hM3Dq [238] and inhibitory hM4Di [239]), photoswitchable tethered ligands linked to metabotropic glutamate receptors [240] and vertebrate rhodopsins [215, 241]. By applying the inhibitory compounds to specific cell types, like molecular layer interneurons [193, 196, 197] or to Purkinje cells directly [111, 228], the net effect on the cerebellar output can be tuned to the specific research questions.

3.3 Optogenetic manipulation of cerebellar nuclei activity

Apart from the vestibulo-cerebellar Purkinje cell projections to the vestibular nuclei, all Purkinje cell axons terminate in the cerebellar nuclei (CN). Most, if not all [242], CN neurons receive Purkinje cell input, which is GABA-mediated. The medial, interposed and lateral CN contain various types of neurons; up to 6 different types in the rodent lateral nucleus [243]. For several of these types of neurons, cell-specific markers have become available in the last years (see **Figure 1** for overview). Vesicular glutamate transporter type-II (vGluT2) is expressed in the CN solely by the glutamatergic projection neurons [244], of

which currently only a single type has been described despite the varying projection patterns (see for instance refs [88, 245]). Apart from using vGluT2-Cre transgenic mice, also the Ntsr1-Cre mouse line has been reported to selectively express in glutamatergic projection neurons of the CN [245]. The other cell types in the CN are inhibitory and release glycine, GABA, or both neurotransmitters from their terminals. By coupling Cre-recombinase to the glutamic acid decarboxylase (GAD), GABAergic neurons can be identified, just as glycinergic neurons can be tagged selectively by coupling Cre to glycine transporter type II (GlyT2) [198]. Ankri and colleagues recently dissected the various types of CN neurons that can be targeted using the GAD-Cre and GlyT2-Cre mice. They convincingly showed that GlyT2-Cre labelled a single type of neuron (based upon somatic diameter and dendritic morphology), which also expresses GAD, and that the GAD-Cre separately labels a smaller type of neuron that is GlyT2-negative and projects to the inferior olive [82, 198, 246, 247]. Using the GlyT2-cre mice it is in principle also possible to target the glycinergic projection neurons that selectively project to the brainstem's vestibular complex [248]. These cell-specific tactics provide researchers with a similar arsenal as previously mentioned for the cerebellar cortex. Importantly, also the same precautions for optical stimulation and recordings will have to be taken into account. Below we will review the currently available data important to design future optogenetic studies that can unravel the impact of afferents on CN neuronal activity and the impact of CN neurons on their downstream targets.

3.3.1 Manipulating afferents to Cerebellar Nuclei neurons

Neurons in the CN have been reported to receive a mixture of excitatory and inhibitory input from external inputs – for the current chapter we disregard the intra-nuclear axon collaterals and local interneurons (for review see ref [242]). The excitatory input may originate from the inferior olive and arrive as climbing fiber (CF) collaterals or from various reticular, pontine or spinal regions as mossy fiber (MF) collaterals [95]. It was concluded from electrical stimulation experiments performed *in vivo* that CF-inputs monosynaptically excited CN neurons [105, 108, 110, 249, 250]. Yet, a more recent study that used optogenetic approaches indicated that CF-evoked responses in CN could only be recorded in a few cells and if present, these responses were relatively weak [251]. A potential confounder for some of the electrical stimulation studies is that not only inferior olive neurons and their axons were stimulated, but also the neurons and axons passing nearby that may give rise to MF-evoked responses [105, 108, 251]. Electrical stimulation of isolated MF-afferents to CN neurons is mostly limited to *in vitro* studies in which the CN-surrounding white matter is stimulated and the excitatory responses are pharmacologically isolated by blocking

inhibitory currents (as reviewed by ref [252]). These data on putative MF-CN transmission reveal that the excitatory input is subject to synaptic plasticity and mediates also inhibitory transmission and cellular excitability levels. Applying selective optogenetic stimulation of MF-inputs will provide more insights in the differences between the MF- and CF-inputs to CN neurons.

For the other major input to CN neurons, the Purkinje cells, it was long thought that this GABA-mediated input had a purely inhibitory effect on CN action potential firing patterns. This thought was fueled by the extreme convergence of Purkinje cell axons onto single CN neurons, the perisomatic location of these axon terminals on CN neuronal membrane and the relatively slow time constants of the inhibitory postsynaptic potentials. However, the landmark paper by Person and Raman [83] revealed that synchronous Purkinje cell firing could elicit time-locked spiking in CN neurons, which can be used to design optogenetic paradigms for Purkinje cell stimulation. For instance, short pulses (1-2 ms pulse width) of 470 nm light on ChR2-expressing Purkinje cells could result in a short inhibition of CN spiking, followed by a well-timed action potential (see for instance refs [83, 105]). This will probably occur once a sufficient number Purkinje cells are synchronously entrained by the optical stimulation, i.e., when a sufficient level of Purkinje cell synchronicity is reached [83, 253]. By lengthening such potent optogenetic stimulation to tens or hundreds of milliseconds it may occur that CN neurons are depolarized to such levels that once the stimulation stops, the membrane potential shows a rebound depolarization (see also refs [105, 107, 108, 253, 254]). The accompanying increase in CN firing has indeed been shown in various optogenetic studies from several labs albeit ranging from a rather limited increases [115, 251] to more pronounced elevations that even accompanied behavioral responses [111, 193, 228]. These responses can be tuned quite precisely by varying the light intensity and/or location of optical Purkinje cell stimulation. It should be noted that the optical stimulation is merely enhancing the synchronicity of Purkinje cell firing for the duration of stimulation and that the local and downstream network will outlast the direct intervention.

3.3.2 Manipulating Cerebellar Nuclei neuron activity

The output neurons of the CN can be inhibitory or excitatory and thus the effect on downstream targets can increase or decrease local action potential firing. In general it is thought that the excitatory projection neurons connect to the di-, mes-, met- and myelencephalon and that the GABA-ergic and glycineric projection neurons project to the inferior olive and vestibular nuclei, respectively (**Figure 1B**). So far, a limited

number of optogenetic studies evaluated the impact of varying CN firing rates on these downstream targets. Nucleo-olivary neurons have been shown by electrical stimulation to provide a tonic and phasic inhibition to olivary neurons at the site of dendro-dendritic gap junctions [255]. When selectively activating these neurons using a GAD-Cre mouse and a double-floxed ChR2(H134R) viral construct, Lefler et al recently showed for the first time that this inhibitory input uncouples inferior olive neurons and thereby manipulates complex spike firing and Purkinje cell activity [247]. Moreover, it was recently shown for these nucleo-olivary neurons that optogenetic stimulation of Purkinje cells evoked post-synaptic responses that decayed 10-fold slower than in excitatory projection neurons [82]. The electrophysiological difference between these two types of neurons also extended into the sluggish action potential half width as well as a narrow dynamic range in action potential firing rates in nucleo-olivary neurons [82]. These apparent differences could be of importance for selecting optogenetic constructs to drive each of these neurons, or their afferents.

So far, the studies which have been applying optogenetics directly in CN to study the impact of glutamatergic neurons all injected a hSyn-promotor driven ChR2-vector into the cerebellar nuclei. In an effort to stop generalized spike-and-wave discharges in epileptic mouse models, Kros et al transfected interposed and lateral CN neurons, optically stimulated in these regions and recorded CN action potential firing patterns and the electrocorticogram [46]. Apart from the fact that the generalized episodes were reliably stopped, the responses recorded in the CN showed a mixture of increased and decreased firing during optical stimulation. This latter finding is most likely due to the fact that using the hSyn-promotor resulted in the transfection of inhibitory neurons, which synapse on the recorded cells. Also Chen et al transfected the lateral CN with the same a-specific promotor [256]. Although they did not extensively report on the CN activity during stimulation, the authors found that the electrophysiological responses in the striatum evoked by optical stimulation in the CN and those evoked by stimulation of the CN axon terminals in the centrolateral thalamic nucleus were in principle the same [256]. These results argue that although the transfection was most likely not specific for excitatory CN neurons the impact of optical stimulation is mediated by the excitatory input in the downstream target nucleus. Although the local stimulation of axon terminals may be an option for many studies, it could still be advantageous to study an isolated subgroup of CN terminals projecting to a particular downstream target. One way to do so is to use a retrogradely transported viral vector and inject it in the downstream nucleus targeted by the CN. Several vectors for such retrograde expression have been generated; currently it seems that AAV-retro provides the best options [257].

Using the cell-specific stimulation options, recently there have been several studies that revealed the functional importance for CN axonal connections back to the cerebellar cortex. These axonal tracts had been described in various anatomical papers, but due to the anatomical specifications it had not been possible to electrophysiologically isolate them sufficiently [258]. Using the a-specific hSyn promotor Gao et al transfected CN neurons with ChR2 and found that their fluorescent mossy fiber-like terminals evoked purely excitatory currents in granule and Golgi cells of the cerebellar cortex [259]. In another recent study, an inhibitory nucleo-cortical projection has been described from neurons that co-express GAD and GlyT2 and specifically target a subpopulation of cerebellar Golgi cells [198]. This latter study utilized GAD-Cre and GlyT2-Cre mice in combination with AAV-vectors encoding for floxed-ChR2 constructs, which warranted cell-specific manipulations of inhibitory neurons that are GABAergic and glycinergic (and excluded GABAergic nucleo-olivary and glutamatergic projection neurons) [198]. Such level of unprecedented anatomical, physiological and functional detail recently also lead to the characterization of Purkinje cell axon collaterals to granule cells and neighboring Purkinje cells in the adult brain [169, 171].

3.4 Final recommendations and conclusions

Utilizing optogenetics will have a positive impact on cerebellar studies. Novel research questions about the functional impact of particular connections can now be adequately addressed. The information content of the results from optogenetic studies will be unprecedented, but will require a multitude of controls and sensitive analyses to filter out artefacts and identify the true impact of optogenetic manipulations. For instance, to recognize subtle changes in action potential firing patterns evoked by the activation of a subset of presynaptic axon terminals, a sufficient number of stimulation repeats have to be recorded to allow for Monte Carlo bootstrapping and subsequently identification of significant changes in firing patterns. Another aspect of optogenetics in cerebellar network physiology that deserves attention is the fact that various recurrent loops exist that can affect the electrophysiological responses in addition to the direct effects of the optical stimulation. These loops come in various shapes and sizes that not only include cortical neurons (MF-granule cell-Golgi cell-granule cell; Purkinje cell-granule cell-Purkinje cell; etc), but also involve the CN neurons and inferior olive neurons (intra-CN, nucleocortical and nucleo-olivary) and thus can have a delayed effect on cerebellar activity patterns. Moreover, the glutamatergic CN output can also return to the MF or CF sources by thalamo-cortical networks and midbrain nuclei, or even via the sensory feedback triggered

by cerebellar-evoked motor responses. Although most of these potential feedback loops will be characterized by a fixed latency, it is very likely that the evoked network effects can last for extended periods and need to be considered when setting inter-stimulus intervals. Likewise, for most optogenetic constructs the inter-stimulus interval needs to be tailored to the desensitization and closed states [260]. Tuning these and other technical details will be decisive for the added value of optogenetics in cerebellar studies. Although the cerebellar field can ride on the constant wave of optogenetic innovations, this does not mean that optogenetic approaches can be bluntly copied from, for instance, the cerebral cortex field. By using the extensive anatomical knowledge of the cerebellar connectivity and cellular physiology the most effective and functionally relevant optogenetic approaches can be achieved.

4

Synchronicity and rhythmicity of Purkinje cell complex spike firing during GSWDs

Accepted in Frontiers in Cellular Neuroscience:

L. Kros*, S. Lindeman*, O.H.J. Eelkman Rooda*, P. Murugesan, L. Bina, L.W.J. Bosman, C.I. De Zeeuw* and F.E. Hoebeek*

*These authors contributed equally

Absence epilepsy is characterized by the occurrence of generalized spike and wave discharges (GSWDs) in electrocorticographical (ECoG) recordings representing oscillatory activity in thalamocortical networks. The oscillatory nature of GSWDs has been shown to be reflected in the simple spike activity of cerebellar Purkinje cells and in the activity of their target neurons in the cerebellar nuclei, but it is unclear to what extent complex spike activity is implicated in generalized epilepsy. Purkinje cell complex spike firing is elicited by climbing fiber activation and reflects action potential firing in the inferior olive. Here, we investigated to what extent modulation of complex spike firing is reflected in the temporal patterns of seizures. Extracellular single-unit recordings in awake, head-restrained homozygous tottering mice, which suffer from a mutation in the voltage-gated CaV2.1 calcium channel, revealed that a substantial proportion of Purkinje cells (26%) showed increased complex spike activity and rhythmicity during GSWDs. Moreover, simultaneous Purkinje cells, recorded either electrophysiologically or by using Ca2+-imaging, showed a significant increase in complex spike synchronicity for both adjacent and remote Purkinje cells during ictal events. These seizure-related changes in firing frequency, rhythmicity and synchronicity were most prominent in the lateral cerebellum, a region known to receive cerebral input via the inferior olive. These data indicate profound and widespread changes in olivary firing that are most likely induced by seizure-related activity changes in the thalamocortical network, thereby highlighting the possibility that olivary neurons can compensate for pathological brain-state changes by dampening oscillations.

4.1 Introduction

Absence epilepsy is a common form of generalized epilepsy that clinically manifests itself as behavioral arrest and diminished consciousness [40, 96, 262, 263]. It is characterized by thalamocortical network oscillations occurring as generalized spike and wave discharges (GSWDs) in electrocorticographical (ECoG) recordings. GSWDs appear as repetitive sharp peaks followed by slow waves reflecting synchronous phasic firing of thalamocortical and corticothalamic neurons [225, 262, 263]. Recruitment of inhibitory reticular thalamic neurons by either of these two cell populations has been shown to be necessary and sufficient for GSWD appearance due to their control of rhythmic burst firing of thalamic relay cells[225, 264]. Apart from the well-studied thalamocortical pathophysiology, generalized epilepsy also involves subcortical structures [96]. One of these subcortical structures that has been shown to be involved in pathological thalamocortical oscillations is the cerebellum [46]. Cerebellar nuclei neurons divergently project to neurons throughout the thalamic complex and a proportion of cerebellar nuclei neurons shows firing that is synchronized with thalamocortical network activity [46, 104]. Likewise the simple spike activity of Purkinje cells in the cerebellar cortex can also be phase-locked to the GSWDs [46, 104].

Thalamocortical information can be conveyed to the cerebellum through two pathways: via mossy fibers that predominantly originate from pontine nuclei, and climbing fibers that exclusively originate from the inferior olive [265, 266]. These afferent pathways both project to the cerebellar cortex and send collaterals to the cerebellar nuclei [243, 267-273]. Typically, cerebellar nuclei neurons fire at frequencies of 20-100 Hz in awake rodents [81, 83, 105]. Given that the intrinsic spiking activity of cerebellar nuclei neurons has been shown to be regular [274, 275], the GSWD-related modulation may be attributed at least in part to synaptic inputs [164]. Although cerebellar nuclei neurons are known to receive both excitatory and inhibitory input from various intra- and extra-cerebellar sources, previous studies indicate that the most potent source of cerebellar nuclei firing modulation occurs from the GABAergic Purkinje cells [83, 105, 107, 251, 254, 267, 276, 277]. In rodents, approximately 30 – 50 Purkinje cell axons converge on a single cerebellar nuclei neuron [83, 95]. Thus, the simple spike modulation of Purkinje cells being phase-locked to the GSWDs [104] might also contribute to the generation and/or control of the seizure. However, to what extent the Purkinje cell simple spike modulation stands on its own and what the impact of oscillatory complex spike activity is, remains to be elucidated.

Purkinje cell simple spike firing is commanded by intrinsic pacemaking activity and mossy fiber input, which is forwarded by granule cells and molecular layer interneurons,

whereas complex spike firing exclusively reflects climbing fiber activation generated in the inferior olive. Given that i) the axons of single olivary neurons branch and synapse in ~7 Purkinje cell dendritic trees [273], ii) olivary neurons tend to synchronize their membrane depolarizations [278], and iii) synchronous olivary activity is a potent way of controlling firing patterns of cerebellar nuclei neurons (as reviewed by [81]), olivo-cerebellar projections appear to be suitable candidates to mediate the oscillatory firing patterns from the cerebral cortex to the cerebellum. Indeed, olivary lesions have been shown to have anti-epileptic effects in epilepsy-prone rats [279] and patients with dentate-olivary dysplasia are reported to suffer from intractable seizures [280, 281].

To establish to what extent activity of the inferior olive contributes to the oscillatory patterns of cerebellar activity during absence seizures, we studied the frequency, rhythmicity and synchronicity of Purkinje cell complex spike firing during episodes of GSWDs. We used a well characterized mouse model for absence epilepsy, the *tottering* mouse, which is characterized by a loss-of-function mutation in the *Cacna1a* gene that codes for the α1-subunit of $Ca_V2.1$-channels [282, 283]. We first investigated single-unit Purkinje cell firing patterns during GSWDs by simultaneously recording ECoG in primary motor and somatosensory cortices to detect any change in firing frequency and subsequently used extracellular multiple-unit Purkinje cell recordings and Ca^{2+}-imaging in Purkinje cell dendrites in awake, head-restrained homozygous *tottering* mice to study synchronicity.

4.2 Materials and methods

All experiments were performed in accordance with the European Communities Council Directive. Protocols were reviewed and approved by an independent animal ethical committee (DEC Consult, Soest, Netherlands).

4.2.1 Animals

Data were collected from male and female homozygous *tottering* mice (4-30 weeks old) and their wild-type littermates, which were bred using heterozygous mice. As described previously [46] the colony, originally purchased from Jackson laboratory (Bar Harbor, ME, USA), was maintained using C57BL/6NHsd mice obtained from Envigo laboratories (Horst, Netherlands). PCR was used to confirm the presence of the *tottering* mutation in the *Cacna1a* gene using 5′-TTCTGGGTACCAGATACAGG-3′ (forward) and 5′-AAGTGTCGAAGTTGGTGCGC-3′ (reverse) primers (Eurogentech, Seraing, Belgium) and subsequent digestion using restriction enzyme NSBI at the age of P9 - P12.

4.2.2 Experimental procedures

Surgery

Mice were anesthetized with isoflurane (4-5% for induction, 1.5-2.5% for maintenance) after which carprofen (5 mg/kg) and buprenorphine (50 µg/kg) were given systemically and lidocaine (2%) was applied subcutaneously to the skull. Hereafter, the skull was exposed, cleaned and treated with OptiBond All-In-One (Kerr Corporation; Orange, CA, USA). Subsequently, five 200 µm teflon-coated silver ball tip electrodes (Advent research materials, Eynsham, Oxford, UK) or five 1 mm stainless steel screws were subdurally implanted for ECoG recordings above the primary motor cortex (+1 mm AP; ± 1 mm ML relative to bregma, bilateral), primary sensory cortex (-1 mm AP; ± 3.5 mm ML, bilateral) and in the rostral portion of the interparietal bone to serve as reference (-1 mm AP relative to lambda). Electrodes and connectors were fixed to the skull and embedded in a pedestal composed of the hybrid composite or dental acrylic (Simplex Rapid; Associated Dental Products, Kemdent works, Purton, Wiltshire, UK and Charisma; Heraeus Kulzer, Hanau, Germany, respectively). To enable cerebellar electrophysiological recordings, bilateral craniotomies (~2 mm diameter) were carefully drilled in the occipital bone. Great care was taken to leave the dura mater intact. Bupivacaine (1 mg/kg) was locally applied to the skull surrounding the craniotomies after which a dental acrylic recording chamber (Simplex rapid) was formed. The recording chamber was sealed with bone wax (Ethicon, Somerville, NJ, USA) after covering the exposed dura with tetracycline-containing ointment (Terra-cortril; Pfizer, New York, NY, USA). An hour after surgery, the mice received another dose of the analgesic carprofen (5 mg/kg) followed by another dose of buprenorphine (50 µg/kg) after 8 hours. The mice were given at least 5 days to recover and then were allowed ~3 hour training sessions with ECoG monitoring for two days prior to the day on which the single-unit electrophysiological recordings started. In case of experiments involving two-photon Ca^{2+}-imaging, a head plate instead of a recording chamber was placed around the craniotomy during surgery. The craniotomy for the two-photon experiments was made on the day of the recording. This procedure was performed under isoflurane anesthesia with local analgesia using lidocaine. Recordings started at least 1 hr after termination of the anesthesia.

Single cell recordings

Recordings were performed in awake, head-fixed animals for no longer than 4 hours while their body temperature was supported using a homeothermic pad (FHC, Bowdoin, ME, USA). Custom-made, borosilicate glass capillaries (OD 1.5 mm, ID 0.86 mm; resistance

8-12 MΩ; taper length ~8 mm; tip diameter ~1 µm) (Harvard Apparatus, Holliston, MA, USA) filled with 2 M NaCl were used for electrophysiological Purkinje cell recordings. Electrodes were positioned stereotactically using an electronic pipette holder (SM7; Luigs & Neumann, Ratingen, Germany). Neurons were recorded extracellularly in both medial (vermis) and lateral (paravermis and hemisphere) areas of the cerebellar cortex, mainly from lobules VI – X. Purkinje cells were identified by the characteristic occurrence of both complex spikes and simple spikes and a minimal pause in simple spike firing following each complex spike of 10 ms. ECoGs were filtered online using a 1-100 Hz band pass filter and a 50 Hz notch filter. Single unit extracellular recordings and ECoGs were simultaneously sampled at 20 kHz (Digidata 1322A, Molecular Devices LLC, Axon Instruments, Sunnyvale, CA, USA), amplified, and stored for off-line analysis (CyberAmp & Multiclamp 700A, Molecular Devices LLC., Axon Instruments, Sunnyvale, CA, USA). ECoG traces were down sampled to 300 Hz.

Multi-unit recordings

Experiments involving multiple single-unit recordings were performed under the same conditions as described above. In these experiments, Purkinje cell recordings were made using glass electrodes or using quartz-coated platinum-tungsten fiber electrodes (2-5 MΩ; 80 µm outer diameter; Thomas Recording, Giessen, Germany). The former electrodes were placed using an electronic pipette holder (SM7; Luigs & Neumann) for each of the two glass electrodes. These pipette holders were mounted on their own oil-drive to position the electrodes independently in the brain. The latter electrodes were placed in a rectangular matrix (Thomas Recording) with an inter-electrode distance of 305 µm. Also these electrodes were independently positioned in the brain. Prior to the recordings using the platinum-tungstun electrodes, the dura was removed under light isoflurane anaesthesia. The recordings were started at least 30 min after termination of the anesthesia. All recordings were made in crus 1, crus 2 and vermis at a minimal depth of 500 µm from the cortical surface. The signals from the glass electrodes were sampled at 20 kHz (Digidata 1322A, Axon Instruments), amplified, and stored for off-line analysis (CyberAmp & Multiclamp 700A, Axon Instruments). The signals from the platinum-tungsten electrodes were sampled at 25 kHz (PZ5 NeuroDigitizer, Tucker-Davis Technologies, Alachua, FL, USA), amplified, filtered online using a 1-6000 Hz band-pass filter and stored offline using a RZ2 multi-channel workstation (Tucker-Davis Technologies). ECoG was recorded as described above (CyberAmp, Molecular Devices).

Ca^{2+}-imaging

The craniotomy required for Ca^{2+}-imaging was performed similarly as described above. During surgery, the surface of the cerebellar cortex was cleaned with extracellular solution composed of (in mM) 150 NaCl, 2.5 KCl, 2 $CaCl_2$, 1 $MgCl_2$ and 10 HEPES (pH 7.4, adjusted with NaOH). After the craniotomy, the mice were allowed to recover from isoflurane anesthesia for at least 30 min and were subsequently head-fixed in the recording setup and received a bolus-loading of the Ca^{2+} indicator Cal-520 (0.2 mM; AAT Bioquest, Sunnyvale, CA) [284, 285]. The dye was first dissolved with 10% w/V Pluronic F-127 in pure DMSO (Invitrogen) and diluted 20 times in the extracellular solution. The dye solution was pressure injected into the molecular layer (50–80 μm below the surface) at 0.35 bar for 5 min. Finally, the brain surface was covered with 2% agarose dissolved in saline (0.9% NaCl) in order to reduce motion artifacts and prevent dehydration.

Starting at least 30 min after dye injection, thus at least 1 hr after the end of isoflurane administration, *in vivo* two-photon Ca^{2+}-imaging was performed of the molecular layer using a setup consisting of a titanium sapphire laser (Chameleon Ultra, Coherent, Santa Clara, CA, USA), a TriM Scope II system (LaVisionBioTec, Bielefeld, Germany) mounted on a BX51 microscope with a 20X 1.0 NA water immersion objective (Olympus, Tokyo, Japan) and a GaAsP photomultiplier detector (Hamamatsu, Iwata City, Japan). A typical recording sampled approximately 20 x 200 μm with a frame rate of ~50 Hz.

4.2.3 Data analyses

Offline GSWD detection

The start and end of GSWD episodes and timing of ECoG 'spikes' (i.e., negative ECoG peaks during episodes of GSWDs) were detected using a custom-written GSWD detection algorithm (LabVIEW, National Instruments, Austin, TX, USA) as described previously [46]. The program detects GSWD-episodes with a minimal duration of 1 s and a minimal interval between seizures of 1 s. Ictal periods were defined as the time from start to end of seizures and interictal periods refer to the time between 2 s after a seizure and 2 s before the next.

Detection of action potentials in extracellular recordings

Extracellular recordings were included if activity was well isolated for >100 s and action potential detection in extracellular traces was performed using threshold-based analyses with customized Matlab (Mathworks Inc. Natick, MA, USA) routines or the Matlab-based program SpikeTrain (Neurasmus BV, Erasmus MC Holding, Rotterdam, Netherlands).

Complex spikes were separated from simple spikes using waveform-based cluster analyses and post-hoc visual inspection.

Detection of calcium events

After motion correction, the dendrites of Purkinje cells were identified using spatial independent component analysis. From each dendrite, the fluorescent signal was used to detect transients as described previously [286].

GSWD-related firing pattern modulation

To assess whether Purkinje cells showed GSWD-modulated firing patterns, a custom-written algorithm in LabVIEW (National Instruments) was used as described previously [46]. Since all ECoG channels (M1 and S1) consistently showed SWDs simultaneously, we only used the M1 recording for GSWD analysis. GSWD-triggered rasterplots and peri-stimulus time histograms (PSTH) with a 10 ms bin width were created for both complex spike and simple spike firing if the total GSWD-episode length was at least 2 s. This allowed us to determine: 1) modulation amplitude: the amplitude difference between the peak and trough near t=0 (corresponding to the spikes of the GSWDs); 2) modulation frequency: dominant frequency in the PSTH as determined with Fast Fourier Transforms (FFT); and 3) mean power at GSWD frequency: based on the average power between 6 and 9 Hz (GSWD frequency range) as determined with FFT. Due to the low complex spike frequency and the low total number of ictal complex spikes, complex spike-based PSTHs of GSWD-modulated cells often did not show a sinusoidal distribution like those seen for GSWD-modulated simple spike firing. Therefore, only modulation amplitude and modulation frequency were considered for complex spike activity. Subsequently, the interspike intervals used for this PSTH were randomly shuffled (500 times) and converted into new PSTHs in order to create normal distributions of modulation amplitude and mean power at GSWD frequency. Z-scores ($Z = (X-\mu)/\sigma$) could now be calculated based on the real and shuffled data. Complex spike firing was identified as GSWD-modulated if: 1) The modulation amplitude was significantly higher than expected by chance ($Z \geq 1.96$, $p \leq 0.05$); and 2) the cell modulated at GSWD frequency (6-9 Hz). For simple spike activity, a third rule was added: the mean power at GSWD frequency was significantly higher than expected by chance ($Z \geq 1.96$, $p \leq 0.05$). Since all ictal simple spike firing that showed significant Z-scores of mean power at GSWD frequency also showed significantly higher modulation amplitudes, the former was used for further analyses. The term 'Z-score' without specification refers to modulation amplitude for complex spike firing and to mean power at GSWD frequency for simple spike firing throughout the manuscript.

Phase differences between the ECoG-spike of GSWDs and the peak of Purkinje cell complex spike and simple spike activity were calculated using the time between 0 (aligned to the peak of the ECoG-spike) and the first peak in the PSTH divided by the median GSWD distance and multiplied by 360.

Firing pattern parameters

Firing pattern parameters were assessed using custom written LabVIEW (National Instruments) based programs described previously [46] and calculating median climbing fiber pause, defined as the median time difference between a complex spike and the first consecutive simple spike, firing frequency, coefficient of variation (CV) of interspike intervals (ISIs) (σ_{ISI}/μ_{ISI}), CV2 $(2|ISI_{n+1} - ISI_n|/(ISI_{n+1} + ISI_n))$ [287] and burst index (number of action potentials within bursts / total number of action potentials) for which we defined 'burst' as a sequence of ≥3 spikes within 100 ms. Firing patterns were specifically calculated for ictal and interictal periods. To make sure these interictal periods were really interictal and without abnormal pre-ictal or post-ictal activity, the 2 seconds before and after each seizure were excluded from analysis.

Synchronicity of Purkinje cell firing

To investigate the synchronicity of inctal Purkinje cell activity, cross-correlograms of pairs of simultaneously recorded Purkinje cells were calculated for both the complex spikes and the simple spikes using the xcorr function from Matlab's Signal Processing Toolbox (Mathworks). Cross-correlograms were normalized so that the autocorrelations at zero lag equaled 1. For the complex spike cross-correlograms, only Purkinje cells with a minimum of 10 ictal complex spikes were included in the analysis. The detected spike times of the complex spikes and simple spikes were binned before calculating the cross-correlogram of each Purkinje cell pair (10 ms bin size). Next we used the bootstrapping method in order to calculate the amount of synchronicity that would occur by chance. For this we randomly shuffled the interspike intervals of complex spikes and simple spikes of each Purkinje cell pair 500 times, creating 500 surrogate spiketrains for each Purkinje cell. From these bootstrapped spiketimes we calculated the cross-correlograms for the complex spikes and simple spikes as described above. Z-scores from the original cross-correlograms could now be calculated using the real and bootstrapped data by applying: $Z=(X-\mu)/\sigma$ where X indicates the values based on the original cross-correlogram, μ indicates the mean of the 500 bootstrapped cross-correlograms and σ indicates the standard deviation. Purkinje cell pairs were identified to be synchronously active if the cross-correlogram amplitude was significantly higher than expected by chance ($Z > 1.96$) at a lag of ~0 ms. In a similar fashion

we also calculated the synchronicity for interictal Purkinje cell activity. The same analyses with the same criteria were applied to the imaging data using the timing of the calcium events.

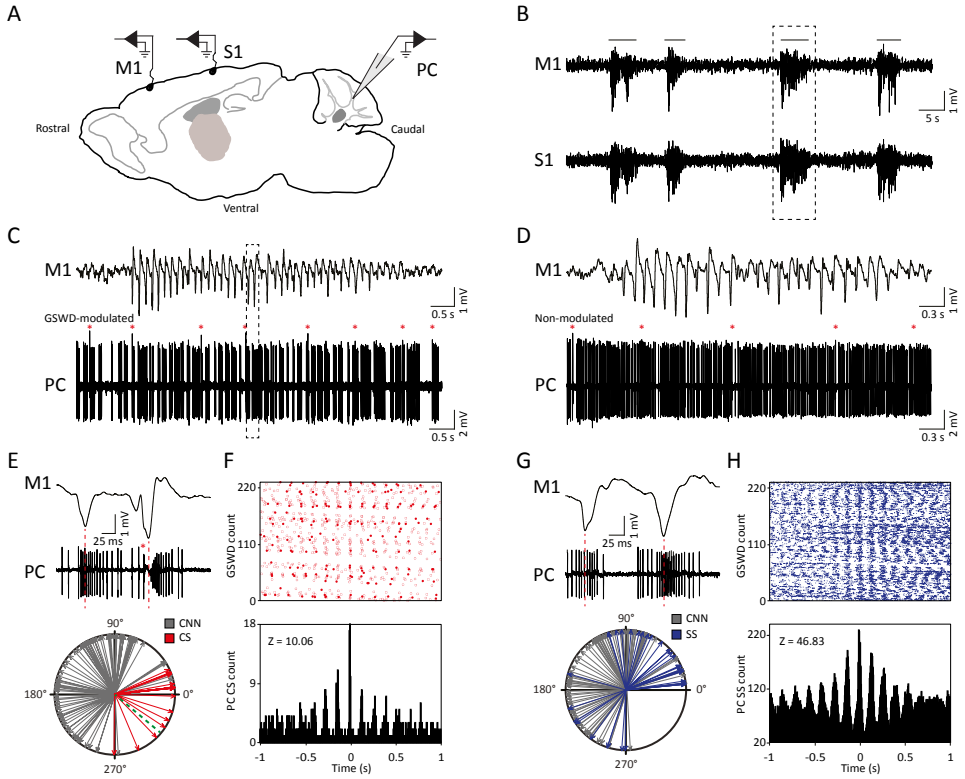

Figure 1. Purkinje cell complex and simple spike firing show GSWD related modulation.

(A) Schematic of recording conditions**. (B**) Example of typical GSWD-episodes in both primary motor (M1) and primary sensory (S1) cortices. Horizontal lines indicate GSWD-episodes. **(C)** Example of Purkinje cell spiking that aligns to boxed GSWD episode in (B). Red asterisks indicate complex spikes. **(D)** Example of non-modulated Purkinje cell firing. **(E)** Example of the timing of a complex spike with respect to the GSWDs. This is activity of the same Purkinje cell as shown in (C) but during a different seizure. Red line aligns ECoG spike to Purkinje cell action potential firing. (Bottom panel) Compass plot of phase difference between modulated Purkinje cell complex spike firing (red) or cerebellar nuclei neuron action potential firing (grey) and ECoG spikes. Dashed green line refers to the onset of the ECoG spike (e.g. the start of the downward deflection in the ECoG). **(F)** Raster plot (top) and PSTH (bottom) for complex spike firing during nine GSWD-episodes in the example in C; t=0 indicates each ECoG spike. **(G, H)** As in (E, F), for GSWD-modulated simple spike firing of the cell shown in C (dashed box in C is magnified in G (top)). The phase information of the cerebellar nuclei data (grey arrows in the compass plots in E and G) was previously published in [46] and is merely shown here for comparison with phase relations of Purkinje cell activity. Abbreviations: Purkinje cell (PC), primary motor cortex (M1), primary somatosensory cortex (S1), cerebellar nuclei neuron (CNN), complex spikes (CS), simple spikes (SS), generalized spike and wave discharge (GSWD).

4.2.4 Statistical analyses

We randomly assigned mice to either electrophysiological recordings or Ca^{2+}-imaging experiments. Statistical differences in firing pattern parameters between independent groups of Purkinje cell recordings (GSWD-modulated, non-modulated and wild-type cells) were determined using MANOVA's with complex spike firing frequency, median climbing fiber pause, simple spike firing frequency, CV, CV2 and burst index as dependent variables and group as independent variable. If a MANOVA showed a significant result, post-hoc ANOVA's were used to assess contributions of individual firing pattern parameters with Bonferroni corrected *p*-values. Statistical differences in firing pattern parameters between ictal and interictal periods were tested with repeated measures ANOVA's with one "within-subjects" factor, *i.e.*, time period, with 2 levels (ictal and interictal) and Bonferroni corrections. Differences in frequency of Ca^{2+}-events between ictal and interictal periods were tested using a paired *t*-test.

A *p*-value ≤0.05 (α) was considered significant unless a Bonferroni correction was used; in that case a *p*-value of α/n was considered significant. Two-tailed testing was used for all statistical analyses and all were performed using SPSS 22.0 software (IBM Corporation, New York, USA). All data throughout the manuscript are represented as mean ± standard deviation (SD). *N* indicates the number of mice; *n* indicates the number of recordings.

4.3 Results

4.3.1 GSWD-related Purkinje cell firing patterns

To establish to what extent activity of the inferior olive and the cerebellar Purkinje cells contribute to the oscillatory activity of cerebellar nuclei neurons during absence seizures, we investigated temporal relations of complex spike and simple spike firing patterns with GSWDs. To this end, extracellular Purkinje cell activity was simultaneously recorded with primary motor and primary sensory ECoG in awake, head fixed *tottering* mice (Fig 1A). These ECoG recordings revealed GSWDs, which are characterized by negative deflections that occur at a mean frequency of 7.74 ± 1.01 Hz (*N* = 23). GSWD-episodes had a mean duration of 3.53 ± 1.12 s (*N* = 23), which is comparable to previously reported values in rodent models for epilepsy [46, 104, 283].

Similar to their main downstream targets, cerebellar nuclei neurons, a portion of Purkinje cells clearly showed GSWD-modulated complex spike or simple spike firing patterns (Fig 1C, D). Complex spike firing that was phase-locked to GSWDs occurred in 26% of Purkinje cells (Fig 1E, F). In these Purkinje cells, the peak of complex spike activity occurred almost exclusively during the ECoG spike, virtually all of them appeared after the onset of the ECoG

spike (green dashed line in the compass plot in Fig 1E). Interestingly, this is the inverse pattern to that seen in cerebellar nuclei neurons (Fig 1E) (cf. [46]). GSWD-modulated simple spike firing tended to occur during the same phase of a GSWD as cerebellar nuclei firing (Fig 1G, H). These data indicate that during GSWD episodes the complex spike firing coincides with a pause in simple spike and cerebellar nuclei firing. Overall, almost half of the recorded Purkinje cells (47 out of 103) showed GSWD-modulated complex spike and/or simple spike firing. Of these modulated Purkinje cells, 15% showed complex spike modulation only, 43% showed both complex spike and simple spike modulation and in the remaining 43%, sole simple spike modulation was observed (Fig 2A-C).

We next investigated whether Purkinje cells that showed either GSWD-modulated complex spike or simple spike activity can be distinguished from non-modulating Purkinje cells (Fig 3A, B). Because firing patterns can be determined using various non-independent parameters that asses rate and regularity (Fig 3C, D), we first tested for differences in overall firing pattern using MANOVAs that, in case of significance, were followed by *post hoc* ANOVAs.

Firing patterns were calculated separately for interictal and ictal periods. This allowed us to compare modulated and non-modulated firing during GSWD-episodes and interictal periods separately and additionally we could assess changes in firing between ictal and interictal periods. These analyses revealed that Purkinje cells showing GSWD-modulated complex spike firing indeed differed from cells that did not show complex spike modulation in both interictal ($p<0.05$) and ictal ($p<0.01$) firing patterns. More specifically, cells with GSWD-modulated complex spike firing showed a shorter interictal climbing fiber pause ($p<0.01$), a higher simple spike burst index during both interictal ($p<0.01$) and ictal periods ($p\leq0.001$), a higher ictal complex spike frequency ($p<0.01$) and a higher coefficient of variation (CV) of ictal simple spike firing ($p<0.01$) when compared to those cells that showed non-modulated firing (Fig 3C, Online Table 1). The same analyses based on modulated simple spike firing resulted in similar differences between modulated and non-modulated Purkinje cells ($p<0.001$ both ictally and interictally; Fig 3D, Online table 3). We also noticed that not only modulated Purkinje cells, but also non-modulated Purkinje cells (based on either complex spike or simple spike firing) showed a change in firing pattern when comparing ictal and inter-ictal firing patterns (Fig 3C, D, Online Table 2, 4). Notably, our data show that during GSWDs, an inverse phase relationship exists between complex spike firing and both simple spike and cerebellar nuclei firing, and that the complex spike frequency increased significantly during seizures. This indicates that at least a proportion of inferior olivary neurons significantly changes activity during seizures. (See Fig 3 and online table 1-4 for all statistical outcomes for the individual firing pattern parameters).

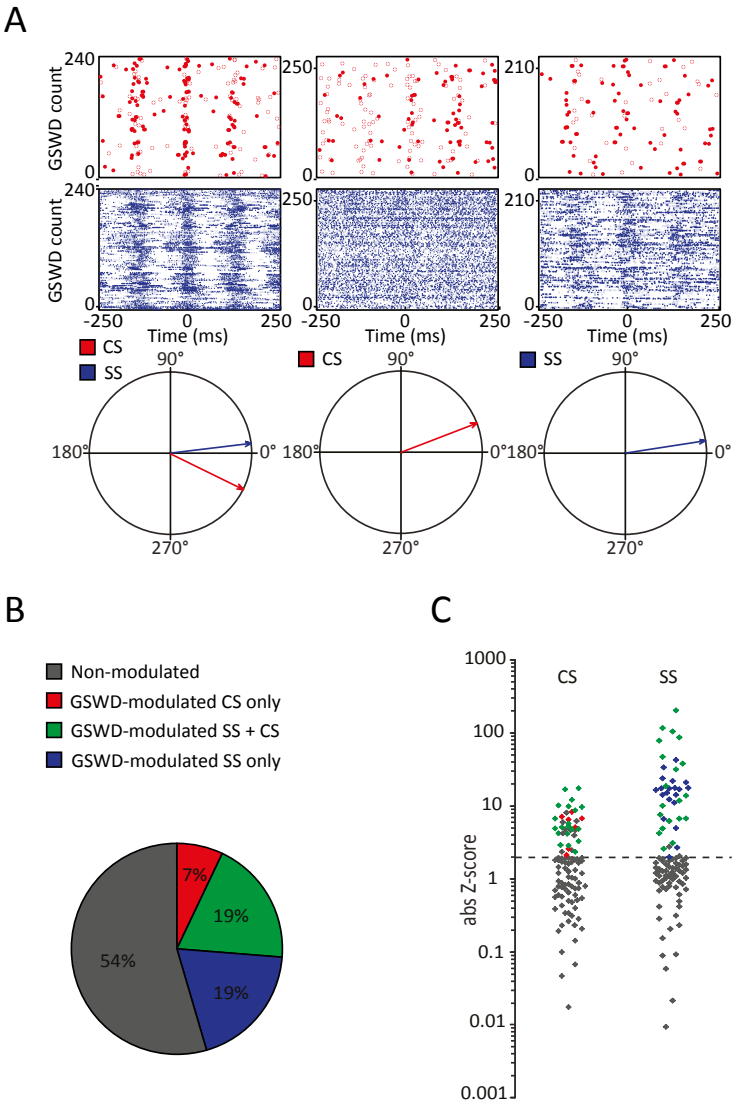

Figure 2. Co-occurrence of GSWD-modulated complex spike and simple spike firing.

(A) Examples of complex spike raster plots (red, top) simple spike raster plots (blue, middle) and compass phase plots (bottom) of Purkinje cells with GSWD-modulated complex spikes and simple spikes (left), GSWD-modulated complex spikes only (middle) and GSWD-modulated simple spike only (right). **(B)** Distribution of Purkinje cells showing GSWD-modulated complex spike firing only (red), GSWD-modulated simple spike firing only (blue), both simple spike and complex spike GSWD-modulated firing (green) and non-modulating (grey). **(C)** Distributions of FFT-based complex spike Z-scores (left) and modulation amplitude-based simple spike Z-scores (right) color coded according to the Purkinje cell distributions described in (B). Dashed line corresponds to the cut-off Z-score of 1.96 (p<0.05). Grey markers above this cut-off in the complex spike-based Z-score plot correspond to cells that showed significant modulation that was not in GSWD frequency range. Abbreviations: generalized spike and wave discharge (GSWD), complex spikes (CS), simple spikes (SS).

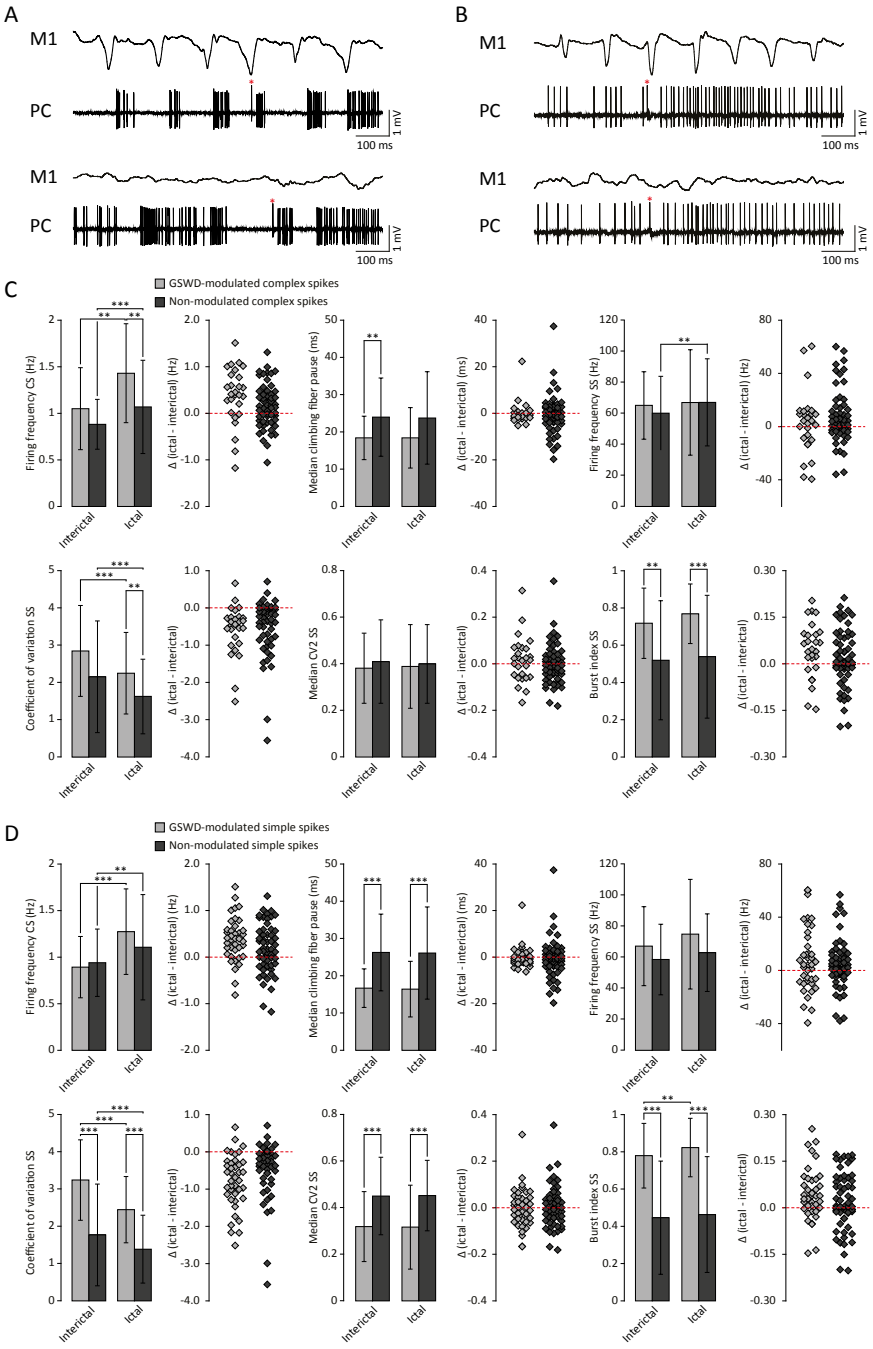

Figure 3. Differences in firing pattern parameters between GSWD-modulated and non-modulated Purkinje cells.

(A) Representative example of ictal (top) and interictal (bottom) spiking from a single Purkinje cell showing GSWD-related modulation. **(B)** As in (A), but for a non-modulated Purkinje cell. **(C)** Spiking parameters for Purkinje cells showing GSWD-modulated (n=27) and non-modulated (n=76) complex spike firing. $^{**}p<0.01$, $^{***}p<0.001$ (Online Table 1 and 2). Error bars denote mean ± SD. Scatterplots correspond to the bar plots and represent for each firing pattern parameter the difference between ictal and interictal conditions per cell (i.e. delta (ictal-interictal)). **(D)** As in (C), but for Purkinje cells that showed GSWD-modulated (n=40) and non-modulated (n=63) simple spike firing. $^{**}p<0.01$, $^{***}p<0.001$ (Online Table 3 and 4). Error bars denote mean ± SD. Abbreviations: Purkinje cell (PC) and primary motor cortex (M1).

When we assessed the location of GSWD-modulated and non-modulated Purkinje cells, we found that Purkinje cells that showed GSWD-modulated complex spikes are found more often in the lateral cerebellum (hemispheres) compared to the medial cerebellum (vermis) (Figs 4A and 4B). When looking at simple spike activity, this difference was even larger (Fig 4C). These data suggest that GSWD-modulated Purkinje cell firing patterns are more likely to be found in cerebellar hemispheres, possibly reflecting a cerebral cortical origin [79].

4.3.2 GSWD related Purkinje cell synchronicity: electrophysiology

The occurrence of robust GSWD related changes in complex spike activity suggests a potential inferior olivary role in seizures. We next aimed to further investigate how olivary firing is affected by thalamocortical network oscillations. Since each olivary neuron innervates ~7 Purkinje cells in the same sagittal plane and different parts of the inferior olive project to different cerebellar zones [95, 265, 273, 288, 289], simultaneously recorded activity from distant Purkinje cells can help elucidate the degree of synchronicity across different olivary zones. Additionally, given the extensive degree of convergence of Purkinje cell to cerebellar nuclei projections, not only the timing of Purkinje cell action potentials but also the synchronicity of the activity plays an important role in shaping cerebellar nuclei firing patterns. Therefore, assessing synchronicity of Purkinje cell activity by combining ECoG with multiple single-unit Purkinje cell recordings in awake *tottering* mice (Fig 5A, B) allowed us to both investigate GSWD related olivary activity and assess its potential contribution to oscillatory cerebellar output.

Cross-correlation analysis revealed no significantly increased interictal average complex spike synchronicity compared to a bootstrapped distribution (Fig 5C). This indicates that complex spikes recorded during interictal periods did not occur simultaneously. During ictal periods however, a significant cross-correlation was found with an average lag of 1.25 ± 24.75 ms (range -50 – 40 ms; n=8) (Fig 5D). These data indicate that there was no indication of increased average complex spike synchronicity during interictal periods, but that distant Purkinje cell pairs do tend to fire complex spikes synchronously during seizures. The degree

of synchronicity of electrophysiologically recorded Purkinje cell activity was not found to be preferentially dependent on relative distance on the mediolateral or the anteroposterior axis (data not shown). This suggests that distant inferior olive neurons show synchronous activity during seizures. Simultaneously occurring complex spikes are also likely to profoundly impact downstream cerebellar nuclei activity. Inducing synchrony in complex spike firing at a general scale has previously been shown to result in a pause followed by a burst of action potentials in cerebellar nuclei neurons [105] and given the high degree of ictal synchrony in Purkinje cell firing, this is also likely to contribute to the burst-like firing pattern of many cerebellar nuclei neurons during GSWD-episodes [46].

Cerebellar nuclei neuron firing has also been shown to be subject to simple spike synchronicity [83, 253, 276]. Whereas asynchronous simple spike activity has been shown to dampen cerebellar nuclei activity, increased synchronous simple spike firing entrained rather than inhibited cerebellar nuclei activity [83]. This would also be in line with the lack of phase difference between GSWD-related simple spike and cerebellar nuclei neuron firing. We therefore performed the same cross-correlation analyses on these Purkinje cell pairs to assess simple spike synchrony. Similar to complex spike firing, average simple spike synchronicity was only increased during GSWD-episodes but not during interictal periods (Fig 5E, F). Seven out of 17 (41%) individual pairs showed significantly correlated interictal simple spike firing, which increased to 13 out of 17 (76.5%) during ictal periods (Fig 5G). Analyses of the timing of the peak cross-correlation shows that during GSWDs, the peak lag is much closer to zero than during interictal periods ($p < 0.05$, Fig 5H, I). The peak amplitude also showed a significant difference between ictal and interictal periods; during GSWDs, the cross-correlation was significantly increased ($p < 0.05$, Fig 5J). The difference in lag between interictal and ictal periods, was not predictive of a difference in amplitude ($p = 0.405$, Fig 5K). Thus, the synchronicity and rhythmicity of Purkinje cell simple spike firing are stronger during ictal periods.

4.3.3 GSWD related Purkinje cell synchronicity: Ca^{2+}-imaging

Whereas the multiple-unit recordings described above can be used to assess interictal and ictal complex spike synchrony of Purkinje cells positioned in different zones or lobules, we did not assess activity patterns of adjacent Purkinje cells, which are much more likely to get climbing fiber input from clusters of coupled olivary neurons [81]. We therefore performed two-photon Ca^{2+}-imaging of awake *tottering* mice while simultaneously recording the ECoG (Fig 6A). Results from these imaging experiments showed a marked increase in both the frequency and synchronicity of Ca^{2+}-events (Fig 6B-H) in ictal periods when compared

to interictal activity. The increase in both frequency (p <0.001, Fig 6D, Online Table 6) and synchronicity (Fig 6F, H) confirmed our electrophysiological data (Fig 5). In these experiments we did, however, find significant complex spike cross-correlations during interictal periods (Fig 6E, G) occurring with a lag of approximately 0 ms (Fig 6I, J). In line with the data shown in Figure 4, ictal synchronicity in all Purkinje cell pairs was again significantly higher than that observed during interictal periods (p <0.001, Fig 6K, Online Table 6). Moreover, this increase in ictal compared to interictal synchronicity remained highly significant even in the subset of Purkinje cell pairs that showed a significant cross-correlation Z-score at a lag of 0 ms (p <0.001, Online Table 6). Synchronicity of Ca^{2+} events did not show a dependence on inter-dendritic distance during interictal periods ($t(1, 118)=0.077$, $R^2=0.00$, $p=0.939$) or ictal periods ($t(1, 118)=-1.105$, $R^2=0.010$, $p=0.271$) as tested with linear regression analyses. Additionally the difference between the interictal and ictal cross-correlation peaks does not show any distance dependency ($t(1, 118)=-0.669$, $R^2=0.004$, $p=0.505$).

4.4 Discussion

The inferior olive has been implicated to play a role in generalized epilepsy [279-281]. In the current study we aimed to investigate absence seizure related complex spike activity patterns with a particular focus on rhythmicity and synchronicity. Simultaneously recording activity in the cerebral cortex and the cerebellar cortex in awake, head-restrained homozygous *tottering* mice revealed pronounced GSWD-related changes in Purkinje cell firing. We show that complex spike and simple spike activity of a substantial subset of Purkinje cells is phase locked to GSWDs during seizures. Simultaneous recordings of ensembles of Purkinje cells, either by multiple single-unit recordings or Ca^{2+}-imaging, showed a significant increase in complex spike activity and synchronicity in both distant and adjacent cells during ictal events, indicating profound and widespread changes in olivary firing during absence seizures.

4.4.1 GSWD-related changes in olivary activity and synchronicity

Complex spike firing frequency, rhythmicity as well as synchronicity were all significantly increased during ictal episodes compared to inter-ictal periods, and the phase-locked complex spike rhythmicity was more prominent in the lateral than medial cerebellar cortex.

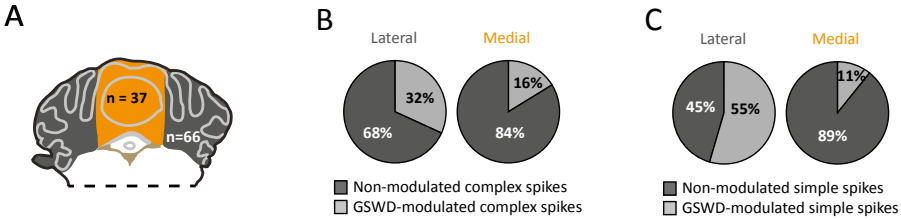

Figure 4. Purkinje cells showing GSWD-modulated complex spike firing are most prominently present in lateral parts.

(A) Schematic representation of lateral cerebellar area (grey) and the vermis (yellow). **(B, C)** Proportion of Purkinje cells showing GSWD-modulated complex spikes (B) or simple spikes (C) in lateral (left) or medial (right) cerebellar areas.

These differences suggest that the GSWD-related activity changes in the inferior olive are induced in the thalamocortical network, rather than the other way around (see also [34, 225]). The cerebral cortex projects to the principal olive (PO) and rostral medial accessory olive (rMAO) mainly via the mesodiencephalic junction [288]. The PO and rMAO in turn provide climbing fibers to the lateral, but not the medial, cerebellum [290]. If the inferior olivary cells would have induced or promoted the GSWDs in the thalamocortical network, because of the fact that the olivary cells also express the *Cacna1a* gene encoding the $Ca_V2.1$-channels [291], one would expect to also observe prominent complex spike rhythmicity and synchronicity phase-locked to GSWDs in the medial cerebellar cortex, which receives its climbing fiber inputs from the caudal MAO and caudal dorsal accessory olive. Moreover, if one looks carefully at the precise moment when the complex spikes during the GSWD-episodes start to occur (dashed line in bottom panel of Fig 1E), one can see that the vast majority (i.e. ~ 90%) of the complex spikes occurs after the start of the falling phase of the spike of the GSWD, which reflects the onset of cortical burst-firing [34]. Together, these data suggest that the increased rhythmicity and synchronicity are more likely to be the consequence rather than the cause of the GSWD.

One might also consider the possibility that the profound changes in olivary activity during seizures form a mechanism to compensate for the over-oscillating brain during seizures. Indeed, the capability of olivary neurons to dampen oscillations is supported by recent work in Dr. Sillitoe's lab [292], who showed that blocking olivary output increases rhythmicity in the motor output, precisely at the frequency (6-9 Hz) that can be optimally dampened by olivary activity [293-295]. Neurons in the inferior olive have unique properties to support such a function; their dendrites are electrically coupled by gap junctions and endowed with conductances that promote oscillations, together enhancing synchrony and

rhythmicity in complex spike firing when the system requires such modification [81, 249]. The concept of the inferior olive and olivocerebellar system as a compensator for potentially pathologicaloscillations is also in line with the finding that children with dentato-olivary dysplasia can suffer from intractable seizures [280, 281]. When the olivary oscillatory activity cannot be properly controlled anymore by the GABAergic feedback from the cerebellar nuclei [247, 288, 296, 297], compensatory effects could be ameliorated. Likewise, the threshold for pharmacologically induced seizures is reduced in rats following chemical ablation of the inferior olive [298-300], supporting the same mechanism.

4.4.2 GSWD-modulated Purkinje cell simple spikes

Much like their downstream targets [46] and in line with previous results in an inbred rat strain characterized with absence epilepsy ('WAG/Rij' strain) [104], about half of the recorded Purkinje cells showed an ictal simple spike firing pattern that was phase-locked to GSWDs. GSWD-modulated simple spike activity showed a similar phase-relation to GSWDs as cerebellar nuclei neurons; bursts of activity during the ECoG waves interspersed with pauses coinciding with ECoG spikes. In contrast, complex spike activity predominantly showed the inverse phase-relation. Simple spike and complex spike firing have been shown to often be reciprocally modulated; periodic decreases in simple spike firing often coincide with increases in complex spike firing and vice versa. This antiphasic temporal relation between complex spike and simple spike firing becomes most prominently evident during sensorimotor control [301-304], but may also explain the antiphasic relation in GSWD modulation.

The firing patterns of *tottering* Purkinje cells have been described in detail using both *in vitro* and *in vivo* recording techniques [231, 305]. One of the most pronounced aberrations is the increased irregularity of simple spike firing, which correlates to impaired motor behavior [305] and has been attributed to the decreased Ca^{2+}-influx and the subsequently decreased Ca^{2+}-dependent K^{+}-channel activity that disrupt the intrinsic pacemaking activity [231]. Our current analyses of ictal and interictal firing patterns confirmed the aberrant Purkinje cell firing pattern in awake *tottering* mice, but also showed that GSWD-modulated cells can be distinguished from non-modulated cells even by analyzing inter-ictal firing patterns. This is particularly noteworthy, since we previously showed that also the interictal activity pattern of cerebellar nuclei neurons was predictive for their firing pattern during GSWD-episodes [46]. Together these data suggest that different populations of cerebellar neurons may have a different level of susceptibility to be modulated by thalamocortical oscillations.

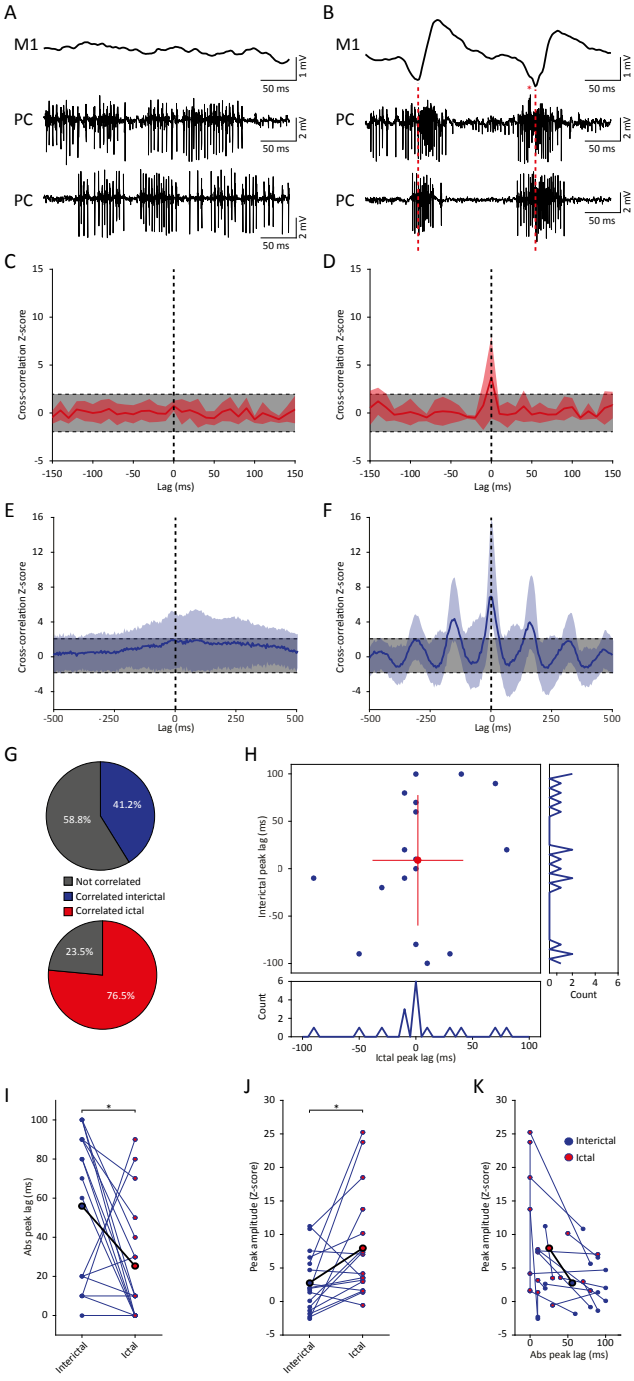

Figure 5. GSWD-related synchronicity in Purkinje cell complex spike and simple spike firing.

(A, B) Example of interictal, non-synchronous Purkinje cell firing (A) and ictal GSWD-modulated, synchronous activity (B) of two simultaneously recorded Purkinje cells. Red dashed lines indicate ECoG-spikes. **(C, D)** Average cross-correlation (red line) ± SD (shaded light red area) of complex spike firing of two cells during interictal periods (C) and GSWD episodes (D). Strength of the correlation is expressed in Z-scores with respect to the cross-correlations of a bootstrapped distribution (grey bar, 500 x; see material and methods section). The vertical, black dashed line depicts a lag of 0 ms. **(E, F)** As in (C, D), but the for average cross-correlation Z-scores ± SD (shaded light blue area) of simple spike firing. **(G)** Proportion of cell pairs that show a significant cross-correlation Z-score during interictal (blue, top graph) and ictal (red, bottom graph) periods. **(H)** Distribution of the peak lags in the individual cross-correlograms. Y-axis shows the interictal peak lag and the horizontal axis shows the ictal peak lag. PSTHs of interictal (right) and ictal (bottom) peak lags (bin size is 10 ms). **(I-J)** Differences in absolute peak lag (I) and peak amplitude (J) between interictal (blue dots) and ictal periods (red dots). Blue lines represent the individual cell pairs and the black line shows the average. *p<0.05 (Online table 5). **(K)** Combined differences in absolute peak lag and peak amplitude between interictal (blue dots) and ictal periods (red dots). (N=8, n=17 pairs). Abbreviations: Purkinje cell (PC) and primary motor cortex (M1).

4.4.3 Potential role of Purkinje cell activity in dampening ictal cerebellar nuclei oscillations

The cerebellar nuclei have been utilized to effectively stop seizure activity in mice [46] and men [12, 48, 49]. During GSWD-episodes, a substantial subset of cerebellar nuclei neurons has been shown to fire in burst-like GSWD-modulated patterns. Pharmacological or optogenetic manipulation of cerebellar nuclei neuronal firing can potently and bidirectionally affect seizure occurrence [46]. Cerebellar nuclei neurons receive input from climbing and mossy fiber collaterals as well as local interneurons, but the majority of their synaptic inputs originates from Purkinje cells [83, 302]. Although the impact of Purkinje cell firing and synchronicity has been addressed at both modeling and experimental level (for references see below), it remains to be elucidated how GSWD-modulated Purkinje cell activity and synchronicity precisely affect cerebellar nuclei neuron firing and thereby the cerebellar output during absence seizures.

Given the inhibitory effect of Purkinje cell activity on cerebellar nuclei neuronal firing [306, 307], one would expect an antiphasic relation between Purkinje cell and cerebellar nuclei activity. Yet such a reciprocal relation was only found with complex spike but not simple spike firing. Large scale synchronization of olivary activity has been shown to evoke a pause followed by increased firing in cerebellar nuclei neurons [105] resembling the pattern of bursts and pauses seen during GSWD-episodes. Although the characteristics of these rebound responses have been particularly well described [109, 267, 308-316], the existence of rebound responses in the cerebellar nuclei is however a heavily debated subject [81, 83, 105, 107, 111, 276, 277, 317-320]. Yet, the large scale synchronization of olivary neurons during these pathological network oscillations may resemble artificial olivary stimulation rather than the smaller scale synchronization associated with normal sensorimotor functions.

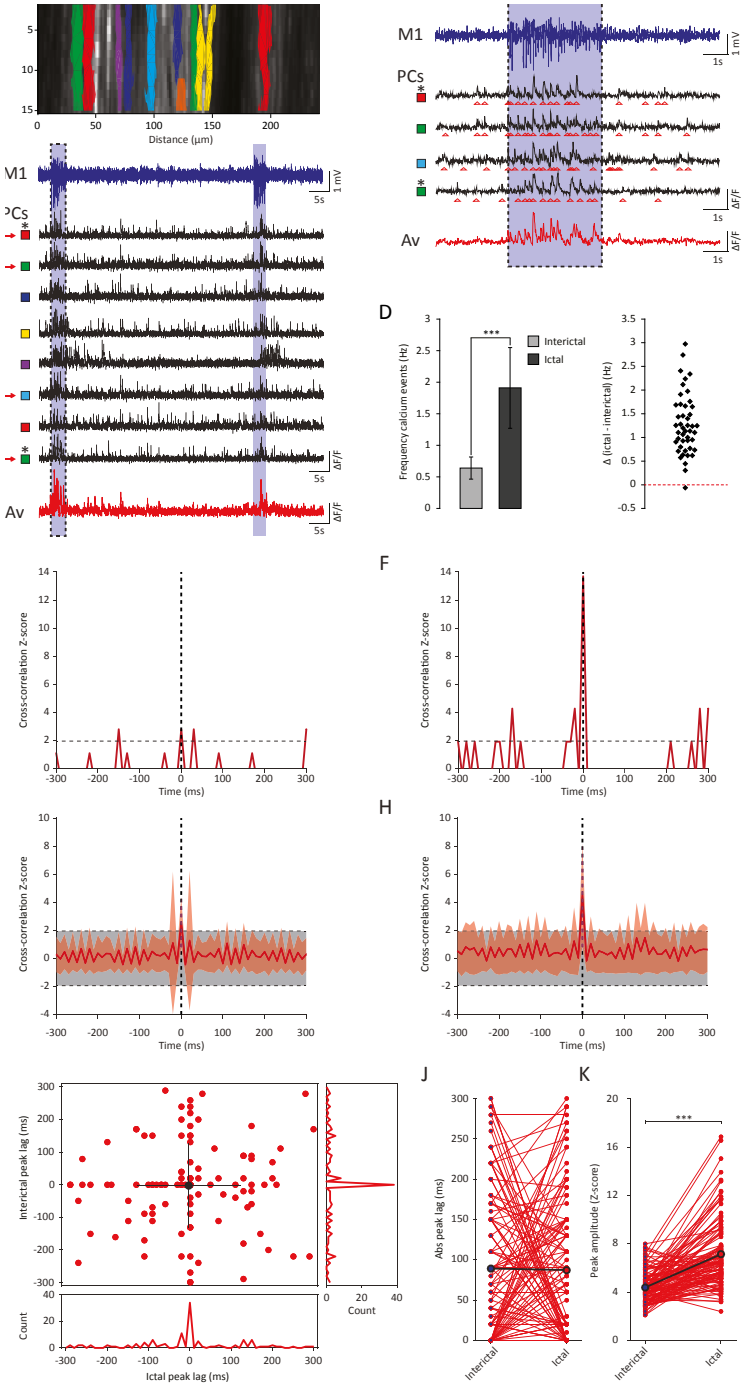

Figure 6. GSWD-related synchronicity of Ca^{2+}-events in adjacent Purkinje cells.

(A) Example of a window showing Purkinje cell dendrites and corresponding dendritic masks during two-photon Ca^{2+}-imaging. Note that the y-axis is magnified and differs from the x-axis in scale. **(B)** Representative example of ECoG (blue top trace) and fluorescent traces recorded from various Purkinje cell dendrites (black traces) during interictal and ictal (light blue shades) periods. The bottom red trace represents the average Ca^{2+}-signal of all black traces above. Colored squares next to the traces refer to the dendritic masks shown in (A). **(C)** Magnification of the boxed data in (B) (marked with red arrows). **(D)** Difference in frequency of Ca^{2+}-events of Purkinje cells (n=46) between interictal and ictal periods (left). Scatterplots correspond to the bar plots and represent for each parameter the difference between ictal and interictal conditions per cell. ***p<0.001 (Online Table 6). Error bars denote mean ± SD. **(E, F)** Example of a cross-correlogram of 2 Purkinje cells marked in B and C with asterisks during interictal (E) and ictal (F) periods. Strength of the correlation is expressed in Z-scores with respect to the cross-correlations of a bootstrapped distribution (horizontal black dashed line). The vertical black dashed line depicts a lag of 0 ms. **(G, H)** As in (E, F) but with the average cross-correlation Z-scores ± SD (shaded light red area) of the population (n=119 pairs). **(I)** Distribution of peak lags in the individual cross-correlograms. Y-axis shows the interictal peak lag and the horizontal axis shows the ictal peak lag. PSTHs of interictal (right) and ictal (bottom) peak lags. **(J-K)** Differences in absolute peak lag (J) and peak amplitude (K) between interictal (blue dots) and ictal periods (red dots). Red lines represent the individual cell pairs and the black the average. *p<0.001 (Online Table 6). Abbreviations: Purkinje cell (PC), primary motor cortex (M1) and average (Av).

Although recent evidence indicates that the direct olivary input to cerebellar nuclei neurons via climbing fiber collaterals provide considerable excitatory drive [251, 321] our data represented in Figure 1 indicate that during GSWDs the excitation from olivary axon collaterals would arrive mostly during the pause in cerebellar nuclei firing, further highlighting the importance of Purkinje cell firing in directing GSWD-related cerebellar activity.

Simple spike activity has also been shown to affect cerebellar nuclei activity in a synchrony-dependent manner; rather than suppressing cerebellar nuclei activity, as has been shown for asynchronous simple spike patterns, synchronous simple spike activity tends to entrain cerebellar nuclei neuron firing [83]. Additionally, the impact of mossy fiber collaterals on cerebellar nuclei activity has been shown to depend on the degree of synchrony of their Purkinje cell inputs with increased levels of excitation upon increased levels of Purkinje cell synchronicity [322]. We found that in a large subset of recorded Purkinje cell pairs, ictal simple spike synchronicity was significantly increased. This synchronicity likely explains the co-occurrence of bursts of simple spike activity and cerebellar nuclei activity. Given that the silencing of cerebellar nuclei firing results in a detrimental increase in GSWD occurrence [46], our current data on Purkinje cell firing implicate that not only complex spikes, but also simple spike firing could in principle dampen seizures by fine-regulating GSWD-modulated firing of cerebellar nuclei neurons.

Acknowledgements

The authors thank the members of the Hoebeek lab for constructive discussions. Elize Haasdijk, Erika Sabel-Goedknegt and Mandy Rutteman provided excellent technical assistance.

5

Cerebellar output controls generalized spike-and-wave discharge occurrence

Annals of Neurology 2015:

L. Kros *, O.H.J. Eelkman Rooda *, J.K. Spanke, P. Alva, M.N. van Dongen, A. Karapatis, E.A. Tolner, C. Strydis, N. Davey, B.H.J. Winkelman, M. Negrello, W.A. Serdijn, V. Steuber, A.M. J. M. van den Maagdenberg, C.I. De Zeeuw, and F.E. Hoebeek

*These authors contributed equally

Abstract

Objective: Disrupting thalamocortical activity patterns has proven to be a promising approach to stop generalized spike-and-wave discharges (GSWDs) characteristic of absence seizures. Here, we investigated to what extent modulation of neuronal firing in cerebellar nuclei (CN), which are anatomically in an advantageous position to disrupt cortical oscillations through their innervation of a wide variety of thalamic nuclei, is effective in controlling absence seizures.

Methods: Two unrelated mouse models of generalized absence seizures were used; the natural mutant *tottering*, which is characterized by a missense mutation in *Cacna1a*, and inbred *C3H/HeOuJ*. While simultaneously recording single CN neuron activity and electrocorticogram (ECoG) in awake animals, we investigated to what extent pharmacologically increased or decreased CN neuron activity could modulate GSWD occurrence and short-lasting on-demand CN stimulation could disrupt epileptic seizures.

Results: We found that a subset of CN neurons shows phase-locked oscillatory firing during GSWDs and that manipulating this activity modulates GSWD occurrence. Inhibiting CN neuron action potential firing by local application of the $GABA_A$-agonist muscimol increased GSWD occurrence up to 37-fold, whereas increasing the frequency and regularity of CN neuron firing with the use of gabazine decimated its occurrence. A single short-lasting (30-300 ms) optogenetic stimulation of CN neuron activity abruptly stopped GSWDs, even when applied unilaterally. Using a closed-loop system GSWDs were detected and stopped within 500 ms.

***Interpretation*:** CN neurons are potent modulators of pathological oscillations in thalamocortical network activity during absence seizures and their potential therapeutic benefit for controlling other types of generalized epilepsies should be evaluated.

5.1 Introduction

Absence epilepsy is one of the most prevalent forms of generalized epilepsy among children and is characterized by sudden periods of impaired consciousness and behavioral arrest [323, 324]. Like other types of generalized epilepsies, absence seizures are electrophysiologically defined by oscillatory activity in cerebral cortex and the thalamic complex [263]. Thalamocortical oscillations are primarily caused by excessive cortical activity and can be identified in the electrocorticogram (ECoG) as generalized spike-and-wave discharges (GSWDs) [96, 263]. The underlying excessive cortical activity not only excites thalamic neurons, but also provides potent bisynaptic inhibition by means of cortical axonal collaterals to the inhibitory reticular thalamic nucleus [86, 263, 325-327]. Excess tonic GABA-mediated inhibition in thalamus may also contribute to absence seizures [37, 263, 327]. Oscillatory cortical activity thereby poses a dual excitation-inhibition effect on thalamic neurons, which drives thalamocortical network oscillations [37, 325, 327, 328].

Recent studies in several rodent models indicate that direct stimulation of thalamic nuclei [126] or cerebral cortex [159] can be effective in disrupting thalamocortical oscillations and thereby stopping generalized oscillations in thalamocortical networks, such as GSWDs. Apart from direct interventions in thalamus and cortex, synaptic thalamic afferents can affect the balance in excitation and inhibition and thereby potentially mediate thalamocortical oscillations. One of the initial stimulation sites to prevent seizures in epileptic patients was the cerebellar cortex [47, 68, 69, 72, 73, 75, 329]. Yet, as shown in three controlled, blind studies [76-78], the impact of these cerebellar surface stimulations was highly variable and probably reflects irregularities in the converging inputs from superficial and deeper parts of the cerebellar cortex neurons in the cerebellar nuclei (CN) [81].

Given the considerable divergence of excitatory axonal projections from the cerebellar nuclei (CN) to a wide range of motor, associative and intralaminar thalamic nuclei [84, 86, 89, 91, 92, 96, 106, 330, 331], we considered this region an ideal candidate to effectively modulate thalamocortical oscillations. We hypothesized that altering the firing patterns of CN neurons should affect GSWD occurrence. To test this hypothesis we utilized homozygous *tottering* (*tg*) mice that frequently show absence seizures and harbor a P601L missense mutation in the *Cacna1a* gene that encodes the pore-forming α_{1A}-subunit of voltage-gated $Ca_V2.1$ Ca^{2+} channels [282, 283]. Once we established that *tg* CN neurons showed oscillatory action potential firing patterns comparable to that found in rat models for absence epilepsy [104], we assessed the effect of increasing or decreasing CN neuronal firing on GSWD occurrence by local pharmacological interventions using modulators of $GABA_A$-mediated neurotransmission. In addition, we generated a closed-loop detection

system for on-demand optogenetic stimulation to stimulate CN neurons with millisecond precision. Finally, to exclude the possibility that our design of intervention is tailored to the specific pathophysiology of *tg* mice we extended our key experiments to an unrelated mouse model for absence epilepsy; the *C3H/HeOuJ* inbred mouse line [332].

5.2 Materials and methods

All experiments were performed in accordance with the European Communities Council Directive. Protocols were reviewed and approved by local Dutch experimental animal committees (DEC).

5.2.1 Animals

Data were collected from 4- to 30-week-old homozygous and wild-type littermates of the natural mutant *tottering* (mouse symbol *tg*) mice and 8- to 10-week-old inbred *C3H/HeOuJ* mice. Male and female *tg* and wild-type littermates were bred using heterozygous parents. The colony, which was originally obtained from Jackson laboratory (Bar Harbor, ME, USA), was maintained in C57BL/6NHsd purchased from Harlan laboratories (Horst, Netherlands). Conformation of the presence of the *tg* mutation in the *Cacna1a* gene was obtained by PCR using 5′-TTCTGGGTACCAGATACAGG-3′ (forward) and 5′-AAGTGTCGAAGTTGGTGCGC-3′ (reverse) primers (Eurogentech, Seraing, Belgium) and subsequent digestion using restriction enzyme *NsbI* at the age of P9 - P12. Male inbred *C3H/HeOuJ* mice were purchased from Charles River Laboratories (Wilmington, MA, USA).

5.2.2 Experimental procedures

Surgery

Mice were anesthetized with isoflurane (4% in 0.5 L/min O_2 for induction and 1.5% in 0.5 L/min O_2 for maintenance). The skull was exposed, cleaned and treated with OptiBond All-In-One (Kerr Corporation; Orange, CA, USA) to ensure adhesion of a light-curing hybrid composite (Charisma; Heraeus Kulzer, Hanau, Germany) to the skull to form a pedestal. Subsequently, five 200-µm teflon-coated silver ball tip electrodes (Advent research materials, Eynsham, Oxford, UK) or five 1-mm stainless steel screws were subdurally implanted for cortical recordings by ECoG. Four of the electrodes were bilaterally positioned above the primary motor cortex (+1 mm AP; ± 1 mm ML relative to bregma) and primary sensory cortex (-1 mm AP; ± 3.5 mm ML). A fifth electrode was placed in the rostral portion of the

interparietal bone to serve as reference (-1 mm AP relative to lambda). The electrodes and their connectors were fixed to the skull and embedded in a pedestal composed of the hybrid composite or dental acrylic (Simplex Rapid; Associated Dental Products, Kemdent works, Purton, Wiltshire, UK). To enable optogenetic control of neuronal activity in CN, a subset of *tg* and *C3H/HeOuJ* mice received two small (~0.5 mm in diameter) craniotomies in the interparietal bone (-2 mm AP relative to lambda; ± 1.5-2 mm ML) to initially accommodate the injection pipette and later the optical fibers. CN were stereotactically injected bilaterally with 100-120 nL of the AAV2-hSyn-ChR2(H134R)-EYFP vector (kindly provided by Prof. K. Deisseroth (Stanford University) through the UNC vector core) at a rate of ~20 nL/min 3-6 weeks prior to recordings. To allow electrophysiological recordings from CN neurons, all mice received bilateral craniotomies (~2 mm diameter) in the occipital bone without disrupting the dura mater. Finally, a dental acrylic recording chamber (Simplex rapid) was constructed. The exposed tissue was covered with tetracycline-containing ointment (Terra-cortril; Pfizer, New York, NY, USA) and the recording chamber was sealed with bone wax (Ethicon, Somerville, NJ, USA). After surgery, the mice recovered for at least 5 days (or 3 weeks in case of virally-injected mice) in their home cage and were allowed two ~3-hr sessions on consecutive days during which the mice were left undisturbed to accommodate to the setup.

Electrophysiological recordings

During the accommodation session the animals' motor behavior was visually inspected for behavioral correlates of the oscillatory cortical activity during episodes of generalized spike-and-wave-discharges (GSWDs). No consistent patterns of movement were identified during such epileptic activity, as described before in *tg* and other rodent models of absence epilepsy [104, 283, 333]. Recordings were performed in awake, head-fixed animals, lasted no longer than 4 consecutive hours and were performed during various times of day. No consistent pattern was identified in ECoG frequency spectra with respect to the day-night cycle [334]. While being head-restrained, mice were able to move all limbs freely. Body temperature was supported using a homeothermic pad (FHC, Bowdoin, ME, USA). For extracellular single unit recordings, custom-made, borosilicate glass capillaries (OD 1.5 mm, ID 0.86 mm; resistance 8-12 MΩ; taper length ~8 mm; tip diameter ~1 µm) (Harvard Apparatus, Holliston, MA, USA) filled with 2 M NaCl were positioned stereotactically using an electronic pipette holder (SM7; Luigs & Neumann, Ratingen, Germany). CN were localized by stereotactic location as well as the characteristic sound and density of neuronal activity [105]. To record from medial CN (MCN), electrodes were advanced

through vermal lobules 6-7 with 0° jaw angle relative to the inter-aural axis to a depth of 1.6-2.4 mm. To record from interposed nuclei (IN), electrodes were advanced through the paravermal or hemispheric part of lobules 6-7 using a yaw angle of ~10° relative to the inter-aural axis to a depth of 1.8-2.7 mm. To record from lateral CN (LCN), electrodes were advanced through the paravermal or hemispheric part of lobules 6-7 using a yaw angle of ~25° relative to the inter-aural axis to a depth of 2.7-4 mm. A subset of electrophysiological recording sites was identifiable following Evans blue injections (see below) and confirmed the accuracy of our localization technique. ECoGs were filtered online using a 1-100 Hz band pass filter and a 50 Hz notch filter. Single-unit extracellular recordings and ECoGs were simultaneously sampled at 20 kHz (Digidata 1322A, Molecular Devices LLC., Axon Instruments, Sunnyvale, CA, USA), amplified, and stored for off-line analysis (CyberAmp & Multiclamp 700A, Molecular Devices LLC.).

Pharmacological modulation of CN neuronal action potential firing

In order to bilaterally target the CN for pharmacological intervention, their location was first determined as described above, after which we recorded one hour of 'baseline' ECoG. Next, a borosilicate glass capillary (Harvard Apparatus; tip diameter of ~5 μm) filled with either one of the following mixtures replaced the recording pipette to allow high spatial accuracy of the injection: to decrease CN neuronal action potential firing, we applied 0.5% muscimol ($GABA_A$-agonist; Tocris) dissolved in 1 M NaCl (Sigma-Aldrich); to increase CN neuronal action potential firing, we applied 100 μM gabazine ($GABA_A$-antagonist; Tocris) dissolved in 1 M NaCl; or 1 M NaCl for sham injections. The solution was bilaterally administered to CN by pressure injections of ~150 nL at a rate of ~50 nL/min following which one hour of post-injection ECoG was recorded. As an additional control, similarly-sized injections of saline with either gabazine or muscimol were administered to lobule 6 and 7 and Crus I and Crus II of the cerebellar cortex. The drugs were injected superficially (0.7-1 mm from the surface) to avoid spread to the CN. The locations of the injections were identified with the use of electrophysiological recordings and stereotactic coordinates and most (19 out of 26) CN injections were histologically confirmed using the fluorescence of Evans blue (1% in 1 M saline; **Fig. S1**) [335]. To verify the effects of muscimol, gabazine, and vehicle, we recorded extracellular activity in the injected area during 20-50 min after the injections. Immediately after acquiring the post-injection ECoG an overdose of sodium-pentobarbital (0.15 mL *i.p.*) was administered allowing transcardial perfusion (0.9% NaCl followed by 4% paraformaldehyde in 0.1 M phosphate buffer (PB); pH=7.4) to preserve the tissue for histological verification of the injections.

Optogenetic stimulation of CN neurons

Optic fibres (200 µm inner diameter; 0.39 NA) were placed ~200 µm from the injection site and connected to 470-nm or 590-nm LEDs, or ~200 µm above the brain, *i.e.,* 'wrong location'. Light intensity at the tip of the implantable fibre was 550 ± 50 µW/mm^2 (measured after each experiment). Activation of LEDs by a single 30 - 300 ms pulse was triggered manually ('open-loop') or by a closed-loop detection system (as described below). In each mouse, 4 stimulation protocols were used: 1) bilateral stimulation (470 nm) 2) unilateral stimulation (470 nm); 3) bilateral stimulation (590 nm); and 4) bilateral stimulation (470 nm) with optical fibres outside of the CN (to exclude potential effects of visual input on the GSWD occurrence – see refs [104, 283]). All hardware used for optogenetic stimulation was purchased from ThorLabs (Newton, NJ, USA). After the last experimental session, animals were sedated and perfused (as described above) to preserve tissue for histological verification of ChR2 expression.

Immunofluorescence

After perfusion, the cerebellum was removed and post-fixed in 4% paraformaldehyde in 0.1 M PB for 1.5 hr, placed in 10% sucrose in 0.1 M PB at 4°C overnight, and subsequently embedded in gelatine in 30% sucrose (in 0.1 M PB). Embedded brains were post-fixed for 2.5-3 hr in 30% sucrose and 10% formaldehyde (in MilliQ) and placed overnight in 30% sucrose (in 0.1 M PB) at 4°C. Forty-µm thick transversal slices were serially collected for immunofluorescent DAPI staining. To confirm correct localization of the injections fluorescence was assessed using images captured using a confocal laser scanning microscope (LSM 700, Zeiss, Lambrecht, Germany) at 555 nm (Evans blue), 405 nm (DAPI) and 488-527 nm (GFP/YFP range) and optimized for contrast and brightness manually using Zen 2009 software (Zeiss). The fluorescent images in Figures 2 and 3 were captured using a tile-scan function of the Zen software with a 10X objective and have been optimized for representation using Adobe Illustrator (creative suite 6).

5.2.3 Data analyses

Offline GSWD detection

In order to accurately determine start and end of absence GSWDs and the locations of ECoG 'spikes' (negative ECoG peaks during episodes of GSWDs), a custom-written GSWD detection algorithm (LabVIEW, National Instruments, Austin, TX, USA) was used. In short, we detected those time points in the ECoG for which the first derivative of the filtered ECoG traces (3rd order Butterworth 1 Hz high-pass) changed polarity. The amplitude differences between each point and both its neighbors were summed in order to detect fast, continuous

amplitude changes and potential GSWDs with a manually set amplitude threshold. Series of GSWDs were marked when: 1) five threshold-exceeding points appeared within 1 s; and 2) each of the intervals between the points was < 300 ms. Furthermore, we separated GSWDs by applying the following four rules: 1) a point is the first spike of a GSWD-episode if there are no other spikes in the previous 300 ms; 2) a point is the last spike of a GSWD-episode if there are no other spikes in the next 350 ms; 3) the inter-GSWD-episode interval is ≥ 1 s; and 4) the minimal GSWD duration is 1 s.

GSWD definition

An ictal period is defined to start at the first ECoG spike of a GSWD and end at the last ECoG spike. Unless stated otherwise SWDs that lasted > 1 s and appeared in both M1 and S1 were considered GSWD. An interictal period is defined as the time in between GSWDs starting 2 s after one GSWD and ending 2 s before the next GSWD.

Detection of action potentials in extracellular recordings

Extracellular recordings were included if activity was well-isolated and held stable for > 100 s. Action potential detection in extracellular traces was performed using threshold based analyses with customized Matlab (Mathworks Inc. Natick, MA, USA) routines incorporating principal component analysis of the spike waveform or with the Matlab-based program SpikeTrain (Neurasmus BV, Erasmus MC Holding, Rotterdam, Netherlands).

GSWD-related firing pattern modulation

A custom-written algorithm in LabVIEW (National Instruments) was used to assess whether CN neurons showed GSWD-modulated firing patterns during GSWDs in the ECoG of the contralateral primary sensory cortex (in case of medial CN neurons) or primary motor cortex (in case of interposed or lateral CN neurons). The minimum total duration per episode was set at 2 s to construct GSWD-triggered rasterplots and peri-GSWD-time-histograms (PSTH) with a 5-ms bin width, which allowed us to determine: 1) modulation amplitude: the amplitude difference between the peak and trough near t = 0; 2) modulation frequency: frequency of the sine wave that fits the PSTH best; and 3) mean power at GSWD frequency: a Fast Fourier Transform between 6 and 9 Hz (GSWD frequency range). Next, the interspike intervals (ISIs) used for this PSTH were randomly shuffled 500 times and converted into a new PSTH with the same bin size to create normal distributions of modulation amplitude and mean power at GSWD frequency. Z-scores could now be calculated for the real and shuffled data by applying: $Z = (X-\mu)/\sigma$ where

X = the value based on the original PSTH, μ = the mean of the bootstrapped normal distribution and σ = its standard deviation. Cells were identified as GSWD-modulated if: 1) the modulation amplitude should be significantly higher than expected by chance ($Z \geq 1.96$, $p \leq 0.05$); 2) the cell should modulate at GSWD frequency (6-9 Hz); and 3) The mean power at GSWD frequency should be significantly higher than expected by chance ($Z \geq 1.96$, $p \leq 0.05$). Since all CN neurons that showed significant Z-scores of mean power at GSWD frequency also showed significantly higher modulation amplitudes; the former was used for further analyses. The term Z-score refers to mean power at GSWD frequency unless stated otherwise.

Coherence

To determine the spectral coherence between the activity of a CN neuron and the ECoG signal during GSWDs, a custom-written Matlab (Mathworks) routine was used. The extracellular signal was time-binned at 1-ms precision, convolved with a sinc(x)-kernel (cut-off frequency = 50 Hz) and down-sampled to 290 Hz. The ECoG signal was directly down-sampled to 290 Hz. The magnitude squared coherence was calculated per GSWD episode using Welch's averaged, modified periodogram method and is defined as: $C_{xy}(f)=|P_{xy}(f)|^2/P_{xx}(f)*P_{yy}(f)$ with the following parameters: window = 290 (Hamming), noverlap = 75%, nfft = 290, sampling frequency = 290 (due to the window size only GSWDs > 1.5 s were considered). The coherence value per GSWD was defined as the maximum coherence in the 6-9 Hz frequency band; a weighted average per cell based on GSWD duration was used.

Firing pattern parameters

Firing patterns parameters were assessed using custom written LabVIEW (National Instruments) based programs calculating firing frequency, coefficient of variation (CV) of inter-spike intervals (ISIs) = σ_{ISI}/μ_{ISI}, $CV2 = 2|ISI_{n+1} - ISI_n|/(ISI_{n+1} + ISI_n)$ and burst index = number of action potentials within bursts / total number of action potentials in a recording, where a burst is defined as ≥ 3 consecutive action potentials with an ISI ≤ 10 ms. CV reports regularity of firing throughout the whole recording and CV2 quantifies the regularity of firing on a spike-to-spike basis [287]. Firing pattern parameters were specifically calculated for ictal and interictal periods.

Regression analyses of inter-ictal CN activity

To evaluate whether there is a type of CN neuron that is predisposed for ictal phase-locking during GSWDs, we analyzed the neurons' interictal activity using a custom-made Matlab routine (Mathworks), aiming to probe the predictability of the ictal activity. We used Gaussian process regression [336], which is considered to be one of the best non-linear regression methods, to determine if the GSWD modulation of the activity was predictable from the interictal activity of the neurons. The measures that enabled the prediction of the modulation amplitude most accurately were CV, log-interval entropy, firing frequency and permutation entropy. The interictal parts of the extracellular recordings were divided into 1-s bins. To calculate the log-interval entropy, in which entropy measures the predictability of a system, first a natural logarithm of the intervals, in milliseconds, was taken to construct a histogram with a bin width of 0.02 log_e (time). Further, a Gaussian convolution was performed using a kernel of one-sixth SD of the *log*(ISIs). The entropy of the ISI histogram $p(I_i)$ was calculated by:

$$\mathrm{Ent(I)} = -\sum_{i=1}^{N} p(I_i)\log_2 p(I_i)$$

Furthermore, we analyzed the permutation entropy, which is calculated as the predictability of the order of neighboring ISIs rather than the actual values of the ISIs [337].

Normalized GSWD occurrence and duration

GSWDs were detected using the off-line ECoG detection algorithm described above. Total number of GSWDs and average GSWD duration were calculated and normalized to baseline values.

Assessment of cellular responses to optogenetic stimulation

Action potentials were detected as described above. A custom-written LabVIEW (National Instruments) program was used to construct light-triggered rasterplots and peri-stimulus-time-histograms with a 5-ms bin width. Changes in CN neuronal firing rate upon optical stimulation were subsequently determined by calculating the total number of action potentials during light pulses divided by the total length of the pulse and compared with the baseline firing rate (calculated from the total recording time excluding the optogenetic stimulation). In the current study we consider differences in action potential firing rate exceeding 25% as responsive.

Assessment of impact of optogenetic stimulation of cerebellar output on GSWDs

The start and end of seizures were identified using the off-line GSWD detection method described above. A custom-written LabVIEW (National Instruments) program was used to assess the effectiveness of optogenetic stimulation in stopping GSWDs. Only light pulses triggered prior to the natural end of the seizure were used for analysis. The time difference between the light pulse and the end of the seizure was calculated. The seizure was considered 'stopped by the optogenetic stimulation' when this time difference did not exceed 150 ms. Mean power at GSWD frequency (6-9 Hz) was calculated using a Fast Fourier Transform of the ECoG signal recorded during 1-s or 0.5-s (in case of closed-loop optogenetic stimulation) time periods before and after the light pulse. Averaged responses to light pulses are represented per animal and per stimulus condition by averaging complex Morlet wavelets of 4-s windows ranging from 2 s before to 2 s after the stimulus.

Assessment of onset of optical cerebellar nuclei stimulation in relation to GSWD cycle

The time difference between the onset of stimulation and the last spike before stimulation was calculated and divided by the median length of one GSWD during that episode, representing one cycle of 360 degrees. The outcome was subsequently multiplied by 360. Note that the optogenetic stimuli were not initiated with a fixed delay after the occurrence of an ECoG-spike; the delay depended on the visual interpretation and reaction speed of the experimenter (for manual activation of the LED) or on the closed-loop detection system for which the delay depends on the variability of the ECoG directly prior to the GSWDs (see below and ref [158]).

Closed-loop GSWD detection

The GSWD detection system has been implemented using a real-time, digital wavelet-filter setup. The analog filter used for digitization has four functions: 1) amplification; 2) offset injection in order to match the signal to the input range of the Analog to Digital Converter (ADC); 3) artefact removal by using a second-order 0.4 Hz high-pass filter; and 4) anti-aliasing by means of a second-order 23.4 Hz low-pass filter. The filter is realized using discrete components on a prototype printed circuit board (PCB). Following the PCB the wavelet filter functionality is implemented on a TI Sitara AM335x ARM® microprocessor (Texas Instruments Inc. Dallas, TX, USA). It first digitizes the signal from the analog filter with its integrated ADC using a sampling frequency (fs) of 100 Hz. Subsequently the signal is filtered using a wavelet filter and the GSWD episode is detected using signal thresholding. Upon detection an output LED is switched on to stimulate the target area in the cerebellum.

Wavelet filters have previously been successfully applied for real-time GSWD detection [338]. Here we applied a complex Morlet wavelet at 6.7 Hz that resembled a GSWD. The wavelet filter was implemented as a Finite-Impulse-Response (FIR) filter by truncating the ideal complex Morlet as described earlier [339]. Using the two thresholds that are set manually during a recording session, the GSWDs are detected during a positive, high-threshold crossing and the detection is ended upon a negative, low-threshold crossing.

5.2.4 Statistical analyses

Statistical differences in firing pattern parameters between independent groups of CN neuronal recordings (*e.g.,* from *tg* mice, their wild-type littermates, GSWD-modulated and -non-modulated, pre- and post-gabazine injection) were determined using MANOVA's with firing frequency, CV, CV2 and burst index as dependent variables and group as independent variable. When a MANOVA showed a significant result, post-hoc ANOVA's were used to assess contributions of individual firing pattern parameters with Bonferroni corrected *p*-values.

Differences in coherence value between GWSD-modulated and -non-modulated cells were assessed using unpaired samples *t* tests. Cochran & Cox adjustment for the standard error of the estimate and the Satterthwaite adjustment for the degrees of freedom were used since equality of variances was not assumed.

Differences in normalized number of GSWD episodes and their duration between traces pre- and post-injection of either muscimol, gabazine or saline were tested by using non-parametric Friedman ANOVA's with one 'within-subjects' factor (*i.e.,* time period) with 2 levels (baseline and post injection).

Differences in mean power at 6-9 Hz before and after a light pulse were tested using values from all individual pulses by use of repeated measures ANCOVA's with one 'within-subjects' factor (*i.e.,* period) with 2 levels (pre and post light pulse) and 'mouse number' added as covariate to correct for variance in the within subjects factor explained by variance between mice. To test whether the time difference between the last ECoG-spike before optogenetic stimulation and the subsequent one deviates from the median interval between two ECoG-spikes in 'stopped seizures' a similar statistical approach was used. A repeated measures ANCOVA was used with one within subjects' factor with 2 levels, both time ECoG-spike intervals. Mouse number was again added as covariate. Since the number of seizures not terminated by the optogenetic stimulation was low, a non-parametric Friedman ANOVA was used to test the same difference.

To determine whether the phase angle of the optogenetic stimulation onset was related to the success rate of stopping GSWDs we compared the phase angle distribution of successful attempts to that of the unsuccessful attempts. We tested for significant differences between these distributions using the non-parametric 2-sample Kuiper test.

A p-value ≤ 0.05 (α) was considered significant unless Bonferroni correction was used; in that case a p-value of α/n was considered significant. Two-tailed testing was used for all statistical analyses and all were performed using SPSS 20.0 software (IBM Corporation, New York, NY, USA). Exact information and outcomes regarding statistical testing are depicted in **Online Tables 1-7**.

5.3 Results

5.3.1 GSWD related CN neuronal activity

We first investigated whether CN neuronal activity and ECoG were correlated during spontaneous episodes of GSWDs in awake head-fixed homozygous *tg* mice (**Fig. 1A**). We found no significant differences in GSWD occurrence ($t(24) = -0.002$, $p = 0.998$) and GSWD duration ($t(24) = 0.195$, $p = 0.847$) between male and female *tg* mice, which is in line with data from other experimental animal models of absence epilepsy (reviewed by [340]). Therefore, we grouped data of both genders. GSWDs appeared simultaneously in bilateral primary motor (M1) and sensory cortices (S1) at 7.6 ± 0.6 Hz with an average duration of 3.6 ± 1.4s ($N = 17$ mice; **Fig. 1B**). The GSWD frequency and appearance were comparable to earlier reports of awake *tg* and other rodent models of absence epilepsy [104, 283, 333, 341]. During these GSWDs, action potential firing of a subset of CN neurons was phase-locked to GSWDs. A typical GSWD-modulated CN neuron showed oscillatory action potential firing at GSWD frequency; repetitive firing was observed during the wave in the ECoG whereas the spike was accompanied by a pause in CN neuronal activity (**Fig. 1C-E**). These GSWD-modulated CN neurons showed significantly increased coherence with ECoG during seizures ($p \leq 0.001$; **Online Table 1**). In each CN (MCN, IN and LCN) a substantial portion of the recorded CN neurons showed GSWD-modulated firing, with the highest percentage (73%; 49 out of 67 neurons) in the IN and 35% (35 out of 100 neurons) and 44% (19 out of 43 neurons) in the MCN and LCN respectively. We found no statistical difference ($p = 0.512$) in the phase of modulation of neuronal firing relative to the GSWD cycle for these three nuclei (**Fig. 1D, F**).

To assess whether GSWD-modulated CN neurons differed from non-modulating CN neurons in baseline activity, we compared their interictal firing patterns. During interictal periods GSWD-modulated CN neurons showed a higher firing frequency and a more

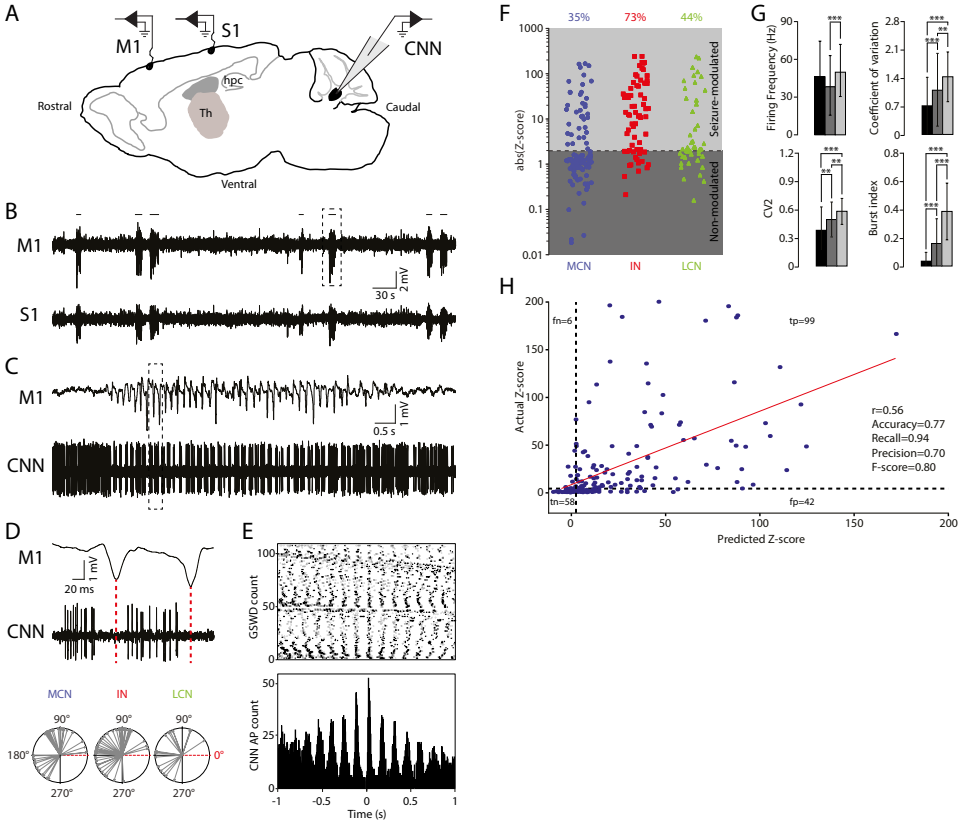

Figure 1. CN neuronal action potential firing patterns are modulated during GSWDs.

(**A**) Schematic of recording sites for ECoG from primary motor (M1) and sensory (S1) cortices and extracellular single-unit CN neuronal (CNN) recordings (Th = thalamus, Hpc = hippocampus). (**B**) ECoG from M1 and S1 with GSWD episodes (horizontal lines), indicating absence seizures. (**C**) Zoom of M1 episode outlined in panel B and simultaneously recorded action potential firing of a single CN neuron. (**D**) (top panel) Zoom of outlined M1 and CN neuronal recording in panel C. Red line aligns ECoG spike with pause in CN neuronal action potential firing. (bottom panel) Compass plot of phase difference between ECoG spike and modulated CN neuronal action potential firing. (**E**) Rasterplot and accompanying peri-SWD-time-histogram of CN neuronal action potentials (AP) for three consecutive seizures (t = 0 is aligned with each ECoG spike). (**F**) Distribution of absolute Z-scores of mean power at GSWD frequency as determined by FFT for medial CN (MCN) interposed nuclei (IN) and lateral CN (LCN). Note that none of the negative Z-scores was below -1.96 and therefore showing absolute Z-scores does not change the number of data points below and above the 1.96 cut-off score (corresponding to $p < 0.05$; horizontal dashed line). Total number recorded neurons: MCN $n = 100$; IN $n = 67$; LCN $n = 43$. (**G**) Barplots representing firing frequency, coefficient of variation, coefficient of variation 2 (CV2) and burst index for CN neurons recorded in wild-type littermate ($n = 94$; black) and seizure-modulated ($n = 103$; light grey) and non-modulated CN neurons recorded in *tg* ($n = 107$; dark grey). For clarity, we truncated the negative error bars. $^{**}p < 0.01$, $^{***}p < 0.001$ (MANOVA, post-hoc ANOVA's with Bonferroni correction; see **Online Table 1**). (**H**) Result of the Gaussian process regression to predict the Z-score from interictal activity parameters (CV, firing frequency, log-interval entropy and permutation entropy) represented as a confusion matrix. The prediction is characterized as being a true positive (tp) when the predicted Z-score > 1.96 (dotted line) and the actual Z-score > 1.96. A true negative (tn) is scored when both predicted and actual Z-scores < 1.96. False positive (fp) and false negative (fn)

refer to neurons which have been incorrectly predicted as "GSWD-modulated" and "GSWD-non-modulated", respectively. Note that we were able to achieve a precision of 0.70 and a recall of 0.94 which means that 70% of CN neurons (n = 210) that were predicted as "GSWD-modulated" were actually "GSWD-modulated" and 94% of all GSWD-modulated neurons has been identified correctly by the model. The Pearson correlation coefficient (r) between the predicted Z-score and the actual Z-score was 0.56 with $p \leq 0.05$. $^{**}p < 0.01$, $^{***}p < 0.001$.

irregular, burst-like firing pattern compared with non-modulated neurons (p-values < 0.01) and both modulated and non-modulated groups showed a more irregular firing pattern and increased burst index compared to CN neurons recorded from wild-type littermates (p-values < 0.01; **Fig. 1G**; **Online Table 1**). Gaussian process regression [336] revealed that in *tg* mice interictal CN neuronal firing was correlated to the ictal firing pattern: 94% of neurons that phase-locked their activity to GSWDs could be predicted correctly, based on their interictal firing pattern (**Fig. 1H**). These data indicate that a large subset of neurons within each CN consistently shows seizure-modulated activity, *i.e.,* that these GSWD-modulated CN neurons are different from non-modulated neurons in basic, interictal firing patterns and that GSWD-related modulation can be predicted based on these interictal firing patterns.

Impact on GSWD occurrence of pharmacological interventions that modulate CN action potential firing

CN neurons provide excitatory input to thalamic neurons [84, 86, 89, 91, 92, 96, 106, 330, 331] and thereby potentially contribute to the excitation-inhibition balance that sets thalamic activity patterns. Excess tonic inhibition of thalamic activity has been linked to the occurrence of absence seizures [37, 263, 327] and therefore we hypothesized that a decrease in CN output in *tg* should increase the occurrence of GSWDs, whereas increased CN output should have the opposite effect. To test this, we locally applied (**Fig. 2A**, **Fig. S1**) either $GABA_A$-agonist muscimol, which stopped CN neuronal action potential firing (**Fig. 2B**) (no statistical comparison was possible due to complete cessation of action potential firing), or $GABA_A$-antagonist gabazine (SR-95531), which consistently increased the frequency ($p < 0.01$) and regularity of CN neuronal firing ($p < 0.001$; **Fig. 2B, C**; **Online Table 2**). Upon bilateral CN injections with muscimol the occurrence of GSWDs increased by 160-3700% post-injection ($p < 0.01$; recorded for 60 min; peak of seizure occurrence 34.5 ± 16.5 min after injection; N = 10; **Fig. 2D-F; Online Table 2**). In contrast, bilateral CN injections with gabazine significantly reduced the occurrence of GSWDs ($p < 0.05$; first seizure occurred 32.5 ± 17.4 min after injection; N = 10) and bilateral sham injections did not change GSWD occurrence (p = 0.18) (**Fig. 2D-F, H**; **Online Table 2**). The duration of

GSWDs was not significantly changed following muscimol, gabazine or saline injections in the CN (muscimol: $p = 0.21$; gabazine: $p = 0.32$; saline: $p = 0.41$; **Fig. 2G**; **Online Table 2**). As a control, we also injected similar quantities of gabazine or muscimol into the cerebellar cortex; this had no significant effect on the GSWD occurrence ($p = 0.66$ and 0.32 respectively) or duration ($p = 0.66$ for both gabazine and muscimol injections) (**Fig. 2H; Online Table 2**). Thus, pharmacological manipulation of neuronal activity in the CN, but not the cerebellar cortex, is highly effective in modulating the occurrence of GSWDs in *tg* mice.

Notably, we observed that muscimol and gabazine were most effective when the injections were in the IN and/or LCN (no statistical difference in impact on GSWD-occurrence after IN and/or LCN injections ($p = 0.70$; Mann Whitey *U* test) compared to injections in the MCN ($p = 0.07$ for muscimol and $p < 0.05$ for gabazine; **Fig. 2F, G**; **Fig. S1; Online Table 3**). To study whether these differences in impact of pharmacological interventions aimed at the MCN or the IN and LCN were due to a variable effect on neuronal activity we also performed single-unit recordings in the injected CN. Regardless of the injected nucleus, muscimol effectively silenced all action potential firing and gabazine consistently increased the firing frequency and the regularity of action potential firing (all p-values < 0.01 for firing frequency, coefficient of variation and CV2; **Online Table 4**). These findings indicate that although effects of muscimol and gabazine on the neuronal activity were similar throughout all CN, the effect of manipulating activity in the IN and LCN seems to exert a larger impact on GSWD-occurrence in the mutants than targeting the MCN. Instead, pharmacological interventions in the CN of wild-type littermates ($N = 2$) did not evoke GSWD-episodes (data not shown).

Although it has been shown that pharmacological interventions can have sex-specific differences in animal models of epilepsy [342] that may contribute to the variability of the current results, our ECoG recordings did not show a trend towards a sex-specific impact of CN-specific muscimol or gabazine application (**Fig. 2F-H**). This finding was corroborated by the finding that muscimol was equally effective in stopping CN action potential firing in both male and female mice. Together, these effects indicate that in the *tg* animal model of absence epilepsy CN output forms an integral component of the neuronal networks involved in generalized epilepsy and may operate as a potent modulator of GSWD occurrence, irrespective of the gender.

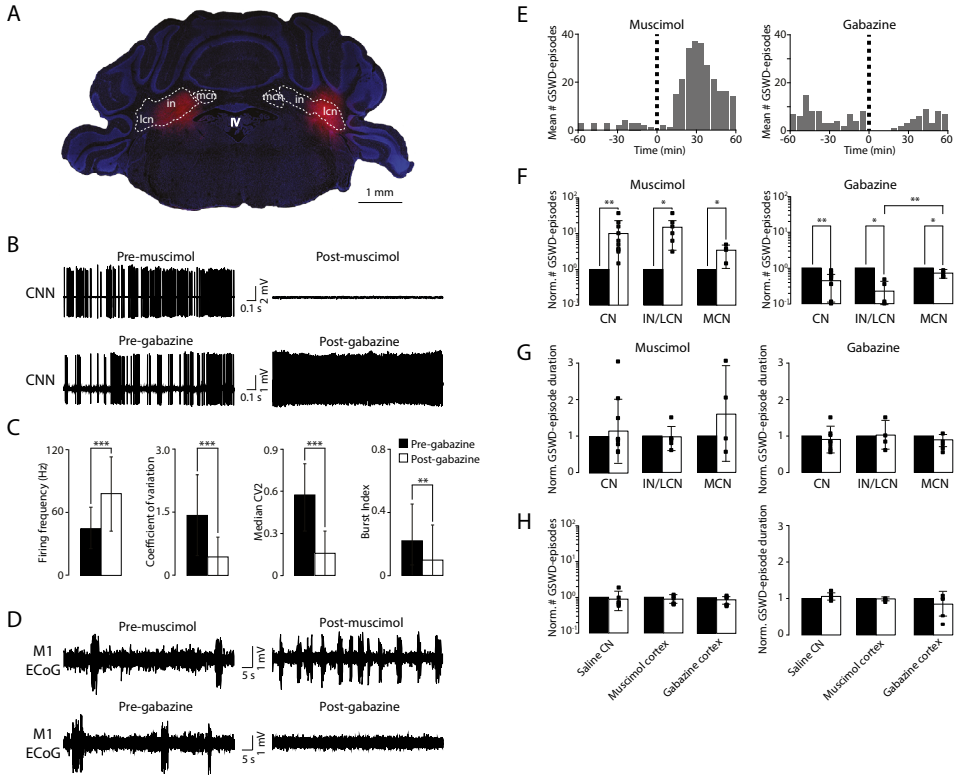

Figure 2. Bimodal modulation of GSWD occurrence by pharmacological manipulation of CN neuronal action potential firing.

(**A**) Confocal image of coronal cerebellar slice with bilateral muscimol injections (blue = DAPI; red = Evans blue indicating the injection sites; IV = 4th ventricle; MCN = medial CN; IN = interposed nucleus; LCN = lateral CN). (**B**) Examples of CN neuronal (CNN) recordings before and after bilateral muscimol (top) and gabazine (bottom) injections. (**C**) Barplots for the impact of gabazine on CN neuronal firing as quantified by the difference between pre- and post-gabazine injections (n = 81 and n = 55, respectively) in firing frequency, coefficient of variation, median CV2 and burst index; $^{**}p < 0.01$, $^{***}p < 0.001$ (MANOVA, post-hoc ANOVA's with Bonferroni corrections; see **Online Table 2**). (**D**) (top) Representative ECoG of primary motor cortex (M1) ECoG pre- and post-muscimol injection and (bottom) representative M1 ECoG pre- and post-gabazine injection. (**E**) Time course of the effects of muscimol (left) and gabazine (right) on the average number of GSWD-episodes (bin-size = 5 minutes) **(F, G)** Normalized number of seizures **(F)** and normalized seizure duration **(G)** pre and post muscimol (left) and gabazine (right) injections (1 hr each) for bilateral injections in all CN (N = 10 for both gabazine and muscimol), in IN/LCN (N = 6 for muscimol and 5 for gabazine) and in MCN (N = 4 for muscimol and 5 for gabazine). Note that for quantification of the seizure duration post-gabazine injection the only 9 mice are included for the 'all CN' and 4 mice for the IN/LCN group, since one mouse did not show any GSWDs post-injection. Blue dots indicate data recorded from male mice and red dots from female. $^{*}p < 0.05$, $^{**}p < 0.01$, (Friedman's ANOVAs and Mann-Whitney U tests; see **Online Tables 2 and 3**). (**H**) Normalized number of GSWD-episodes (left) and normalized GSWD-episode duration (right) for control experiments; saline injections in the CN and muscimol and gabazine injections in superficial cerebellar cortical areas.

Optogenetic stimulation of cerebellar nuclei

The promising impact of long-lasting pharmacological interventions at the level of the cerebellar output prompted us to explore whether short-lasting neuromodulation would be equally effective in stopping GSWDs, *i.e.,* whether disrupting oscillatory CN neuronal activity immediately stops GSWDs. To test this hypothesis we virally expressed light-sensitive channelrhodopsin-2 (ChR2) cation-channels in CN neurons (**Fig. 3A**). The optically-evoked alteration of CN neuronal firing (see below; **Fig. 5A**) had a robust effect on GSWD occurrence, in that most, if not all, episodes abruptly stopped within 150 ms of the onset of bilateral stimulation ($N = 4$; presented per mouse: 76% (male), 84% (female), 92% (female) and 100% (female) stopped) (**Fig. 3B, C**) and that the power at GSWD frequency was significantly reduced ($p < 0.001$) (**Fig. 3F**; **Online Table 5**). Moreover, unilateral optical stimulation of CN neurons proved equally effective in stopping GSWDs in all recorded cortices, regardless of the laterality ($N = 3$ female; presented per mouse: 89%, 92% and 100% stopped; power reduction: $p < 0.001$) (**Fig. 3C, F**; **Online Table 5**). Bilateral cerebellar stimulation was ineffective when a different wavelength (590 nm) was applied ($N = 3$ female; presented per mouse: 0%, 0% and 5% stopped; power reduction: $p = 0.37$) or when the optical fiber was placed outside the CN region ($N = 3$ female; presented per mouse: 0%, 5% and 8% stopped; power reduction: $p = 0.28$) (**Fig. 3D, F**; **Online Table 5**).

The type of seizure detection and on-demand stimulation described above renders the procedure conceptually unsuitable for clinical implementation in that it would require constant on-line evaluation and decision making by medics [39]. Therefore, we developed a brain-machine-interface (BMI) approach by engineering a closed-loop system for online detection of GSWDs and subsequent optogenetic stimulation [158]. Using off-line analysis we optimized the performance of a wavelet-based GSWD detection filter up to an accuracy of 96.5% and a median latency of 424 ms. When applied online this on-demand, closed-loop stimulation proved efficient in detecting and stopping GSWDs; bilateral optical stimulation of ChR2-expressing CN neurons stopped 93.4% of GSWDs and unilateral stimulation stopped 91.8% of GSWDs, which is also represented by the GSWD frequency power reduction ($N = 3$ female; $p < 0.001$; **Fig. 3E, 3F**; **Online Table 5**). Together, these data highlight that also in a clinically applicable BMI setting single-pulse stimulation of CN neurons suffices to stop GSWDs and that unilateral stimulation is sufficiently powerful to disrupt bilateral thalamocortical oscillations.

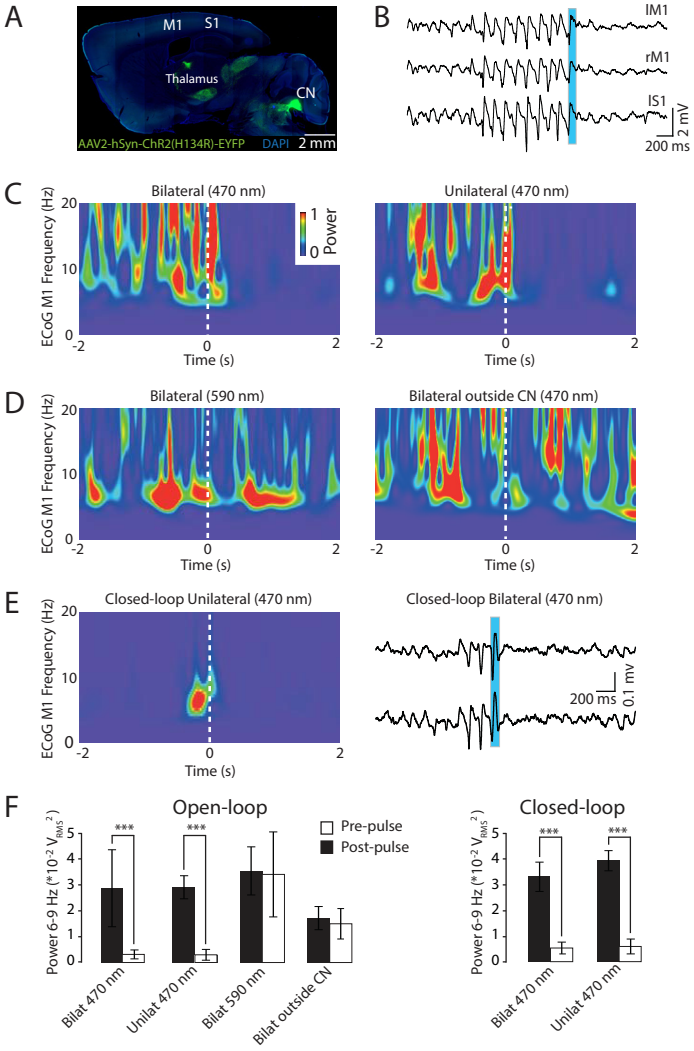

Figure 3. Optogenetic stimulation of cerebellar nuclei reliably stops GSWDs.

(**A**) Confocal image of sagittal brain section showing ChR2-expression in cerebellar nuclei (CN) with projections to the thalamus (Th) (M1, S1 represent primary motor and sensory cortex respectively). (**B**) Representative ECoG of bilateral M1 (left (l) and right (r) M1) and left S1 recording (lS1) which exemplifies how bilateral optogenetic stimulation (470 nm light pulse of 100 ms indicated by the vertical blue bar) stops GSWDs in all recorded cortices. (**C**) Mean ECoG wavelet spectrogram of contralateral M1 for all bilateral (n = 25; left panel) and unilateral stimuli (n = 11; right panel) presented to a single mouse at 470 nm. (**D**) As in panel d for (left) 590 nm stimuli (n = 36) and stimulation at 470 nm outside of CN (right) (n = 18). (**E**) (Right panel) Typical example of the effect of bilateral closed-loop stimulation on GSWD recorded in contralateral M1 and S1 and (left panel) mean ECoG wavelet spectrogram of all unilateral stimuli (n = 44) presented to one mouse. (**F**) ECoG theta-band power before and after open-loop (bilateral N = 3 female, 1 male; n = 178); unilateral N = 3 female; n = 43), stimulations with the wrong wavelength (590 nm) (N = 3 female; n = 107) and stimulations outside the CN (N = 3 female; n = 185) as well as the responses to closed-loop stimulation at 470 nm in the CN (bilateral N = 3 female; n = 227; unilateral N = 3 female; n = 49). *** $p < 0.001$ (repeated-measures ANCOVA; see **Online Table 5**).

Key findings are replicated in an unrelated mouse model of absence epilepsy

To exclude the possibility that our current findings in *tg* are unique to their pathophysiology [283, 305, 319], we repeated key experiments in *C3H/HeOuJ*, an inbred strain with an absence epilepsy phenotype [332] that is unrelated to *tg*. Extracellular recordings in awake ECoG-monitored *C3H/HeOuJ* mice confirmed that a smaller but substantial portion (35%) of CN neurons showed phase-locked action potential firing (**Fig. 4A, B**) and significant coherence with ECoG ($p < 0.001$; **Online Table 6**) during GSWDs and that this oscillatory firing was more irregular than their interictal firing pattern ($p < 0.001$; **Fig. 4C**; **Online Table 6**). Similar to *tg* mutants (**Fig. 2**), *C3H/HeOuJ* mice showed significantly more seizures following local muscimol injections into CN ($p < 0.05$; **Fig. 4D, E**; **Online Table 6**). Moreover, also in *C3H/HeOuJ* optogenetic stimulation reliably stopped GSWD-episodes ($N = 3$; presented per mouse: 82%, 87% and 91% stopped) and both bilateral and unilateral stimuli significantly reduced power at GSWD frequency ($p < 0.01$ and $p < 0.001$, respectively); the closed-loop detection and intervention system reduced the GSWD frequency power ($p < 0.001$ for bilateral and $p < 0.05$ for unilateral stimulation); and neither optical stimulation at 590 nm nor stimulation outside of CN significantly reduced the GSWD frequency power ($p = 0.43$ and $p = 0.81$, respectively; **Fig. 4H**; **Online Table 6**). Thus, the main findings done on CN treatment of absence seizures in *tg*, could be replicated in *C3H/HeOuJ* mutants.

Optogenetic stimulation of presumptively excitatory CN neurons affects GSWDs

To investigate the mechanism underlying the potent interruption of GSWDs by optogenetic stimulation of CN in *tg* and *C3H/HeOuJ*, we quantified the responses of CN neurons to bilateral optical stimulation.

In *C3H/HeOuJ* and *tg* injected with AAV2-hSyn-ChR2(H134R)-EYFP 33 out of 50 responsive cells (66%) showed increased action potential firing, whereas 17 (34%) showed decreased firing (**Fig. 5A**). A further 16 recorded neurons showed no response to optical stimulation. This variety of responses is in line with the properties of the construct that was used to transfect CN neurons with ChR2. Since human synapsin (hSyn) is not specific to a certain type of CN neuron [343] both excitatory and inhibitory neurons expressed ChR2. Excitatory responses can be recorded from neurons that express ChR2, inhibitory responses can be recorded from neurons that do not express ChR2 but that receive input from ChR2-positive inhibitory neurons, while neurons devoid of ChR2 expression either in their membrane or synaptic afferents will not show any response.

Next, we questioned to what extent the impact of optogenetic stimulation of CN neuronal action potential firing depends on the phase of the thalamocortical oscillations, *i.e.*, to what extent the disruption of GSWD-modulated CN firing was evoked during cortical excitation

(the ECoG spike) and/or cortical inhibition (the ECoG wave) [99]. Since we did not design our stimulation protocol to be activated with a fixed delay relative to the GSWDs, we could answer this question by comparing the phase values of the onset of effective stimuli relative to the Spike-and-Wave cycle in M1 and S1 cortices with those of ineffective stimuli (**Fig. 5B**).

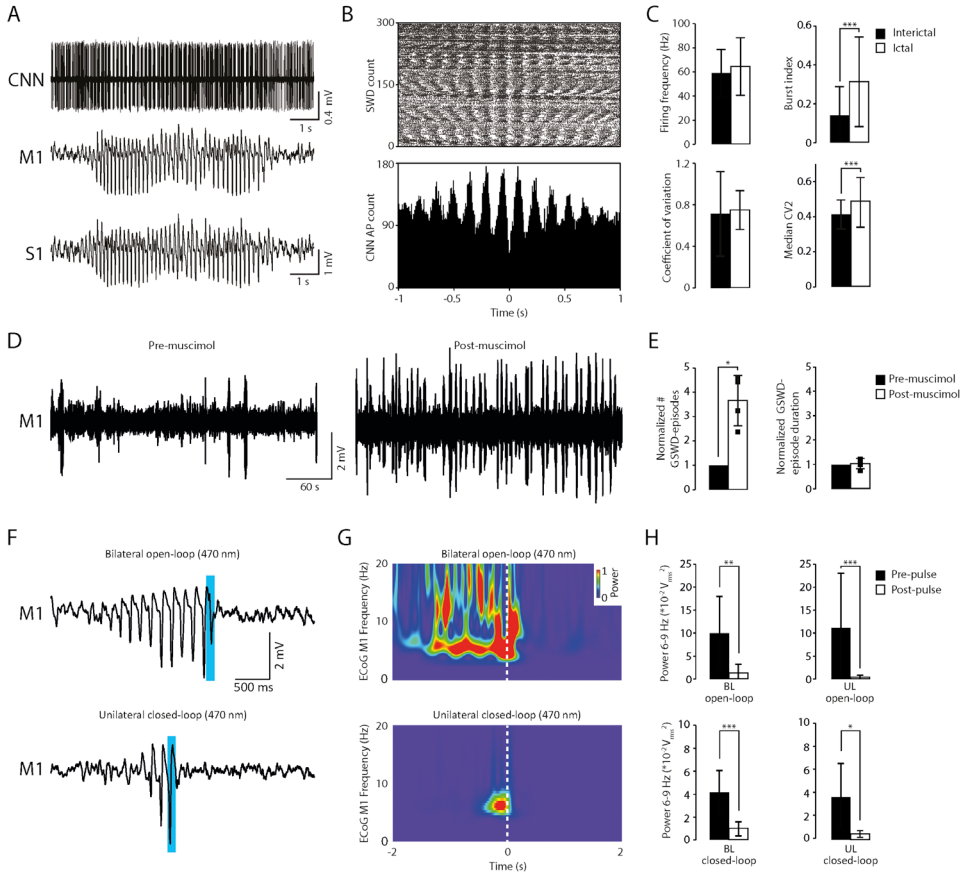

Figure 4. Modulation of phase-locked CN neuronal activity stops GSWDs in *C3H/HeOuJ mice*.

(**A**) Simultaneously recorded primary motor (M1) and sensory (S1) cortex ECoGs and CN neuronal activity. (**B**) Rasterplot and peri-stimulus time histogram of single CN neuronal activity (t = 0 indicates each ECoG spike). (**C**) Summary barplots representing the mean differences in firing pattern parameters between interictal and ictal periods (n = 28). *** $p < 0.001$ (repeated-measures ANOVA with Bonferroni corrections; see **Online Table 6**). (**D**) Representative M1 ECoG of pre- and post-muscimol injection and (**E**) corresponding normalized seizure occurrence and duration. * $p < 0.05$ (Friedman's ANOVA; see **Online Table 6**). (**F-H**) Open- (top) and closed-loop (bottom) optogenetic stimulation stops GSWDs as shown by: (**F**) typical example trace; by (**G**) ECoG wavelet spectrogram averaged over all bilateral open-loop (n = 11; top panel) stimuli in a single mouse and over all unilateral closed-loop stimuli (n = 18; bottom panel) in another mouse; and by (**H**) ECoG theta-band power before and after optical stimulation for bilateral open-loop stimuli (N = 3, n = 19; top left panel), unilateral open-loop stimuli (N = 3, n = 19), bilateral closed-loop stimuli (N = 3, n = 46) and unilateral closed-loop stimuli (N = 3, n = 30). *** $p < 0.001$ (repeated-measures ANCOVA; see **Online Table 6**).

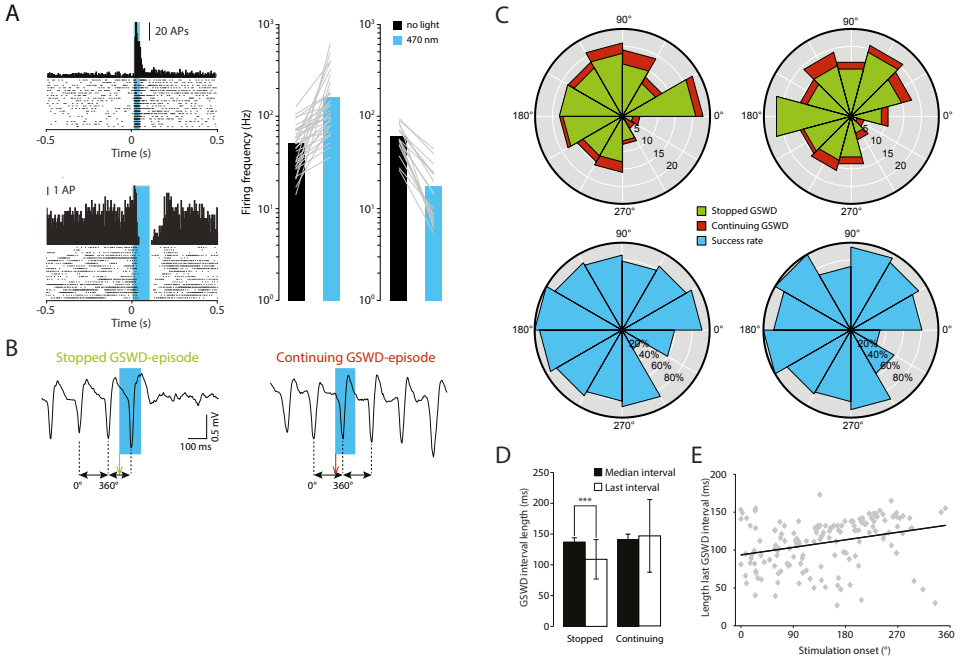

Figure 5. Excitatory impact of optical CN stimulation on cortical activity stops GSWD-episodes.

(**A**) (Left panels) Peri-stimulus time histogram and rasterplot indicating increased (top) or decreased (bottom) action potential (AP) firing for individual CN neurons evoked by 470 nm light pulses (blue bars). (Right panels) Scatterplots represent the individual changes in CN neuronal firing following optical stimulation: (left) increased firing (n = 33); (right) decreased firing n = 17). Black and blue bars indicate mean firing frequency when the 470 nm LED was turned off or on, respectively (**B**) Examples of stopped (left) and continuing (right) GSWD episodes upon optogenetic stimulation. Black horizontal arrows represent the median time interval between ECoG 'spikes', which correspond to one cycle of cortical oscillation, here represented as 360 degrees. Green and red vertical arrows represent the onset of the light stimulus. (**C**) Rose plots of the start of successful and unsuccessful optical stimulation in the 360° GSWD cycle for both primary motor cortex (M1; left) and primary sensory cortex (S1; right). (**D**) Comparison between the median and the last interval (between the last two ECoG-spikes) for stopped and continuing GSWD episodes. *** $p < 0.001$ (repeated measures ANCOVA; see **Online Table 7**). (**E**) Scatterplot representing the predictability of the stimulus-related time interval between GSWDs by the phase of stimulation-onset ($p < 0.001$; linear regression analysis; see **Online Table 7**).

For both M1 and S1 success rates were lowest when the stimulus was applied up to 60 degrees before the peak of a spike (*i.e.*, 300°-360° in **Fig. 5C** lower panels), but the overall differences of these distributions did not reach statistical significance (M1: $p = 0.13$; S1: $p = 0.29$). However, effective stimuli evoked a significant shortening ($p < 0.01$) of the interval between the last two ECoG-spikes, which is indicative of an excitatory effect on cortical activity [99] (**Fig. 5D; Online Table 7**), and the timing of the last ECoG-spike could be predicted by the time of the stimulus onset relative to the Spike-and-Wave cycle ($p < 0.001$; **Fig. 5E; Online Table 7**). Together, our combined electrophysiological and optogenetic

data indicate that optogenetic CN stimulation is most effective when applied during the 'Wave' of the GSWD, during which cortical neurons are normally silent.

5.4 Discussion

In this study we show that in two unrelated mouse models of absence epilepsy the activity of CN neurons can be utilized to modulate the occurrence of GSWDs. We provide evidence that pharmacological interventions at the level of CN can exert slow, but long-term, effects and that optogenetic stimulation of CN neurons can exert fast, short-term control. The different dynamics of these experimental approaches, with converging outcomes, align with the hypothesis that CN neurons can control the balance of excitation and inhibition in the thalamus, thereby resetting the oscillatory activity in thalamocortical loops.

In both *tg* and *C3H/HeOuJ* strains of mice a substantial subset of CN neurons showed phase-locked action potential firing during GSWDs, which is in line with a previous study of oscillating cerebellar activity during GSWDs in WAG/Rij and F344/BN rats [104]. We observed that 35% of neuronal recordings in the MCN showed GSWD-modulated patterns, whereas the portions of GSWD-modulated neurons in the IN and LCN were higher (73% and 44%, respectively). Except for an anatomical evaluation of the local density of large and small soma-diameter CN neurons in the mouse brain [344] and computational studies on the clustering analysis of CN neuronal action potential firing in *tg* [345, 346], little experimental data are available that allow us to unequivocally pinpoint the type(s) of CN neurons responsible for modification of GSWD activity. With respect to the extracellular recordings we presumably recorded mostly from CN neurons with a large soma-diameter [347], which incorporates mainly excitatory glutamatergic neurons [243], but in the MCN also inhibitory glycinergic projection neurons [248]. Interestingly, GSWD-modulated CN neurons also showed characteristic firing patterns during the periods in between the seizures. During these interictal periods they fired at higher frequencies with a more irregular and burst-like pattern than the CN neurons that did not co-modulate with GSWDs. Thus, the interictal firing pattern of CN neurons in *tg* and *C3H/HeOuJ* mice appears to reliably predict whether these cells will show oscillations phase-locked to GSWDs during seizures.

Pharmacological manipulation of neuronal activity in the cerebellum proved effective when the injections of muscimol or gabazine were aimed at the CN, but not when the cerebellar cortex was targeted. We found that gabazine application was effective in reducing GSWD occurrence in all CN with the most pronounced effects in IN and LCN. Along the same line, muscimol injections in IN and LCN evoked the biggest increase in GSWD occurrence. Effects of MCN injections were smaller but still significant. Since we know

little about the density of individual types of neurons throughout the murine MCN, IN and LCN [243, 344], and considering the similarity in effects of gabazine and muscimol on neuronal activity in these nuclei, we cannot draw a firm conclusion about a potentially differential effect of either gabazine or muscimol on the respective nuclei. These data raise the possibility that the difference in impact on GSWD occurrence between manipulation of MCN vs. that of IN and LCN does not reflect a difference in intrinsic activity, but rather a difference in their efferent projections to the brainstem, midbrain and thalamus [89]. Although all CN have been shown to project to a wide range of thalamic subnuclei, like the ventrolateral, ventromedian, centrolateral, centromedian and parafascicular nuclei [89, 348] and thereby connect to a variety of thalamocortical networks, the impact of IN and LCN has been shown to focus on the primary motor cortex whereas MCN impacts more diffusely on thalamocortical networks [349].

CN axons that project to the thalamus have been shown to originate from glutamatergic neurons, which synapse predominantly perisomatically and evoke substantial excitatory responses [84, 86, 89, 91, 92, 96, 106, 330, 331]. Upon CN injections with muscimol, we must in effect have substantially reduced the level of excitation of thalamic neurons and thereby disturbed the balance of inhibition and excitation in thalamocortical networks in favor of inhibition. One of the main consequences of hyperpolarizing the membrane potential of thalamic neurons through this inhibition is activation of hyperpolarization-activated depolarizing cation currents (I_h) and $Ca_V3.1$ (T-type) Ca^{2+}-currents, which typically results in the burst-like action potential firing that can drive GSWDs in thalamocortical networks [37, 327, 350, 351]. Moreover, in *tg* thalamic relay neurons show increased T-type Ca^{2+} channel currents [352], which probably act synergistically with the decreased excitation following muscimol treatment, likely further increasing GSWD occurrence. In contrast, when we applied gabazine to CN, the balance of inhibition and excitation in the thalamocortical networks probably shifted towards excitation and thereby may have prevented the activation of I_h and T-type Ca^{2+}-channel currents, reducing the occurrence of burst firing and GSWDs. The successful application of short periods of optogenetic excitation of CN neurons did not only confirm the de-oscillating impact of gabazine, but further refined it by revealing that GSWDs can be most efficiently stopped when the interval between ECoG spikes, *i.e.,* wavelength of the oscillations, is instantly shortened and thereby reset. Given the relatively low success rate of optogenetic stimulation in the period just preceding the 'Spike' state of the GSWDs, which reflects the excitation state of the thalamocortical relay neurons, it is parsimonious to explain the effective resetting through optimal interference during the inhibitory or 'Wave' state of the GSWD [99]. This explanation centered on the resetting hypothesis argues against the possibility that GSWDs were terminated by optogenetic

activation of the CN neurons that were inhibited. Regardless of the *netto* effect of CN stimulation on thalamocortical networks, the current approach proved equally effective when applied bilateral or unilateral. Most likely, instantly resetting the balance of excitation and inhibition in thalamocortical relay neurons on one side of the brain will also engage the other side through combined ipsi- and contralateral projections from the CN to the thalamus and through interthalamic and intercortical connections [86, 89, 353].

It remains to be established to what extent the current findings for absence epilepsy can help to treat epileptic patients suffering from other types of seizures. Our findings on the impact of optogenetic manipulation of CN firing patterns on GSWD occurrence seem to support that (pre-)clinical studies that apply DBS [354, 355] in the CN may be an option to treat epilepsy patients. So far, only three clinical studies applying electrical deep brain stimulation (DBS) to the CN have been reported, which is in contrast to the dozens of studies performed to investigate the therapeutic use of cerebellar surface stimulation (as reviewed by ref [74]). Although initially promising, the clinical studies on the effects of cerebellar surface stimulation reported inconsistent results [47, 68, 69, 72, 73, 75-78, 329], which may partially be due to suboptimal placement of electrodes. Unlike the current results which show a regional preference for the effect of lateral CN stimulation on GSWD occurrence, it was recently shown that manipulating Purkinje cells in the medial cerebellum is most effective in controlling kainate-induced temporal lobe epilepsy [45]. So far, the studies that applied DBS at the level of CN in an uncontrolled fashion report highly effective decreases in the level of seizures (corresponding to class IC and IIIA of the Engel scale [356]) in a low number of patients characterized with various types of epilepsy [48, 49, 129]. Apart from the coherence in location of stimulation (laterally located nucleus dentatus) these studies used a wide variety in CN stimulus regimes, ranging from 3 min per day to continuous electrical stimulation for 12-14 hrs per day. It appears that high-frequency stimulation (> 50 Hz), but not low-frequency stimulation (1-40 Hz), is most effective when applied to the cerebellar dentate nucleus. In the present study we found that the increase in CN neuronal action potential firing frequency upon optogenetic stimulation was highly variable **(Fig. 5)** and thus our current results do not provide any ground for a conclusion on whether low- or high-frequency stimulation would be advantageous to stop GSWD-episodes. Yet, our results do provide sufficient data to conclude that the temporal precision determines the level of efficiency, *e.g.*, by stimulating with short pulses as soon as an epileptic event starts to occur and if possible in a proper temporal relation with respect to the inhibitory wave of the GSWDs.

Since absence epilepsy is a commonly prevalent but in essence a benign form of generalized epilepsy [323], DBS will not very likely be considered as a serious option. However, patients

diagnosed with other forms of epilepsy whom do not benefit sufficiently from medication, may be eligible for (cerebellar) DBS [39]. Currently, the options for applying DBS are (too) limited; only the anterior thalamic nucleus is currently described in the FDA-guidelines to treat intractable epilepsy, and although promising, the outcome is limited and can result in cognitive and emotional problems [357, 358]. Given the powerful impact of CN stimulation on thalamocortical activity that is shown in the present study, we hypothesize that CN stimulation may also exert very positive effects in these other, more severe kinds of epilepsies.

Acknowledgements

We thank Dr. Karl Deisseroth for providing the AAV-hSyn-ChR2(H134R)-EYFP and we thank Drs. T.J. Ruigrok, L. Bosman and P. Holland, K. Voges, R. Seepers, E. Haasdijk, E. Goedknegt, M. Rutteman, D. Groeneweg and P. Plak for technical assistance and/or constructive discussions.

6

Diversifying cerebellar impact on thalamic nuclei

Submitted to Cell Reports:

S.V. Gornati*, C.B. Schäfer*, O.H.J. Eelkman Rooda, A. Nigg,
C.I. De Zeeuw and F.E. Hoebeek

The cerebellum plays a role in coordination of movements and possibly also non-motor functions. Cerebellar nuclei (CN) axons connect to various parts of the thalamo-cortical network, but detailed information on the characteristics of cerebello-thalamic connections is lacking. Here, we assessed the cerebellar input to the ventrolateral (VL), ventromedial (VM) and centrolateral (CL) thalamus. Confocal and electron microscopy showed an increased density and size of CN axon terminals in VL compared to VM or CL. Electrophysiological recordings in vitro revealed that optogenetic CN stimulation resulted in enhanced charge transfer and action potential firing in VL neurons compared to VM or CL neurons, despite that the paired-pulse ratio was not significantly different. Together these findings indicate that the impact of CN input onto neurons of different thalamic nuclei varies substantially, which highlights the possibility that cerebellar output differentially control various parts of the thalamo-cortical network.

6.1 Introduction

Cerebellar best-known functions are involved in coordinating motor activities. It contributes for example to learning new motor skills and prediction of the sensory consequences of action [290, 359, 360]. The anatomical connections that underlie this broad impact include cerebellar axons to premotor centers in the brainstem, like the red nucleus and the thalamic complex [89, 348, 361-366]. The glutamatergic projection neurons from cerebellar nuclei (CN) are known to connect to a wide range of thalamic regions encompassing primary relay nuclei, i.e. 'core nuclei', like the ventrolateral (VL) nucleus, but also association nuclei such as the ventromedian (VM) nucleus, i.e., a 'matrix nuclei', as well as intralaminar nuclei [86]. Single axon reconstructions of cerebellar-recipient zones within VL and VM reveal that although both of these nuclei connect to motor and pre-motor cortices, their axons also spread throughout other regions [367, 368]. The diffuse character of the cerebellar input on thalamo-cortical networks is further highlighted by the divergent CN-projections to the intralaminar thalamic nuclei, like the centromedian, parafascicular and centrolateral (CL) nuclei [84, 89, 308] which are considered to project non-specifically throughout cortical regions and layers [369-372].

Apart from their connectivity, neurons in thalamic nuclei are also characterized by a heterogenic dendritic morphology. For instance, the cerebellar recipient zones of the VL and VM have been shown to contain neurons with 'bushy' dendrites [367, 368, 373-375] and thereby have a different appearance than CL neurons that show polarized dendritic branching [370]. Besides the difference in the cytoarchitecture, thalamic cells have been found to show different neurochemical profiles. For instance, a subpopulation of VM cells express elevated levels of calbindin, whereas intralaminar neurons show also parvalbumin-immunoreactivity [367, 376-379]. This variability in the neurochemical and morphological aspects of thalamic neurons in the cerebellar-recipient nuclei suggests that the impact of cerebellar output on thalamic neurons varies for each target nucleus.

Due to its divergent nature, the thalamo-cortical projection is likely to affect a multitude of functions [349, 367, 380, 381]. As a consequence, cerebellar lesions can result in a wide range of symptoms that span both the motor and non-motor domains [382-384]. Cerebellar-specific mutations affect not only the motor coordination, but also the social interaction between mice [385, 386]. Several *in vivo* experiments recently showed that manipulating the cerebellar output affects sensorimotor integration by somatosensory and motor cortices and thereby could direct the thalamo-cortical activity related to voluntary movements [90, 387]. Cerebellar projections to VL and VM nuclei might also influence motor preparation and movement initiation [388]. Moreover, a recently uncovered pathway from CN to the thalamic CL neurons enables short-latency control of striatal activity [256].

So far, the electrophysiological studies that investigated the cerebello-thalamic projections focused on the VL nucleus. It has been established that mono-synaptic responses evoked by CN axon stimulation results exclusively in excitatory responses in VL neurons [90-92, 380, 387, 389]. In order to elucidate how the cerebellar impact on thalamic neurons correlates to the specific nuclei we studied the postsynaptic responses to cerebellar stimulations using *in vitro* whole cell recordings. We focused on neurons in the VL, VM and CL and correlated the electrophysiological data to the morphological and cytological details of the target neurons. Our results show that both pre- and post-synaptic aspects of the cerebello-thalamic transmission vary between these thalamic nuclei and thereby provide the first evidence for the functional diversification of the cerebellar impact on thalamo-cortical networks.

6.2 Experimental procedures

6.2.1 Animals

All experiments were performed in accordance with the European Communities Council Directive. Protocols were reviewed and approved by the Dutch national experimental animal committees (DEC) and every precaution was taken to minimize stress, discomfort and the number of animals used. Data were collected from 21-56 day old C57BL/6NHsd mice of both sexes, which were purchased from Envigo laboratories (Horst, Netherlands).

6.2.2 Virus injections

We performed stereotaxic injections of adeno-associated virus carrying Channelrhodopsin2 AAV2-hSyn-ChR2(H134R)-EYFP into CN at 2 mm anterior-posterior and 1.5-2 mm medial-lateral to lambda. For localization of the injection sites 40 µm thick horizontal sections were obtained on a freezing microtome. The tissue was incubated with DAPI (300nM). Sections where rinsed and mounted on glass.

6.2.3 Electrophysiological recordings in slices and optogenetics

Electrophysiological recordings in coronal or horizontal slices were performed at 34 ± 1˚C aCSF 40 min after dissection. Internal solution was supplemented with biocytin for morphological reconstruction. Full-field optogenetic stimulation (1 ms, 470 nm peak excitation, 0.1 to 6.65 mW/mm^2) was generated using a Polygon4000 (Mightex, Toronto, Canada) or a pE2 (CoolLED, Andover, UK). Pharmacology experiments were assessed adding AMPA- (10 µM NBQX), NMDA- (10 µM APV), mGluR1- (10 µM JNJ-16259685) and mGluR5- (50 µM MPEP) blockers to the aCSF.

6.2.4 Immunofluorescence and reconstruction

To visualize the recorded neurons and CN terminals, slices were stained for Streptavidin-Cy3 (Jackson Immunoresearch) and vGluT2 anti-guinea pig Cy5 (Millipore Bioscience Research Reagent). Using custom-written Fiji-scripts (ImageJ) we identified putative synaptic contacts that were isolated and morphologically studied using a LSM 700 microscope (Carl Zeiss). Stack's subsets of the connection were deconvolved using Huygens software (Scientific Volume Imaging) and the volume measured using a custom-written Fiji macro. To quantify the distance from soma for vGluT2-positive CN terminals we calculated the distance in 3 dimensions (using x-, y-, z-coordinates) between the center of the terminal and the center of the soma by Pythagorean Theorem. To determine the dendritic arborization of biocytin filled cells, we used the 3D Sholl analysis macro implemented in Fiji software [390].

6.2.5 Electron microscopy

Ultrastructural morphology was analyzed using electron microscope (CM 100, Philips). Staining for DAB and preparation of ultrathin section was performed as previously described [319].

6.3 Data analysis and statistics

All numerical values are given as means and error bars are SEM. Parametric and non-parametric tests were chosen as appropriate and were reported in figure legends. Data analyses were performed using SPSS 22.0 software package.
Detailed experimental procedures and statistical analyses for each experiment can be found in Supplemental Experimental Procedures.

6.4 Results

6.4.1 Thalamic nuclei receive various densities of CN axons and terminals

To assess the innervation of VL, VM and CL thalamic nuclei by cerebellar axons in the mouse brain, we transfected neurons in the interposed and lateral CN with a virally encoded YFP-expressing construct (**Figure 1A**). We found the level of intensity in the VL (55.9 ± 8.0 a.u.) to be highest compared to VM (38.7 ± 3.9 a.u.) and CL (25.8 ± 2.3 a.u.) (p=0.529 for VL *vs* VM; p=0.002 for VL *vs* CL, p=0.136 for VM *vs* CL, K-W tests, Dunn's correction; **Figure 1B** and **Online Table S1**).

In order to establish whether the regional variability in fluorescence also reflects a variable size and density of CN axon terminals, we next evaluated tissue samples that were additionally stained for vGluT2, a widely used marker to selectively label glutamatergic terminals [248, 367, 379, 391, 392]. High–magnification confocal microscopic images and custom-written image analysis scripts revealed that the VL nucleus was most densely populated by CN terminals (total count 499 terminals; N=5 mice; **Figure 1C-D**) with a mean volume of 12.45±0.74 μm^3. As previously reported [348], VM is mostly a region where cerebellar fibers pass through by sending some branches in the most medial part of the nucleus (**Figure 1E**). The number of vGLUT2 positive terminals was lower compared to VL and their size was significantly smaller (6.65±0.71 μm^3 mean value for 172 terminals isolated, $p<0.0001$, K-S test; **Figure 1F,I** and **Table S1**). The centrolateral nucleus showed the lowest number of terminals and the volume was statistically different from VL but not VM (73 terminals with mean volume size of 5.85±0.9 μm^3; p=0.0002 for VL vs CL and p=0.966 for VM vs CL, K-S test; **Figure 1G-I** and **Table S1**). Moreover we could observe a significantly higher density of vGluT2-positive CN terminals compared to CL (p=0.024; K-W test), whereas the differences in density between VL-VM and VM-CL were not significantly different (p=0.334 and p=0.865, respectively; K-W tests; **Figure 1J** and **Online Table S1**). This data demonstrate that the cerebellar projection innervates preferentially VL and that their terminals are not only more abundant, but also bigger compared to VM and CL.

Basic transmission properties of cerebello-thalamic synapses differ across thalamic nuclei

It has been shown by sharp electrode recordings in anesthetized cats and rats that electrical stimulation of the cerebellar nuclei axons could elicit monosynaptic excitatory post-synaptic potentials (EPSPs) from which a fast spike could arise in VL relay cells [91, 92]. To our knowledge, no data have been published about the postsynaptic currents underlying these changes in VL potentials, or about the postsynaptic responses of thalamic VM or CL cells. To gather these data we performed whole cell patch-clamp recordings of VL, VM and CL neurons in acutely prepared thalamic slices that contained YFP-labelled, ChR2-expressing CN axons (see material and methods section). Overall, we found that the resting membrane potential of VL (-71.6±0.9 mV), VM (-72.2±2.0 mV) and CL (-70.0±1.4 mV) neurons was not significantly different (p=0.736, one-way ANOVA), but that the input resistance of CL neurons was significantly higher than in VL neurons (p=1 for VL *vs* VM, p=0.012 for VL *vs* CL and p=0.175 for VM *vs* CL; n=49; K-W test). In all three thalamic nuclei single light pulses (1 ms, 470 nm, applied through the objective) elicited an EPSC (**Figure 2A**).

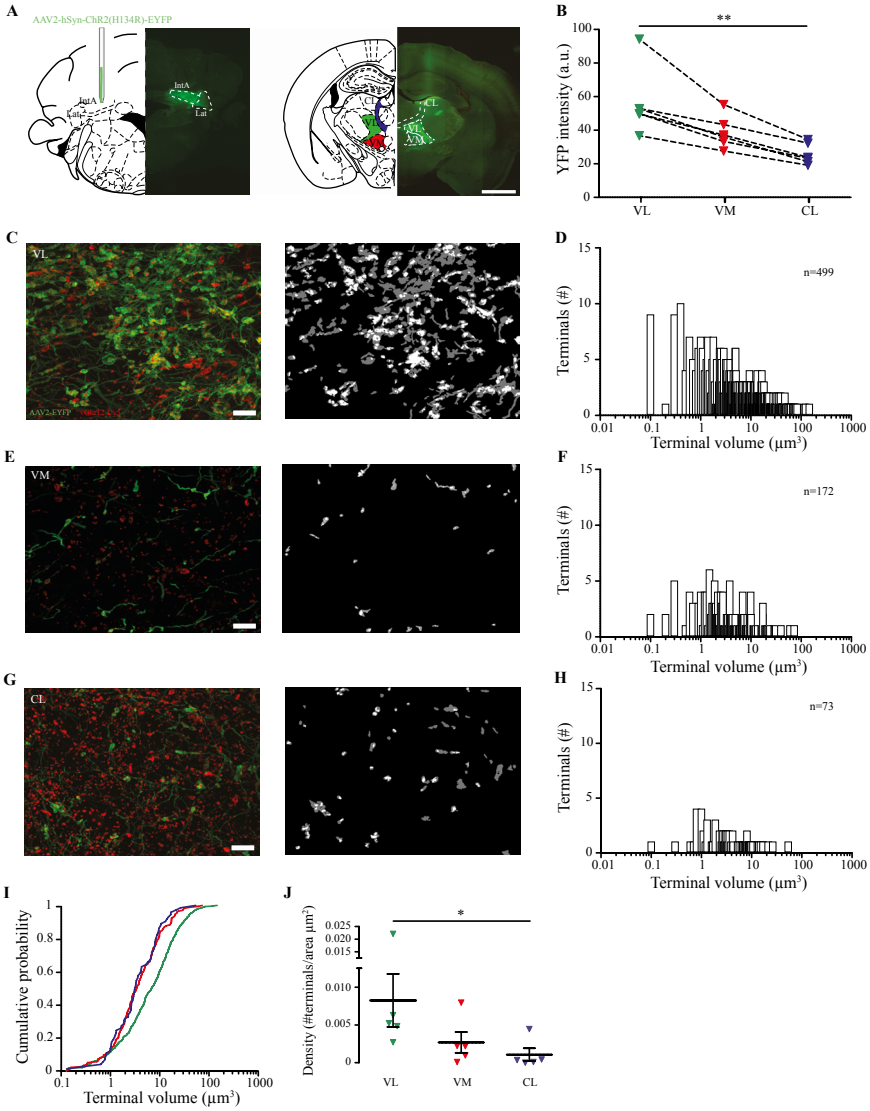

Figure 1. Variable innervation of VL, VM and CL nuclei by CN axons.

A schematic representation of the experiment. (left) AAV-injection in the interposed nucleus and (right) fluorescent (ChR2-EYFP) CN axons throughout the thalamic complex (3 weeks post-injection). The nuclei of interest are highlighted in green (VL), red (VM) and blue (CL). This color code will be applied throughout all the figures. Scale bar indicates 1 mm. ***B*** percentage of YFP signal in the three nuclei of interest (N = 6 mice) normalized to fluorescence in VL. ***C,E,G*** (left) maximum intensity projection of *Z-stack* (14 µm thick) showing in green ChR2-EYFP stained CN axons, in red vGluT2 staining and (right) the result of the colocalization mask; gray indicates ChR2-EYFP-stained axons and white vGluT2-staining. ***D,F,H*** histograms showing terminal volume and number for VL, VM and CL (N = 5 mice). ***I*** cumulative plot of the terminal volume (green: VL; red: VM; blue: CL). (VL vs CL $p<0.001$: VL vs VM $p<0.001$ and VM vs CL $p=0.966$; N = 5 mice, K-S test). ***J*** Average density of vGluT2-stained CN terminals (VL vs CL $p=0.024$). Data are presented as mean ± S.E.M; * $p<0.05$, *** $p<0.001$. K-W test was used. For full statistical report see Online Table 1.

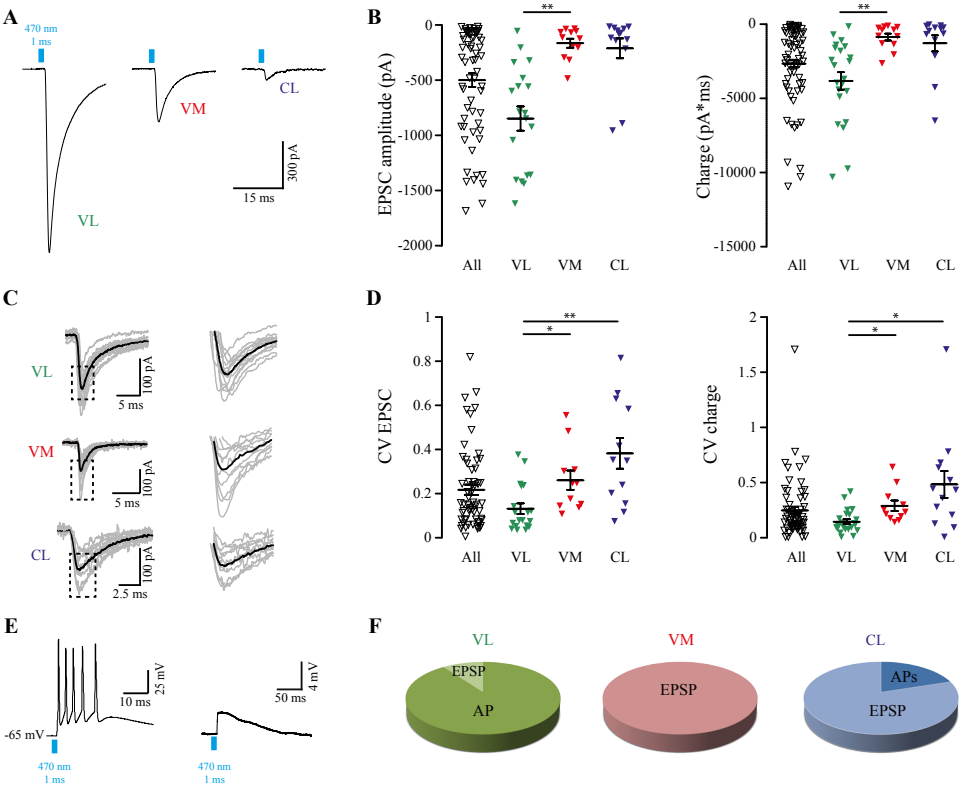

Figure 2. Charge transfer between CN axons and thalamic neurons differs for VL, VM and CL.

A, optical wide field stimulation of CN terminals (470 nm, 1 ms pulse length) evoked EPSCs of variable amplitude in VL, VM and CL. ***B*** quantification of EPSCs amplitude and charge for all recorded cells (n = 63 for EPSC amplitude and n = 65 for charge) and for the nuclei of interest (EPSC: VL: n = 19; VM: n = 12; CL: n = 13; charge: VL: n = 22; VM = 12; CL = 13 respectively; 'All' category represents all cells recorded, of which some were not recovered by histology and therefore were not classified to a specific nucleus – note that all cells in VL, VM and CL are also represented in 'All'). ***C*** example traces of EPSCs amplitude in gray and average trace in black. Note the variability in EPSC amplitude of individual responses. ***D*** coefficient of variation (CV) for (left) EPSCs amplitude and (right) EPSC charge. ***E*** example traces of (left) action potential (AP) firing or (right) excitatory postsynaptic potential (EPSP) evoked by single pulse CN stimulation. ***F*** Pie charts representing responses to CN stimulation recorded in current-clamp mode (VL: n = 9 AP, n = 1 EPSP; VM: n = 3 EPSP; CL: n = 1 AP, n = 4 EPSP). Data are presented as mean ± S.E.M; * $p<0.05$, ** $p<0.01$, *** $p<0.001$. K-W was used. For full statistical report see Online Table 2.

These events were reliably blocked by bath-application of the voltage-gated Na^+-channel blocker tetrodotoxin (TTX) (n = 5 cells; >99% decrease in charge transfer), which indicates that the postsynaptic events were triggered by action potential-driven release of glutamate from CN terminals. The mean EPSC amplitude that we could maximally evoke was significantly higher in VL than in VM and CL (VL: -847.7 ± 109.5 pA; VM: -165.0

± 40.2 pA; CL: -210.8 ± 89.2 pA; p=0.001 for VL *vs* VM, p<0.001 for VL *vs* CL and p=1 for VM *vs* CL; K-W tests), which was also represented in the evoked charge (VL: -3820 ± 595 pA*ms; VM: -862 ± 235 pA*ms; CL: -1284 ±542 pA*ms; p=0.002 for VL *vs* VM; p=0.001 for VL *vs* CL, p=1 for VM *vs* CL; K-W tests; **Figure 2B** and **Online Table S2**). The variability in optically stimulated EPSC amplitude and charge was quantified by calculating the coefficient of variation (CV) (**Figure 2C**). We found significant differences in the CV of EPSC amplitudes (VL: 0.13 ± 0.02; VM: 0.25 ± 0.04; CL: 0.38 ± 0.07; p=0.031 for VL *vs* VM, p=0.001 for VL *vs* CL; p=1 for VM *vs* CL, K-W tests, Dunn's correction; **Figure 2D** and Online Table S2) and of EPSC charge (VL: 0.13 ± 0.02; VM: 0.28 ± 0.04; CL: 0.47 ± 0.12; p=0.03 for VL *vs* CL, p=0.025 for VL *vs* VM, p=1 for VM *vs* CL, K-W tests, Dunn's correction and Online Table S2). We found no significant correlation of the incubation time to the EPSC amplitude, nor to the CV of the EPSC amplitude (p=0.470, r_s=0.116 for EPSCs and p=0.269, r_s=0.161 for CV, Spearman correlation), which supports the notion that the difference in postsynaptic responses is actually due to a difference in the charge transfer between CN axons in VL, VM and CL neurons.

To establish the impact of neurotransmitter release from CN terminals on thalamic neurons' membrane potential we also recorded a subset of cells in current clamp (**Figure 2E**). When stimulated at maximum light intensity most VL neurons fired action potentials (9 cells out of 10) whereas most VM (3 out of 3) and CL neurons (4 cell out of 5; **Figure 2F**) were not able to elicit action potential firing. The probability to elicit an action potential was not related to the resting membrane potential of the cell (p=0.628; r_s=-0.127, Spearman correlation). As we expected from the EPSC amplitudes, neurons in VL fired action potentials more readily than those in VM and CL.

Thalamic responses show paired-pulse depression and are predominantly sensitive to ionotropic glutamate receptor blockers

Thalamic afferents are often categorized as 'driver' or 'modulator' [150, 393]. This classification is partially determined by the response to repetitive stimulation of presynaptic terminals: driver synapses are thought to show paired-pulse depression (PPD) whereas modulator synapses evoke paired-pulse facilitation (PPF) [394-396]. Although cerebellar input to motor thalamus has been listed as driver input [150], short-term synaptic dynamics of thalamic responses following repetitive CN stimulation in VL, VM and CL still need to be evaluated. Here we performed voltage-clamp recordings while stimulating the CN terminals repetitively with trains of light pulses at 10, 20 and 50 Hz (**Figure 3A-C**). To evaluate the time course of the depression we normalized EPSC amplitudes to the first peak amplitude (**Figure 3D-F**).

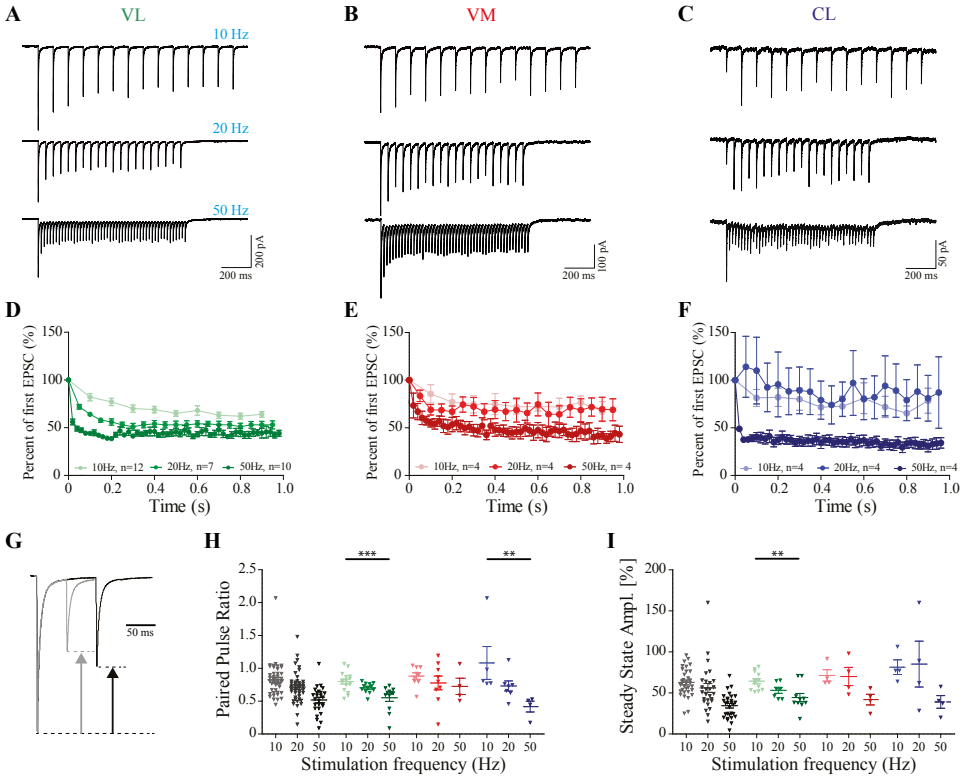

Figure 3. High-frequency stimulation results in paired-pulse depression of EPSC.

A,B,C Averaged responses of VL, VM and CL neurons (of 5 repeats) to 1 sec trains of 10 Hz, 20 Hz or 50 Hz stimuli. ***D,E,F*** Average normalized EPSC amplitudes for 10, 20 and 50 Hz stimulus trains. ***G*** superimposed example responses (average of 5 repeats) to paired-pulse stimulation at 10 Hz (black) and 20 Hz (grey). ***H*** average paired pulse ratio at 10, 20 and 50 Hz for each recorded cell in each nucleus. ***I*** average normalized steady state response amplitude during the last 5 stimuli of the train for each cell in each nucleus. (For panels H and I: VL: n=29; VM: n=12; CL: n=12) ** $p<0.01$, *** $p<0.001$. For full statistical report see Online Table 3.

In general, we found that the ratio between the amplitudes of the first two EPSCs showed a PPD at all frequencies tested (**Figure 3G**). At 50 Hz the second EPSC showed a twofold reduction in amplitude compared to the initial one (VL: 0.52 ± 0.06; VM: 0.72 ± 0.12; CL: 0.41 ± 0.08), whereas lower frequency stimulations showed a smaller effect on the paired-pulse depression. At 20 Hz the depression was around 30% of the first EPSC in all the nuclei (VL 0.70 ± 0.02, VM 0.77 ± 0.10, CL 0.73 ± 0.07) whereas at 10 Hz only VL (0.80 ± 0.03) and VM (0.88 ± 0.04) neurons showed on average PPD but CL did not (1.08 ± 0.25) (**Figure 3H**). When we compared the paired-pulse depression across all nuclei for each frequency, we found that the ratio between the first two responses did not show any

significant difference between the nuclei (10 Hz: p=0.344; 20 Hz: p=0.168; 50 Hz: p=0.137, K-W tests, Dunn's correction; **Figure 3H** and Online Table S3).

Next, we analyzed the subsequent responses to the train stimulation to determine the average sustained release of presynaptic terminals during high frequency steady-state synaptic transmission (**Figure 3A**). For this analysis, the average phasic EPSC amplitude within the train was normalized to the average first EPSC amplitude for each frequency and each nucleus. Across all recorded cells, we find normalized steady state amplitudes of 64.4 ± 3.1% (VL), 71.3 ± 6.9% (VM) and 81.4 ± 8.9% (CL) at 10 Hz: 53.1 ± 3.6% (VL), 70.1 ± 11.1% (VM) and 85.2 ±28.0% (CL) at 20 Hz and 44.4 ± 5.0% (VL) 41.9 ± 6.5% (VM) and 39.1 ± 7.7% (CL) at 50 Hz (**Figure 3I** and Table S3). We found no significant differences between the values recorded per nucleus, but did find that in VL the steady-state depression was significantly higher at 50 Hz than at 10 Hz (p =0.005, K-W test, **Figure 3I** and Table S3). These data indicate that the general tendency for transmission at cerebello-thalamic synapses in VL, VM and CL is to show a depression of neurotransmitter release in response to repetitive stimulation.

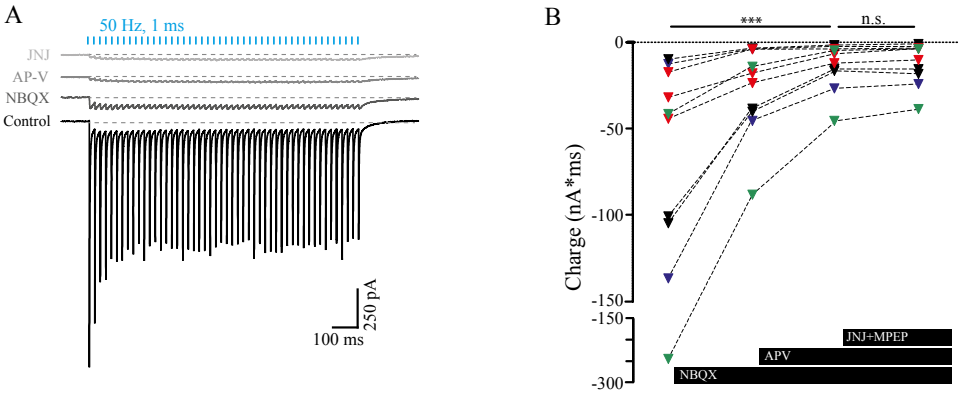

Figure 4. Thalamic responses to CN-stimulation are sensitive to ionotropic receptor blockers.

A example traces of averaged EPSCs evoked by 1 sec train of 1 ms pulses at 50 Hz in control (ACSF) conditions and following application of NBQX, APV and JNJ+MPEP to block AMPA, NMDA and mGluR1 and 5 receptors, respectively. ***B*** summary data showing the decrease of charge after drugs application (VL in green, VM in red, CL in blue, undefined location in black;n=10 in total). *** p<0.001. For full statistical report see Online Table 4.

Our results indicate that the synaptic transmission at cerebello-thalamic synapses in VL, VM and CL are glutamatergic, which matches previous *in vivo* findings on the excitatory responses of VL neurons evoked by microstimulation of the brachium conjunctivum or the neurons in CN [91, 92, 380, 389]. To elucidate whether these excitatory postsynaptic

responses where mediated by ionotropic and/or metabotropic receptors we next tested the effects of their selective blockage on the responses to 50 Hz stimulus trains. Upon wash-in of AMPAR-antagonist NBQX the EPSC charge decreased from -74.6 ± 2.4 nA*ms to -28.0 ± 8.3 nA*ms and following the wash-in of NMDAR-antagonist APV the EPSC charge decreased even further to -13.5 ± 4.3 nA*ms (p<0.001, Friedman test; **Figure 4A-C** and Online Table S4). Further application of blockers for the mGluRs most abundantly expressed in thalamic neurons (JNJ for mGluR1 and MPEP for mGluR5 [395, 397] did not affect the remaining current (-12.1 ± 3.9 nA*ms; Friedman test, p=1; **Figure 4D** and Online Table S4), suggesting the absence of a substantial mGluR1- or mGluR5-mediated component in cerebellar transmission on thalamic neurons.

Postsynaptic determinants of variable CN-impact in thalamic cells

Next we evaluated whether the electrophysiological characteristics described above could be linked to the morphology of the thalamic neurons, bearing in mind that in rat thalamus the neuronal morphology in VL, VM and CL neurons varies [367-370, 373, 381, 398]. By reconstructing biocytin-filled neurons throughout the VL, VM and CL nuclei (**Figure 5A**) and analyzing their dendritic branching using a 3D-Sholl analysis (**Figure 5B**) we found that 23 VL neurons on average show a more elaborate branching pattern than the 14 CL neurons at 55 μm distance from the soma (p<0.05, 2-way ANOVA; Mann Whitney comparison, **Figure 5C,D** and Online Table S5). The number of proximal dendrites (VL: 8.13 ± 0.47; VM: 7.83 ± 0.83; and CL: 6.83 ± 0.34) was not significantly different between nuclei (p=0.115, K-W test; **Figure 5E** and Online Table S5). To better illustrate the dendritic architecture of cells in each of the three defined nuclei we also quantified the radial distance between dendrites at 15 μm from the soma. We found no significant difference in the distance (VL: 40.2 ± 2.6 degrees; VM: 41.1 ± 3.5; CL: 47.0 ± 2.8; p=0.14, K-W test; **Figure 5F,G** and Online Table S5). Although limited, these morphological distinctions between the neurons in VL, VM and CL in combination with the electrophysiological characteristics, suggest differential impact of cerebellar input to thalamic neurons.

Distribution and morphology of reconstructed CN terminals

Previous anatomical studies in rats suggested that in VL cerebellar terminals are larger than those in intralaminar nuclei [84]. To further characterize the identity of cerebellar terminals that we optogenetically stimulated, we stained the slicing containing the patched neurons for VGluT2 and assessed the morphology of the cerebello-thalamic contacts for each recorded neuron using high magnification confocal microscopy (**Figure 6A**).

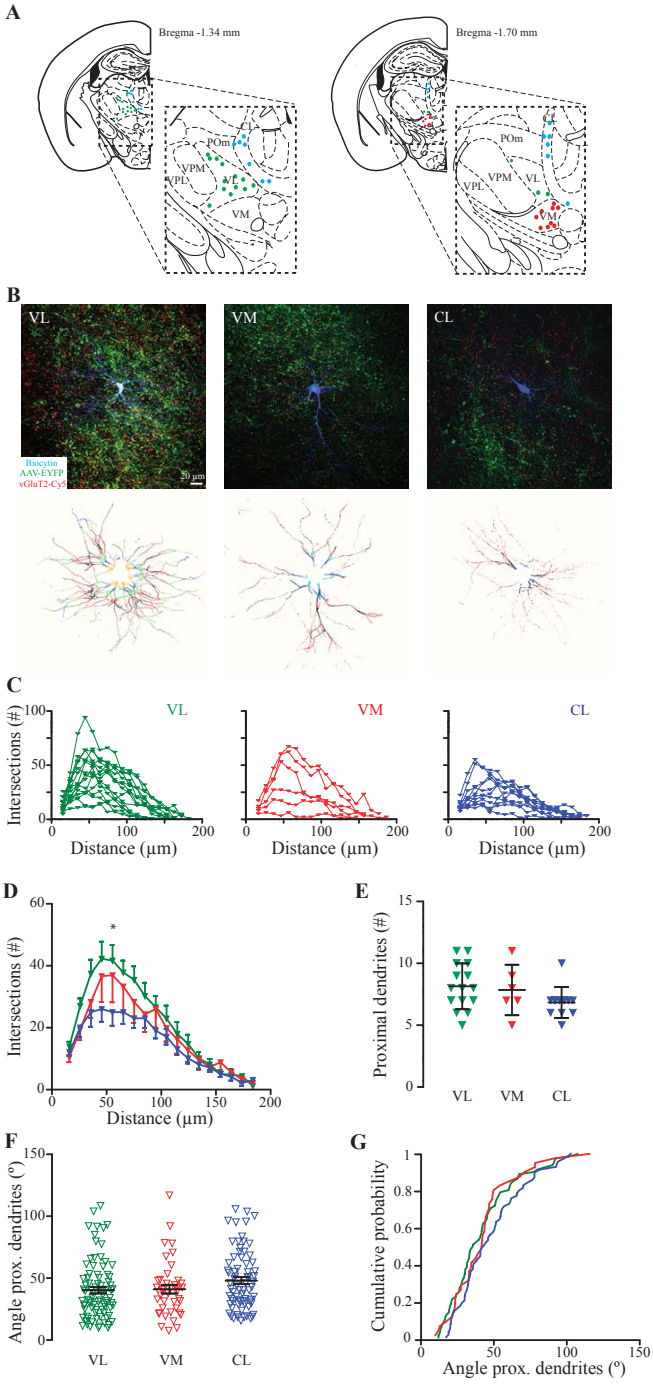

Figure 5. Morphological characterization of thalamic cells recorded in VL, VM and CL.

A Location of all recorded cells in VL, VM and CL projected on two coronal planes [422] ***B*** (top) maximum projections of the somatodendritic morphology of biocytin-filled cells (blue), surrounding ChR2-EYFP labelled CN axons (green) and vGluT2-staining (red) for VL (left), VM (middle) and CL (right). (bottom) maximum projections of 10 µm-thick 3D-spheres surrounding an example neuron from VL, VM and CL (as indicated by the different colors along dendritic trees). ***C*** Sholl analysis shows dendritic arborisation by the number of intersections of the concentric spheres for VL (left), VM (middle) and CL (right) (VL: n=15; VM: n=6; CL: n=11). ***D*** average number of dendritic intersections is shown in 10 µm steps from the soma and each nucleus. ***E*** number of proximal dendrites as quantified at 15 µm distance from soma for VL, VM and CL (VL: n=15; VM: n=6; CL: n=11). ***F*** directionality of proximal dendrites (at 15 µm from soma center) determined by the angle between individual dendrites. Note that the angle is proportional to the angular distance between two neighboring dendrites. ***G*** cumulative distribution of data represented in panel *F*. * $p<0.05$, ** $p<0.01$. For full statistical report see Online Table 5.

The number of vGluT2-positive CN axon terminals on the recorded cells did not vary significantly between the nuclei (VL: 4.5 ± 0.7; VM: 3.66 ± 1.17; CL: 3.08 ± 0.83; p=0.37, K-W test, **Figure 6C**, Online
Table S6) neither their distance from soma (VL: 26.7 ± 1.9 µm; VM: 33.8 ± 5.7 µm; CL: 26.6 ± 2.5 µm; p=0.58, K-W test, **Figure 6D**; Online Table S6). To enhance the *x-y* resolution and reduce the blurring caused by the point spread function, we deconvolved the images and selected the vGluT2-positive terminals to measure their volume (**Figure 6B**). We found that terminals onto recorded VL neurons had a larger volume (11.67 ± 1.30 µm^3) than those onto recorded CL neurons (CL: 7.23 ± 1.57 µm^3) (p=0.02, K-W test, **Figure 6E-F** and Online Table S6), whereas no significant differences were found comparing VM terminals (9.26 ± 1.93 µm^3) to VL and CL (p=1.00 and p=0.35, respectively, K-W tests, **Figure 6E-F** and Online Table S6).
To further investigate CN axon terminal dimensions and characteristics of the post-synaptic structures we studied synaptic contacts at the ultrastructural level. Representative examples of the synaptic profiles formed by BDA-stained CN axons and thalamic neurons are shown in **Figure 7A**. Measurements made from the profiles included terminal surface, number and size of mitochondria, dendritic diameter, PSD length and number of release sites per terminal (**Figure 7B**). Although we observed in the fluorescent images that the terminal size was significantly different between VL and CL, at the ultrastructural level the difference was not significant even though on average VL terminals appeared to be bigger (VL: 2.35 ± 0.38 µm^2; VM: 2.07 ± 0.31 µm^2; CL: 1.23 ± 0.11 µm^2 p=0.099, K-W test). We did observe a significant difference in the mitochondrial surface between VL and CL (VL: 0.13 ± 0.01 µm^2; VM: 0.10 ± 0.01 µm^2; CL: 0.06 ± 0.005 µm^2; VL vs VM p=0.034; VL vs CL $p<0.001$; VM vs CL $p< 0.001$; K-W test; **Figure 7B** and Online Table S7). Another characteristic of cerebello-thalamic synapses we could observe in all three nuclei is that most terminals contained several release sites (VL: 2.97 ± 0.38; VM: 3.08 ± 0.47; CL: 2.96 ± 0.29; p=0.667; K-W test) [348].

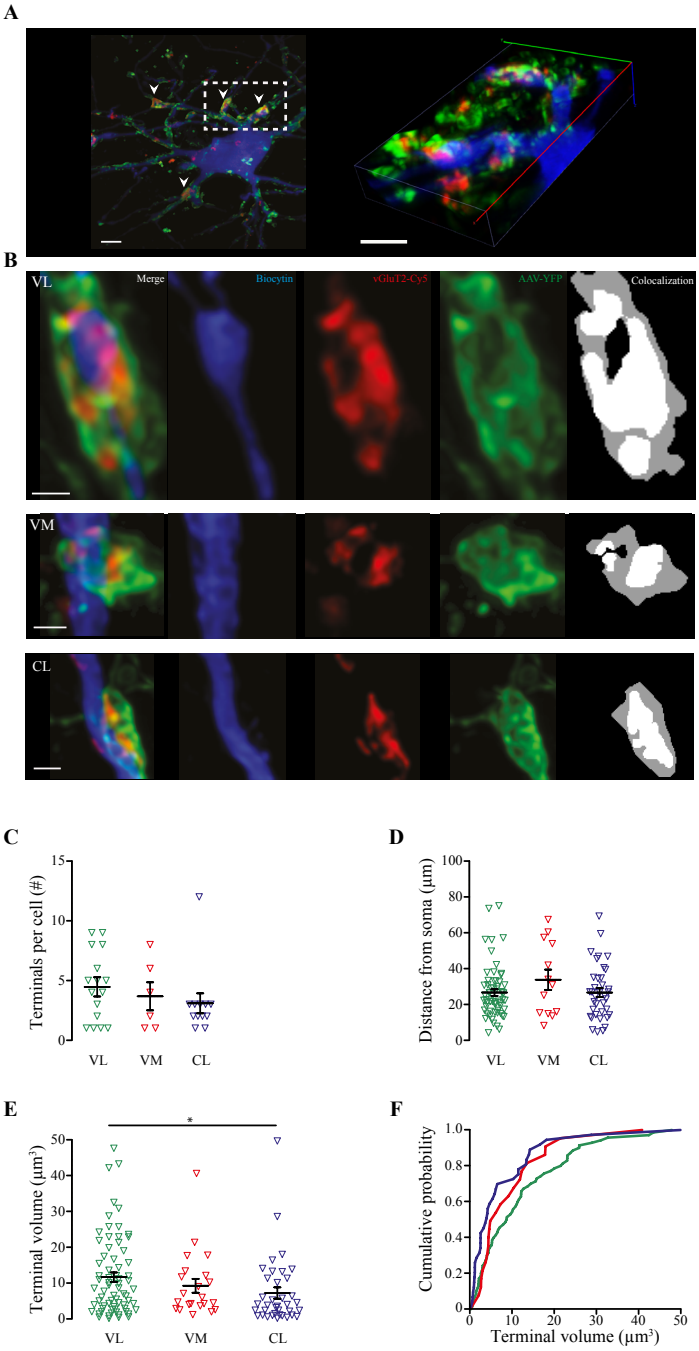

Figure 6. CN terminals of variable volume are similarly positioned along dendrites of recorded thalamic neurons.

A maximum intensity projection of Z-stack image (22 µm thick) of biocytin filled neuron (blue: streptavidin-Cy3; green: ChR2-YFP terminals; Red: vGluT2-Cy5. Arrowheads indicate the vGluT2-positive terminals onto proximal thalamic dendrites. ***B*** summary data of reconstructed vGluT2-positive terminals (VL: n = 16; VM: n = 6; CL: n = 12). ***C*** summary data of distance of reconstructed terminals from soma (VL: n = 60; VM: n = 13; CL: n = 37. ***D*** (left four panels) example of isolated terminals (blue: thalamic dendrite; red: vGluT2; green: CN terminal). (right panel) colocalization of ChR2-EYFP and vGluT2-staining to identify active terminals and calculate their volume based on ChR2-EYFP signal. ***E*** terminal volume (VL: n=71; VM n=22; CL n=37). ***F*** cumulative distribution of terminal volume (data as in panel *E*). * $p<0.05$. For full statistical report see Online Table 6.

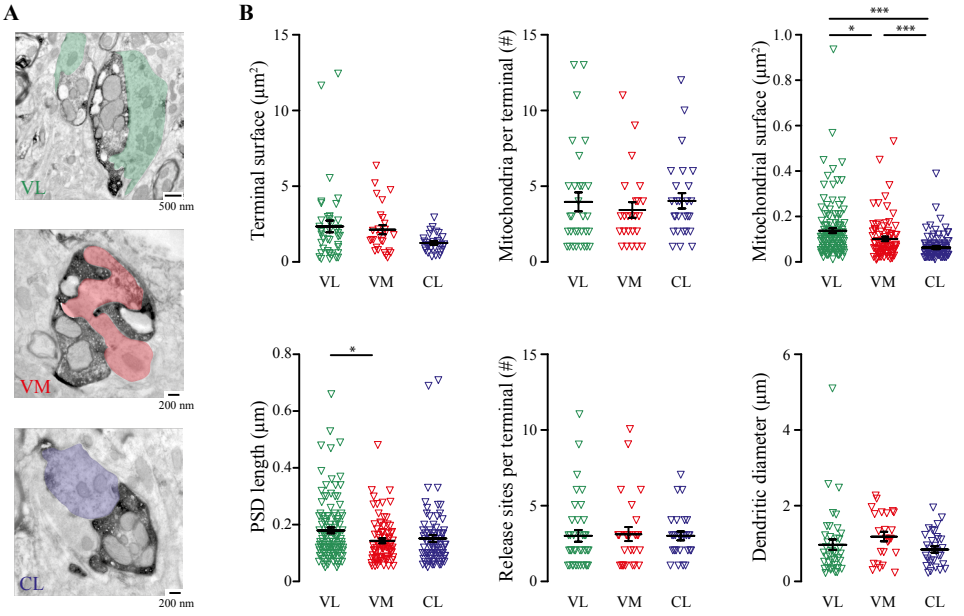

Figure 7. Ultrastructure of CN terminals in VL, VM and CL reveals pre- and post-synaptic specialization.

A Pseudo-colored ultramicrographs of CN terminal in VL (top), VM (middle) and CL (bottom). Note the complex structure of these terminals. ***B*** Quantification of terminal surface (top left; VL: n=48; VM: n=28; CL: n=27, number of mitochondria (top middle; VL: n=32; VM: n=27; CL: n=24;), mitochondrial surface (top right; VL: n=124; VM: n=109; CL: n=82; VL vs VM $p=0.034$; VL vs CL $p<0.001$; VM vs CL $p<0.001$, K-W tests), length of post-synaptic density (PSD) (bottom left; VL: n=114; VM: n=81; CL: n=80; VL vs VM $p=0.024$; VL vs CL $p=0.055$; VM vs CL $p=1$; K-W test), release sites per terminal (bottom middle; VL: n=37; VM: n=27; CL: n=26; $p=0.667$, K-W test) and diameter of the contacted dendrite (bottom right; VL: n=40; VM: n=31; CL: n=25; $p=0.080$, K-W test). * $p<0.05$, *** $p<0.001$. For full statistical report see Online Table 7.

At the post-synaptic side we found that although the dendritic diameter opposing CN terminals did not show any difference between the nuclei (VL: 0.97 ± 0.13 µm; VM: 1.18 ± 0.12 µm; CL: 0.84 ± 0.08 µm; $p=0.08$; K-W test), we did find that length of post-synaptic densities (PSD) were longer in VL (0.17 ± 0.01 µm) compared to VM (0.14 ± 0.01 µm) and CL (0.15 ± 0.01 µm; VL vs VM: $p=0.024$; VL vs CL: $p=0.055$; VM vs CL: $p=1$; K-W

test). Altogether, these ultrastructural findings support the notion that CN axons tend to synapse on proximal dendrites in all three studies nuclei, but that there may be a structural difference in the constellation of the pre- and post-synaptic sites which could correlate to the difference in transmission at CN-synapses throughout the thalamic complex.

Discussion

Our study provides a detailed description of the synaptic transmission at identified cerebello-thalamic synapses in the thalamic VL, VM and CL nuclei onto neurons of which it is known that their axons project throughout various parts and layers of the cerebral cortex, thereby CN axons can exert a strong impact on cortical activity and the encoded behavior. The electrophysiological properties of thalamic neurons in different cerebellar-recipient nuclei were studied with presynaptic optical stimulation and postsynaptic whole-cell recordings. Single-pulse and train stimulation to CN terminals elicited EPSCs of variable amplitudes in thalamic neurons of VL, VM and CL. Still, repetitive stimulation consistently evoked PPD of the responses in VL, VM and CL neurons. The evoked responses in all nuclei were reduced by blockers of ionotropic glutamate receptors, but no further effect was observed upon subsequent application of metabotropic receptors blockers. The differential physiological properties were reflected to some extent by the cellular morphology of VL, VM and CL nuclei as quantified by confocal and electron microscopy.

Our data show that in mouse brain CN neurons innervate the VL thalamic nucleus more densely compared to VM and CL. Although the distribution matches that in other species [89, 348, 362-364, 366, 399, 400] our study does provide one of the first quantitative comparisons of active CN axon terminals in VL, VM and CL, since we exclusively quantified the ChR2-EYFP labeled CN terminals that were co-labeled by vGluT2-staining. Our density values of CN terminals per nucleus (**Figure 1**) may very well be an underestimate given that i) the injections of viral particles did not transfect the complete CN population and ii) the use of vGluT2-antibodies most likely resulted in a limited penetrance into the slices, leaving those CN terminals that are located deeper into the slice unstained. These aspects are also likely to confound the number and location of CN axon terminals on a single thalamic neuron (**Figure 6**) in that there may have been more CN terminals that contributed to the evoked charge transfer, but that due to their location, i.e., depth in the slice, some were identified as vGluT2-negative. Still, we would like to emphasize that the difference in the number of CN terminals between VL, VM and CL is likely to be independent from viral transfection rates or antibody penetrance since these data have been gathered from the

same tissue samples. Our ultrastructural analysis of CN terminals further revealed that, at least for VL, the characteristics described earlier for rat brain, i.e., large terminal surface, fragmented release sites and large diameter of opposing dendritic structure [331, 348, 400], are also found in mouse brain.

The electrophysiological characterization of thalamic responses to CN stimulation revealed that on average VL neurons showed larger EPSCs than those in VM or CL. As expected, these voltage-clamp results translated to a higher chance of action potential firing upon stimulation for VL than for VM and CL when recorded in current-clamp. Our data from VL and VM match earlier reports about faithful action potential firing by VL neurons upon CN or brachium conjunctivum stimulation [91, 92, 349, 380, 389, 401]. Electrophysiological data about CN-CL transmission have not been published before, although recent data indicate that responses of CN neurons to optogenetic stimulation may be faithfully transmitted by CL neurons [256]. Previous electrophysiological data gathered in cats indicate that axons from lateral and interposed CN converge on single VL neurons [106, 389]. Given that our viral transfections reached both lateral and interposed nuclei it may be that at least part of the variability in the recorded responses is due to differential origin of the axons. Yet, to our knowledge no data have been published that suggest a differential impact of lateral and interposed axon terminals on downstream targets.

Referring to intracellular *in vivo* recordings, the cerebellar input on VL neurons has been classified as a driver input to neurons in the motor domain of the thalamus [91, 92, 150]. However, several recent papers classify thalamic inputs in more than two categories: in addition to the 'driver' and 'modulator' inputs a third category of 'driver-like' input has been defined [402]. In the tecto-geniculate system the driver-like inputs have also been identified at the anatomical level by medium-sized terminals that contain round vesicles and innervate proximal dendrites, and at the electrophysiological level stable response amplitudes to trains of stimuli of up to 20 Hz [403, 404]. Our *in vitro* data showed that responses in VL neurons to stimulation of CN terminals meet a number of criteria used to define driver inputs [393]: *i*) CN stimulation evokes a large post-synaptic current that *ii*) is solely mediated by ionotropic receptors and *iii*) depresses upon higher-frequency stimulation, *iv*) CN axons form large synaptic boutons that *v*) contact proximal thalamic dendrites. For CN terminals in VM and CL the categorization is less clear, since these only show some of the 'driver' characteristics. They lack mGluR-mediated transmission and proximal terminal location and their terminal volume is smaller. Moreover, the responses of VM and CL neurons to CN stimulation are significantly smaller, and CL neurons tend to show a stable paired-pulse ratio in response to 10 Hz stimulus trains. At the ultrastructural level, we also found a trend, although not significant, to a reduced terminal surface in CL compared to VL and

a significantly smaller CL mitochondrial surface. Given that previous studies revealed that terminals with larger surface have a higher chance to release neurotransmitter compared to smaller terminals [405-407], our data may at least partially explain why the evoked response amplitude and charge in CL were smaller and more variable (**Figure 2**). Further explanation for the difference in post-synaptic responses to CN stimulation between VL and the other nuclei may come from the difference in PSD length, which previously has been linked to neurotransmission efficacy [408].

Paired-pulse depression is suggested to play an important role in information processing by helping the system to adapt to ongoing levels of activity [395, 409, 410]; this aspect may be of particular interest for cerebellar inputs to thalamic nuclei, since the firing rates reported for CN projections recorded *in vivo* range from ~30-100 Hz (as reviewed by [81]). In our current experiments the ChR2 off-kinetics limited us to stimulus frequencies well below the maximal CN firing rates, which may also have prevented us from recording a significant effect of mGluR-receptor blockage, in that the total mGluR-mediated currents in thalamic neurons evoked by a stimulus frequency of 50 Hz tends to be limited (see also [411]). Therefore, we cannot rule out that the activation of either pre- or postsynaptic modulatory mechanisms have affected the responses we recorded, or those that may be recorded *in vivo*. A dedicated set of future experiments should be designed to study the release probability of individual CN synapses in the thalamic nuclei, the data of which will help to further classify the input of CN terminals to the different thalamic nuclei.

Our findings provide new building blocks to construct the frame of reference for the impact of the cerebellar output on thalamic neurons. Given that mouse thalamus VL, VM and CL are free of interneurons, we argue that all our recordings are from thalamic relay neurons that synapse throughout the various regions of the cerebral cortex. By adapting the classification of relay neurons from rat thalamus (reviewed by [373], our data from VL and VM represent matrix (M)-type neurons and data from CL represent intralaminar (IL)-type, which to some extent is supported by the reduced dendritic branching of CL neurons (**Figure 6**). If we assume that the axonal branching of M- and IL-neurons in mouse brain indeed shows lamina-specific termination as described for rat [367, 368, 370, 412], our data indicate that the information conveyed by M-type neurons in VL will excite corticocallosal or pyramidal tract neurons [413] in the middle and output layers of motor cortices [367] that contribute to initiation of movement [414]. In contrast, M-type VM neurons projections are more dense in layer 1 of widespread cortical areas, including the motor-associated, orbital, cingulate and visual areas in the rat [368], activation which desynchronizes cortical activity patterns [349, 415]. For IL-type CL neurons it has been shown that their axons excite striatal, but also cortical neurons affecting motor, premotor, parietal, prelimbic and

anterior cingulate processing, as well as regulating behavioral arousal levels [256, 416, 417]. Although it remains to be investigated how in *in vivo* conditions thalamic responses may differ between the different types of neurons, our study provides new insights into the diversity of the cerebellar impact on thalamo-cortical networks. Thalamocortical activity exhibits two distinct states, i.e., tonic and burst firing, which are related to different conditions such as waking, non-REM state, slow-wave sleep or even epileptogenic activity [418]. Thalamic afferents, like CN axons, are likely to modulate the activity of thalamo-cortical relay neurons from tonic to burst firing and vice versa. Indeed, single-pulse stimulation of CN neurons efficiently stops thalamo-cortical oscillations in epileptic mutant mice [46]. The underlying mechanism may at least partially depend on the variable impact of CN axons on thalamic neurons, as we showed for VL, VM and CL. Also other synaptic inputs, alike glycinergic or cholinergic projections arising from brainstem [419, 420] or GABAergic projections from substantia nigra [421], may further diversify the cerebellar impact on thalamo-cortical processes throughout the various (non-) motor domains.

7

Single-pulse stimulation of cerebellar nuclei desynchronizes epileptic thalamus and cerebral cortex

Submitted to Current Biology:

O.H.J. Eelkman Rooda*, L. Kros*, S.J. Faneyte, P.J. Holland, S.V. Gornati, T.B. Houben, H.J. Poelman, N.A. Jansen, E.A. Tolner, A.M.J.M. van den Maagdenberg, C.I. De Zeeuw and F.E. Hoebeek

*These authors contributed equally

Experimental treatments for refractory epilepsy are currently remarkably diverse and range from no-invasive strategies like cannabidiol supplements and ketogenic diets to invasive deep brain stimulation. In the current era of optogenetic approaches and increasing understanding of neural networks, we revisited the first site that was used for neurostimulation in epilepsy patients, the cerebellum. Utilizing various electrophysiological and anatomical techniques, we addressed how controlling the cerebellar nuclei (CN) activity allows a highly effective control over generalized seizure activity in thalamocortical networks of the well-characterized CaV2.1 mutant mouse line tottering. Our multi-unit activity and single-unit recordings reveal that neuronal activity in thalamic nuclei, which is hypersynchronous during seizures, becomes desynchronized upon single-pulse optogenetic stimulation of CN neurons. We also found that throughout the thalamic complex CN stimulation results in a kaleidoscope of responses. We conclude that this cerebellar mediated desynchronization of thalamic activity is a crucial factor in the anti-epileptic effects of cerebellar stimulation and is well-worth further (clinical) investigation.

7.1 Introduction

Reorganization of local networks in the cerebral cortex following focal insults can facilitate the induction of more widespread hypersynchronized activity [423-427] and thereby lead to generalized seizures [428]. Directly restoring the activity of the cortical networks themselves forms a promising therapeutic strategy [97, 429], but manipulating the activity of upstream brain regions that provide prominent and specific synaptic inputs to these networks may be an interesting alternative. Here, we investigated how optogenetic stimulation of the cerebellar nuclei (CN) or their efferents affects the neuronal spiking patterns during seizures in the thalamus, which forms the major upstream hub of the cerebral cortex [97]. We show that single-pulse stimulation of CN neurons, which provide not only mono-synaptic but also multi-synaptic inputs to the thalamic nuclei [89, 430], is highly effective in stopping generalized absence seizures in tottering mice [46, 283] by instantly reducing synchronicity and rhythmicity in the thalamus. Notably, optogenetic stimulation of CN axons in the thalamic nuclei alone was less effective in stopping seizures than direct stimulation of CN neurons, supporting that the putative relevance of the upstream multi-synaptic cerebello-thalamic pathway is relevant. In between the seizures, thalamic responses to CN stimulation varied from short-latency increases to bimodal, inhibitory and delayed network effects. Our data show that single-pulse stimulation of CN neurons can stop epileptic seizures by desynchronizing thalamic neuronal firing, and they highlight the importance of cerebellar activity for controlling thalamo-cortical information processing in general.

7.2 Methods

Data were collected from male and female homozygous *tottering* mice (4- to 30-weeks-old) and their wild-type littermates, which were bred using heterozygous mice. The colony, originally purchased from Jackson laboratory (Bar Harbor, ME, USA), was maintained using C57BL/6NHsd mice obtained from Envigo laboratories (Horst, the Netherlands). PCR was used to confirm the presence of the tottering mutation in the *Cacna1a* gene using 5′-TTCTGGGTACCAGATACAGG-3′ (forward) and 5′-AAGTGTCGAAGTTGGTGCGC-3′ (reverse) primers (Eurogentech, Seraing, Belgium) and subsequent digestion using restriction enzyme *Nsb*I at the age of P9 - P12. All surgical and experimental procedures were performed in accordance with the European Communities Council Directive. Protocols were reviewed and approved by the institutional experimental animal committee (DEC).

7.2.1 Viral infection

Stereotactic viral injections were performed as previously described [46]. Briefly, the mice were kept under anesthesia in a custom made stereotactic frame. Craniotomies in the sagittal bone allowed us access to the cerebellar surface. We bilaterally injected virus-containing solutions (100 to 120 nL at a rate of ~20 nL/min) to transfect neurons in the interposed and lateral CN with Channelrhodopsin-2 (AAV2-hSyn-Chr2(H134R)-EYFP) [431]. After 10 minutes the injection pipette was slowly retracted and optic fibers were implanted ~200 μm above the injection site. Stereotaxic coordinates for CN injections were 2.5 mm posterior to lambda, 2.2 mm lateral to the midline and 2.2 mm below the pial surface. Viral vectors were originally designed by Dr. K. Deisseroth and were acquired from the University of North Carolina vector core.

7.2.2 Preparation for freely behaving recordings

Chronic electrode implantation was performed under isoflurane anesthesia (induction 4%; maintenance 1.5% in oxygen-enriched air) at the following coordinates (mm to bregma): -1.0 AP; +3.5 ML; -0.6 DV (right S1; single 75 μm platinum (Pt)/iridium (Ir) electrodes, PT6718; Advent Research Materials, Oxford, UK); or 1.0 mm AP; -1.5 mm ML; -0.6 mm V (right M1; single Pt/Ir electrodes) for LFP recordings; -1.3 mm AP; +1.25 mm ML; -3.1 mm DV (right VL; paired Pt/Ir); or -1.8 mm AP; +0.75 mm ML; -3.0 mm V (right CL; paired Pt/Ir); or -1.8 mm AP; +1.6 mm ML; -3.0 mm V (right VPL/VPM; paired Pt/Ir) for MUA recordings; two ball-tip electrodes (Ag, 75 μm) were positioned just posterior from lambda above cerebellum to serve as reference and ground electrodes. To enable optogenetic control of neuronal activity in CN, mice received 2 craniotomies in the interparietal bone for viral vector injection and placement of two optical fibers (200 μm diameter; CFML22L05, Thorlabs, Newton, NJ, USA) (-2.5 mm relative to lambda; 2.0 ML; 2.0 DV). CN were stereotactically injected bilaterally with 100-150 nl of the AAV2-hSyn-ChR2(H134R)-EYFP vector (kindly provided by Dr K. Deisseroth from Stanford University through the Vector Core at the University of North Carolina). Electrodes were connected to a 7-channel pedestal (E363/0 socket contacts and MS373 pedestal; Plastics One, Roanoke, VA, USA) and secured to the skull together with the optic fibers using light-activated bonding primer and dental cement (Kerr optibond / premise flowable, DiaDent Europe, Almere, the Netherlands) Carprofen (5 mg/kg, s.c.) and Temgesic (0.1 mg/kg, s.c.) was administered for post-operative pain relief.

7.2.3 Preparation for head-fixed in vivo recording

Male and female mice were anesthetized with a mixture of isoflurane (2% mixed with O_2. Body temperature was supported by a heating pad (FHC, Bowdoin, ME, USA). ECoG electrode implantation in M1 and S1 cortices was performed as previously described [46]. To enable extracellular recordings from thalamic neurons, a subset of mice received bilateral craniotomies (~ 1.5 mm diameter) in the parietal bone and great care was taken to preserve the dura mater. In another subset of mice the thalamic complex was implanted with optic fibers. These fibers were positioned using the following coordinates (in degrees (°) relative to the interaural axis and in mm relative to bregma): VL: 22° roll angle, -1.2 AP, -3.0 ML, -3.1 depth; VM: 2° roll angle, -1.2 AP, -1.1 ML, 3.3 depth; CL/CM: 0° roll angle, -1.3 AP, -0.75 ML, -3.0 depth; zona incerta: 0° roll angle, -2.5 AP, -1.75 ML, -3.6 depth). The positioning of the optic fibers was confirmed using immunofluorescent staining (see below). The exposed tissue was surrounded by a recording chamber, covered with tetracycline-containing ointment (Terra-cortril; Pfizer, New York, NY, USA) and sealed with silicon wax (Twinsil speed; Picodent, Wipperfurth, Germany). To allow the use of precise stereotactic coordinates during recording sessions we marked the position of bregma. After surgery, the mice recovered for at least five days in their home cage before experiments were performed.

7.2.4 *In vivo* extracellular electrophysiology

Following ~2-hour daily accommodation session in the setup on the first two days we performed recordings in awake, head-fixed mice on the third day lasting no longer than 4 hours. Although being head-fixed, the mice were able to move all limbs freely. The recording sessions typically were between 9:00 and 17:00, i.e., during the light period. Body temperature was supported using a heating pad (FHC). For extracellular single-unit recordings, custom-made, borosilicate glass capillaries (OD 1.5 mm, ID 0.86 mm; resistance 8–12 MΩ; taper length ~5 µm; tip diameter 0.5 µm) (Harvard Apparatus, Holliston, MA, USA) filled with 2 M NaCl were positioned stereotactically using an electronically driven pipette holder (SM7; Luigs & Neumann, Ratingen, Germany). Stereotactic coordinates for the thalamic recordings were tailored to the different thalamic nuclei. Thalamic neurons were localized by stereotactic location and a subset of recording sites was identified using iontophoretic injections of biocytin (1.5%, ~ 1 min, 4 sec on/off, 50% duty cycle, 4 µA), which was present in the NaCl-filled recording pipette.

ECoG recordings were filtered online using a 1–100 Hz band pass filter and a 50 Hz notch filter, sampled at 500 Hz and amplified before being stored for off-line analysis. Single-unit extracellular recordings were filtered online using a 30 Hz high pass filter and a 50 Hz notch

filter, sampled at 20 kHz and stored for off-line analysis. All electrophysiological recordings were performed using either a combination of CyberAmp 380 (Molecular Devices, LLC, Sunnyvale, Ca, USA), Neurodelta IR 183A or IR283A (Cygnus Technology Inc., Delaware Water Gap, PA, USA) and CED power 1401-3 (Cambridge England), or the combination of Multiclamp 700B and Digidata 1322A (Molecular Devices).

7.2.5 Optogenetics and electrophysiology in head-fixed *in vivo* preparation

For extracellular recordings combined with optogenetic CN or thalamic stimulation brief pulses (50 ms) of blue (470 nm) light were used to activate ChR2-infected CN neurons. Optic fibers (for CN stimulation: inner diameter = 200 μm, numerical aperture (NA) = 0.39; for thalamic stimulation: inner diameter = 105 μm, NA = 0.22; Thor Labs, Newton, NJ, USA) were placed ~200 μm from the injection site and connected to 470 nm LED sources (Thor Labs). Light intensity at the tip of the implantable fiber was 550 ± 50 μW/mm^2. We chose these optic fiber diameters following estimation of the light intensity in the brain so as to ensure that in CN sufficient neurons would be activated and that in thalamus a sufficient number of CN axons were activated. LEDs were activated for 50 ms at 0.2 Hz or by a closed-loop GSWD-detection system [46, 158].

7.2.6 Freely behaving electrophysiological recordings and optogenetic stimulation

After a 2-3 weeks recovery period, electrophysiological recordings were performed in freely behaving animals as described previously [432]. Electrophysiological signals were 3x pre-amplified and fed into separate ECoG (0.5-500 Hz, 800x gain) and MUA amplifiers (500-5,000 Hz; 12,000X gain). Signals were digitized (Power1401 and Spike2 software; CED) at 5,000 Hz (ECoG) or 25,000 Hz (MUA). Synchronized video-recordings made using a digital CCD camera at 30 frames/s (acA1300-60gmNIR; Basler, Ahrensburg, Germany). Optic fibers were connected to 470 nm LEDs (Thor Labs). Manual stimulation was performed to test efficacy of single pulse stimulation (0.5 mW/mm^2, 50 ms) for the disruption of GSWDs using a pulse generator (Prizmatix, Givat-Shmuel, Is) as previously described [46].

7.2.7 Pharmacological modulation of CN neurons

Procedure to increase CN action potential firing was performed as described previously [46]. Briefly, we located CN neurons after which we recorded one hour of 'baseline' ECoG. After this an injection was made with 100 μM gabazine ($GABA_A$-antagonist; Tocris)

dissolved in 1 M NaCl combined with fluorescence of Evans Blue (1% in 1 M NaCl) for histological verification. Next, we recorded during 20-50 min after the injection thalamic activity. The data on GSWD-occurrence following gabazine injection from 4 out of the 6 mice have been reported previously (**Fig. 2** in ref [46]).

7.2.8 Immunohistochemistry

Animals were anesthetized with pentobarbital (0.15 mL, intraperitoneal) immediately after acquiring the postinjection ECoG and perfused transcardially with saline followed by 4% paraformaldehyde (Sigma-Aldrich) in 0.1 M phosphate buffer (Sigma-Aldrich, pH = 7.4). Brains were removed and postfixed for 1–3 hours in 4% phosphate-buffered paraformaldehyde at room temperature, placed overnight in 10% sucrose in 0.1 M PB at 4°C and subsequently embedded in gelatine with 30% sucrose. We serially collected 50-µm-thick coronal sections for immunofluorescent staining. Cerebellar sections were incubated for 10 min with DAPI (300 nM) to verify the locations of viral injections and diencephalic sections were processed for parvalbumin staining (primary staining: 1:7,000 α-mouse, Swant #Pv-235; secondary staining: 1:200 mouse-α-donkey, Jackson Immunoresearch #715-175-150 (Westgrove, PA, USA) to locate thalamic nuclei and for biocytin staining to locate the recording sites. We confirmed the correct localization of the injections of gabazine and biocytin with images captured using a confocal laser scanning microscope (LSM 700; Zeiss, Lambrecht, Germany) at 555 nm (Evans Blue, Sigma), 488 (ChR2-EYFP) and 647 nm (parvalbumin).

7.2.9 Offline GSWD and extracellular action potential analysis

Both analysis of extracellular recordings and spontaneous GSWD characteristics were performed using previously described offline statistical analysis [46]. In brief, action potential analysis was performed using custom-written Matlab-based program SpikeTrain (Neurasmus, Erasmus MC Holding, Rotterdam, the Netherlands). Extracellular recordings were included if activity was stable and well isolated for at least 100 s. GSWD analysis was performed using a custom-written GSWD detection algorithm (LabVIEW, National Instruments, Austin, TX, USA). Co-efficient of variance (CV) was calculated as the ratio between the average and standard deviation of the interspike intervals (σ_{ISI}/μ_{ISI}), CV2 as $(2|ISI_{n+1} - ISI_n|/(ISI_{n+1} + ISI_n))$ [287] and burst index as (BI = number of action potentials within bursts / total number of action potentials) for which we defined 'burst' as a sequence of ≥3 spikes within 100 ms.

7.2.10 Offline MUA analysis

MUA data were analyzed using the template-matching method for spike sorting with an optimal spike threshold of 3 times SD from a 60-sec baseline recording. Sorted spikes were exported and analyzed following a custom-written algorithm in MATLAB to generate spike histograms. The spike-to-spike correlation (autocorrelation) was plotted based on a previous method [433]. Data points (x) were normalized (X_s) in a [0,1] range using the maximum spike count (x_{max}) and the minimum spike count (x_{min}): $X_s = x - x_{min} / x_{max} - x_{min}$. Mean correlation values were calculated by taking the ratio of the greatest correlation peak and the peak at t=0. The same time range was used to determine the greatest correlation in baseline and post-stimulation. Trials were included when the seizure ended 10 ms before stimulation and 150 ms after stimulation.

7.2.11 Assessment of modulation of TRN units

GSWD triggered rasterplots and peri-stimulus-time-histograms (PSTHs; 5 ms bin width) were used to calculate the modulation amplitude and frequency. ISIs of the data used for the rasterplots were subsequently shuffled randomly 500 times to create a normal distribution of modulation amplitudes. Cells were considered GSWD-modulated if the modulation amplitude was significantly higher than expected by chance, as indicated by a Z-score ($Z = (X-\mu)/\sigma$; $Z \geq 1.96$, $p \leq 0.05$) using the shuffled data as described previously [46], and if cells modulated at seizure frequency (6–9 Hz). The phase difference between the occurrence of the most negative deflection of a GSWD-episode and the time of the peak in thalamic activity was calculated by dividing this time difference by the median time difference between two GSWDs in that particular seizure.

7.2.12 Response of optogenetic stimulation

To determine if thalamic single units were significantly modulated following optogenetic CN stimulation we performed a random permutation calculation following a Monte-Carlo Bootstrap method, using 2 ms bin width PSTHs. For every recording we calculated the ISIs of action potentials 4 s prior to every pulse and combined them in a single ISI distribution, which was randomly permutated 250 times. We created PSTHs from these 'fake' spike times and calculated the average and standard deviation. If the PSTH of the 'true' spiking response to optogenetic stimuli breached the mean + 2SD threshold we noted the recording to have an increased firing response. For a subset of neurons we noticed a compelling inhibition. We marked the recording to have a decreased firing response if at any time during the post-stimulus period (5 s in total) 25 consecutive bins, i.e., 50 ms, the spike count was zero.

7.2.13 Assessment of fluorescence in thalamic nuclei

Guided by a reference atlas [434] we outlined the thalamic nuclei of interest. For each nucleus the expression pattern of ChR2-YFP was quantified with RGB measure function of Fiji (ImageJ) to calculate the mean intensity (in arbitrary units; a.u.) among the region of interest (ROI).

7.2.14 Interictal ECoG analysis

Analysis of EcoG data was performed with the fieldtrip toolbox (http://www.fieldtriptoolbox.org) in MATLAB. For the optogenetic data, stimuli that occurred during manually identified inter-ictal periods were extracted and subsequently any found to contain artefacts or short periods of increased oscillatory activity were removed from further analysis. Extracted epochs contained 4 s of activity both before and after the stimulus and data was bandpass filtered between 2 and 125 Hz prior to further analysis. Replacement of the stimulus artefact was performed by removing the section of data 700 ms prior to the stimulus to 300 ms after the stimulus and replacing it with a section of data extracted from 3 s prior to the stimulus on a trial by trial basis the ends of the replaced section were then smoothed to reduce edge effects. Spectrograms were calculated using Morlet wavelets with a width of 7 and evaluated at every sample.

For the Gabazine injection data, 100 epochs of 10 s were extracted from inter-ictal periods prior to injection (Baseline), immediately following injection (Early Post) and after ~1 hr (Late Post). Epochs with artefacts were rejected on the same basis as for the optogenetic data. The frequency content of the signals was calculated using Morlet Wavelets and normalized to the total power in the 2 to 115 Hz frequency band.

7.3 Statistical analysis

We examined the variance in each group using Kolmogorov-Smirnov and Shapiro-Wilk's test for normality. We analyzed the data using parametric (two-samples, one/two-tailed Student's *t*-test or (repeated measures) (M)ANOVA) or non-parametric (one/two-tailed Mann-Whitney U) depending on whether data was normally distributed. For the ECoG data statistical analysis of the power in each frequency band was carried out via repeated measures ANOVA with time point (Baseline, Early Post and Late Post) as the within-subject factor and recording location as the between subject factor. Only frequency bands which displayed a significant main effect of time point were subjected to post-hoc paired sample *t*-tests, Bonferroni-corrected *p*-values are reported in the figure legends. $P < 0.05$ is

considered significantly different. A single asterisk indicates $p < 0.05$, two asterisks indicate $p < 0.01$, three asterisks indicate $p < 0.001$.

7.4 Results

7.4.1 Cerebellar nuclei stimulation desynchronizes thalamic spiking activity

To examine the effects of CN stimulation on seizure-related thalamo-cortical neuronal activity patterns we recorded neuronal multi-unit activity (MUA) throughout the thalamic complex while monitoring cortical activity by ECoG in awake, freely behaving *tottering* mice (**Fig. 1A-C**). We observed that cortical generalized spike-and-wave discharges (GSWDs) were accompanied by rhythmic neuronal firing, i.e., characteristic for synchronized firing, in the thalamic complex. During interictal periods, however, thalamic MUA was relatively arrhythmic, i.e., characteristic for desynchronized firing (**Fig. 1C**).

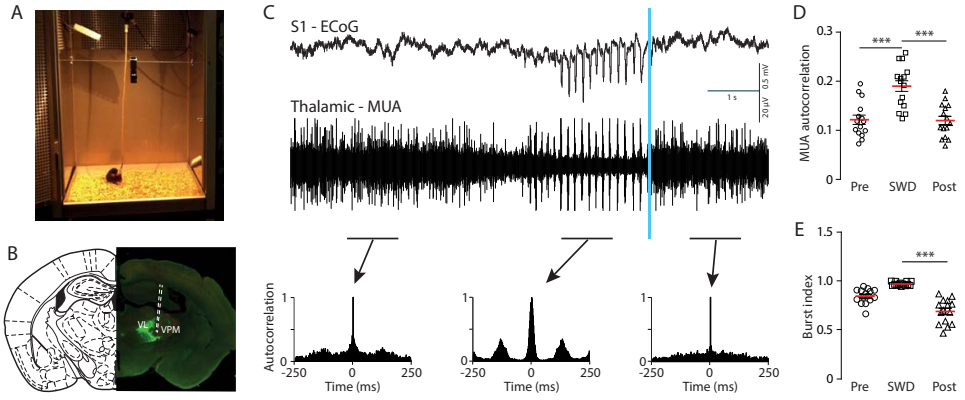

Figure 1. Single-pulse optogenetic CN stimulation stops rhythmic thalamic spiking.

(**A**) Tethered recording system for optogenetic stimulation in CN and thalamic neuronal multi-unit activity (MUA) and ECoG recordings from primary motor (M1) and sensory (S1) cortices in freely behaving *tottering* mice. (**B**) ChR2-EYFP-expressing CN axons in the thalamus complex with the location of the MUA electrode indicated by white-dashed lines. (**C**) (*Top - middle*) Example of spike-and-wave discharges (SWDs) in S1-ECoG (*top*) in synchrony with thalamic MUA (*middle*), during which mice developed behavioral arrest. Single-pulse optogenetic stimulation (vertical blue line; 50 ms, 470 nm, 0.5 mW/mm^2) in CN stopped synchronous burst firing in thalamic neurons and ended the SWDs, upon which behavioral arrest was typically ended. On average, SWDs occurred every 72.6 ± 19.8 s (N = 8 mice, 1-hour recording per mouse). (*Bottom*) Accompanying normalized autocorrelograms of MUA in 1-second periods of the pre-SWD, SWD and post-SWD phase. (**D**) Average MUA autocorrelation for pre-SWD, SWD and post-SWD multi-unit recordings. (**E**) As (D) but for burst index. Data are represented as mean ± SEM. * indicates $p < 0.05$, *** indicate $p < 0.001$ (see Online **Suppl. Table 1** for statistics).

Termination of seizure activity by optogenetic CN stimulation (single-pulse, 50 ms, 470 nm) (see also [46]) instantly reverted the phase-locked thalamic MUA to a desynchronized state, as shown by a reduction of the MUA autocorrelation (**Fig. 1C,D** and **Online Suppl. Table 1**). We also found that upon ictal CN stimulation the MUA burst index reverted to baseline levels (**Fig. 1E**). These findings indicate that single-pulse CN stimulation can consistently desynchronize seizure-related rhythmic thalamic MUA.

7.4.2 Thalamic responses to single-pulse cerebellar nuclei stimulation is variable

Our MUA recordings of thalamic neurons suggest that single-pulse stimulation in CN, which was shown to promote synchronous action potential firing [46], may have a differential effect on thalamic neurons. To further investigate the thalamic responses to CN stimulation, we recorded single-unit responses during interictal periods in head-fixed *tottering* mice (see STAR experimental procedures). Out of the 201 recorded neurons 165 neurons were responsive to single-pulse CN stimulation (50 ms pulse of 470 nm and 0.5 mW/mm^2 at 0.2 Hz) (**Fig. 2A**). Both the response latency and the type of response were variable (**Fig. 2B-D**) (see also **Suppl. Fig. 1** and **Online Suppl. Table 2**).

We observed a significant negative correlation between the pre-stimulus firing frequency and the number of spikes during the pulse (**Fig. 2C**). Most thalamic neurons increased their firing rate during CN stimulation (group 'increased'; 114 out of 165 neurons; 69.1%). Other thalamic neurons responded in a bi-phasic manner, i.e. following the initial excitatory response the firing rate was significantly reduced (group 'bi-phasic'; 17 out of 165; 10.3%). Again other thalamic neurons only showed a reduction of their firing rate upon CN stimulation (group 'decreased'; 15 out of 165; 9.1%). Finally we recorded neurons that did not show a significant response during the 50-ms stimulus, but only thereafter (group 'delayed'; 19 out of 165; 11.5%). Given that in a mouse brain the CN projection neurons that synapse onto thalamic neurons are known to be glutamatergic [245, 259], these recordings of bi-phasic-, decreased- and delayed-responses are most likely representing a combination of direct CN-input and additional afferent input possibly gated via CN-afferents to pre-thalamic nuclei [430]. To investigate the impact single-pulse CN stimulation has on cortical activity we analyzed M1 and S1 ECoG activities. As shown in the ECoG traces single-pulse CN stimulation resulted in a clear change of frequency and amplitude (**Fig. 2E,F**). A broadband decrease in power was observed lasting ~1 s; the most prominent suppression was found within in the seizure-related θ*-band (7-10 Hz) across the recording sites. We found that this response was reliably evoked, as can be seen from the averaged responses and power spectrogram (**Fig. 2G,H** and **Online Suppl. Table 3**).

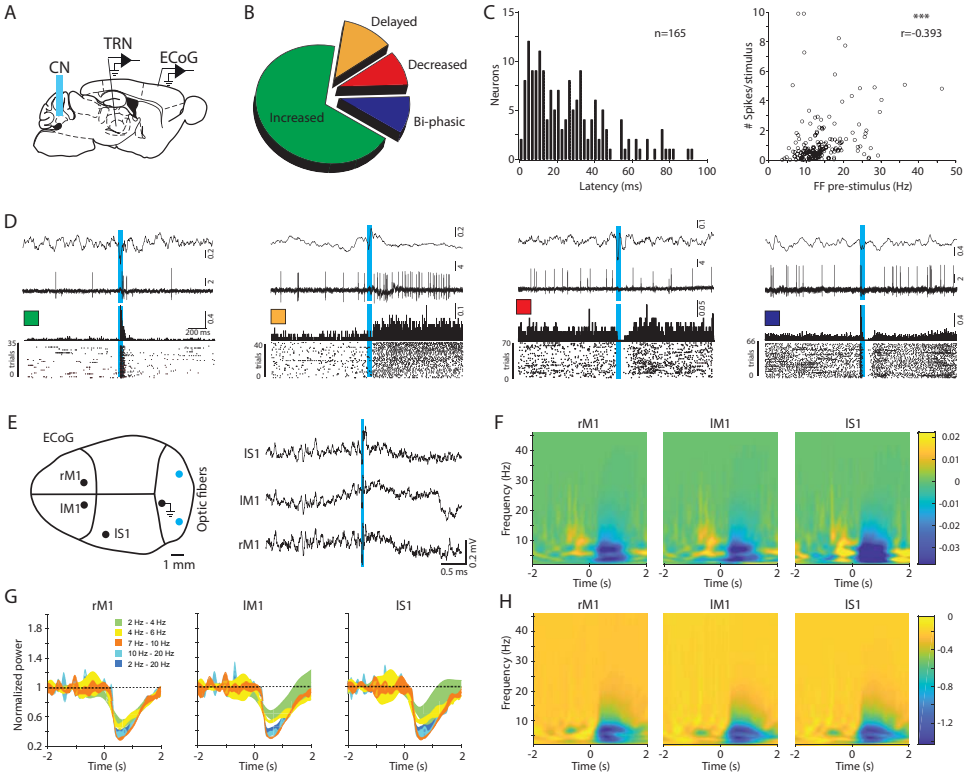

Figure 2. CN stimulation induces variable changes in interictal thalamic firing and cortical activity.

(**A**) Schematic outline of head-fixed experiment in *tottering* mice for CN optogenetic stimulation, single-unit extracellular recordings from thalamic relay neurons (TRN) and multi-site ECoG recordings from M1 and S1 regions. (**B**) Distribution of response types for the 165 thalamic neurons that showed a significant response to CN stimulation (as determined by Z-score based diagnostics; see STAR methods). See main text for number of cells per type of response. (**C**) (*Left*) Cumulative histogram of response latencies of thalamic neurons (n = 165 neurons) to single-pulse (50 ms) CN stimulation. (*Right*) Scatterplot for the correlation between the pre-stimulus firing frequency (FF) and the number of spikes recorded during the CN stimulus (Pearson's correlation coefficient: r = -0.393; $p < 0.001$). (**D**) Example traces of ECoG (*top traces*) and simultaneously recorded TRN (*bottom traces*) with accompanying per-stimulus histograms and scatterplots for each type of response. Green: 'increased' (see also **Suppl. Fig. 1B**); orange: 'delayed' (see also **Suppl. Fig. 1D**); red: 'decreased' (see also **Suppl. Fig. 1E**); and blue: 'bi-phasic' (see also **Suppl. Fig. 1C**). Vertical blue lines indicate time of optogenetic CN stimulation (50 ms). (**E**) (*Left)* Placement of craniotomies for ECoG recording electrodes and optic fibers in CN. (*Right*) Example ECoG trace from left S1 (lS1), left M1 (lM1) and right M1 (rM1) suggesting widespread effect of single-pulse optogenetic stimulation to bi-lateral CN (50 ms). (**F**) Normalized ECoG spectrogram from a single mouse (n = 246 stimuli) calculated following the masking of the large-amplitude ECoG response directly following the CN stimulation – to accurately analyze the post-stimulus response in all frequency bands (see STAR methods). This procedure is also applied to panels G and H. Note the clear drop in all frequency bands. (**G**) Normalized power in the separate frequency bands, indicating that in all recorded cortices a single-pulse CN stimulation resulted in a significant decrease in all channels, or in rM1 θ (4–7 Hz), θ* (7–10 Hz), β (10–20 Hz), and the broadband 2–20 Hz, but not in rM1 δ- (2–4 Hz) and γ (25–40 Hz) bands (N = 7 mice) (see Online **Suppl. Table 3** for statistics). (**H**) Normalized spectrogram accompanying panel G.

7.4.3 Pharmacological intervention of CN activity affects firing patterns of thalamic neurons

We previously showed that infusing $GABA_A$-receptor blocker gabazine (SR-95531) into the CN of *tottering* mice blocked GSWD occurrence and increased the frequency and regularity of CN spike firing [46]. To assess whether such long-term increases in CN firing had differential effects on interictal thalamic firing, as opposed to single-pulse CN stimulation, we recorded the effect of gabazine infusions into CN and found that the firing pattern of thalamic neurons was affected (**Suppl. Fig. 2A-C**). Comparison of the interictal activity recorded before and after gabazine infusion revealed that thalamic spiking contained less bursts and an increased level of regularity, while the average firing frequency was not significantly altered (**Suppl. Fig. 2D** and **Online Suppl. Table 4**). These alterations in thalamic firing indicate that upon gabazine infusion in CN, thalamic neurons shifted from the characteristic burst-pause firing pattern (related to a down-state of the membrane potential) to a more regular firing pattern (related to an up-state of the membrane potential) [99]. In parallel, the power of most ECoG frequency bands was changed (**Suppl. Fig. 2E-G**). Most notably, the power in the seizure-related θ*-band (7–10 Hz) was significantly decreased (**Suppl. Fig. 2H,I** and **Online Suppl. Table 5**). Together these data indicate that pharmacological interventions at the level of the CN affect the interictal firing pattern of thalamic neurons.

7.4.4 Factors contributing to the variability of thalamic responses to CN stimulation

Our current data indicate that single-pulse stimulation at a millisecond timescale and long-lasting pharmacological interventions, both of which increase CN firing [46], have a profound but variable effect on thalamic firing patterns and cortical network activity during interictal periods. This wide range of thalamic responses to optogenetic CN stimulation (**Fig. 2**) may have various causes. It may be that we recorded from different cell types [373]. Hereto we evaluated the firing pattern of thalamic neurons during GSWDs. We observed that 56.6% (69 out of 122 thalamic neurons) of the neurons revealed firing associated with GSWD patterns, i.e. 'GSWD-modulated' (**Fig. 3A-C**) (see also **Suppl. Fig. 3** and **Online Suppl. Table 6**), with a variable level of rhythmic spiking (**Fig. 3C**).

To assess whether the location of the recordings and thereby the afferent connections related to the rhythmic firing could contribute to the wide range of responses to CN stimulation we labelled the recording sites of 70 thalamic neurons (from 8 mice) using iontophoretic injections of biocytin (**Fig. 3D**).

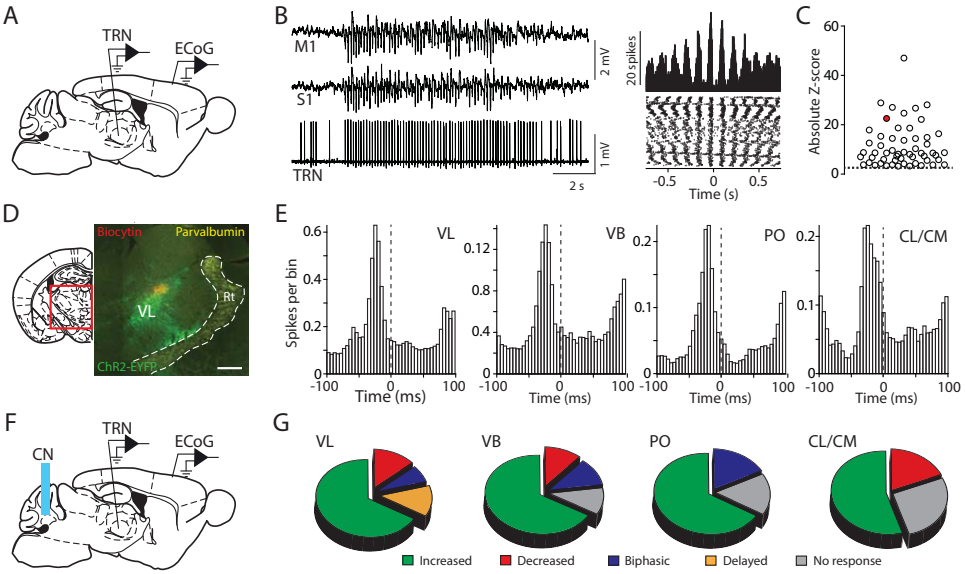

Figure 3. Varying thalamic responses to CN stimulation, but constant modulation by GSWDs.

(**A**) Schematic outline of head-fixed experiment for single-unit extracellular recordings from thalamic relay neurons (TRN) and multi-site ECoG recordings from M1 and S1 regions. (**B**) (*Left*) Typical example of TRN from which the firing becomes strongly associated with M1- and S1-recorded GSWDs. (*Right*) Accompanying per-ECoG-spike-histogram and scatterplot. (**C**) Absolute Z-score range for GSWD-modulated TRN recordings (Z-score = 9.97 ± 0.99; range 1.74 – 47.17; n = 69 cells from 8 mice). Note that all recordings (n = 53) with a Z-score < 1.96 are not represented in this panel for clarity of representation. The red circle indicates the neuron shown in (**B**). (**D**) Schematic and example image of immunohistological staining indicating the thalamic recording location (biocytin, red) in the VL nucleus that is innervated by ChR2-EYFP expressing CN axons (green). Reticular nucleus neurons are stained by parvalbumin (yellow). (**E**) Per-ECoG-spike histogram for all GSWD-modulated neurons recorded in VL (n = 15 cells; 7138 ECoG spikes from 3284 GSWD episodes), VB (n = 4 cells, 2064 ECoG spikes from 1369 GSWD episodes), PO (n = 5 cells, 2342 ECoG spikes from 1149 GSWDs) and CL/CM (n = 7 cells, 1645 ECoG spikes from 1066 GSWD episodes). Note that the time lag between histogram peaks only differs marginally (VL 23.1 ms, VB 16.0 ms, PO 16.2 ms, CL/CM 20.4 ms). (**F**) As (**A**) including optogenetic CN stimulation. (**G**) Proportions of neurons in VL (n = 20 neurons), VB (n = 9 neurons), PO (n = 6 neurons) and CL/CM (n = 11 neurons) that showed an 'increase', 'decrease', 'bi-phasic' or 'delayed' response upon single-pulse CN stimulation.

We found that a subpopulation of neurons throughout the various nuclei showed firing patterns directly associated with ECoG GSWDs. For these neurons the periodicity with the ECoG spikes was remarkably consistent per nucleus, ranging between 16.7 and 23.5 ms (**Fig. 3E**). In sharp contrast to these consistent firing patterns recording during ECoG GSWDs, we found that interictally the responses to single-pulse CN stimulation ranged widely throughout thalamic nuclei (**Fig. 3F**). In VL neurons we found that all recorded neurons changed their firing pattern upon CN stimulation. Most VL neurons increased the firing frequency, but the other response types (decreased, bi-phasic and delayed), which putatively can be linked to a multi-synaptic effect of CN stimulation, were also readily recorded (**Fig. 3G**).

Likewise, in the VB, PO and the intralaminar CL/CM nuclei we found several types of responses to CN firing, albeit that in these nuclei we also recorded several neurons the firing pattern of which did not change (**Fig. 3G**). These findings highlight not only that the various response types are not restricted to a particular thalamic nucleus, but also that throughout the various thalamic nuclei CN stimulation evokes a variety of changes in spiking patterns.

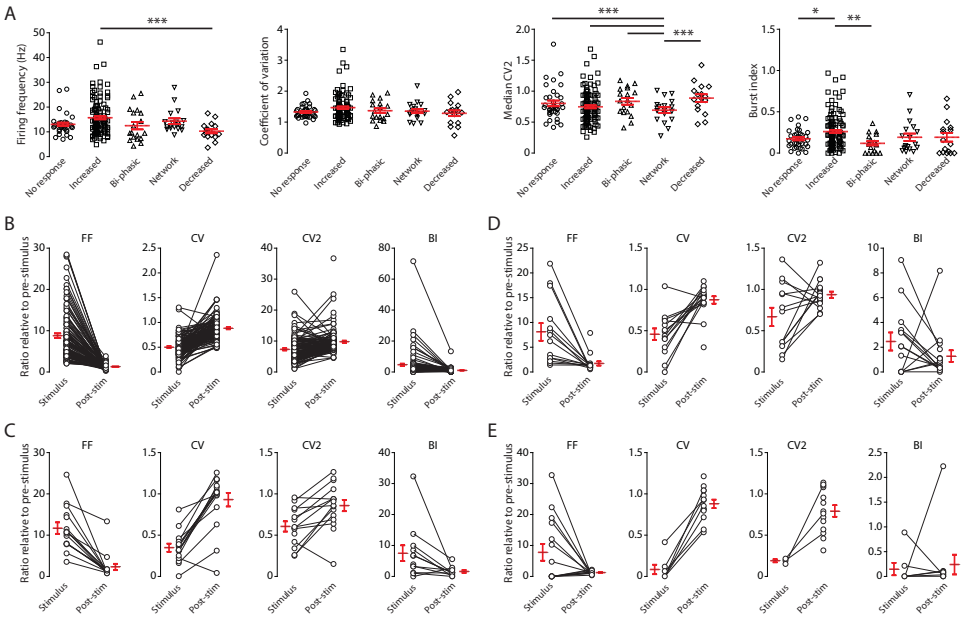

Supplemental Figure 1: Spiking pattern characteristics of thalamic relay neurons in relation to CN stimulation.

(**A**) Pre-stimulus firing frequency, coefficient of variation, median CV2 and burst index recorded from neurons that did not respond with a significantly altered spiking pattern to CN stimulation ('no response'; n = 36 neurons) and from neurons that responded with increased firing patterns during the 50-ms CN stimulation pulse ('increased'; n = 114 neurons), a bi-phasic modulation of spiking during the stimulus and post-stimulus period ('bi-phasic'; n = 17 neurons), a delayed response, i.e., no significant change in firing rate during the CN but only during the post-stimulus period ('delayed'; n = 15 neurons) or solely a decreased firing rate during the stimulus and/or post-stimulus periods ('decreased'; n = 19 neurons). See **Fig. 2D** for typical examples of each type of response. (**B**-**E**) Relative difference in firing frequency (FF), CV, CV2 and burst index (BI) during the stimulus and the post-stimulus period compared to the pre-stimulus period for all 'increased' (**B**), 'bi-phasic' (**C**), 'delayed' (**D**) and 'decreased' neurons (**E**). Only when the number of spikes allowed a calculation of all parameters the data points of the individual recordings are connected. Red markers indicate mean ± SEM. * indicates $p < 0.05$, ** $p < 0.01$ and *** $p < 0.001$. (see Online **Suppl. Table 2** for statistics).

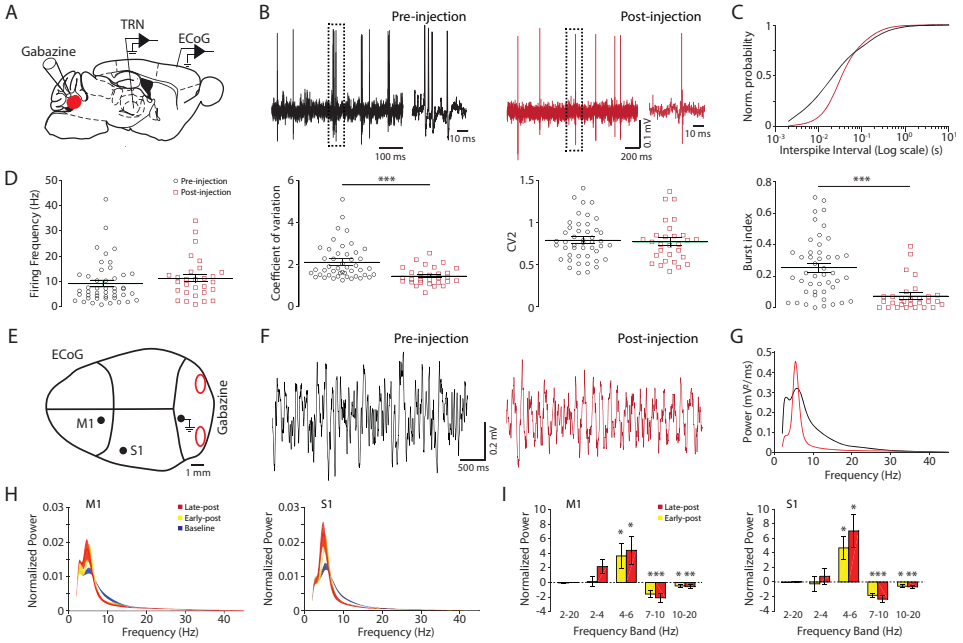

Supplemental Figure 2. Long-term modulation of cerebellar output by bilateral gabazine injections.

(**A**) Schematic outline of head-fixed experiment for CN injection of gabazine, single-unit extracellular recordings from thalamic relay neurons (TRN) and multi-site ECoG recordings from M1 and S1 regions. (**B**) Example traces of two single-unit TRNs: one in the absence (pre-injection; black) and one in the presence (post-injection; red) of gabazine in the bilateral CN. Note the presence (left trace) and absence (right) of burst-firing. (**C**) Normalized cumulative distribution for the interspike interval of thalamic neurons pre-injection (black) and post-injection of gabazine in the bilateral CN. (**D**) Average firing frequency, coefficient of variation (CV), CV2 and burst-index calculated for neurons recorded pre-gabazine (n = 46 neurons, N = 4 mice) and another set of neurons post-gabazine (n = 29 neurons, N = 4 mice). ** indicate $p < 0.01$. (**E**) Placement of craniotomies for ECoG recording electrodes and gabazine injections into the CN. (**F**) Four seconds of M1 ECoG recording pre-gabazine (*left*, black) and post-gabazine (*right*, red) from a single mouse. (**G**) Result of fast-Fourier transform of pre-gabazine (black) and post-gabazine (red) M1 ECoG. (**H**) Normalized ECoG power in M1 (*left*) and S1 (*right*) recordings from 4 mice, comparing pre-gabazine (baseline), ~5–20 min after gabazine (early-post) and ~1 hour after gabazine (late-post). (**I**) Relative change in ECoG power (normalized to pre-gabazine condition) showing an increase in θ- (4–7 Hz) power and a significant decrease in the β-band (10–20 Hz) and the θ*-band (7–10 Hz). The power in δ- (2–4 Hz), γ (25–40 Hz) and broadband 2–20 Hz activity was not affected. Note that there was no difference between M1 and S1 responses (see also [68]). * indicates $p < 0.05$, ** indicate $p < 0.01$ and ** indicate $p < 0.001$. See Online **Suppl. Tables 4 and 5** for statistics.

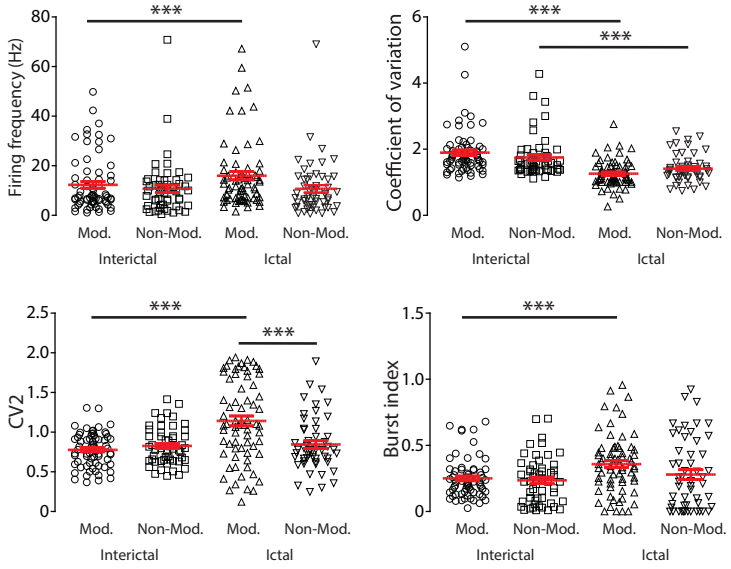

Supplemental Figure 3: Spiking pattern characteristics of thalamic relay neurons in relation to ECoG spike-and-wave discharges.

Firing frequency, coefficient of variation, CV2 and burst index for thalamic relay neurons that revealed spike-and-wave discharge (GSWD)-modulated or non-modulated spiking. Each firing parameter is represented for the interictal and ictal phases (determined by the occurrence of SWDs; see STAR methods section). Red markers indicate mean ± SEM. *** indicate $p < 0.001$ (see Online **Suppl. Table 6** for statistics).

7.4.5 CN neuron stimulation is more effective than activation of cerebellar efferents inside thalamus

To determine whether controlling the activity of a portion of CN axonal input to thalamic neurons is sufficient to stop GSWDs, we implanted optic fibers directly in nuclei of the thalamic complex. We initially focused on VL and VM since the density of CN axons, as evidence by the level of fluorescence from AAV-ChR2-EYFP transfected CN axons, in these nuclei was highest (VL: 47.5 ± 11.2 a.u.; VM: 54.5 ± 14.0 a.u.; N = 5 mice) (see also [435]). Given that VL and VM not only innervate M1, but also prefrontal, sensory and associative cortical regions [367, 368], we reasoned that stimulating only the CN axons in these nuclei may be sufficient to stop the widespread cortical oscillations underlying absence seizures. To test this premise, we implanted optic fibers bilaterally in VL and VM and ensured that the level of light intensity was sufficient to in principle activate ChR2-expressing CN axons throughout the thalamic nuclei (see STAR Methods). Surprisingly, optogenetic stimulation of these regions stopped only a proportion of seizures, regardless of whether we stimulated uni- or bilaterally (**Fig. 4A-C**).

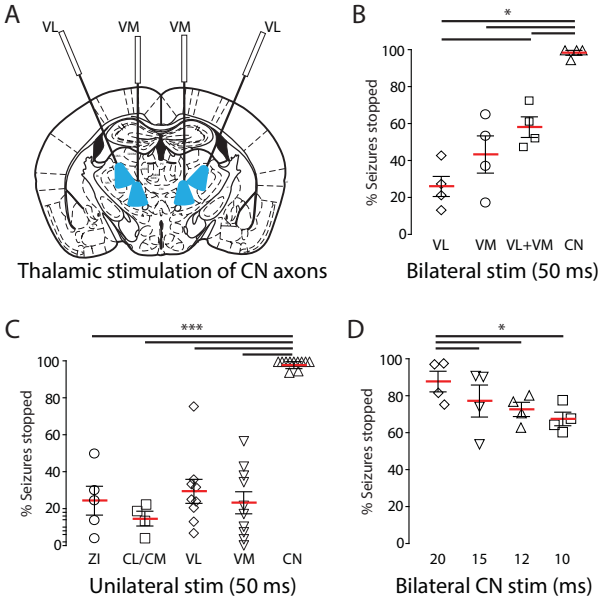

Figure 4. Activation of cerebellar afferents in thalamic nuclei is less sufficient in stopping GSWDs compared with direct cerebellar nuclei neuron stimulation.

(**A**) Experimental setup with four optic fibers implanted in thalamic nuclei. (**B**) Proportion of the seizures that stopped following bilateral VL (bilateral VL 25.8 ± 1.8% N = 4 animals; 244 seizures), bilateral VM (56.2 ± 6.0% N = 4 animals; 185 seizures), quadruple VL/VM (57.3 ± 3.9%, N = 4 mice, 250 seizures) or bilateral CN stimulation (98.7 ± 1.3% N = 4 animals; 3,254 seizures). (**C**) Proportion of the seizures that stopped following unilateral zona incerta (ZI) (24.4 ± 7.8 %; N = 5 sites; 302 seizures), CL/CM (16.8 ± 2.2 %, N = 4 animals; 205 seizures), VL (31.7 ± 2.7 %, N = 5 mice, 281 seizures), VM (32.9 ± 5.0%, N = 6 mice, n = 417 seizures) or CN stimulation (98.0 ± 1.9%, N = 11 sites; 199 seizures). (**D**) Proportion of the seizures that stopped following bilateral CN stimulation with varying pulse lengths. Data from the same mice as reported in B. Note that at 10-ms pulse length, CN stimulation is still effective in stopping most seizures. Data are represented as mean ± SEM. * indicates $p < 0.05$, *** indicate $p < 0.001$ (see Online Suppl. Table 7 for statistics).

In an attempt to increase the efficacy of seizure termination we activated all thalamic optic fibers simultaneously, but 50-ms pulses applied bilaterally to both VL and VM still only stopped a proportion of seizures (**Fig. 4B** and **Online Suppl. Table 7**). In the same mice, we also implanted optic fibers in the CN. In contrast to VL/VM stimulation bilateral CN stimulation stopped nearly all seizures (98.7 ± 1.3%); significantly more than in any of the VL/VM stimulation conditions. Even when we decreased the pulse length to 10 ms the efficacy of stopping GSWDs by direct CN stimulation (71.4 ± 6.8%) was at least as effective as applying 50 ms pulses to the VL and VM optic fibers simultaneously (**Fig. 4D** and **Online Suppl. Table 7**). To evaluate whether selective activation of CN axons in other thalamic nuclei is more effective in stopping seizures, we also implanted fibers in the zona incerta and in the intralaminar CL and CM nuclei, for which unilateral electrical or optogenetic stimulation was

shown to dampen cortical seizure activity [60, 436]. However, neither unilateral stimulation of CN terminals in zona incerta nor in CL/CM was as effective as unilateral stimulation of CN neurons (**Fig. 4C** and **Online Suppl. Table 7**). Collectively these data reveal that direct optogenetic CN stimulation has a more reliable effect in GSWD termination than activating proportions of cerebellar axons throughout the thalamic complex.

7.5 Discussion

Using a combination of *in vivo* electrophysiological and optogenetic techniques we could show that single-pulse stimulation of CN has a varying effect on neuronal spiking patterns throughout the thalamic complex, causing desynchronization of thalamic activity that disrupts epileptogenic GSWDs. Controlling the activity in CN for a fraction of a second was sufficient to desynchronize thalamic neurons for a prolonged period of time. Thereby our findings unveil a previously unknown function of cerebellar output in potentially directly affecting information processing in thalamo-cortical networks. We suggest that both under healthy and pathological conditions CN firing can direct the extent of thalamic synchronization and thereby contribute to neuronal network patterns encoded in various cerebral regions.

In freely behaving *tottering* mice thalamic neuronal activity recordings showed phase-locked action potential firing during GSWDs, which parallels earlier reports on cellular excitability and hypersynchronicity in thalamo-cortical networks in this model [36, 352, 437], and other rodent models of absence epilepsy [438]. Our single-cell recordings showed that ~50% of neurons recorded in primary, associative and intralaminar thalamic nuclei fire most of their action potentials ~20 ms prior to the peak of the ECoG spikes during GSWD episodes. In the other rodent models this delay in thalamo-cortical activity ranged from 9 ms in GAERS to 28 ms in Long-Evans rats [35, 99]. In contrast to a rather fixed periodicity in thalamic firing, cerebellar firing is known to be far more variable when compared to cortical GSWDs [46, 104, 439]. Although it is not known whether CN neurons show increased levels of synchrony during GSWDs and thus could contribute to driving synchronous thalamic firing [123, 124], our findings indicate that CN output has a rather opposite effect: synchronizing CN firing by direct CN stimulation desynchronizes thalamic firing. Our previous pharmacological interventions confirm this anti-seizure effect of cerebellar output, and showed that GSWD occurrence was prevented by enhancing CN firing, whereas dampening of CN action potential firing strongly increased the seizure load [46]. Also in refractory epilepsy dentate CN stimulation has such dual effect, which was recognized to have therapeutic value [12, 48, 49].

Increasing cerebellar output resulted in a variable effect on thalamic nuclei. Anatomical connections between cerebellum and thalamus and the impact on cerebral cortical activity revealed that in various species CN axonal projections to VL neurons and the interconnected motor cortex are excitatory [84, 89-92, 363, 364, 366, 380, 387, 399, 440, 441]. However, early reports indicated bi-modal responses following electrical stimulation of the cerebellar nuclei in cats [92, 330, 389]. Although such responses may be easily caused by intra-thalamic inhibitory projections that run through the reticular thalamic nucleus, we speculate that axonal connections from CN to other pre-thalamic nuclei, such as the middle and deeper layers of the superior colliculus, the zona incerta and the anterior pretectal nucleus, contribute to the differential thalamic responses to CN stimulation (see also [430, 442]. Other sources that could contribute to a desynchronizing effect of CN stimulation on thalamic firing come from: *i*) inhibitory afferents that manipulate thalamic responses [443] to CN stimulation, as has been shown for substantia nigra pars reticulata input to VM neurons [421]; *ii*) an increased contribution of $Ca_V2.2$ (N-type) voltage-gated Ca^{2+} channels to neurotransmitter release to compensate the loss of $Ca_V2.1$ (P/Q-type) channel function in *tottering* mice, which may increase the asynchronous release of neurotransmitter (as discussed by [444]); *iii*) excitation of pre-motor CN that do not project to the thalamus but rather to premotor nuclei in the brainstem and thereby drive behavioral motor responses [111]; such behavioral responses are likely to affect thalamo-cortical synchrony through the coding of proprioceptive input (see for instance ref [445]).

In conclusion, our data show that targeted stimulation of CN neurons results in desynchronization of thalamic firing in line with termination of GSWDs in *tottering* mice. We thereby suggest CN as an important node in the neuronal network underlying generalized seizures. Stimulating this node can not only acutely stop hypersynchrony in the thalamo-cortical networks during seizures, but may also have more general effects. For example, cerebellar output has been implicated in cognitive processes, like social interaction [385, 386], sensory coding [90, 387], and language [446], all of which have also been linked to the integrity of the thalamic structure and its activity [447]. Therefore, we argue that cerebellar stimulation may also have important effects on cognitive functioning in epilepsy patients (as reviewed by [448]).

8

Potassium current deficit underlies thalamic hyperexcitability and seizures in Scn1a-deficient Dravet syndrome

Submitted to Nature Neuroscience:

S. Ritter-Makinson, A. Clemente-Perez, B. Higashikubo, E. Bennett, A. Chkaidze, O.H.J. Eelkman Rooda, M.-C. Cornet, F.E. Hoebeek, K. Yamakawa, M. Roberta Cilio, B. Delord, J.T. Paz

Dravet syndrome (DS) is a severe form of early-onset epileptic encephalopathy associated with intractable seizures, developmental delay, autistic features, sleep disorders, and sudden unexpected death. Approximately 80% of patients with DS have a loss-of-function mutation in one allele of the sodium channel gene SCN1A, which is mainly expressed in inhibitory neurons. The brain circuits causing seizures in these patients have not yet been identified, but runaway excitation has been thought to result from reduced activity in inhibitory neurons. Here, we show that runaway excitation results instead from enhanced activity in the inhibitory reticular thalamus, a region that regulates thalamocortical rhythms and contains intrinsically oscillatory neurons. In a well-established mouse model of a human Scn1a mutation, we found that reticular thalamic cells exhibited abnormally high pacemaker burst firing due to reduced SK current, which is conducted by a subfamily of calcium-activated potassium channels that normally limit firing. The dorsal thalamic complex was hyperexcitable in Scn1a mutant mice, as indicated by abnormally long evoked circuit oscillations. In vivo, we observed that non-convulsive seizures also occur in Scn1a mutant mice, and have similar EEG signatures as in humans with DS. These cellular abnormalities and seizures were all rescued by enhancing SK currents in the reticular thalamus. Further, optogenetically toggling between burst and tonic firing

in thalamic neurons launched and aborted seizures, respectively. Finally, computational modeling and electrophysiology indicate that reticular thalamic hyperexcitability can cause abnormal bursting in thalamocortical relay neurons to promote cortical seizure expression. These correlational, loss-of-function, and gain-of-function results support a model in which the most common and intractable seizures in DS are caused by a hypoactive SK current that makes the reticular thalamus hyperexcitable. Our study identifies the SK current as a novel therapeutic target in Dravet syndrome.

8.1 Introduction

The SCN1A gene encodes the alpha subunit of the voltage-gated sodium channel Nav1.1, which is widely expressed in the brain and the heart. As a key regulator of cardiac and brain rhythms, mutations in SCN1A dramatically affect human health. SCN1A is one of the most commonly mutated genes associated with epilepsy, including Dravet syndrome (DS) [449, 450]. This age-dependent, early-onset epileptic encephalopathy is characterized by intractable seizures, developmental delay, intellectual and motor disabilities, autistic features, sleep impairment, and high risk of sudden unexplained death. Reduced Scn1a function in GABAergic cortical and hippocampal inhibitory neurons is thought to reduce action potential (AP) firing and network inhibition, leading to runaway excitation (altered excitatory/inhibitory balance) and deadly seizures [451-454]. Global knockout of Scn1a in parvalbumin and somatostatin neurons increases susceptibility to thermally induced seizures, whereas selective knockout in either neuron subtype phenocopies distinct DS neuropsychiatric behavioral phenotypes [455]. However, the molecular and brain circuit mechanisms by which reduced SCN1A causes seizures is unknown. Uncovering how SCN1A mutations disrupt brain function could identify novel therapeutic strategies. SCN1A is abundant in the GABAergic nucleus reticularis thalami (nRT) [456], a brain structure known as the "guardian of the gateway" because of its role in dynamically modulating interactions between the thalamus and cerebral cortex [442, 457]. Scn1a–expressing GABAergic neurons of the nRT are intrinsic oscillators that inhibit the excitatory relay thalamus [458, 459], positioning them to regulate thalamocortical oscillations, including seizures. Given the abundant expression of Scn1a in nRT and the disruptions in nRT that correlate with neurological [460, 461] and psychiatric disorders [462, 463], we tested the hypothesis that Scn1a deficiency in nRT neurons is causally involved in DS in a well-established mouse model containing a human Scn1a mutation [452]. Mice with Scn1a haploinsufficiency due to this mutation are hereafter referred to as Scn1a DS mice.

8.2 Results

8.2.1 Scn1a deficiency leads to thalamic microcircuit hyperexcitability

Interactions between nRT and thalamocortical relay neurons generate rhythmic circuit oscillations. Because nRT neurons express high levels of Scn1a, [456] we asked whether the intra-thalamic micro-circuit rhythmogenesis is altered in Scn1a DS mice. We used horizontal thalamic slice preparations that conserve the connectivity between the nRT and 86 the ventrobasal complex of the somatosensory thalamus (VB) to assess nRT-VB

intrathalamic network oscillations independent of other structures (i.e., cortex) (**Fig. 1a, c**) [464].

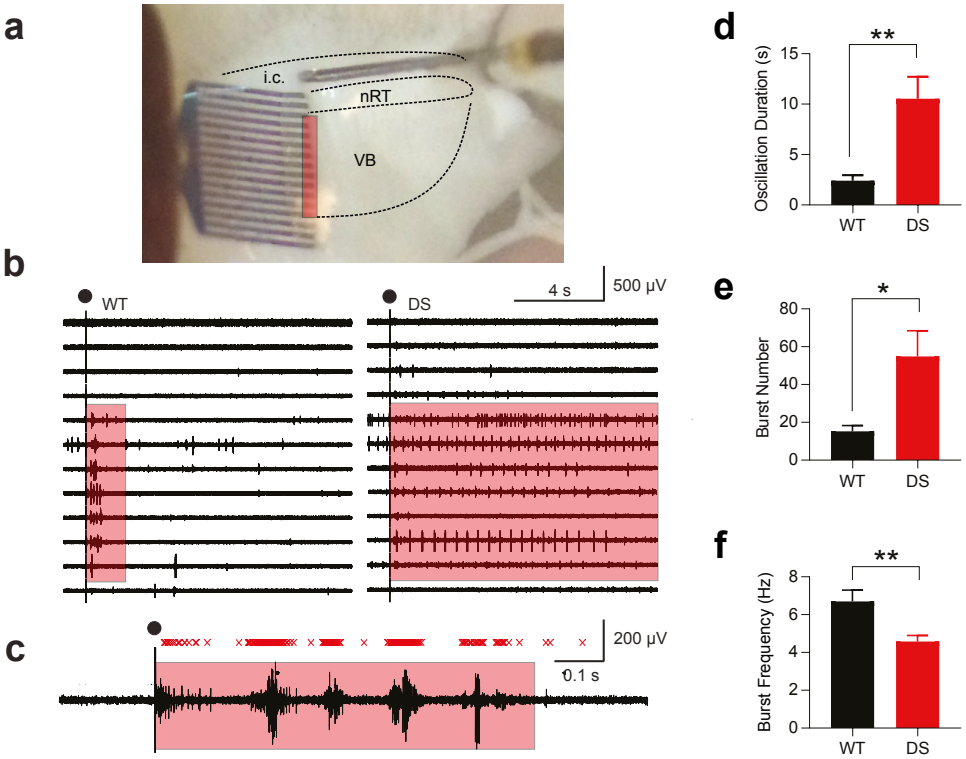

Figure 1. Scn1a deficiency in nRT neurons enhances intra-thalamic circuit oscillations.

a, Horizontal slice preparation to study intra-thalamic circuit oscillations. Position of 16-channel linear array silicon probe showing the region of the ventrobasal thalamus studied. Evoked oscillations were elicited via stimulation of the internal capsule. b, Representative example of evoked intra-thalamic circuit oscillations in slices prepared from WT and Scn1a DS mice. Black circles indicate stimulation artifact. Pink box indicates region of analysis in which evoked oscillations were observed. c, Detection of extracellular multiunit spikes (red "X") and bursts that compose a thalamic oscillation (duration is marked by orange box). Oscillation example taken from a slice prepared from a WT mouse. d, Duration of evoked oscillation. Mann-Whitney U test. WT: n = 9 mice, Scn1a DS: n = 12 mice. ** $p < 0.01$. e, Number of bursts within the evoked oscillation. Mann-Whitney U test. WT: n = 9 mice, Scn1a DS: n = 12 mice. * $p < 0.05$. f, Interburst interval within the evoked oscillation. Mann-Whitney U test. WT, n = 9 mice, DS, n = 12 mice. ** $p < 0.01$. Abbreviations: i.c., internal capsule; nRT, thalamic reticular nucleus; VB, ventrobasal somatosensory complex of the thalamus; WT, wild-type; DS, Scn1a Dravet syndrome.

Stimulation of the internal capsule consistently evoked rhythmic oscillatory bursting activity in VB (**Fig. 1b, left, C**), in the spindle frequency range (~10 Hz), similar to reports using electrical stimulation to activate intra-thalamic oscillations [126, 325, 464] or optogenetic activation in vivo [465]. Similar stimulations in Scn1a DS mice induced more bursts and

longer circuit oscillations in the thalamus (**Fig. 1b, right,** and **d, e**), with slower circuit oscillations in Scn1a DS mice (**Fig. 1f**). Thus, the nRT-VB microcircuit is hyperexcitable in Scn1a DS mice. This finding is surprising, given that nRT-VB 5 oscillations require robust firing in nRT neurons, which we expected to be lower in Scn1a-deficient mice, as reported [466].

8.2.2 Scn1a deficiency leads to enhanced high-frequency burst firing in nRT neurons

The nRT-VB microcircuit loop regulates rhythm generation, because thalamocortical VB cells fire low-threshold-spike (LTS)-mediated rebound bursts after hyperpolarization induced by nRT GABAergic inputs [467]. LTS-mediated burst firing is needed for the nRT to generate spindle oscillatory activity in the normal thalamocortical circuit [424, 468-470] and is also important for sensory processing [471, 472]

To determine if nRT-VB thalamic circuit hyperexcitability in Scn1a DS mice is explained by alterations in the electric membrane properties of nRT neurons, we performed whole-cell patch-clamp recordings of nRT neurons. We measured membrane potential changes in response to intracellular square current pulses (**Fig. 2a**). We studied PV-like bursting nRT cells because of their major involvement in thalamocortical rhythmogenesis. After similar responses to membrane potential hyperpolarizations, the number of APs within the initial rebound burst was ~1.5x higher in nRT neurons from Scn1a DS mice than 110 wild-type (WT) littermates (**Fig. 2a, b**). These data show that Scn1a mutation paradoxically enhances the post-inhibitory rebound bursts. We asked whether the prolonged rebound burst firing could result from enhanced T-type calcium currents that underlie the postinhibitory LTS and high-frequency burst firing [467]. We recorded T-currents from Scn1a DS and WT mice using identical steady-state inactivation (SSI) protocols (**Extended Data Fig. 1a**). The peak T-current density, voltage-dependence, and biophysical properties of the SSI T-type calcium currents were not altered in Scn1a DS nRT neurons (**Extended Data Fig. 1b-e**). These results show that enhanced post-hyperpolarization firing in Scn1a DS nRT neurons is not due to a stronger T-current. Since Scn1a was reduced in our DS mice, the AP threshold was depolarized, the AP width was increased as expected, and the input resistance was enhanced (**Extended Data Fig. 1**). The properties of spontaneous synaptic excitatory currents (sEPSCs) were not altered in nRT (**Extended Data Fig. 1**).

8.2.3 SK current deficit in nRT neurons underlies the enhanced cellular and circuit rhythmogenesis

Because burst firing in nRT neurons depends on interactions between T-type Ca2+ and small conductance calcium-activated (SK) K+ channels [473], we asked whether the function of SK channels was impaired in the Scn1a DS mice. Patch-clamp recordings showed that the density of SK currents in nRT neurons was reduced (**Fig. 2c, d**). Quantitative PCR for a predominant SK2 subtype in nRT [474] showed that mRNA levels of a variant of the SK2 channel (Kcnn2S) were reduced in nRT tissue isolated from DS mice (**Fig. 2d**). Notably, in a rescue experiment, we found that the SK agonist 1-ethyl-2-benzimidazolinone (EBIO) normalizes nRT bursting properties in Scn1a DS nRT neurons to WT levels (**Fig. 2e**).

In a biophysical model of an nRT neuron (**Fig. 2f**), reducing SK conductance was sufficient to account for the enhanced number of APs within the burst, as found in Scn1a DS nRT neurons (**Fig. 2g**). This increase proved general: the mean AP number in the entire DS parameter domain was larger than for WT (**Fig. 2h**, see Methods for domain definitions).

We assessed the impact of reduced SK conductance in the nRT neuron at the circuit level in a model, including thalamocortical (TC) and nRT neurons (**Fig. 3a**). We found that reduced SK phenocopied enhanced network oscillations (**Fig. 3b**), displayed longer oscillations (**Fig. 3c, d**), had more bursts within each oscillation (**Fig. 3e, f**), and showed lower oscillation frequency (**Fig. 3g, h**) in the DS domain, quantitatively predicting the features found in Scn1a DS thalamic circuits.

Mechanistically, in the DS condition, the increased number of APs per burst in the nRT neuron produces stronger inhibition and a larger post-inhibitory rebound in the TC neuron, which increased the excitatory TC-to-nRT feedback. Synaptic transmission was stronger in the circuit and more robust to noise, enabling more bursts and longer oscillations. The model showed how longer nRT bursts and TC inhibitory post-synaptic potentials explain the counterintuitive decrease in bursting frequency in DS mice. Remarkably, modifying the fast sodium conductance was not required to account for experimental results. Thus, reduced SK function in nRT neurons makes the thalamus "epileptic" by enhancing thalamic rhythmogenesis.

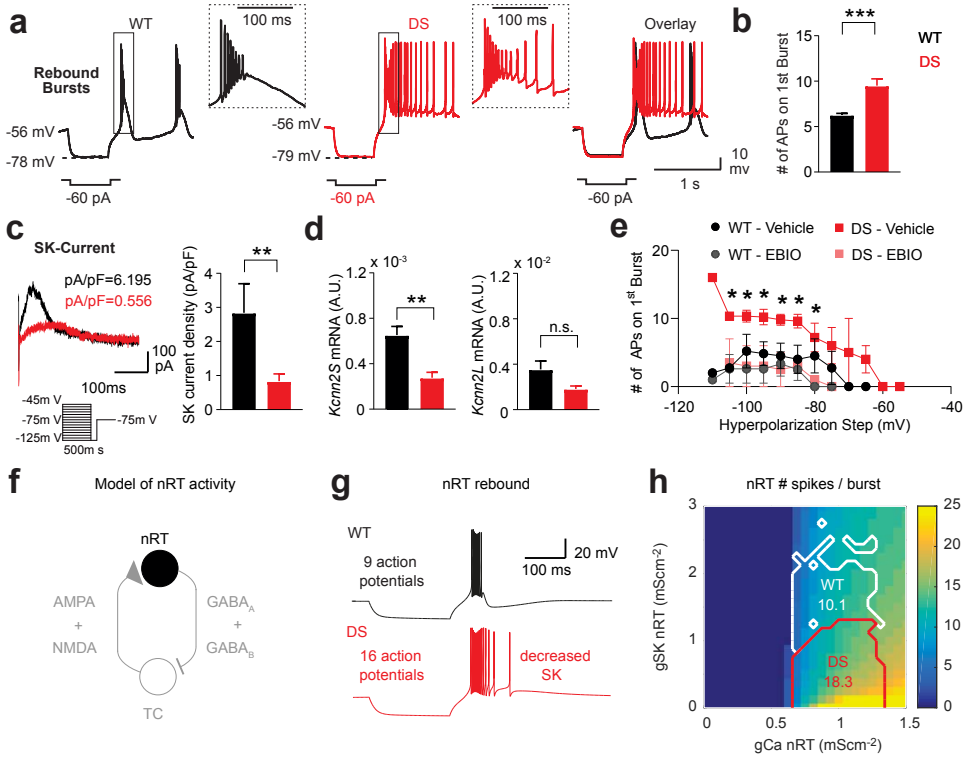

Figure 2. SK current deficiency in nRT neurons underlies the enhanced cellular bursting in Scn1a DS mice.

a, Representative traces showing that Scn1a DS neurons (red trace) exhibit enhanced post-inhibitory rebound burst firing upon hyperpolarization induced by −60 pA current pulses, compared to WT neurons (black trace). Insets show zoom of APs on first rebound burst. b, Number of APs on first rebound burst (WT: n = 30 cells, 4 mice; Scn1a DS, n = 43 cells, 6 mice). Data = mean ± SEM, compared with 14 parametric t-test with Welch's correction and α = 0.05, *** $p < 0.001$. c, Representative SK current traces obtained by digital subtraction in nRT neurons from WT (black) and Scn1a DS mutant (red) mice with respective current density. d. Left, Quantification of SK current density defined as the maximal current divided by individual cell capacitance. Data are represented as mean ± SEM, compared with Mann-Whitney U test (** $p = 0.0085$). WT: n = 8 cells, 3 mice; Scn1a DS: n = 10 cells, 3 mice. Right, SK2 relative mRNA expression levels (encoded by the gene Kcnn2, short and long transcript variants) normalized to Gapdh mRNA, in nRT. Expression levels were calculated using the ΔΔCT method and are expressed as arbitrary units. Mann-Whitney U test, ** $p < 0.01$. e, Number of APs on the first rebound burst, plotted against hyperpolarization step (mV) with vehicle or 100μM EBIO treatment. WT: n = 6 neurons, 3 mice; Scn1a DS: n = 6 neurons, 3 mice. Data = mean ± SEM. Data points compared by individual unpaired t-test, not corrected for multiple comparisons, * $p < 0.03$. f, Schematic of the minimal thalamic circuit used for computational modeling, including a thalamocortical (TC) and an nRT neuron, TC to nRT AMPA and NMDA excitatory synapses, and nRT to TC GABA–A and GABA–B inhibitory synapses. Synaptic currents are absent in the simulations of the nRT neuron mimicking intracellular recordings (**Figure 2g-h**). g, Voltage traces of a nRT neuron in the WT parameter domain (black trace; $\overline{g}_{CaT}^{nRT} = 0.85 mScm^{-2}$ and $\overline{g}_{SK}^{nRT} = 2 mScm^{-2}$) and of a neuron in the DS domain with decreased SK maximum conductance (red trace; $\overline{g}_{CaT}^{nRT} = 0.85 mScm^{-2}$ and $\overline{g}_{SK}^{nRT} = 0.1 mScm^{-2}$, in response to a hyperpolarizing injected current $I_{Inj}^{nRT} = -0.5 \mu A cm^{-2}$ for 500 ms h, Map of the average number of APs in the rebound burst in the nRT neuron model as a function of maximal conductance parameters. APs numbers are computed over 30 simulations with different realizations of the stochastic current mimicking the noise in the thalamic circuit. The mean of these average numbers of APs are indicated in the WT (white) and DS (red) domains. See Methods for the definition of WT and DS domains. Abbreviations: SK channel, small conductance calcium-activated potassium channels; WT, wild-type; DS, Scn1a Dravet syndrome; APs, action potentials; nRT, thalamic reticular nucleus; TC, thalamocortical.

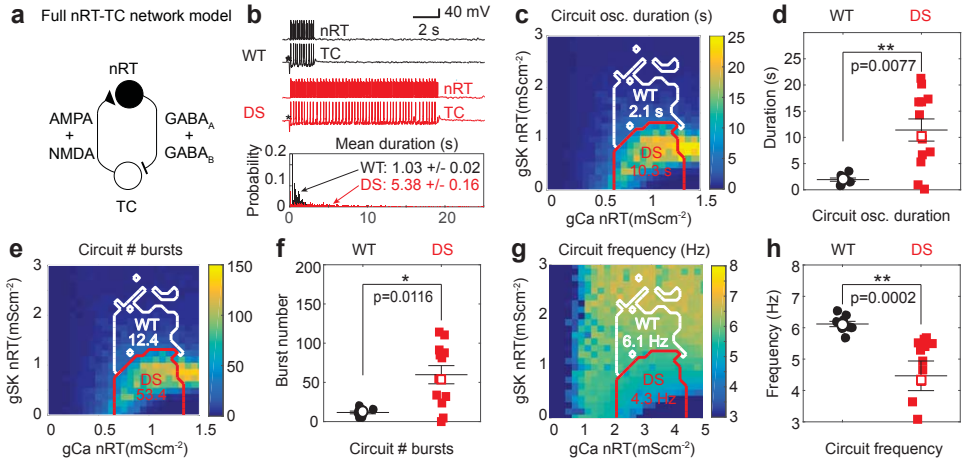

Figure 3. SK current deficiency in nRT underlies enhanced micro-circuit rhythmogenesis in SCN1A DS mice.

a, Schematic of the full nRT-TC circuit used for the computational modeling of thalamic oscillations in WT and DS conditions. b, (above) Example of nRT and TC voltage traces triggered by a stimulus (star) mimicking optogenetic stimulation, in the WT and DS conditions. (below) Probability distributions of the duration of oscillations in the circuit over 10^3 simulations with different realizations of the stochastic current. The mean oscillation duration in the TC-nRT circuit model in the DS condition was ~5 times that in the WT condition. The maximal conductances are as in **Figure 2g. c**, Map of the average oscillation duration of the TC-nRT circuit model as a function of maximal conductances, computed over 10^3 simulations with different realizations of the stochastic current. The mean of these averages in the WT and DS domains (white and red boundaries, respectively) are indicated. d, Duration of evoked oscillation for 9 samples with randomly maximal conductances drawn from the WT domain and 12 samples with randomly maximal conductances drawn from the DS domain. The difference of sample means is statistically significant (Mann–Whitney U test, WT: n = 9 mice, Scn1a DS: n = 12 mice. ** p = 0.0062). e, Same as in (c) for the average number of bursts of the oscillation. f, Same as in (d) for the average number of bursts of the oscillation. The difference of sample means is statistically significant (Mann– Whitney U test, WT: n = 9 mice, Scn1a DS: n = 12 mice. * p = 0.0208). g, Same as in (c) for the average frequency of the oscillation. h, Same as in (d) for the average frequency of the oscillation. The difference of sample means is statistically significant (Mann– Whitney U test, WT: n = 9 mice, Scn1a DS: n = 12 mice. ** p = 0.0002) Abbreviations: SK channel, small conductance calcium-activated potassium channels; WT, wild-type; DS, Scn1a Dravet syndrome; nRT, thalamic reticular nucleus; TC, thalamocortical.

8.2.4 "Silent" non-convulsive seizures are a major phenotype in human and mouse DS

Dravet syndrome presents with a complex seizure phenotype including multiple convulsive seizures – such as generalized tonic-clonic seizures (GTCS), myoclonic seizures, and febrile seizures – in addition to non-convulsive seizures – such as typical and atypical absence seizures. Notably, non-convulsive seizures are often intractable, contribute to the intellectual impairment observed in DS patients, and can progress in so-called obtundation status, resulting in a prolonged impairment of consciousness; yet, they are under-recognized and understudied, compared with convulsive seizures, mainly because they are clinically

difficult to diagnose. To date, non-convulsive seizures have not been described in the Scn1a DS mouse model. Thus, we set out characterize this phenotype in both human patients and our Scn1a DS mice (**Fig. 4 a-d**). Non-convulsive seizures occurred on average 15 ± 8 times per hour in mice, lasting 0.5-6 seconds (n=9 mice), and 7 ± 4 times 166 per hour in our human DS patient, lasting 10 seconds (n=1 patient). Notably, non- convulsive seizures in Scn1a DS mice and DS patients exhibited similar spectral EEG signatures with fundamental frequencies of 5-7 Hz (**Fig. 4**). To our knowledge, this study is the first to compare DS seizures in the Scn1a mouse model and human patients.

8.2.5 Optogenetic toggling of thalamic bursting bi-directionally modulates seizures in 172 SCN1A-deficient mice

We next asked whether the high-frequency burst firing in vitro in the thalamus occurs during spontaneous seizures in freely behaving mice. Optrode recordings in nRT (**Extended Data, Fig. 2d**) and VB (**Fig. 4g-i**) TC neurons showed high-frequency burst firing, phase-locked with spontaneously occurring non-convulsive seizures.

Notably, nRT does not project directly onto the cortex and thus exerts its effects on cortical rhythms through its TC targets. To test the causality of the nRT-VB pathway in non-convulsive seizures, which predominate in the S1 ECoG, we perturbed the VB firing using Stable Step Function Opsin (SSFO). SSFO is a bistable opsin, which was used to show that activation in TC cells causes depolarization and a switch from bursting to tonic firing [225]. We unilaterally activated SSFO in VB after seizure detection. SSFO activation reliably and rapidly eliminated TC bursts, toggled tonic firing, and stopped ongoing seizures (**Fig. 4g-j**). Thus, TC VB bursting output may be causally required to maintain non-convulsive seizures in DS. We tested more clinically tractable strategies for interrupting hyperthermia-triggered GTCS in DS patients using electrical stimulation. The spectrogram of these seizures showed a pronounced increase in broad gamma-band (30-100 Hz) power (**Extended Data, Fig. 3a, b**). Because we pinpointed the thalamus as a potential choke point for DS seizure control, we employed unilateral electrical stimulation of VB (**Extended Data, Fig. 3c, d**) and the anterior thalamic nuclei, (**Extended Data, Fig. 3e, f**) upon the start of temperature-induced GTCS in our Scn1a DS model. Moreover, we also investigated another potential clinical target – the medial and interposed cerebellar nuclei – which send divergent projections throughout the thalamic complex and modulate various cerebral cortical regions. Although no significant anti-epileptic effects were observed when unilaterally manipulating VB or AN, we did see a seizure-modifying effect of electrical stimulation of the cerebellar nuclei (**Extended Data, Fig. 3g, h**). Together, these data indicate that simultaneous recruitment of multiple thalamic nuclei and/or recruitment of thalamic nuclei together with parts of the cortex are more effective for modification of ongoing GTCS in DS.

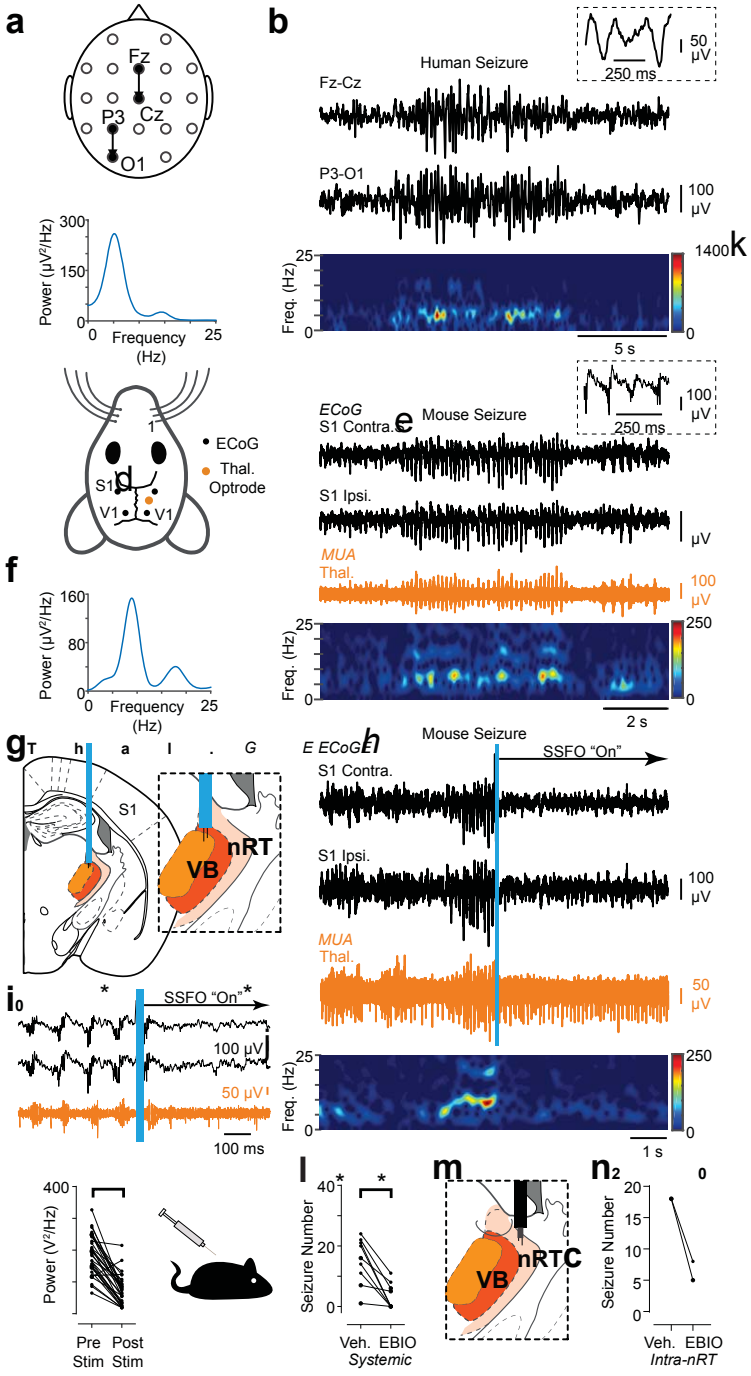

Figure 4. Dual strategy for seizure control in Dravet patients converge on the thalamus.

a, Diagram of human EEG recording montage. b, top: Example of the EEG signature of a typical non-convulsive seizure in a patient with DS recorded in two different locations on the scalp. inset, Note the spikes are not typical spike-and-wave discharges and have a higher frequency component in addition to the slower oscillation. bottom: Spectrogram showing frequency components of the recorded seizure. c, Power spectral density of the seizure shown in b. Note the peak fundamental frequency is ~5 Hz. d, Diagram of the mouse ECoG and thalamic depth electrode recording montage. ECoG was recorded from somatosensory (S1) and visual (V1) cortices, with depth electrodes implanted in the thalamus. e, top: Example of an ECoG signature of a typical non-convulsive seizure in Scn1a DS mice recorded from S1 (black), along with simultaneous multi-unit (MU) recordings in the thalamus (orange). inset, Note the spikes are not typical spike-and-wave discharges and have a higher frequency component in addition to the slower oscillation. bottom: Spectrogram showing frequency components of the recorded seizure. f, Power spectral density of the seizure shown in e. Note the peak fundamental frequency is 6–7 Hz. g, Diagram of optogenetic targeting of the thalamus. inset, Depth electrodes were positioned in VB thalamus. h, top: Example of optogenetic seizure interruption of an ongoing non-convulsive seizure in a Scn1a DS mouse. The blue bar corresponds to a brief (50 ms) pulse of blue light to activate SSFO-expressing thalamocortical neurons. Unilateral activation of SSFO in the thalamus immediately interrupts an ongoing seizure. bottom: Spectrogram showing frequency components of the recorded seizure and decrease in power after SSFO activation. i, Magnification of the seizure interruption shown in (h). Activation of SSFO switches rebound burst firing in the thalamus to tonic firing. j, Quantification of 1-25 Hz broadband power 2 s before and after optogenetic manipulation. Data are from 32 trials across 4 mice. **** $p < 0.0001$ Mann-Whitney test. k, Diagram of systemic administration of EBIO (s.c. 25 mg/kg). l, Quantification of effects of systemic administration of EBIO (25 mg/kg, s.c.) on non-convulsive seizure number within 30 minutes of EBIO infusion. Data are from n = 9 Scn1a DS mice. ** $p = 0.0039$ Wilcoxon Signed-Rank test. m, Diagram of unilateral intra-nRT infusion of EBIO in conjunction with simultaneous multiunit recordings. n, Quantification of effects of intra-nRT administration of EBIO (800 nl of 0.4 mM) on non-convulsive seizure number within 1 hour of infusion. Data are from n = 2 Scn1a DS mice. Abbreviations: EEG, electroencephalogram; S1, somatosensory cortex; V1, visual cortex; ECoG, electrocorticogram; Thal., thalamus; Ipsi., ipsilateral; Contra., contralateral; MUA, multiunit activity; VB, ventrobasal thalamus; nRT, thalamic reticular nucleus; SSFO, stable step-function opsin.

We next asked whether mimicking rhythmic hyperpolarization in the nRT-to-VB pathway was sufficient to cause seizures during normal baseline behavior. We expressed halorhodopsin (eNpHR) in TC neurons as in Sorokin et al. (2017) and showed that unilaterally driving TC bursting causes bilateral GTCS in Scn1a DS mice (**Extended Data, Fig. 4**). The finding is striking, given that TC neurons of primary thalamic nuclei project exclusively to ipsilateral cortex. These results suggest the nRT-VB pathway is sufficient to initiate and necessary to maintain seizures in Scn1a DS mice.

8.2.6 SK enhancement treats seizures in SCN1A-deficient mice

Next we asked whether pharmacological boosting of SK channels could rescue seizures in Scn1a DS mice. Acute injection of EBIO, either systemically or locally in the nRT, reduced the number of spontaneously occurring non-convulsive seizures in Scn1a DS mice (**Fig. 4k-n**). These results support the idea that a reduction in SK channels in nRT underlies behavioral epileptic seizures in DS.

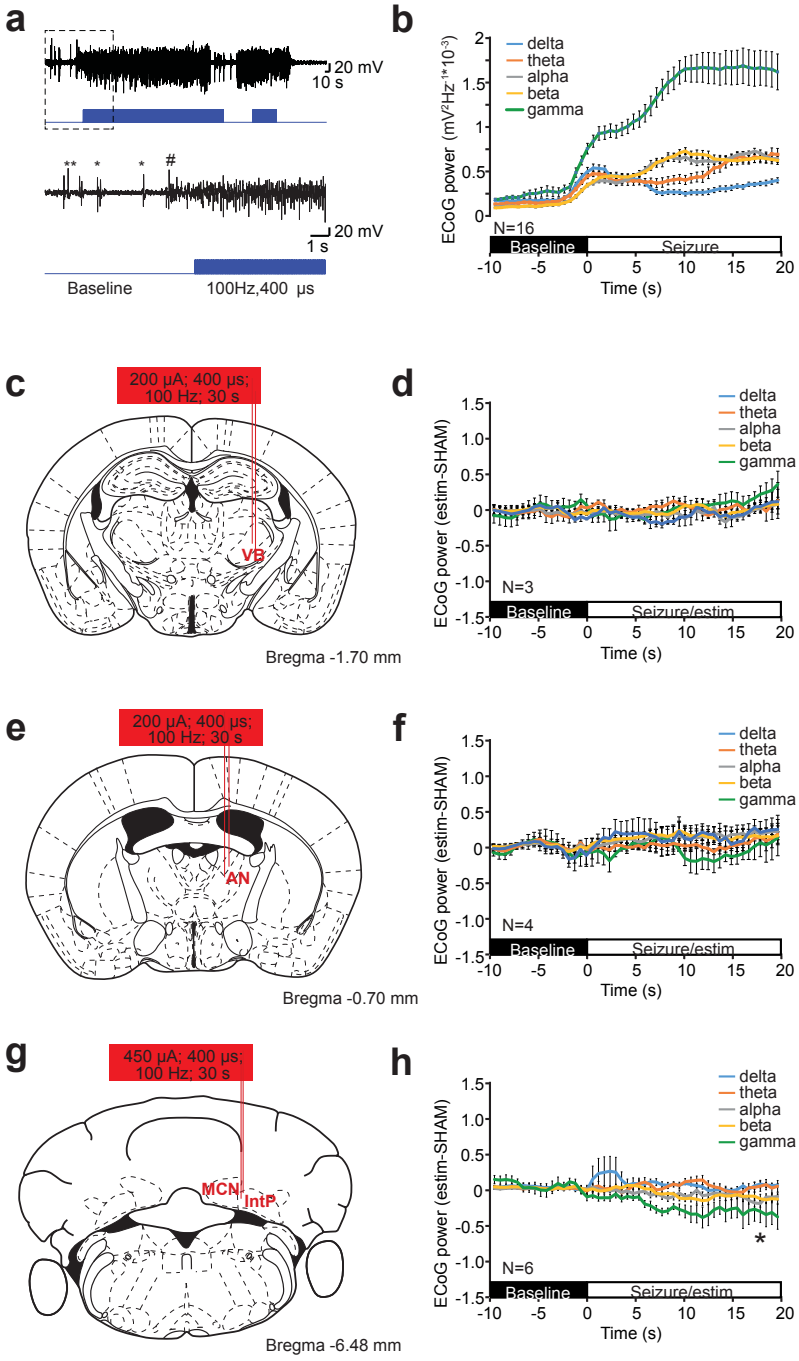

Extended Data Figure 3. Hyperthermia-triggered GTCS cannot be halted by thalamic or cerebellar stimulation.

a) ECoG recorded from S1 electrodes in a freely moving mouse indicates the clear onset of seizure-related activity. Manually started electrical stimulation (in this case sham condition is shown) was triggered after GTCS onset (pound sign). Asterisks indicate myoclonic jerks that precede seizure onset. b) Using a line length algorithm we determined the onset of the seizures and aligned the recordings of GTCS seizures from 16 mice. Note the steep increase in ECoG power at the gamma band (30-100 Hz) upon seizure onset. c) Schematic representation of stimulus electrode location in the ventral basal nucleus of the thalamus (VB). d) Difference in ECoG power at various frequency band between electrical stimulation (estim) and sham stimulation experiments. No consistent effect was observed (Wilcoxon-Signed Rank Test, n = 3 mice, all bands n.s.). e-h) Similar to (c,d) but for AN and CN stimulation experiments, respectively. Note, * in (h) corresponds to p = 0.046 for significant reduction in gamma power between 5 s of seizure (sham) versus 5 s of stimulation (estim) using a Wilcoxon-Signed Rank Test (AN, n = 4 DS mice, all bands n.s.; CN n = 6 DS mice, all bands except gamma n.s.).

Stereotactic atlas panels were adapted from Paxinos atlas for mouse brain (3rd edition). Error bars indicate SEM. Abbreviations: ECoG, electrocorticogram; S1, somatosensory cortex; GTCS, generalized tonic-clonic seizure; VB, ventral basal thalamus; AN, anterior nuclei of the thalamus; CN; cerebellar nuclei; MCN; medial cerebellar nucleus; IntP, interposed cerebellar nucleus.

8.3 Discussion

Using a well-established model of DS with Scn1a haploinsufficiency, we uncovered a novel and unexpected mechanism to explain intractable seizure pathology in DS, whereby Scn1a reduction, together with reduced SK current in nRT, drives thalamic hyperexcitability to promote cortical seizures.

Unlike previous work showing that dissociated cells from the GABAergic nRT of Scn1a-deficient mice are hypoexcitable and fire fewer APs, we find in the intact thalamic circuit in a comparable Scn1a-deficient model of DS that nRT neurons are hyperexcitable: they are more likely to fire bursts of APs. We show that this paradoxical increase in cell firing results from a compensatory decrease in SK2 channel expression and membrane conductance in nRT neurons. Our findings are distinct from previous work on DS, which suggested that sodium channel deficits in inhibitory neurons result in reduced firing and reduced network inhibition in neocortex and hippocampus to promote seizures [386, 451, 452, 454]. Moreover, our results contrast with another study in which a missense mutation in Scn1a associated with genetic epilepsy with febrile seizures resulted in reduced firing in nRT neurons. Instead, our data suggest that thalamic circuit dysfunction and seizure pathology in DS involve complex interactions among Scn1a, its particular mutation, and the brain circuits in which Scn1a is found. Our results support the view that DS pathology cannot simply be explained by cortical inhibitory neuron hypoexcitability by defining a novel role for Scn1a in the thalamus.

Identification and manipulation of SK2 as a modifier of DS seizures is novel and expands upon the growing list of genetic modifiers of SCN1A-epilepsies. Notably, our study not only found that Kcnn2 is reduced in the thalamus, but that pharmacological enhancement of SK2

can treat seizures in our Scn1a DS mouse model. Additionally, our findings complement existing literature on SK2 function in thalamic circuitry and other symptoms associated with DS. Notably, mice lacking SK2 show fragmented sleep patterns and reduced sleep spindles similar to DS mice, supporting the idea that reductions in SK2 underlie thalamic circuit dysfunction and its associated sleep impairments in DS. Overexpressing SK2 increases sleep spindles and reduces sleep fragmentation, further supporting that enhancement of SK2 function in DS might restore sleep impairments, in addition to treating intractable seizures.

To our knowledge, we are also the first to describe and define a mechanism for non-convulsive seizures in DS and compare this phenomenon with human patients. Although understudied, non-convulsive seizures are often intractable and may account for the cognitive decline, behavioral disorders, and reduction in social life associated with DS. Interestingly, the absence of non-convulsive seizures is typical of borderline forms of DS, in which cognitive ability is at least partially preserved, as reported in 1987.

Indeed, non-convulsive seizures, in particular atypical absence seizures, are co-morbid with autism spectrum disorders in multiple mouse models. By identifying the SK current as a novel therapeutic target for the non-convulsive seizures in DS, we also posit that enhancing SK function might treat deficits in cognition and social interaction in DS.

Given the recently uncovered framework of nRT organization and function, we hypothesize that the nRT is a key brain substrate responsible for the co-morbidity between neurological (seizure) and psychiatric (autism) components in DS. Within this framework, we propose that the nRT, through its respective projections to sensory and limbic thalamocortical nuclei, underlies the complex intractable seizures and autism, respectively, in DS. This nucleus thus can act as a final common pathway to treat the multi-faceted DS.

9

General Discussion

This dissertation primarily focusses on the neural mechanisms underlying cerebellar impact on thalamocortical networks, particular during pathological oscillations. We have in detail investigated how the cerebellum and its up- and downstream targets are and can be modulated during epilepsy. This was not possible without the preexisting evidence regarding functional research mostly performed in the 20th century about the anatomical organization of cerebello-thalamo-cortical and cortico-ponto-cerebellar projections. We focused upon cerebellar's primary output, i.e. cerebellar nuclei, and combined this with the use of different (epilepsy) mouse models. These models are well-characterized, reliable and 'easy to use'. The combination of the wealth of knowledge about the cerebellum and the existence of different well-known epilepsy models created close to ideal circumstances to understand the functioning and potency of this remote structure of control. In this general discussion I will only briefly touch upon the main findings of this thesis and further discuss and coordinate the findings to suggest future lines of animal and clinical research.

9.1 Seizures are hard-wired but also tend to dial in

In **Chapter 5** we demonstrate a limited occurrence of phase-locked modulation of Cerebellar Nuclei (CN) firing during GSWDs which is in line with previous work [104]. Modulation of CN activity during GSWDs has previously been suggested as a potential brain node essential for maintaining cortical GSWD activity [104], which was supported by anatomical connectivity in cerebello-thalamo-cortical networks of various mammalian species [89, 103, 104, 475]. Question remains why some CN neurons do modulate and some don't.

In addition to the discussion of Chapter 5 I came to think about a brain which is not as black and white as often suggested. We show significant interictal firing differences between modulatory and non-modulatory CN neurons [46] while supervised machine-learning algorithms could not clearly identify particular cell types [346]. These results were somewhat surprising to us, since previous in vitro data showed clear differences in activity patterns between CN cell-types [243]; and reviewed by [112, 242]. One of the reasons for interictal firing activity differences might be due to the variance in afferent connections. In other words, axonal projections ('hard-wiring') predefine partially if a cell 'participates' in a seizure or not. Furthermore it is likely that seizures differ in the number of participating cells. It has been suggested that there is always a most-committed group of cells which modulate back and forth other groups of cells within a seizure [476]. This so called 'waxing and waning' phenotype is also resembled in our data where we see differences in the maximal amplitude of GSWDs within a seizure and a large group of CN cells which has Z-scores not clearly indicative of being 'modulatory' although they fall in that category because of values slightly above significance (**Chapter 5**). Therefore it wouldn't surprise me if CN neurons which have a high Z-score (and thus are likely to modulate very reliably) are directly connected in a core-network of SWD occurrence while others are not. These show per GSWD much less reliable modulation or are not modulated during every seizure like the most-committed group.

These results are in line with our results from **Chapter 4** where we show that modulating Purkinje cells occur more often in lateral parts of the cerebellum compared to medial. As with CN neurons they also exhibit a wide range of Z-scores. The representation of modulating Purkinje and CN cells from medial to lateral is in line with data evidencing that cerebello-cerebral communication is represented by fundamental architectural closed-loop circuits [383, 477, 478]. The value of these closed-loop circuits for GSWD generation remains to be seen but it does raise the question if the amount and likelihood of CN neurons being modulated determines or is contributory to the spread and/or length of GSWDs.

This is shown in other brain areas such as the robust correlation between the participation probability of Reticular thalamic neurons at the first cycle and the length and spread of sleep spindles [465]. A similar although much weaker relationship existed for thalamocortical relay cells and spindle duration [465]. In **Chapter 7** we show that some GSWD-modulated thalamocortical relay neurons have a low but still significant Z-score. Seeing the weak relation between thalamocortical relay neurons and spindle-activity and the fact that unnatural spindle-activity is believed to underlie absence epilepsy and thus GSWDs [328, 479-481] I think it is hard to expect a strong correlation between thalamocortical relay neurons and GSWD duration. This suggests that low-Z-score modulated thalamocortical relay neurons are relatively unimportant for seizure maintenance.

9.2 The impact of enhancing cerebellar output

In **Chapter 5** we show that enhancing cerebellar output reduces GSWD activity either directly by optogenetic activation of CN or chronically by pharmacologic modulation. It is interesting to know if on-demand interruption of CN activity is also capable of stopping GSWDs. In that case it would hint towards a mechanism which is about breaking the closed-loop circuit like earlier discussed. For this reason I performed unpublished experiments in which I tested on-demand optogenetic interruption of CN activity using Archaerhodopsin during GSWDs. This was achieved by injecting AAV2.2-hSyn-Arch(eArch3.0)-EYFP bilaterally in cerebellar nuclei basically according to the same protocols and stereotactic locations as used in **Chapter 5 and 7** (Figure 1A, 1B)**.** Inhibition stopped only 21 out of 286 seizures (7.3%) (Fig 1C, 1D). Of 47 thalamic neurons was not capable of stopping GSWDs. (please note that I used 590nm ligt pulses whereas the ideal stimulation of Archaerhodopsin is reached with 540 nm light pulses).

Because of the purely excitatory nature of cerebellar output these results are in line with the suggested mechanism of action in **Chapter 7** where our thalamic recordings hint to signs of desynchronization upon enhancing cerebellar output.

The profound impact of CN activity raises to me the question if there are thalamic cells which are purely driven by excitatory CN input. I think it is likely that many thalamic cells have differential tasks processing different input but regarding cerebellar's motor task it must be that the cerebellum needs to rely on a 1:1 feedforward messaging system to the cortex which means that some thalamic cells will be purely driven by cerebellar input. Evidence for this is given in **Chapters 6 en 7** where we show both for *in vitro* and *in vivo* experiments the existence of cells which show a very reliable and high (amplitude) response. Although the evidence is meager I found one thalamic cell during my Archaerhodopsin

experiment which shows a near complete collapse of firing upon inhibition of CN firing. If we extrapolate this as a given fact this suggests there are thalamic cells which significantly need CN input to overcome either their own action potential generation threshold or other (inhibitory) input to fire action potentials. The function of these cells might be that the cerebellum is involved in preparing future motor actions for which it needs such a reliable feedforward system as was shown for inhibition of thalamic motor nuclei neurons causing a near complete stop of firing in anterior lateral motor cortex [388]. The specifics about this will need further research before even thinking about implementation in a broader line of perspective in epilepsy.

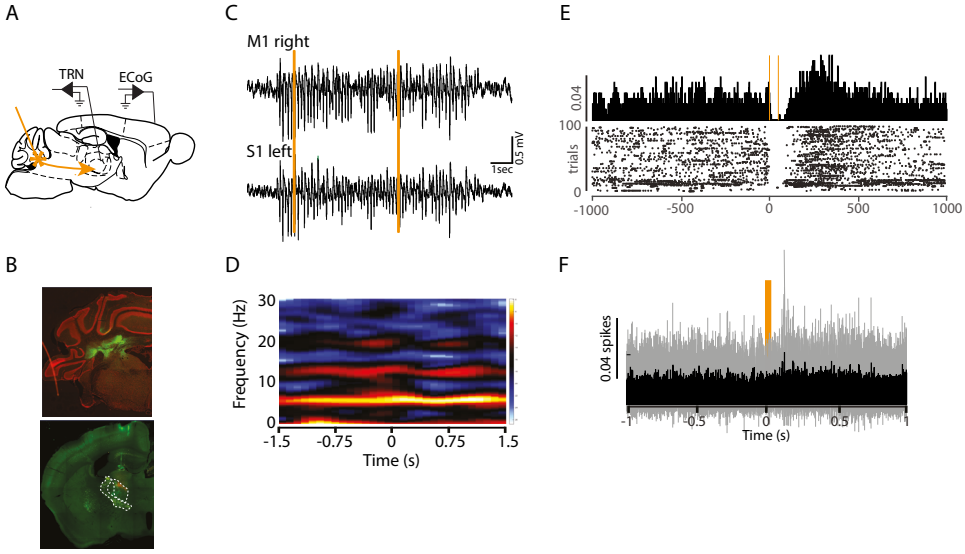

Figure 1. Optogenetic inhibition of cerebellar nuclei (CN) does not stop generalized spike-and-wave discharges (GSWDs).

(A) Schematic of sites for CN inhibition and recording for thalamic relay neurons and electroccorticogram (ECoG) from primary motor and sensory cortices. (B) Confocal image of coronal brain section showing Archaerhodopsin expression in CN (top panel) with projections to thalamus (bottom panel) with a biocytin mark (red; bottom panel) after recording thalamic single units. (C) Representative ECoG of primary motor and sensosry cortices which exemplifies how bilateral optogenetic inhibition (590nm ligt pulse of 50 milliseconds indicated by the vertical orange bar) is not capable of stopping GSWDs. (D) Mean ECoG wavelet spectrogram for all bilateral stimuli (n = 286 seizures; n = 2 animals). (E) Peri-stimulus time histograms (PSTH) and raster plot indicating decreased action potential (AP) firing for one individual thalamic neuron evoked by 590 nm light pulse in CN. (F) Average PSTH (n = 47 thalamic neurons) with in black mean and in gray SD action potential firing upon 590 nm inhibition in CN

9.3 The likelihood of cerebral desynchronization

One of the general objectives of this thesis was to establish a first view on cerebellar impact on the thalamus in the epilepsy-prone brain. In particular my thesis shows different types of responses in thalamic cells upon cerebellar stimulation in the epileptic brain (**Chapter 7**). This was in part evidenced by our results in **Chapter 6** where we found variable amplitudes in thalamic neurons upon cerebellar pulse and train stimulation. Although our results fuels further research of cerebellar communication with thalamocortical networks the polysynaptic individuality of cerebellar projections remains far from elucidated. Experiments in cats and monkeys have identified functional anatomical projections to thalamic motor nuclei and motor cortex in concordance with activation which was depended upon microstimulation in cerebellar nuclei [399, 401, 482-485]. Over the past years evidence accumulated indicating that the cerebellum is also considerably important for neurological non-motor disorders such as autism and schizophrenia [486]. This is supported by anatomical evidence regarding projections extending to premotor and non-motor parietal regions [487, 488]. Nevertheless there are relatively few studies investigating cerebellar effect on cerebral cortices regarding epilepsy (see **Chapter 2** of this thesis for a review of studies) and other neurological diseases [384].

The way cerebral cortices respond to cerebellar modulation remains to be elucidated. Our data using chronic (gabazine) or optogenetic activation of CN neurons shows enhancement of its output to frequency rates > 50 Hz (gabazine) and > 100 Hz (optogenetic). It has been suggested that increasing cerebellar output enhances cortical excitability by activation of the ascending di-synaptic glutamatergic excitatory dentate-thalamo-cortical pathway [489]. This however seems in sharp contrast with the anti-seizure effect proposed in this thesis and the multi-observed increased cortical excitability in juvenile myoclonic, idiopathic generalized and focal epilepsy in humans [490, 491]. It is believed however that increased sensorimotor cortex excitability and desynchronization go hand in hand [492-495].

Another question which stands out is how this desynchronization comes about. Major CN projections towards subcortical nuclei as superior colliculus, anterior pretectal nucleus and Zona Incerta (ZI) have been shown [84-86, 88, 89]. Since cerebellothalamic output is thought to be purely excitatory, the feed-forward excitation-inhibitory responses as recorded in neurons of group 2 in **Chapter 7** might originate from the non-thalamic innervation of extra-thalamic centers of inhibition (see also [442]) by CN axons. The ZI is one of these centers and receives cerebellar projections [89]. The ZI is related to motor-sensory integration and provides massive GABAergic feedback to virtually the entire neocortex [496, 497]. During my research I tried to bidirectionally control cerebellar

injected channelrhodospin and zona incertal injected halorhodopsin in an effort to find dorsal thalamic cells which would be alleviated from inhibition upon optogenetic activation of both opsins. Although my recordings and reconstructions of recording locations did not yet provide unequivocal evidence for this, I strongly believe zona incerta is capable of providing dorsal thalamus with gabaergic inhibition mediated by cerebellum [498].

9.4 Cerebellar control of human refractory epilepsy

An emanating question for the near future regarding CN stimulation in refractory epilepsy is whether or not different CN are capable of influencing various cortical areas involved in contrasting seizure types (Figure 2). In principle the cerebellar nuclei are perfectly suited for different epileptic phenotypes.

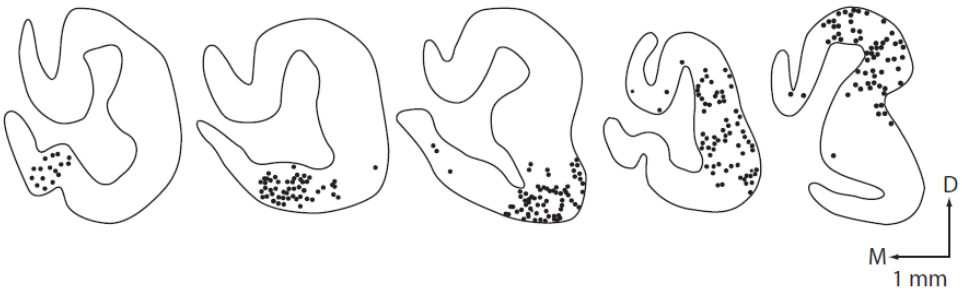

Figure 2. Output Channels in the dentate.

The dots on representative coronal sections show the location of dentate neurons that project to a specific area of the cerebral cortex in the cebus monkey. The cortical target is indicated above each section. (Abbreviations: M1, primary motor cortex; PMv, ventral premotor area) (Taken from Strick 2009).

The impact of cerebellar output changed over the last years significantly from being predominantly thought to influence motor coordination and control to also affecting cortical nonmotor areas important for visuospatial, cognitive and affective processes [499]. In **Chapter 3** we suggested that medial CN project more densely to the limbic system and thus in principle can be effective in stopping temporal seizures. Thus the possibilities of reaching several brain areas via different CN (medial to lateral) indicates that differently positioned stimulation is effective against several types of seizures, as is not uncommonly occurring in epilepsy patients [45, 46, 48, 89]. However, will medial CN be targeted? Seeing the relative small size of more medial CN compared to dentate nucleus and the

vicinity of brainstem structures I think changes are small [127, 128]. A good start in general would be to reestablish recent results [48] regarding CN efficacy in humans. That is why in combination with this thesis' results we started to work towards a clinical trial regarding DBS modulation of CN in pediatric refractory epilepsy patients, regardless of the numerous (ethical) considerations for experimental, invasive treatment options in pediatric patients. Still, given the long-term effects of refractory pediatric epilepsy on cognition, psychological health in adulthood and quality of life in general [500] I feel that efforts to push for CN DBS as a potential novel treatment is justified. However, physicians (and researchers!) must never forget that patients and parents feel undertaking DBS is a life altering decision. The perceived risks, uncertainty of neurosurgical intervention and its outcome, personal fears and the hope for a better life is an unimaginable delicate balance [501].

9.5 Cerebellar induced structural network changes

Structural network changes can occur after epilepsy surgery which not only controls seizures, but also substantially improves patients' behavior, quality of life and cognition [502]. Furthermore it is known that functional and structural brain abnormalities in epilepsy patients are not restricted to the epilepsy onset zone but reach out to other regions of the brain whichever are connected to this zone [503, 504]. This suggests that if focal lesions can give downstream changes in a neuronal system it seems not farfetched to think that a neuronal intervention, such as cerebellar stimulation, is also capable of inducing structural network changes in downstream targets. Any estimates on the most beneficial cerebellar stimulation is difficult seeing the knowledge gaps regarding which cerebellar cell subtypes project to which areas and the many differential non-pathological operating firing frequencies between cell subtypes (let alone seeing this in perspective of the many behavioral states; sleep, drowsy, awake etc) in combination with the problem of a neuromodulation probe being not capable of targeting a specific cell type but only an area. To achieve long lasting changes in downstream targets like the thalamus and further I believe open-loop chronic burst firing superimposed on high frequency (50-80 Hz) activity might be most beneficial.

The thalamus was recently shown to have subdivisions contributing to thalamocortical network abnormalities [505] which makes the CN with its widespread and divergent thalamic projections an ideal candidate for implementing structural cortical network changes as is evidenced over the last years by Machado and colleagues [152, 489, 506-508]. Besides from this evidence that structural changes can occur after lesion like damage from both epilepsy surgery and artificial infarcts, long-term follow-up of studies which were

initially started to evidence efficacy of neurostimulation show that outcome improves over time to over 60% when looking at median seizure reduction compared to baseline [15, 56]. To my knowledge there are no studies which investigate properties of cortical phase amplitude coupling or structural dynamics, e.g. by DTI imaging, several years after the start of neuromodulation. Nevertheless, all this evidence is suggestive for longlasting changes in network activity as a consequence of neuromodulation. In general I think that adding cerebellar output stimulation to the line of possibilities for treating refractory epilepsy is a step towards unraveling the best possible treatment. Among others future research goals need to seek for targets which can cause interictal changes to network activity for reducing the chance on an epileptic attack. Achieving this by implementing one of the most controversial aspects of DBS, i.e. its mechanism of action, will be the most challenging task for the near future.

It has been proposed that AN thalamic stimulation reduces seizure susceptibility because of increasing short-interval intracortical inhibition and increasing motor thresholds (and thus decreasing motor cortex excitability) [509]. This same group showed that stimulating cerebello-thalamo-cortical pathway using DBS VIM activates cortical M1 [510]. However, it remains highly speculative what the exact mechanism is of CN stimulation. Most likely it causes predominantly excitatory effects on thalamic neurons causing widespread desynchronization in thalamus and cortex. Pre and or postsynaptic neurotransmitter depletion or depolarization blockade of the CN soma because of high-frequency stimulation is unlikely when taking into account the natural high firing rate of CN neurons. Our **Chapter 6** results indicate however that optogenetic trains of high frequency stimulation lead to paired pulse depression in VL, VM and CL when measured *in vitro* at 32 degrees. Other unpublished observations from our group indicate that short interval pauses using electrical stimulation is sufficient to regain neurotransmitters in the synapse. Something which seems in concordance with the burst-like firing behavior of natural firing CN neurons. Another option for DBS to fail is somatic hyperpolarization which also seems unlikely because of mounting evidence that DBS is enhancing target output instead of causing lesions. Regarding plasticity it has been shown that upon subthalamic nucleus stimulation potentiation of field potentials did occur in substantia nigra but only following oral L-dopa administration [511]. Direct evidence regarding cerebellar induced LTP or LTD in dorsal thalamic neurons is very scarce [512]. Although evidence is mostly lacking regarding cerebellar induced LTP or LTD in thalamic neurons both in animals and in humans it is hard to come with any arguments why this will not be possible [512]. Furthermore I would like to point out that any ideas regarding downstream thalamic effects upon CN stimulation lacks information regarding the effects of dorsal thalamic

interneurons. Until date GABAergic interneurons have not been recognized in the dorsal thalamus in rodents apart from the lateral geniculate nuclei where they represent 20-25% of the total neurons [513, 514]. On the contrary primates and humans have neuronal thalamic populations containing between 20 and 30% interneurons [86, 515]. Apart from all these considerations future research can guide ideal stimulation parameters and whether or not crucial windows of opportunity exist to intervene in epileptic networks and inducing above described changes.

9.6 How to translate cerebellar epilepsy research?

Irving Cooper (1922-1985) set the stage by pioneering with functional neurosurgery. He aimed to manage neurological disorders such as cerebral palsy and epilepsy. Techniques under his command evolved into scientific reports where he described cerebellar stimulation for spasticity, cerebral palsy and epilepsy and deep brain stimulation for managing tremor and dystonia [69, 516-518]. I think it is safe to assume that his clinical research was at least in part initiated due to the work of Horsley (see the introduction of this thesis) and Sherrington who independently reported after anterior cerebellar lobe stimulation the release of decerebrate rigidity [47, 519, 520]. Over the years many more evidence about the cerebello-cerebral connection revealed first starting with primarily physiology related cerebellar cortex papers which subsequently were followed by reports about cerebello-thalamic connectivity [92, 307, 380, 401, 440, 441, 521, 522]. These results might have even further fueled Cooper's efforts. However, because of his anecdotal style of reports, lack of notion for the need of scientific validated reports of his results, lack of effort to collaborate and lack of criticism on his own work, his work on cerebellar stimulation was met with a lot of skepticism. Over the last years I have met that skepticism. Cerebellar stimulation for epilepsy was, according to many 'established scientists' at international conferences, already investigated and proved not to work. Case closed. Even referring to the work of Dr. Sozari Chkhenkeli [48] was put down as 'work performed in Georgia, so do the math'. Looking at all the work in this thesis performed in the experimental setting, using optogenetics and electrophysiological recording techniques, I would like to state that some of our findings confirm previous findings, but also allowed us to improve the understanding of the cerebellar impact on thalamo-cortical network activity in health and disease. Confirming previous results is very important in today's scientific environment since the human brain is skilled in self-deception which creates a neglect for our own biases. This has been evidenced multiple times over the last years and the fast rising pile of research results inevitably leads to more bias and incorrect results [523-525]. I feel that now the time has come to

re-introduce cerebellar stimulation into the clinic and establish the therapeutic value for patients of refractory seizures.

In that perspective our results in the Dravet Mouse model are difficult to interpret. On one hand we have results in different benign epileptic mouse models showing that cerebellar stimulation can be efficient stopping attacks using on-demand and chronic activation [46]. Furthermore others have shown that cerebellar cortex stimulation is capable of decreasing seizure duration in a temporal lobe seizure mouse model [45]. On the other hand our **Chapter 7** results clearly show that on-demand electrical stimulation of several brain targets, among which the cerebellar, cannot stop generalized epileptic attacks in the Dravet mouse model. It is a possibility that cerebellar projections do not reach all necessary brain areas to stop ongoing severe epileptic attacks. Motor and sensory cerebellothalamic nuclei projections have been shown but cerebellar projections to brain stem nuclei are far from evident [89] while explicitly the combination of stimulation of centrolateral thalamic nucleus and pontine nucleus oralis was shown to be crucial for seizure control in a focal limbic seizure model [433]. Whether or not this was limiting in our experiments is not clear. Furthermore ECoG characteristics and behavior during epileptic attacks in the Dravet mouse model were much more severe compared to our absence epilepsy models. This however does not need to be limiting since human experience of (sub)thalamic stimulation is considerably meager but results were presented as a moderate to significant seizure frequency reduction in a very low number of patients [526, 527]. This is a soft argument that although we were not able to stop epileptic attacks this does not exclude the possibility of reducing seizure frequency for which our research was not setup for [48].

Figure 3. Irving Cooper placing a probe into the thalamus with patient awake in a seated position (Picture taken from [528])

To conclude, whether or not CN neurons are capable of suppressing pathological oscillations remains an intriguing open one. Mouse transgenics is a very promising approach to examine this but we need more specific methods to target specific subtypes of CN neurons and a better understanding of their impact on thalamus. In this way, decades later after Irving Cooper started pioneering with functional neuromodulation we can further identify the potential benefit of cerebellar impact on thalamocortical networks in epilepsy (Figure 3).

R

References

[1] P. Kwan, S. C. Schachter, and M. J. Brodie, "Drug-Resistant Epilepsy," *N. Engl. J. Med.,* vol. 365, pp. 919-926, 2011.

[2] E. H. Reynolds and J. V. Kinnier Wilson, "Psychoses of epilepsy in Babylon: the oldest account of the disorder," *Epilepsia,* vol. 49, pp. 1488-1490, 2008.

[3] H. Cushing, "A note upon the faradic stimulation of the postcentral gyrus in conscious patients," *Brain,* vol. 32, pp. 44-53, 1909a.

[4] J. Hughlings Jackson, "Note on the comparison and contrast of regional palsy and spasm," *Lancet,* pp. 295-297, 1867.

[5] J. Hughlings Jackson, "Remarks on the disorderly movements of chorea and convulsion," *Med Times Gazette,* vol. ii, pp. 642-643, 1867.

[6] J. Hughlings Jackson, "A study of convulsions," *Trans St Andrews Med Grad Assoc,* vol. 3, pp. 162-204, 1870.

[7] J. Hughlings Jackson, "On the anatomical, physiological, and pathological investigation of epilepsies. A study of convulsions.," *West Riding Lunatic Asylum Med Reports,* vol. 3, pp. 315-319, 1873.

[8] V. Horsley, "The function of the so-called motor area of the brain," *British Medical Journal,* vol. 11, pp. 125-132, 1909.

[9] E. A. Spiegel, H. T. Wycis, M. Marks, and A. J. Lee, "Stereotaxic apparatus for operations on the human brain," *Science,* vol. 106, pp. 349-350, 1947.

[10] D. E. Sheer, *Electrical stimulation of the brain. An interdisciplinary survey of Neurobehavioral integrative systems*. Austin, Texas: University of Texas Press, 1961.

[11] I. S. Cooper, A. R. Upton, and I. Amin, "Reversibility of chronic neurologic deficits. Some effects of electrical stimulation of the thalamus and internal capsule in man," *Applied neurophysiology,* vol. 43, pp. 244-258, 1980.

[12] M. Šramka, G. Fritz, M. Galanda, and P. Nádvorník, "Some observations in treatment stimulation of epilepsy," *Acta Neurochir. (Wien),* vol. 23 (Suppl), pp. 257-262, 1976.

[13] A. R. Upton, I. S. Cooper, M. Springman, and I. Amin, "Suppression of seizures and psychosis of limbic system origin by chronic stimulation of anterior nucleus of the thalamus," *International journal of neurology,* vol. 19-20, pp. 223-230, 1986.

[14] E. B. Geller, T. L. Skarpaas, R. E. Gross, R. Goodman, G. Barkley, C. Bazil, *et al.*, "Brain-responsive neurostimulation in patients with medically intractable mesial temporal lobe epilepsy," *Epilepsia,* vol. 58, pp. 994-1004, 2017.

[15] V. Salanova, T. Witt, R. Worth, T. R. Henry, R. E. Gross, J. M. Nazzaro, *et al.*, "Long-term efficacy and safety of thalamic stimulation for drug-resistant partial epilepsy," *Neurology,* vol. 84, pp. 1017-1025, 2015.

[16] G. Buszaki, *Rhytms of the Brain*. New York: Oxford University Press, 2006.

[17] H. Berger, "Uber das Elektrenkephalogramm des Menschen," *Archiv fur Psychiatrie und Nervenkrankheiten,* vol. 87, pp. 527-570, 1929.

[18] D. Contreras and M. Steriade, "Cellular basis of EEG slow rhythms: a study of dynamic corticothalamic relationships," *Journal of Neuroscience,* vol. 15, pp. 604-622, 1995.

[19] S. Diekelmann and J. Born, "The memory function of sleep," *Nature Reviews Neuroscience,* vol. 11, 2010.

[20] M. A. Busche, M. Kekus, H. Adelsberger, T. Noda, H. Forstl, I. Nelken, *et al.*, "Rescue of long-range circuit dysfunction in Alzheimer's disease models," *Nature Neuroscience,* vol. 18, pp. 1623-1630, 2015.

[21] L. I. Schmitt, R. D. Wimmer, R. Nakajima, M. Happ, S. Mofakham, and M. M. Halassa, "Thalamic amplification of cortical connectivity sustains attentional control," *Nature,* vol. 545, pp. 219-223, 2017.

[22] M. F. Wells, R. D. Wimmer, L. I. Schmitt, G. Feng, and M. M. Halassa, "Thalamic reticular impairment underlies attention deficit in Ptchd1(Y/-) mice," *Nature,* vol. 532, pp. 58-63, 2016.

[23] R. D. Wimmer, L. I. Schmitt, T. J. Davidson, R. Nakajima, K. Deisseroth, and M. M. Halassa, "Thalamic control of sensory selection in divided attention," *Nature,* vol. 526, pp. 705-709, 2015.

[24] D. Williams, "A study of thalamic and cortical rhythms in petit mal," *Brain,* vol. 76, pp. 50-69, 1953.

[25] P. Andersen, S. A. Andersson, and T. Lomo, "Nature of thalamo-cortical relations during spontaneous barbiturate spindle activity," *Journal of Physiology,* vol. 192, pp. 283-307, 1967.

[26] T. Bal, "Synaptic and membrane mechanisms underlying synchronized oscillkations in the ferret lateral geniculate nucleus *in vitro*," *Journal of Physiology,* vol. 483, pp. 641-663, 1995.

[27] J. Gotman, "Interhemispheric relations during bilateral spike-and-wave activity," *Epilepsia,* vol. 22, pp. 453-466, 1981.

[28] M. Steriade and R. R. Llinás, "The functional states of the thalamus and the associated neuronal interplay," *Physiological Reviews,* vol. 68, pp. 649-742, 1988.

[29] M. von Krosigk, T. Bal, and D. A. McCormick, "Cellular mechanisms of a synchronized oscillation in the thalamus," *Science,* vol. 261, pp. 361-364, 1993.

[30] J. R. Huguenard and D. A. Prince, "Intrathalamic rhytmicity studied in vitro: nominal T-current modulation causes robust antioscillatory effects," *Journal of Neuroscience,* vol. 14, pp. 5485-5502, 1994.

[31] U. Kim, M. V. Sanchez-Vives, and D. A. McCormick, "Functional dynamics of GABAergic inhibition in the thalamus," *Science,* vol. 278, pp. 130-134, 1997.

[32] M. V. Sanchez-Vives and D. A. McCormick, "Functional properties of perigeniculate inhibition of dorsal lateral geniculate nucleus thalamocortical neurons in vitro," *Journal of Neuroscience,* vol. 17, pp. 8880-8893, 1997.

[33] H. K. Meeren, J. P. Pijn, E. L. Van Luijtelaar, A. M. Coenen, and F. H. Lopes da Silva, "Cortical focus drives widespread corticothalamic networks during spontaneous absence seizures in rats," *J. Neurosci.,* vol. 22, pp. 1480-1495, 2002.

[34] P. O. Polack, I. Guillemain, E. Hu, A. Depaulis, and S. Charpier, "Deep layer somatosensory cortical neurons initiate spike-and-wave discharges in a genetic model of absence seizures," *J. Neurosci.,* vol. 27, pp. 6590-6599, 2007.

[35] P. O. Polack, S. Mahon, M. Chavez, and S. Charpier, "Inactivation of the somatosensory cortex prevents paroxysmal oscillations in cortical and related thalamic neurons in a genetic model of absence epilepsy," *Cerebral Cortex,* vol. 19, pp. 2078-2091, 2009.

[36] S. Sasaki, K. Huda, T. Inoue, M. Miyata, and K. Imoto, "Impaired feedforward inhibition of the thalamocortical projection in epileptic Ca2+ channel mutant mice, tottering," *Journal of Neuroscience,* vol. 26, pp. 3056-3065, 2006.

[37] D. W. Cope, G. Di Giovanni, S. J. Fyson, G. Orbán, A. C. Errington, M. L. Lorincz*, et al.*, "Enhanced tonic GABAA inhibition in typical absence epilepsy," *Nat. Med.,* vol. 15, pp. 1392-1398, 2009.

[38] J. H. Jackson, "Case of tumour of the middle lobe of the cerebellum," *Brain,* vol. 29, pp. 425-440, 1906.

[39] R. S. Fisher and A. L. Velasco, "Electrical brain stimulation for epilepsy," *Nat. Rev. Neurol.,* vol. 10, pp. 261-270, 2014.

[40] R. S. Fisher, C. Acevedo, A. Arzimanoglou, A. Bogacz, J. H. Cross, C. E. Elger*, et al.*, "ILAE official report: a practical clinical definition of epilepsy," *Epilepsia,* vol. 55, pp. 475-482, 2014.

[41] S. L. Moshé, E. Perucca, P. Ryvlin, and T. Tomson, "Epilepsy: new advances," *Lancet,* vol. 385, pp. 884-898, 2015.

[42] M. P. Kerr, "The impact of epilepsy on patients' lives," *Acta Neurologica Scandinavia,* vol. 194, pp. 1-9, 2012.

[43] P. Perucca and F. G. Gilliam, "Adverse effects of antiepileptic drugs," *Lancet Neurology,* vol. 11, pp. 792-802, 2012.

[44] B. C. Jobst and G. D. Cascino, "Resective epilepsy surgery for drug-resistant focal epilepsy: a review," *JAMA,* vol. 313, pp. 285-293, 2015.

[45] E. Krook-Magnuson, G. G. Szabo, C. Armstrong, M. Oijala, and I. Soltesz, "Cerebellar Directed Optogenetic Intervention Inhibits Spontaneous Hippocampal Seizures in a Mouse Model of Temporal Lobe Epilepsy," *eNeuro,* vol. 1, 2014.

[46] L. Kros, O. H. J. Eelkman Rooda, J. K. Spanke, P. Alva, M. N. Van Dongen, A. Karapatis*, et al.*, "Cerebellar output controls generalized spike-and-wave discharge occurrence," *Annals of Neurology,* vol. 77, pp. 1027-1049, 2015.

[47] I. S. Cooper, "Effect of chronic stimulation of anterior cerebellum on neurological disease," *Lancet,* vol. 1, p. 206, 1973.

[48] S. A. Chkhenkeli, M. Šramka, G. S. Lortkipanidze, T. N. Rakviashvili, E. S. Bregvadze, G. E. Magalashvili*, et al.*, "Electrophysiological effects and clinical results of direct brain stimulation for intractable epilepsy," *Clin. Neuro.l Neurosurg.,* vol. 106, pp. 318-329, 2004.

[49] M. Šramka and I. S. Chkhenkeli, "Clinical experience in intraoperational determination of brain inhibitory structures and application of implanted neurostimulators in epilepsy," *Stereotact. Funct. Neurosurg.,* vol. 54-55, pp. 56-59, 1990.

[50] D. J. Englot, E. F. Chang, and K. I. Auguste, "Vagus nerve stimulation for epilepsy: a meta-analysis of efficacy and predictors of response," *Journal of Neurosurgery,* vol. 115, pp. 1248-1255, 2011.

[51] C. Bodin, S. Aubert, G. Daquin, R. Carron, D. Scavarda, A. McGonigal*, et al.*, "Responders to vagus nerve stimulation (VNS) in refractory epilepsy have reduced interictal cortical synchronicity on scalp EEG," *Epilepsy Research,* vol. 113, pp. 98-103, 2015.

[52] C. C. de Vos, L. Melching, J. van Schoonhoven, J. J. Ardesch, A. W. de Weerd, H. C. van Lambalgen, *et al.*, "Predicting success of vagus nerve stimulation (VNS) from interictal EEG," *Seizure,* vol. 20, pp. 541-545, 2011.

[53] M. Fraschini, M. Puligheddu, M. Demuru, L. Polizzi, A. Maleci, G. Tamburini, *et al.*, "VNS induced desynchronization in gamma bands correlates with positive clinical outcome in temporal lobe pharmacoresistant epilepsy," *Neuroscience Letters,* vol. 536, pp. 14-18, 2013.

[54] R. Fisher, V. Salanova, T. Witt, R. Worth, T. Henry, R. Gross, *et al.*, "Electrical stimulation of the anterior nucleus of thalamus for treatment of refractory epilepsy," *Epilepsia,* vol. 51, pp. 899-908, 2010.

[55] M. J. Morrell, "Responsive cortical stimulation for the treatment of medically intractable partial epilepsy," *Neurology,* vol. 77, pp. 1295-1304, 2011.

[56] G. K. Bergey, M. J. Morrell, E. M. Mizrahi, A. Goldman, D. King-Stephens, D. Nair, *et al.*, "Long-term treatment with responsive brain stimulation in adults with refractory partial seizures," *Neurology,* vol. 84, pp. 810-817, 2015.

[57] U. Eckert, C. D. Metzger, J. E. Buchmann, J. Kaufmann, A. Osoba, M. Li, *et al.*, "Preferential networks of the mediodorsal nucleus and centromedian-parafascicular complex of the thalamus--a DTI tractography study," *Human brain mapping,* vol. 33, pp. 2627-2637, 2012.

[58] S. Haber and N. R. McFarland, "The place of the thalamus in frontal cortical-basal ganglia circuits," *Neuroscientist,* vol. 7, pp. 315-324, 2001.

[59] Y. D. van der Werf, M. P. Witter, and H. J. Groenewegen, "The intralaminar and midline nuclei of the thalamus. Anatomical and functional evidence for participation in processes of arousal and awareness," *Brain Research. Brain research reviews,* vol. 39, pp. 107-140, 2002.

[60] A. Valentín, E. García Navarrete, R. Chelvarajah, C. Torres, M. Navas, L. Vico, *et al.*, "Deep brain stimulation of the centromedian thalamic nucleus for the treatment of generalized and frontal epilepsies," *Epilepsia,* vol. 54, pp. 1823-1833, 2013.

[61] F. Velasco, A. L. Velasco, M. Velasco, F. Jiménez, J. D. Carrillo-Ruiz, and G. Castro, "Deep brain stimulation for treatment of the epilepsies: the centromedian thalamic target," *Acta Neurochir. (Suppl.),* vol. 97, pp. 337-342, 2007.

[62] F. Velasco, M. Velasco, C. Ogarrio, and G. Fanghanel, "Electrical stimulation of the centromedian thalamic nucleus in the treatment of convulsive seizures: a preliminary report," *Epilepsia,* vol. 28, pp. 421-430, 1987.

[63] F. Velasco, M. Velasco, A. L. Velasco, and F. Jiménez, "Effect of chronic electrical stimulation of the centromedian thalamic nuclei on various intractable seizure patterns: I. Clinical seizures and paroxysmal EEG activity," *Epilepsia,* vol. 34, pp. 1052-1064, 1993.

[64] F. Velasco, M. Velasco, A. L. Velasco, F. Jimenez, I. Marquez, and M. Rise, "Electrical stimulation of the centromedian thalamic nucleus in control of seizures: long-term studies," *Epilepsia,* vol. 36, pp. 63-71, 1995.

[65] F. Velasco, M. Velasco, A. L. Velasco, D. Menez, and L. Rocha, "Electrical stimulation for epilepsy: stimulation of hippocampal foci," *Stereotact. Funct. Neurosurg.,* vol. 77, pp. 223-227, 2001.

[66] G. Moruzzi, "Effects at different frequencies of cerebellar stimulation upon postural tonus and myotatic reflexes," *Electroencephalography and Clinical Neurophysiology,* vol. 2, pp. 463-469, 1950.

[67] K. D. Graber and R. S. Fisher, "Deep Brain Stimulation: Animal Models," in *Jasper's Basic Mechanisms of the Epilepsies*, J. L. Noebels, M. Avoli, M. A. Rogawski, R. W. Olsen, and A. V. Delgado-Escueta, Eds., ed Bethesda, US: National Center for Biotechnology Information, 2012.

[68] J. Bidziński, T. Bacia, K. Ostrowski, and L. Czarkwiani, "Effect of cerebellar cortical electrostimulation on the frequency of epileptic seizures in severe forms of epilepsy," *Neurol. Neurochir. Pol.,* vol. 15, pp. 605-609, 1981.

[69] I. S. Cooper, I. Amin, M. Riklan, J. M. Waltz, and T. P. Poon, "Chronic cerebellar stimultion in epilepsy. Clinical and anatomical studies," *Arch. Neurol.,* vol. 33, pp. 559-570, 1976.

[70] R. Davis, "Cerebellar stimulation for cerebral palsy spasticity, function and seizures," *Arch. Med. Res.,* vol. 31, pp. 290-299, 2000.

[71] R. Davis and S. E. Emmonds, "Cerebellar stimulation for seizure control: 17-year study," *Stereotactic Functional Neurosurgery,* vol. 58, pp. 200-208, 1992.

[72] R. S. Dow, W. Smith, and L. Maukonen, "Clinical experience with chronic cerebellar stimulation in epilepsy and cerebral palsy," *Electroencephalogr. Clin. Neurophysiol.,* vol. 43, p. 906, 1977.

[73] S. Gilman, G. W. Dauth, V. M. Tennyson, L. T. Kremzner, R. Defendini, and J. W. Correll, "Clinical, morphological, biochemical, and physiological effects of cerebellar stimulation," in *Functional Electrical Stimulation: Applications in Neural Prosthesis*, 5 ed New York: Marcel Dekker, 1977.

[74] G. L. Krauss and M. Z. Koubeissi, "Cerebellar and thalamic stimulation treatment for epilepsy," *Acta. Neurochir. Suppl.,* vol. 97, pp. 347-356, 2007.

[75] L. F. Levy and W. C. Auchterlonie, "Chronic cerebellar stimulation in the treatment of epilepsy," *Epilepsia,* vol. 20, pp. 235-245, 1979.

[76] J. M. Van Buren, J. H. Wood, J. Oakley, and F. Hambrecht, "Preliminary evaluation of cerebellar stimulation by double-blind stimulation and biological criteria in the treatment of epilepsy," *J. Neurosurg.,* vol. 48, 1978.

[77] F. Velasco, J. D. Carrillo-Ruiz, M. Velasco, A. L. Velasco, I. Marquez, and R. Davis, "Double-blind, randomized controlled pilot study of bilateral cerebellar stimulation for treatment of intractable motor seizures," *Epilepsia,* vol. 46, pp. 1071-1081, 2005.

[78] G. D. Wright, D. McLellan, and J. G. Brice, "A double-blind trial of chronic cerebellar stimulation in twelve patients with severe epilepsy," *J. Neurol. Neurosurg. Psych.,* vol. 47, pp. 769-774, 1984.

[79] J. Voogd, "The human cerebellum," *Journal of chemical neuroanatomy,* vol. 26, pp. 243-252, 2003.

[80] H. Zhou, Z. Lin, K. Voges, C. Ju, Z. Gao, L. W. Bosman*, et al.*, "Cerebellar modules operate at different frequencies," *Elife,* vol. 3, p. e02536, 2014.

[81] C. I. De Zeeuw, F. E. Hoebeek, L. W. J. Bosman, M. Schonewille, L. Witter, and S. K. Koekkoek, "Spatiotemporal firing patterns in the cerebellum," *Nat. Rev. Neurosci.,* vol. 12, pp. 327-344, 2011.

[82] M. Najac and I. M. Raman, "Integration of Purkinje cell inhibition by cerebellar nucleo-olivary neurons.," *Journal of Neuroscience,* vol. 35, pp. 544-549, 2015.

[83] A. L. Person and I. Raman, "Purkinje neuron synchrony elicits time-locked spiking in the cerebellar nuclei," *Nature,* vol. 481, pp. 502-505, 2012.

[84] T. D. Aumann and M. K. Horne, "Ramification and termination of single axons in the cerebellothalamic pathway of the rat," *J. Comp. Neurol.,* vol. 376, pp. 420-430, 1996.

[85] A. C. Bostan, R. P. Dum, and P. L. Strick, "Cerebellar networks with the cerebral cortex and basal ganglia," *Trends in cognitive sciences,* vol. 17, pp. 241-254, 2013.

[86] E. G. Jones, "The Thalamus 2nd Edition," 2 ed. New York: Cambridge University Press, 2007.

[87] F. Palesi, J. D. Tournier, F. Calamante, N. Muhlert, G. Castellazzi, D. Chard, *et al.*, "Contralateral cerebello-thalamo-cortical pathways wih prominent involvement of associative areas in humans in vivo," *Brain structure & function,* vol. 220, pp. 3369-3384, 2015.

[88] T. J. Ruigrok and T. M. Teune, "Collateralization of cerebellar output to functionally distinct brainstem areas. A retrograde, non-fluorescent tracing study in the rat," *Frontiers in systems neuroscience,* vol. 8, p. 23, 2014.

[89] T. M. Teune, J. van der Burg, J. van der Moer, J. Voogd, and T. J. Ruigrok, "Topography of cerebellar nuclear projections to the brain stem in the rat," *Progress in brain research,* vol. 124, pp. 141-172, 2000.

[90] R. D. Proville, M. Spolidoro, N. Guyon, G. P. Dugué, F. Selimi, P. Isope, *et al.*, "Cerebellum involvement in cortical sensorimotor circuits for the control of voluntary movements," *Nature Neuroscience,* vol. 17, pp. 1233-1239, 2014.

[91] S. F. Sawyer, S. J. Young, P. M. Groves, and J. M. Tepper, "Cerebellar-responsive neurons in the thalamic ventroanterior-ventrolateral coplex of rats: in vivo electrophysiology," *Neuroscience,* vol. 63, pp. 711-724, 1994.

[92] M. Uno, M. Yoshida, and I. Hirota, "The mode of cerebello-thalamic relay transmission investigated with intracellular recording from cells of the ventrolateral nucleus of cat's thalamus," *Exp. Brain Res.,* vol. 10, pp. 121-39, 1970.

[93] H. Arnts, M. Kleinnijenhuis, J. G. Kooloos, A. N. Schepens-Franke, and A. M. van Cappellen van Walsum, "Combining fiber dissection, plastination, and tractography for neuroanatomical education: Revealing the cerebellar nuclei and their white matter connections," *Anatomical sciences education,* vol. 7, pp. 47-55, 2014.

[94] B. J. Hunnicutt, B. R. Long, D. Kusefoglu, K. J. Gertz, H. Zhong, and T. Mao, "A comprehensive thalamocortical projection map at the mesoscopic level," *Nature Neuroscience,* vol. 17, pp. 1276-1285, 2014.

[95] I. Sugihara, H. Fujita, J. Na, P. N. Quy, B. Y. Li, and D. Ikedia, "Projection of reconstructed single Purkinje cell axons in relation to the cortical and nuclear aldolase C compartments of the rat cerebellum," *J. Comp. Neurol.,* vol. 512, pp. 282-304, 2009.

[96] A. D. Norden and H. Blumenfeld, "The role of subcortical structures in epilepsy," *Epilepsy Behav.,* vol. 3, pp. 219-231, 2002.

[97] J. T. Paz and J. R. Huguenard, "Microcircuits and their interactions in epilepsy: is the focus out of focus?," *Nature Neuroscience,* vol. 18, pp. 351-359, 2015.

[98] R. S. Fisher, C. Acevedo, A. Arzimanoglou, A. Bogacz, J. H. Cross, C. E. Elger, *et al.*, "ILAE official report: a practical clinical definition of epilepsy," *Epilepsia,* vol. 55, pp. 475-482, 2014.

[99] P. O. Polack and S. Charpier, "Intracellular activity of cortical and thalamic neurones during high-voltage rhythmic spike discharge in Long-Evans rats in vivo," *Journal of Physiology,* vol. 571, pp. 461-476, 2006.

[100] T. Bal and D. A. McCormick, "Mechanisms of oscillatory activity in guinea-pig nucleus reticularis thalami in vitro: a mammalian pacemaker," *Journal of Physiology,* vol. 468, pp. 669-691, 1993.

[101] C. C. Huang, K. Sugino, Y. Shima, C. Guo, S. Bai, B. D. Mensh, *et al.*, "Convergence of pontine and proprioceptive streams onto multimodal cerebellar granule cells," *Elife,* vol. 2, p. e00400, 2013.

[102] P. M. Cooke and R. S. Snider, "Some cerebellar influences on electrically-induced cerebral seizures," *Epilepsia,* vol. 4, 1955.

[103] A. Fernandez-Guardiola, E. Manni, J. H. Wilson, and R. S. Dow, "Microelectrode recording of cerebellar and cerebral unit activity during convulsive afterdischarge," *Exp. Neurol.,* vol. 6, pp. 48-69, 1962.

[104] A. Kandel and G. Buzsáki, "Cerebellar neuronal activity correlates with spike and wave EEG patterns in the rat," *Epilepsy Res.,* vol. 16, pp. 1-9, 1993.

[105] F. E. Hoebeek, L. Witter, T. J. Ruigrok, and C. I. De Zeeuw, "Differential olivo-cerebellar cortical control of rebound activity in the cerebellar nuclei," *Proc. Natl. Acad. Sci. U.S.A.,* vol. 107, pp. 8410-8415, 2010.

[106] Y. Shinoda, M. Kano, and T. Futami, "Synaptic organization of the cerebello-thalamo-cerebral pathway in the cat. I. Projection of individual cerebellar nuclei to single pyramidal tract neurons in areas 4 and 6," *Neuroscience Research,* vol. 2, pp. 133-156, 1985.

[107] K. Alvina, J. T. Walter, A. Kohn, G. Ellis-Davies, and K. Khodakhah, "Questioning the role of rebound firing in the cerebellum," *Nature Neuroscience,* vol. 11, pp. 1256-1258, 2008.

[108] F. Bengtsson, C. F. Ekerot, and H. Jorntell, "In vivo analysis of inhibitory synaptic inputs and rebounds in deep cerebellar nuclear neurons," *PLoS One,* vol. 6, 2011.

[109] M. L. Molineux, J. E. McRory, B. E. McKay, J. Hamid, W. H. Mehaffey, R. Rehak, *et al.*, "Specific T-type calcium channel isoforms are associated with distinct burst phenotypes in deep cerebellar nuclear neurons," *PNAS,* vol. 103, pp. 5555-5560, 2006.

[110] N. C. Rowland and D. Jaeger, "Responses to tactile stimulation in deep cerebellar nucleus neurons result from recurrent activation in multiple pathways," *Journal of Neurophysiology,* vol. 99, pp. 704-717, 2008.

[111] L. Witter, C. B. Canto, T. M. Hoogland, J. R. de Gruijl, and C. I. De Zeeuw, "Strength and timing of motor responses mediated by rebound firing in the cerebellar nuclei after Purkinje cell activation," *Frontiers in neural circuits,* vol. 7, pp. 1-14, 2013.

[112] M. Uusisaari and T. Knöpfel, "Diversity of neuronal elements and circuitry in the cerebellar nuclei," *Cerebellum,* vol. 11, pp. 420-421, 2012.

[113] R. R. Myers, K. J. Burchiel, J. J. Stockard, and R. G. Bickford, "Effects of acute and chronic paleocerebellar stimulation on experimental models of epilepsy in the cat: studies with enflurane, pentylenetetrazol, penicillin, and chloralose," *Epilepsia,* vol. 16, pp. 257-267, 1975.

[114] R. G. Heath and J. W. Harper, "Ascending projections of the cerebellar fastigial nucleus to the hippocampus, amygdala, and other temporal lobe sites: evoked potential and histological studies in monkeys and cats," *Experimental Neurology,* vol. 45, pp. 268-287, 1974.

[115] J. Chaumont, N. Guyon, A. M. Valera, G. P. Duqué, D. Popa, P. Marcaggi, *et al.*, "Clusters of cerebellar Purkinje cells control their afferent climbing fiber discharge," *PNAS,* vol. 110, pp. 16223-16228, 2013.

[116] T. L. Babb, A. G. J. Mitchell, and P. H. Crandall, "Fastigiobulbar and dentatothalamic influences on hippocampal cobalt epilepsy in the cat," *Electroencephalography and Clinical Neurophysiology,* vol. 36, pp. 141-154, 1974.

[117] R. S. Dow, A. Fernandez-Guardiola, and E. Manni, "The influence of the cerebellum on experimental epilepsy," *Electroencephalography and Clinical Neurophysiology,* vol. 14, 1962.

[118] D. C. Hemmy, S. J. Larson, A. J. Sances, and E. A. Millar, "The effect of cerebellar stimulation on focal seizure activity and spasticity in monkeys," *Journal of Neurosurgery,* vol. 46, pp. 648-653, 1977.

[119] R. A. Badawy, A. Lai, S. J. Vogrin, and M. J. Cook, "Subcortical epilepsy?," *Neurology,* vol. 80, pp. 1901-1907, 2013.

[120] J. F. Fulton, "A case of cerebellar tumor with seizures of head retraction described by Wurffbain in 1691," *J. Nerv. Ment. Dis.,* vol. 70, pp. 577-583, 1929.

[121] P. R. McCrory, P. F. Bladin, and S. F. Berkovic, "The cerebellar seizures of Hughlings Jackson," *Neurology,* vol. 52, pp. 1888-1890, 1999.

[122] S. Boop, J. Wheless, K. Van Poppel, A. McGregor, and F. A. Boop, "J. Neurosurg. Pediatr.," *12,* vol. 3, 2013.

[123] M. D. Mark, T. Maejima, D. Kuckelsberg, J. W. Yoo, R. A. Hyde, V. Shah, *et al.*, "Delayed postnatal loss of P/Q-type calcium channels recapitulates the absence epilepsy, dyskinesia, and ataxia phenotypes of genomic Cacna1a mutations," *J. Neurosci.,* vol. 31, pp. 4311-4326, 2011.

[124] T. Maejima, P. Wollenweber, L. Teusner, J. L. Noebels, S. Herlitze, and M. D. Mark, "Postnatal loos of P/Q-type channels confined to rhombic-lip-derived neurons alters synaptic transmission at the parallel fiber to Purkinje cell synapse and replicates genomic Cacna1a mutation phenotype of

ataxia and seizures in Mice," *J. Neurosci.,* vol. 33, pp. 5162-5174, 2013.

[125] E. Galliano, Z. Gao, M. Schonewille, B. Todorov, E. Simons, A. S. Pop, *et al.*, "Silencing the majority of cerebellar granule cells uncovers their essential role in motor learning and consolidation," *Cell Reports,* vol. 3, pp. 1239-1251, 2013.

[126] J. T. Paz, T. J. Davidson, E. S. Frechette, B. Delord, I. Parada, K. Peng, *et al.*, "Closed-loop optogenetic control of thalamus as a tool for interrupting seizures after cortical injury," *Nat. Neurosci.,* vol. 16, pp. 64-70, 2013.

[127] A. Hayaran, S. Wadhwa, G. Gopinath, and V. Bijlani, "Developing dentate nucleus in man: a qualitative and quantitative study," *Experimental Brain Research,* vol. 89, pp. 640-648, 1992.

[128] S. Tellmann, S. Bludau, S. Eickhoff, H. Mohlberg, M. Minnerop, and K. Amunts, "Cytoarchitectonic mapping of the human brain cerebellar nuclei in stereotaxic space and delineation of their co-activation patterns," *Frontiers in neuroanatomy,* vol. 9, 2015.

[129] M. Šramka, G. Fritz, M. Galanda, and P. Nádvorník, "Some observations in treatment stimulation of epilepsy," *Acta Neurochir. (Suppl.),* vol. 23, pp. 257-262, 1976.

[130] B. P. Hermann, K. Bayless, H. R., J. Parrish, and M. Seidenberg, "Cerebellar atrophy in temporal lobe epilepsy," *Epilepsy & Behavior,* vol. 7, pp. 279-287, 2005.

[131] R. Crooks, T. Mitchell, and M. Thom, "Patterns of cerebellar atrophy in patients with chronic epilepsy: a quantitative neuropathological study," *Epilepsy Res.,* vol. 41, pp. 63-73, 2000.

[132] M. Sévin, G. Lesca, N. Baumann, G. Millat, O. Lyon-Caen, M. T. Vanier, *et al.*, "The adult form of Niemann-Pick disease type C," *Brain,* vol. 130, pp. 120-133, 2007.

[133] A. M. J. M. van den Maagdenberg, T. K. Pizzorusso, S., N. Terpolilli, M. Shapovalova, F. E. Hoebeek, C. F. Barrett, *et al.*, "High cortical spreading depression susceptibility and migraine-associated symptoms in Ca(v)2.1 S218L mice," *Annals of Neurology,* vol. 67, pp. 85-98, 2010.

[134] T. Joensuu, S. Tegelberg, E. Reinmaa, M. Segerstråle, P. Hakala, H. Pehkonen, *et al.*, "Gene expression alterations in the cerebellum and granule neurons of Cstb(-/-) mouse are associated with early synaptic changes and inflammation," *PLoS One,* vol. 8, p. 89321, 2014.

[135] V. Villanueva, J. Alvarez-Linera, P. Gómez-Garre, J. Gutiérrez, and J. M. Serratosa, "MRI volumetry and proton MR spectroscopy of the brain in Lafora disease," *Epilepsia,* vol. 47, pp. 788-792, 2006.

[136] U. Specht, T. May, R. Schulz, M. Rohde, A. Ebner, R. C. Schmidt, *et al.*, "Cerebellar atrophy and prognosis after temporal lobe resection," *Journal of neurology, neurosurgery, and psychiatry,* vol. 62, pp. 501-506, 1997.

[137] J. W. Miller, B. C. Gray, and G. M. Turner, "Role of the fastigial nucleus in generalized seizures as demonstrated by GABA agonist microinjections," *Epilepsia,* vol. 34, pp. 973-978, 1993.

[138] N. Tsuru, H. Kawasaki, S. Genda, K. Hara, H. Hashiguchi, and Y. Ueda, "Effect of unilateral dentate nucleus lesions on amygdaloid kindling in rats," *Epilepsia,* vol. 33, pp. 213-221, 1992.

[139] N. R. Ghatak, R. A. Santoso, and W. M. McKinney, "Cerebellar degeneration following long-term phenytoin therapy," *Neurology,* vol. 26, pp. 818-820, 1976.

[140] I. Savic and J. O. Thorell, "Localized cerebellar reductions in benzodiazepine receptor density in human partial epilepsy," *Archives of neurology,* vol. 53, pp. 656-662, 1996.

[141] J. Annese, N. M. Schenker-Ahmed, H. Bartsch, P. Maechler, C. Sheh, N. Thomas, *et al.*, "Postmortem examination of patient H.M.'s brain based on histological sectioning and digital 3D reconstruction," *Nature Communications,* vol. 5, p. 3122, 2014.

[142] J. C. Augustinack, A. J. van der Kouwe, D. H. Salat, T. Benner, A. A. Stevens, J. Annese, *et al.*, "H.M.'s contributions to neuroscience: a review and autopsy studies," *Hippocampus,* vol. 24, pp. 126-1286, 2014.

[143] Y. Li, H. Du, B. Xie, N. Wu, J. Wang, G. Wu, *et al.*, "Cerebellum abnormalities in idiopathic generalized epilepsy with generalized tonic-clonic seizures revealed by diffusion tensor imaging," *PLoS One,* vol. 5, pp. 1-7, 2010.

[144] K. M. Park, Y. H. Han, T. H. Kim, C. W. Mun, K. J. Shin, S. Y. Ha, *et al.*, "Cerebellar white matter changes in patients with newly diagnosed partial epilepsy of unknown etiology," *Clinical neurology and neurosurgery,* vol. 138, pp. 25-30, 2015.

[145] K. M. Park, T. H. Kim, Y. H. Han, C. W. Mun, K. J. Shin, S. Y. Ha, *et al.*, "Brain morphology in juvenile myoclonic epilepsy and absence seizures," *Acta Neurologica Scandinavia,* 2015.

[146] E. Calabrese, P. Hickey, C. Hulette, J. Zhang, B. Parente, S. P. Lad, *et al.*, "Postmortem diffusion MRI of the human brainstem and thalamus for deep brain stimulator electrode localization," *Human brain mapping,* vol. 36, pp. 3167-3178, 2015.

[147] S. Groppa, J. Herzog, D. Falk, C. Riedel, G. Deuschl, and J. Volkmann, "Physiological and anatomical decomposition of subthalamic neurostimulation effects in essential tremor," *Brain,* vol. 137, pp. 109-121, 2014.

[148] A. M. Lozano and N. Lipsman, "Probing and regulating dysfunctional circuits using deep brain stimulation," *Neuron,* vol. 77, pp. 406-424, 2013.

[149] M. S. LeDoux, J. F. Lorden, and J. Meinzen-Derr, "Selective elimination of cerebellar output in the genetically dystonic rat," *Brain research,* vol. 697, pp. 91-103, 1995.

[150] S. M. Sherman, "The function of metabotropic glutamate receptors in thalamus and cortex," *Neuroscientist,* vol. 20, pp. 136-149, 2014.

[151] P. Mahlknecht, P. Limousin, and T. Foltynie, "Deep brain stimulation for movement disorders: update on recent discoveries and outlook on future developments," *Journal of neurology,* vol. 262, pp. 2583-2595, 2015.

[152] J. Cooperrider, H. Furmaga, E. Plow, H. J. Park, Z. Chen, G. Kidd*, et al.*, "Chronic deep cerebellar stimulation promotes long-term potentiation, microstructural plasticity, and reorganization of perilesional cortical representation in a rodent model," *Journal of Neuroscience,* vol. 34, pp. 9040-9050, 2014.

[153] C. W. Hess, D. E. Vaillancourt, and M. S. Okun, "The temporal pattern of stimulation may be important to the mechanism of deep brain stimulation," *Experimental Neurology,* vol. 247, pp. 296-302, 2013.

[154] R. Apps and R. Hawkes, "Cerebellar cortical organization: a one map hypothesis," *Nat. Rev. Neurosci.,* vol. 10, pp. 670-681, 2009.

[155] D. Jaeger, "Mini-review: synaptic integration in the cerebellar nuclei--perspectives from dynamic clamp and computer simulation studies," *Cerebellum,* vol. 10, pp. 659-666, 2011.

[156] K. J. van Dijk, R. Verhagen, A. Chaturvedi, C. C. McIntyre, L. J. Bour, C. Heida*, et al.*, "A novel lead design enables selective deep brain stimulation of neural populations in the subthalamic region," *Journal of neural engineering,* vol. 12, p. 046003, 2015.

[157] K. Gadhoumi, J. M. Lina, F. Mormann, and J. Gotman, "Seizure prediction for therapeutic devices: A review," *Journal of Neuroscience Methods,* vol. 260, pp. 270-282, 2016.

[158] M. N. van Dongen, A. Karapatis, L. Kros, O. H. J. Eelkman Rooda, R. M. Seepers, C. Strydis*, et al.*, "An implementation of a wavelet-based seizure detection filter suitable for realtime closed-loop epileptic seizure suppression," in *IEEE Biomedical Circuits and Systems Conference*, ed, 2014, pp. 504-507.

[159] A. Berényi, M. Belluscio, D. Mao, and G. Buzsàki, "Closed-loop control of epilepsy by transcranial electrical stimulation.," *Science,* vol. 337, pp. 735-737, 2012.

[160] E. Krook-Magnuson, C. Armstrong, M. Oijala, and I. Soltesz, "On-demand optogenetic control of spontaneous seizures in temporal lobe epilepsy," *Nature Communications,* vol. 4, p. 1376, 2013.

[161] P. Suffczynski, S. Kalitzin, and F. H. Lopes Da Silva, "Dynamics of non-convulsive epileptic phenomena modeled by a bistable neuronal network," *Neuroscience,* vol. 126, pp. 467-484, 2004.

[162] P. N. Taylor, Y. Wang, M. Goodfellow, J. Dauwels, F. Moeller, U. Stephani*, et al.*, "A computational study of stimulus driven epileptic seizure abatement," *PLoS One,* vol. 9, p. 114316, 2014.

[163] U. Seneviratne, M. Cook, and W. D'Souza, "The electroencephalogram of idiopathic generalized epilepsy.," *Epilepsia,* vol. 53, pp. 234-248, 2012.

[164] L. Kros, O. H. J. Eelkman Rooda, C. I. De Zeeuw, and F. E. Hoebeek, "Controlling cerebellar output to treat refractory epilepsy," *Trends in Neurosciences,* vol. 38, pp. 787-799, 2015.

[165] R. Hawkes, S. Blyth, V. Chockkan, D. Tano, Z. Ji, and C. Mascher, "Structural and molecular compartmentation in the cerebellum," *The Canadian Journal of neurological sciences,* vol. 20, pp. S29-S35, 1993.

[166] A. Pijpers, J. Voogd, and T. J. Ruigrok, "Topography of olivo-cortico-nuclear modules in the intermediate cerebellum of the rat," *Journal of Comparative Neurology,* vol. 492, pp. 193-213, 2005.

[167] O. Yizhar, L. E. Fenno, T. J. Davidson, M. Mogri, and K. Deisseroth, "Optogenetics in neural systems," *Neuron,* vol. 71, pp. 9-34, 2011.

[168] A. R. Houweling and M. Brecht, "Behavioural report of single neuron stimulation in somatosensory cortex," *Nature,* vol. 451, pp. 65-68, 2008.

[169] C. Guo, L. Witter, S. Rudolph, H. L. Elliott, K. A. Ennis, and W. G. Regehr, "Purkinje cells directly inhibit granule cells in specialized regions of the cerebellar cortex," *Neuron,* vol. 91, pp. 1330-1341, 2016.

[170] A. M. Valera, F. Binda, S. A. Pawlowski, J. L. Dupont, J. F. Casella, J. D. Rothstein, *et al.*, "Stereotyped spatial patterns of functional synaptic connectivity in the cerebellar cortex," *Elife,* vol. 5, 2016.

[171] L. Witter, S. Rudolph, R. T. Pressler, S. I. Lahlaf, and W. G. Regehr, "Purkinje cell collaterals enable output signals from the cerebellar cortex to feed back to purkinje cells and interneurons," *Neuron,* vol. 91, pp. 312-319, 2016.

[172] B. Sauer and N. Henderson, "Site-specific DNA recombination in mammalian cells by the Cre recombinase of bacteriophage P1," *Proc. Natl. Acad. Sci. U. S. A.,* vol. 85, pp. 5166-5170, 1988.

[173] GENSAT. (2016). *Gensat website for Cre mice*.

[174] L. Madisen, A. R. Garner, D. Shimaoka, A. S. Chuong, N. C. Klapoetke, L. Li, *et al.*, "Transgenic mice for intersectional targeting of neural sensors and effectors with high specificity and performance," *Neuron,* vol. 85, pp. 942-958, 2015.

[175] L. Madisen, T. Mao, H. Koch, J. M. Zhuo, A. Berenyi, S. Fujisawa, *et al.*, "A toolbox of Cre-dependent optogenetic transgenic mice for light-induced activation and silencing," *Nature Neuroscience,* vol. 15, pp. 793-802, 2012.

[176] J. Oberdick, R. J. Smeyne, J. R. Mann, S. Zackson, and J. I. Morgan, "A promoter that drives transgene expression in cerebellar purkinje and retinal bipolar neurons," *Science,* vol. 248, pp. 223-226, 1990.

[177] J. J. Barski, K. Dethleffsen, and M. Meyer, "Cre recombinase expression in cerebellar Purkine cells," *Genesis,* vol. 28, pp. 93-98, 2000.

[178] T. D. Nguyen-Vu, R. R. Kimpo, J. M. Rinaldi, A. Kohli, H. Zeng, K. Deisseroth, *et al.*, "Cerebellar Purkinje cell activity drives motor learning," *Nature Neuroscience,* vol. 16, pp. 1734-1736, 2013.

[179] L. Petreanu, D. Huber, A. Sobczyk, and K. Svoboda, "Channelrhodopsin-2-assisted circuit mapping of long-range callosal projections," *Nature Neuroscience,* vol. 10, pp. 663-668, 2007.

[180] M. Yamada, Y. Seto, S. Taya, T. Owa, Y. U. Inoue, T. Inoue, *et al.*, "Specification of spatial identities of cerebellar neuron progenitors by ptf1a and atoh1 for proper production of GABAergic and glutamatergic neurons," *Journal of Neuroscience,* vol. 34, pp. 4786-4800, 2014.

[181] J. Szcurkowska, A. W. Cwetsch, M. dal Maschio, D. Ghezzi, G. M. Ratto, and L. Cancedda, "Targeted in vivo genetic manipulation of the mouse or rat brain by in utero electroporation with a triple-electrode probe," *Nature Protocols,* vol. 11, pp. 399-412, 2016.

[182] V. Lukashchuk, K. E. Lewis, I. Coldicott, A. J. Grierson, and M. Azzouz, "AAV9-mediated central nervous system-targeted gene delivery via cisterna magna route in mice," *Molecular therapy. Methods & clinical development,* vol. 3, 2016.

[183] J. R. McLean, G. A. Smith, E. M. Rocha, M. A. Hayes, J. A. Beagan, P. J. Hallett, *et al.*, "Widespread neuron-specific transgene expression in brain and spinal cord following synapsin promoter-driven AAV9 neonatal intracerebroventricular injection," *Neuroscience Letters,* vol. 576, pp. 73-78, 2014.

[184] H. Hirai, "Progress in transduction of cerebellar Purkinje cells in vivo using viral vectors," *Cerebellum,* vol. 7, pp. 273-278, 2008.

[185] T. Tsubota, Y. Ohashi, K. Tamura, and Y. Miyashita, "Optogenetic inhibition of Purkinje cell activity reveals cerebellar control of blood pressure during postural alterations in anesthetized rats," *Neuroscience,* vol. 210, pp. 137-144, 2012.

[186] T. Tsubota, Y. Ohashi, K. Tamura, A. Sato, and Y. Miyashita, "Optogenetic manipulation of cerebellar Purkinje cell activity in vivo," *PLoS One,* vol. 6, p. e22400, 2011.

[187] M. K. Bosch, J. M. Nerbonne, and D. M. Ornitz, "Dual transgene expression in murine cerebellar Purkinje neurons by viral transduction in vivo," *PLoS One,* vol. 9, p. e104062, 2014.

[188] J. C. Dodge, J. Clarke, A. Song, J. Bu, W. Yang, T. V. Taksir, *et al.*, "Gene transfer of human acid sphingomyelinase corrects neuropathology and motor deficits in a mouse model of Niemann-Pick type A disease," *Proc. Natl. Acad. Sci. U. S. A.,* vol. 102, pp. 17822-17827, 2005.

[189] W. F. Kaemmerer, R. G. Reddy, C. A. Warlick, S. D. Hartung, R. S. McIvor, and W. C. Low, "In vivo transduction of cerebellar Purkinje cells using adeno-associated virus vectors," *Molecular therapy,* vol. 2, pp. 446-457, 2000.

[190] D. F. Aschauer, S. Kreuz, and S. Rumpel, "Analysis of transduction efficiency, tropism and axonal transport of AAV serotypes 1, 2, 5, 6, 8 and 9 in the mouse brain," *PLoS One,* vol. 8, p. e76310, 2013.

[191] B. Asrican, G. J. Augstine, K. Berglund, S. Chen, N. Chow, K. Deisseroth, *et al.*, "Next-generation transgenic mice for optogenetic analysis of neural circuits," *Frontiers in neural circuits,* vol. 7, 2013.

[192] M. R. Celio and C. W. Heizmann, "Calcium-binding protein parvalbumin as a neuronal marker," *Nature,* vol. 293, pp. 300-302, 1981.

[193] S. A. Heiney, J. Kim, G. J. Augustine, and J. F. Medina, "Precise control of movement kinematics by optogenetic inhibition of purkinje cell activity," *Journal of Neuroscience,* vol. 34, pp. 2321-2330, 2014.

[194] M. I. Aller, A. Jones, D. Merlo, M. Paterlini, A. H. Meyer, U. Amtmann, *et al.*, "Cerebellar granule cell Cre recombinase expression," *Genesis,* vol. 36, pp. 97-103, 2003.

[195] Y. Kim, T. Kim, J. K. Rhee, D. Lee, K. Tanaka-Yamamoto, and Y. Yamamoto, "Selective transgene expression in cerebellar Purkinje cells and granule cells using adeno-associated viruses together with specific promoters," *Brain research,* vol. 1620, pp. 1-16, 2015.

[196] G. Astorga, J. Bao, A. Marty, G. J. Augustine, R. Franconville, A. Jalil*, et al.*, "An excitatory GABA loop operating in vivo," *Frontiers in cellular neuroscience,* vol. 9, 2015.

[197] J. Kim, S. Lee, S. Tsuda, X. Zhang, B. Asrican, B. Gloss*, et al.*, "Optogenetic mapping of cerebellar inhibitory circuitry reveals spatially biased coordination of interneurons via electrical synapses," *Cell Reports,* vol. 7, pp. 1601-1613, 2014.

[198] L. Ankri, Z. Husson, K. Pietrajtis, R. Proville, C. Léna, Y. Yarom*, et al.*, "A novel inhibitory nucleo-cortical circuit controls cerebellar Golgi cell activity," *Elife,* vol. 4, 2015.

[199] T. Tsubota, Y. Ohashi, and K. Tamura, "Optogenetics in the cerebellum: Purkinje cell-specific approaches for understanding local cerebellar functions," *Behavioural brain research,* vol. 255, pp. 26-34, 2013.

[200] Q. Wang, A. M. Henry, J. A. Harris, S. W. Oh, K. M. Joines, J. Nyhus*, et al.*, "Systematic comparison of adeno-associated virus and biotinylated dextran amine reveals equivalent sensitivity between tracers and novel projection targets in the mouse brain," *Journal of Comparative Neurology,* vol. 522, pp. 1989-2012, 2014.

[201] E. S. Boyden, F. Zhang, E. Bamberg, G. Nagel, and K. Deisseroth, "Millisecond-timescale, genetically targeted optical control of neural activity," *Nature Neuroscience,* vol. 8, pp. 1263-1268, 2005.

[202] W. Kruse, M. Krause, J. Aarse, M. D. Mark, D. Manahan-Vaughan, and S. Herlitze, "Optogenetic modulation and multi-electrode analysis of cerebellar networks in vivo," *PLoS One,* vol. 9, p. e105589, 2014.

[203] s. u.-d. lab. (2016, 22 december 2016). *irradiance calculator tool*. Available: http://web.stanford.edu/group/dlab/cgi-bin/graph/chart.php

[204] S. I. Al-Juboori, A. Dondzillo, E. A. Stubblefield, G. Felsen, T. C. Lei, and A. Klug, "Light scattering properties vary across different regions of the adult mouse brain," *PLoS One,* vol. 8, p. e67626, 2013.

[205] Y. Liu, S. L. Jacques, M. Azimipour, J. D. Rogers, R. Pashaie, and K. W. Eliceiri, "OptogenSIM: a 3D Monte Carlo simulation platform for light delivery design in optogenetics," *Biomedical optics express,* vol. 6, pp. 4859-4870, 2015.

[206] C. Brabec, V. Dyakonov, J. Parisi, and N. S. Sariciftci, *Organic photovoltaics: Concepts and Realization*. Berlin Heidelberg: Springer-Verlag, 2003.

[207] M. Gratzel, "Photoelectrochemical cells," *Nature,* vol. 414, pp. 338-344, 2001.

[208] R. Williams, "Becquerel photovoltaic effect in binary compounds," *Journal of chemical physics,* vol. 32, pp. 1505-1514, 1960.

[209] P. Ledochowitsch, A. Yazdan-Shahmorad, K. E. Bouchard, C. Diaz-Botia, T. L. Hanson, J. W. He*, et al.*, "Strategies for optical control and simultaneous electrical readout of extended cortical circuits," *Journal of neuroscience Methods,* vol. 256, pp. 220-231, 2015.

[210] D. W. Park, A. A. Schendel, S. Mikael, S. K. Brodnick, T. J. Richner, J. P. Ness*, et al.*, "Graphene-based carbon layered electrode array technology for neural imaging and optogenetic applications," *Nature Communications,* vol. 5:5258, 2014.

[211] F. Wu, E. Stark, P. C. Ku, K. D. Wise, G. Buzsáki, and E. Yoon, "Monolithically Integrated μLEDs on Silicon Neural Probes for High-Resolution Optogenetic Studies in Behaving Animals," *Neuron,* vol. 88, pp. 1136-1148, 2015.

[212] T. C. Pappas, W. M. S. Wickramanyake, E. Jan, M. Motamedi, M. Brodwick, and N. A. Kotov, "Nanoscale engineering of a cellular interface with semiconductor nanoparticle films for photoelectric stimulation of neurons," *Nano Letters,* vol. 7, pp. 513-519, 2007.

[213] A. Berndt, S. Y. Lee, C. Ramakrishnan, and K. Deisseroth, "Structure-guided transformation of channelrhodopsin into a light-activated chloride channel," *Science,* vol. 344, pp. 420-424, 2014.

[214] X. Han, X. Qian, J. G. Bernstein, H. H. Zhou, G. T. Franzesi, P. Stern*, et al.*, "Millisecond-timescale optical control of neural dynamics in the nonhuman primate brain," *Neuron,* vol. 62, pp. 191-198, 2009.

[215] X. Li, D. V. Gutierrez, M. G. Hanson, J. Han, M. D. Mark, H. Chiel*, et al.*, "Fast noninvasive activation and inhibition of neural and network activity by vertebrate rhodopsin and green algae channelrhodopsin," *Proceedings of the National Academy of Sciences of the United States of America,* vol. 102, pp. 17816-17821, 2005.

[216] C. Mateo, M. Avermann, L. J. Gentet, F. Zhang, K. Deisseroth, and C. C. Petersen, "In vivo optogenetic stimulation of neocortical excitatory neurons drives brain-state-dependent inhibition," *Current Biology,* vol. 21, pp. 1593-1602, 2011.

[217] G. Nagel, M. Brauner, J. F. Liewald, N. Adeishvili, E. Bamberg, and A. Gottschalk, "Light activation of channelrhodopsin-2 in excitable cells of Caenorhabditis elegans triggers rapid behavioral responses," *Current Biology,* vol. 15, pp. 2279-2284, 2005.

[218] S. Zhao, J. T. Ting, H. E. Atallah, L. Qiu, J. Tan, B. Gloss*, et al.*, "Cell type-specific channelrhodopsin-2 transgenic mice for optogenetic dissection of neural circuitry function," *Nature Methods,* vol. 8, pp. 745-752, 2011.

[219] A. M. Herman, L. Huang, D. K. Murphey, I. Garcia, and B. R. Arenkiel, "Cell type-specific and time-dependent light exposure contribute to silencing in neurons expressing Channelrhodopsin-2," *Elife,* vol. 3, 2014.

[220] M. Mahn, M. Prigge, S. Ron, R. Levy, and O. Yizhar, "Biophysical constraints of optogenetic inhibition at presynaptic terminals," *Nature Neuroscience,* vol. 19, pp. 554-556, 2016.

[221] I. N. Christie, J. A. Wells, P. Southern, N. Marina, S. Kasparov, A. V. Gourine*, et al.*, "fMRI response to blue light delivery in the naive brain: implications for combined optogenetic fMRI studies," *Neuroimage,* vol. 66, pp. 634-641, 2013.

[222] M. A. Long and M. S. Fee, "Using temperature to analyse temporal dynamics in the songbird motor pathway," *Nature,* vol. 456, pp. 189-194, 2008.

[223] E. Moser, I. Mathiesen, and P. Andersen, "Association between brain temperataure and dentate field potentials in exploring and swimming rats," *Science,* vol. 259, pp. 1324-1326, 1993.

[224] J. M. Stujenske, T. Spellman, and J. A. Gordon, "Modeling the spatiotemporal dynamics of light and heat propagation for in vivo optogenetics," *Cell Reports,* vol. 12, pp. 525-534, 2015.

[225] J. M. Sorokin, T. J. Davidson, E. Frechette, A. M. Abramian, K. Deisseroth, J. R. Huguenard*, et al.*, "Bidirectional Control of Generalized Epilepsy Networks via Rapid Real-Time Switching of Firing Mode," *Neuron,* Dec 14 2017.

[226] L. M. Palmer, B. A. Clark, J. Grundemann, A. Roth, G. J. Stuart, and M. Hausser, "Initiation of simple and complex spikes in cerebellar Purkinje cells," *J Physiol,* vol. 588, pp. 1709-17, May 15 2010.

[227] P. Vetter, A. Roth, and M. Hausser, "Propagation of action potentials in dendrites depends on dendritic morphology," *J Neurophysiol,* vol. 85, pp. 926-37, Feb 2001.

[228] K. H. Lee, P. J. Mathews, A. M. Reeves, K. Y. Choe, S. A. Jami, R. E. Serrano*, et al.*, "Circuit mechanisms underlying motor memory formation in the cerebellum," *Neuron,* vol. 86, pp. 529-40, Apr 22 2015.

[229] I. M. Raman and B. P. Bean, "Ionic currents underlying spontaneous action potentials in isolated cerebellar Purkinje neurons," *J Neurosci,* vol. 19, pp. 1663-74, Mar 01 1999.

[230] Z. Gao, B. Todorov, C. F. Barrett, S. van Dorp, M. D. Ferrari, A. M. van den Maagdenberg*, et al.*, "Cerebellar ataxia by enhanced Ca(V)2.1 currents is alleviated by Ca2+-dependent K+-channel activators in Cacna1a(S218L) mutant mice," *J Neurosci,* vol. 32, pp. 15533-46, Oct 31 2012.

[231] J. T. Walter, K. Alvina, M. D. Womack, C. Chevez, and K. Khodakhah, "Decreases in the precision of Purkinje cell pacemaking cause cerebellar dysfunction and ataxia," *Nat Neurosci,* vol. 9, pp. 389-97, Mar 2006.

[232] S. L. Jackman, B. M. Beneduce, I. R. Drew, and W. G. Regehr, "Achieving high-frequency optical control of synaptic transmission," *Journal of Neuroscience,* vol. 34, pp. 7704-7714, 2014.

[233] B. Y. Chow, X. Han, A. S. Dobry, X. Qian, A. S. Chuong, M. Li*, et al.*, "High-performance genetically targetable optical neural silencing by light-driven proton pumps," *Nature,* vol. 463, pp. 98-102, 2010.

[234] E. G. Govorunova, O. A. Sineshchekov, R. Janz, X. Liu, and J. L. Spudich, "Natural light-gated anion channels: A family of microbial rhodopsins for advanced optogenetics," *Science,* vol. 349, pp. 647-650, 2015.

[235] J. Wietek, J. S. Wiegert, N. Adeishvili, F. Schneider, H. Watanabe, S. P. Tsunoda*, et al.*, "Conversion of channelrhodopsin into a light-gated chloride channel," *Science,* vol. 344, pp. 409-412, 2014.

[236] A. S. Chuong, M. L. Miri, V. Busskamp, G. A. Matthews, L. C. Acker, A. T. Sorensen*, et al.*, "Noninvasive optical inhibition with a red-shifted microbial rhodopsin," *Nature Neuroscience,* vol. 17, pp. 1123-1129, 2014.

[237] F. Zhang, L. P. Wang, M. Brauner, J. F. Liewald, K. Kay, N. Watzke*, et al.*, "Multimodal fast optical interrogation of neural circuitry," *Nature,* vol. 446, pp. 633-639, 2007.

[238] G. M. Alexander, S. C. Rogan, A. I. Abbas, B. N. Armbruster, Y. Pei, J. A. Allen*, et al.*, "Remote control of neuronal activity in transgenic mice expressing evolved G protein-coupled receptors," *Neuron,* vol. 63, pp. 27-39, Jul 16 2009.

[239] T. J. Stachniak, A. Ghosh, and S. M. Sternson, "Chemogenetic synaptic silencing of neural circuits localizes a hypothalamus-->midbrain pathway for feeding behavior," *Neuron,* vol. 82, pp. 797-808, May 21 2014.

[240] J. Levitz, C. Pantoja, B. Gaub, H. Janovjak, A. Reiner, A. Hoagland*, et al.*, "Optical control of metabotropic glutamate receptors," *Nature Neuroscience,* vol. 16, pp. 507-516, 2013.

[241] D. V. Gutierrez, M. D. Mark, O. Masseck, T. Maejima, D. Kuckelsberg, R. A. Hyde*, et al.*, "Optogenetic control of motor coordination by Gi/o protein-coupled vertebrate rhodopsin in cerebellar Purkinje cells," *J Biol Chem,* vol. 286, pp. 25848-58, Jul 22 2011.

[242] M. Uusisaari and E. De Schutter, "The mysterious microcircuitry of the cerebellar nuclei," *J Physiol,* vol. 589, pp. 3441-57, Jul 15 2011.

[243] M. Uusisaari and T. Knöpfel, "Functional classification of neurons in the mouse lateral cerebellar nuclei," *Cerebellum,* vol. 10, pp. 637-646, 2011.

[244] L. Borgius, C. E. Restrepo, R. N. Leao, N. Saleh, and O. Kiehn, "A transgenic mouse line for molecular genetic analysis of excitatory glutamatergic neurons," *Mol Cell Neurosci,* vol. 45, pp. 245-57, Nov 2010.

[245] B. D. Houck and A. L. Person, "Cerebellar premotor output neurons collateralize to innervate the cerebellar cortex," *The Journal of Comparative Neurology,* vol. 523, pp. 2254-2271, 2015.

[246] Z. Husson, C. V. Rousseau, I. Broll, H. U. Zeilhofer, and Dieudonné, "Differential GABAergic and glycinergic inputs of inhibitory interneurons and purkinje cells to principal cells of the cerebellar nuclei," *J. Neurosci.,* vol. 34, pp. 9418-9431, 2014.

[247] Y. Lefler, Y. Yarom, and M. Y. Uusisaari, "Cerebellar inhibitory input to the inferior olive decreases electrical coupling and blocks subthreshold oscillations," *Neuron,* vol. 81, pp. 1389-1400, 2014.

[248] M. W. Bagnall, B. Zingg, A. Sakatos, S. H. Moghadam, H. U. Zeilhofer, and S. du Lac, "Glycinergic projection neurons of the cerebellum," *Journal of Neuroscience,* vol. 29, pp. 10104-10110, 2009.

[249] T. A. Blenkinsop and E. J. Lang, "Synaptic action of the olivocerebellar system on cerebellar nuclear spike activity," *J Neurosci,* vol. 31, pp. 14708-20, Oct 12 2011.

[250] S. T. Kitai, R. A. McCrea, R. J. Preston, and G. A. Bishop, "Electrophysiological and horseradish peroxidase studies of precerebellar afferents to the nucleus interpositus anterior. I. Climbing fiber system," *Brain Res,* vol. 122, pp. 197-214, Feb 18 1977.

[251] H. Lu, B. Yang, and D. Jaeger, "Cerebellar Nuclei Neurons Show only small excitatory responses to optogenetic olivary stimulation in transgenic mice: In vivo and in vitro studies," *Frontiers in neural circuits,* vol. 10, 2016.

[252] N. Zheng and I. M. Raman, "Synaptic inhibition, excitation, and plasticity in neurons of the cerebellar nuclei," *Cerebellum,* vol. 9, pp. 56-66, Mar 2010.

[253] V. Gauck and D. Jaeger, "The control of rate and timing of spikes in the deep cerebellar nuclei by inhibition," *J Neurosci,* vol. 20, pp. 3006-16, Apr 15 2000.

[254] S. Dykstra, J. D. Engbers, T. M. Bartoletti, and R. W. Turner, "Determinants of rebound burst responses in rat cerebellar nuclear neurons to physiological stimuli," *J Physiol,* vol. 594, pp. 985-1003, Feb 15 2016.

[255] A. R. Best and W. G. Regehr, "Inhibitory regulation of electrically coupled neurons in the inferior olive is mediated by asynchronous release of GABA," *Neuron,* vol. 62, pp. 555-65, May 28 2009.

[256] C. H. Chen, R. Fremont, E. E. Arteaga-Bracho, and K. Khodakhah, "Short latency cerebellar modulation of the basal ganglia," *Nature Neuroscience,* vol. 17, pp. 1767-1775, 2014.

[257] D. G. Tervo, B. Y. Hwang, S. Viswanathan, T. Gaj, M. Lavzin, K. D. Ritola, *et al.*, "A Designer AAV Variant Permits Efficient Retrograde Access to Projection Neurons," *Neuron,* vol. 92, pp. 372-382, Oct 19 2016.

[258] B. D. Houck and A. L. Person, "Cerebellar loops: a review of the nucleocortical pathway," *Cerebellum,* vol. 13, pp. 378-85, Jun 2014.

[259] Z. Gao, M. Proietti-Onori, Z. Lin, M. M. Ten Brinke, H. J. Boele, J. W. Potters, *et al.*, "Excitatory Cerebellar Nucleocortical Circuit Provides Internal Amplification during Associative Conditioning," *Neuron,* vol. 89, pp. 645-657, 2016.

[260] J. Y. Lin, "A user's guide to channelrhodopsin variants: features, limitations and future developments," *Exp Physiol,* vol. 96, pp. 19-25, Jan 2011.

[261] A. I. Chen, C. N. Nguyen, D. R. Copenhagen, S. Badurek, L. Minichiello, B. Ranscht, *et al.*, "TrkB (tropomyosin-related kinase B) controls the assembly and maintenance of GABAergic synapses in the cerebellar cortex," *J Neurosci,* vol. 31, pp. 2769-80, Feb 23 2011.

[262] F. Andermann and S. F. Berkovic, "Idiopathic generalized epilepsy with generalized and other seizures in adolescence," *Epilepsia,* vol. 43, pp. 317-320, 2001.

[263] O. C. Snead, 3rd, "Basic mechanisms of generalized absence seizures," *Ann. Neurol.,* vol. 37, pp. 146-57, 1995.

[264] A. Clemente-Perez, S. R. Makinson, B. Higashikubo, S. Brovarney, F. S. Cho, A. Urry, *et al.*, "Distinct thalamic reticular cell types differentially modulate normal and pathological cortical rhythms," *Cell Reports,* vol. 19, pp. 2130-2142, 2017.

[265] R. Apps and M. Garwicz, "Anatomic and physiological foundations of cerebellar processing," *Nat. Rev. Neurosci.,* vol. 6, pp. 297-311, 2005.

[266] J. C. Eccles, "The development of the cerebellum of vertebrates in relation to the control of movement," *Naturwissenschaften,* vol. 56, pp. 525-534, 1969.

[267] V. Gauck and D. Jaeger, "The contribution of NMDA and AMPA conductances to the control of spiking in neurons of the deep cerebellar nuclei," *J. Neurosci.,* vol. 23, pp. 8109-8118, 2003.

[268] H. J. Groenewegen, J. Voogd, and S. L. Freedman, "The parasagittal zonation within the olivocerebellar projection. II. Climbing fiber distribution in the intermediate and hemispheric parts of cat cerebellum," *J. Comp. Neurol.,* vol. 183, pp. 551-601, 1979.

[269] J. J. Van der Want, L. Wiklund, M. Guegan, T. J. Ruigrok, and J. Voogd, "Anterograde tracing of the rat olivocerebellar system with Phaseolus vulgaris leucoagglutinin (PHA-L). Demonstration of climbing fiber collateral innervation of the cerebellar nuclei," *J. Comp. Neurol.,* vol. 288, pp. 1-18, 1989.

[270] V. Chan-Palay, "Fine structure of labelled axons in the cerebellar cortex and nuclei of rodents and primates after intraventricular infusions with tritiated serotonin," *Anat. Embryol. (Berl.),* vol. 148, pp. 235-265, 1975.

[271] V. Chan-Palay, "Fine structure of labelled axons in the cerebellar cortex and nuclei of rodents and primates after intraventricular infusions with tritiated serotonin," *Anatomy and Embryology,* vol. 148, pp. 235-265, 1975.

[272] H. J. Groenewegen, J. Voogd, and S. L. Freedman, "The parasagittal zonation within the olivocerebellar projection. II. Climbing fiber distribution in the intermediate and hemispheric parts of cat cerebellum," *Journal of Comparative Neurology,* vol. 183, pp. 551-601, 1979.

[273] J. J. Van der Want, L. Wiklund, M. Guegan, T. J. Ruigrok, and J. Voogd, "Anterograde tracing of the rat olivocerebellar system with Phaseolus vulgaris leucoagglutinin (PHA-L). Demonstration of climbing fiber collateral innervation of the cerebellar nuclei," *Journal of Comparative Neurology,* vol. 288, pp. 1-18, 1989.

[274] H. Jahnsen, "Electrophysiological characteristics of neurones in the guinea-pig deep cerebellar nuclei in vitro," *Journal of Physiology,* vol. 372, pp. 129-147, 1986.

[275] D. Mouginot and B. H. Gahwiler, "Characterization of synaptic connections between cortex and deep nuclei of the rat cerebellum in vitro," *Neuroscience,* vol. 64, pp. 699-712, 1995.

[276] C. I. de Zeeuw, F. E. Hoebeek, and M. Schonewille, "Causes and consequences of oscillations in the cerebellar cortex," *Neuron,* vol. 58, pp. 655-658, 2008.

[277] M. M. Ten Brinke, H. J. Boele, J. K. Spanke, J. W. Potters, K. Kornysheva, P. Wulff*, et al.*, "Evolving Models of Pavlovian Conditioning: Cerebellar Cortical Dynamics in Awake Behaving Mice," *Cell Reports,* vol. 13, pp. 1977-1988, 2015.

[278] A. Devor and Y. Yarom, "Electrotonic coupling in the inferior olivary nucleus revealed by simultaneous double patch recordings," *Journal of Neurophysiology,* vol. 87, pp. 3048-3058, 2002.

[279] J. P. Welsh, B. Chang, M. E. Menaker, and S. A. Aicher, "Removal of the inferior olive abolishes myoclonic seizures associated with a loss of olivary serotonin," *Neuroscience,* vol. 82, pp. 879-897, 1998.

[280] B. N. Harding and S. G. Boyd, "Intractable seizures from infancy can be associated with dentato-olivary dysplasia," *Journal of neurological sciences,* vol. 104, pp. 157-165, 1991.

[281] Y. Saito, M. Hayashi, Y. Miyazono, T. Shimogama, and K. Ohno, "Arthrogryposis multiplex congenita with callosal agenesis and dentato-olivary dysplasia.," *Brain & Development,* vol. 28, pp. 261-264, 2006.

[282] C. F. Fletcher, C. M. Lutz, T. N. O'Sullivan, J. D. Shaughnessy, R. Hawkes, W. N. Frankel*, et al.*, "Absence epilepsy in tottering mutant mice is associated with calcium channel defects," *Cell,* vol. 87, pp. 607-617, 1996.

[283] J. L. Noebels and R. L. Sidman, "Spike-Wave and focal motor seizures in the mutant mouse tottering," *Science,* vol. 204, pp. 1334-1336, 1979.

[284] C. Stosiek, O. Garaschuk, K. Holthoff, and A. Konnerth, "In vivo two-photon calcium imaging of neuronal networks.," *Proc Natl Acad Sci U S A,* vol. 100, pp. 7319-7324, 2003.

[285] S. Tsutsumi, M. Yamazaki, T. Miyazaki, M. Watanabe, K. Sakimura, M. Kano*, et al.*, "Structure-function relationships between aldolase C/zebrin II expression and complex spike synchrony in the cerebellum.," *J. Neurosci.,* vol. 35, pp. 843-852, 2015.

[286] J. R. de Gruijl, T. M. Hoogland, and C. I. de Zeeuw, "Behavioral correlates of complex spike synchrony in cerebellar microzones," *Journal of Neuroscience,* vol. 34, pp. 8937-8947, 2014.

[287] G. R. Holt, W. R. Softky, C. Koch, and R. J. Douglas, "Comparison of discharge variability in vitro and in vivo in cat visual cortex neurons," *J. Neurophys.,* vol. 75, pp. 1806-1814, 1996.

[288] C. I. de Zeeuw, J. I. Simpson, C. C. Hoogenraad, N. Galjart, S. K. Koekkoek, and T. J. Ruigrok, "Microcircuitry and function of the inferior olive," *Trends in Neurosciences,* vol. 21, pp. 391-400, 1998.

[289] J. Voogd and T. J. Ruigrok, "The organization of the corticonuclear and olivocerebellar climbing fiber projections to the rat cerebellar vermis: the congruence of projection zones and the zebrin pattern," *Journal of neurocytology,* vol. 33, pp. 5-21, 2004.

[290] C. I. de Zeeuw and M. M. Ten Brinke, "Motor Learning and the Cerebellum," *Cold Spring Harbor perspectives in biology,* vol. 7, 2015.

[291] S. Choi, E. Yu, D. Kim, F. J. Urbano, V. Makarenko, H. S. Shin*, et al.*, "Subthreshold membrane potential oscillations in inferior olive neurons are dynamically regulated by P/Q- and T-type calcium channels: a study in mutant mice," *Journal of Physiology,* vol. 588, pp. 3031-3043, 2010.

[292] J. J. White and R. V. Sillitoe, "Genetic silencing of olivocerebellar synapses causes dystonia-like behaviour in mice," *Nature Communications,* vol. 8, 2017.

[293] S. Khosrovani, R. S. van der Giessen, C. I. de Zeeuw, and M. T. De Jeu, "In vivo mouse inferior olive neurons exhibit heterogeneous subthreshold oscillations and spiking patterns," *Proc. Natl. Acad. Sci. U. S. A.,* vol. 104, pp. 15911-15916, 2007.

[294] R. llinás, "Inferior olive oscillation as the temporal basis for motricity and oscillatory reset as the basis for motor error correction," *Neuroscience,* vol. 162, pp. 797-804, 2009.

[295] R. llinás and Y. Yarom, "Properties and distribution of ionic conductances generating electroresponsiveness of mammalian inferior olivary neurones in vitro," *Journal of Physiology,* vol. 315, 1981.

[296] P. Bazzigaluppi, T. J. Ruigrok, P. Saisan, C. I. de Zeeuw, and M. T. de Jeu, "Properties of the nucleo-olivary pathway: an in vivo whole-cell patch clamp study," *PLoS One,* vol. 7, p. e46360, 2012.

[297] P. Svensson, F. Bengtsson, and G. Hesslow, "Cerebellar inhibition of inferior olivary transmission in the decerebrate ferret," *Experimental Brain Research,* vol. 168, pp. 241-253, 2006.

[298] M. C. Anderson, E. Y. Chung, and M. H. Van Woert, "Effect of inferior olive lesion on seizure threshold in the rat," *Life Sciences,* vol. 40, pp. 2367-2375, 1987.

[299] M. C. Anderson, E. Y. Chung, and M. H. Van Woert, "Strychnine seizure potentiation by azaspirodecanedione anxiolytics in rats," *European Journal of Pharmacology,* vol. 155, pp. 279-283, 1988.

[300] M. C. Anderson, E. Y. Chung, and M. H. Van Woert, "The effects of inferior olive lesion on strychnine seizure," *Brain research bulletin,* vol. 25, pp. 599-603, 1990.

[301] A. Badura, M. Schonewille, K. Voges, E. Galliano, N. Renier, Z. Gao*, et al.*, "Climbing fiber input shapes reciprocity of Purkinje cell firing," *Neuron,* vol. 78, pp. 700-713, 2013.

[302] C. I. De Zeeuw and A. S. Berrebi, "Postsynaptic targets of Purkinje cell terminals in the cerebellar and vestibular nuclei of the rat," *Eur. J. Neurosci.,* vol. 7, pp. 2322-2333, 1995.

[303] W. Graf, J. I. Simpson, and C. S. Leonard, "Spatial organization of visual messages of the rabbit's cerebellar flocculus. II. Complex and simple spike responses of Purkinje cells.," *Journal of Neurophysiology,* vol. 60, pp. 2091-2121, 1988.

[304] V. Yakhnitsa and N. H. Barmack, "Antiphasic Purkinje cell responses in mouse uvula-nodulus are sensitive to static roll-tilt and topographically organized," *Neuroscience,* vol. 143, pp. 615-626, 2006.

[305] F. E. Hoebeek, J. S. Stahl, A. M. Van Alphen, M. Schonewille, C. Luo, M. Rutteman, *et al.*, "Increased noise level of purkinje cell activities minimizes impact of their modulation during sensorimotor control," *Neuron,* vol. 45, pp. 953-965, 2005.

[306] M. Ito, M. Yoshida, and K. Obata, "Monosynaptic inhibition of the intracerebellar nuclei induced from the cerebellar cortex," *Experientia,* vol. 20, pp. 575-576, 1964.

[307] M. Ito, M. Yoshida, K. Obata, N. Kawai, and M. Udo, "Inhibitory control of intracerebellar nuclei by the purkinje cell axons," *Experimental Brain Research,* vol. 10, pp. 64-80, 1970.

[308] C. D. Aizenman and D. J. Linden, "Rapid, synaptically driven increases in the intrinsic excitability of cerebellar deep nuclear neurons," *Nature Neuroscience,* vol. 3, pp. 109-111, 2000.

[309] K. Alvina, G. Ellis-Davies, and K. Khodakhah, "T-type calcium channels mediate rebound firing in intact deep cerebellar neurons," *Neuroscience,* vol. 158, pp. 635-641, 2009.

[310] J. D. Engbers, D. Anderson, R. Tadayonnejad, W. H. Mehaffey, M. L. Molineux, and R. W. Turner, "Distinct roles for I(T) and I(H) in controlling the frequency and timing of rebound spike responses," *Journal of Physiology,* vol. 589, pp. 5391-5413, 2011.

[311] S. S. Feng and D. Jaeger, "The role of SK calcium-dependent potassium currents in regulating the activity of deep cerebellar nucleus neurons: a dynamic clamp study," *Cerebellum,* vol. 7, pp. 542-546, 2008.

[312] S. S. Feng, R. Lin, V. Gauck, and D. Jaeger, "Gain control of synaptic response function in cerebellar nuclear neurons by a calcium-activated potassium conductance," *Cerebellum,* vol. 12, pp. 692-706, 2013.

[313] V. Gauck, M. Thomann, D. Jaeger, and A. Borst, "Spatial distribution of low- and high-voltage-activated calcium currents in neurons of the deep cerebellar nuclei," *Journal of Neuroscience,* vol. 21, 2001.

[314] J. R. Pugh and I. M. Raman, "Potentiation of mossy fiber EPSCs in the cerebellar nuclei by NMDA receptor activation followed by postinhibitory rebound current," *Neuron,* vol. 51, pp. 113-123, 2006.

[315] T. Sangrey and D. Jaeger, "Analysis of distinct short and prolonged components in rebound spiking of deep cerebellar nucleus neurons," *European Journal of Neuroscience,* vol. 32, pp. 1646-1657, 2010. [316] N. Zheng and I. Raman, "Ca currents activated by spontaneous firing and synaptic disinhibition in neurons of the cerebellar nuclei," *Journal of Neuroscience,* vol. 29, pp. 9826-9838, 2009.

[317] D. Aksenov, N. Serdyukova, K. Irwin, and V. Bracha, "GABA neurotransmission in the cerebellar interposed nuclei: involvement in classically conditioned eyeblinks and neuronal activity," *Journal of Neurophysiology,* vol. 91, pp. 719-727, 2004.

[318] D. H. Heck, C. I. de Zeeuw, D. Jaeger, K. Khodakhah, and A. L. Person, "The neuronal code(s) of the cerebellum," *Journal of Neuroscience,* vol. 33, pp. 17603-17609, 2013.

[319] F. E. Hoebeek, S. Khosrovani, L. Witter, and C. I. De Zeeuw, "Purkinje cell input to cerebellar nuclei in tottering: ultrastructure and physiology," *Cerebellum,* vol. 7, pp. 547-558, 2008.

[320] R. N. Holdefer, J. C. Houk, and L. E. Miller, "Movement-related discharge in the cerebellar nuclei persists after local injections of GABA(A) antagonists," *Journal of Neurophysiology,* vol. 93, pp. 35-43, 2005.

[321] M. Najac and I. Raman, "Synaptic excitation by climbing fibre collaterals in the cerebellar nuclei of juvenile and adult mice," *Journal of Physiology,* vol. 595, pp. 6703-6718, 2017.

[322] Y. Wu and I. Raman, "Facilitation of mossy fibre-driven spiking in the cerebellar nuclei by the synchrony of inhibition," *Journal of Physiology,* vol. 595, pp. 5245-5264, 2017.

[323] A. T. Berg, S. F. Berkovic, M. J. Brodie, J. Buchhalter, J. H. Cross, W. van Emde Boas*, et al.*, "Revised terminology and concepts for organization of seizures and epilepsies: Report of the ILAE Commission on Classification and Terminology, 2005–2009," *Epilepsia,* vol. 51, pp. 676-685, 2010 2010.

[324] P. Jallon, P. Loiseau, and J. Loiseau, "Newly diagnosed unprovoked epileptic seizures: presentation at diagnosis in CAROLE study. Coordination Active du Réseau Observatoire Longitudinal de l' Epilepsie," *Epilepsia,* vol. 42, pp. 464-475, 2001.

[325] J. T. Paz, A. S. Bryant, K. Peng, L. Fenno, O. Yizhar, W. N. Frankel*, et al.*, "A new mode of corticothalamic transmission revealed in the Gria4(-/-) model of absence epilepsy," *Nat. Neurosci.,* vol. 14, pp. 1167-1173, 2011.

[326] H. Blumenfeld and D. A. McCormick, "Corticothalamic inputs control the pattern of activity generated in thalamocortical networks," *J. Neurosci.,* vol. 20, pp. 5153-5162, 2000.

[327] H. Blumenfeld and D. A. McCormick, "Corticothalamic inputs control the pattern of activity generated in thalamocortical networks," *Journal of Neuroscience,* vol. 20, pp. 5153-5162, 2000.

[328] J. R. Huguenard and D. A. McCormick, "Thalamic synchrony and dynamic regulation of global forebrain oscillations," *Trends Neurosci.,* vol. 30, pp. 350-356, 2007.

[329] I. S. Cooper, M. Riklan, S. Watkins, and D. McLellan, "Safety and efficacy of chronic stimulation," *Neurosurgery,* vol. 1, pp. 203-205, 1977.

[330] A. Bava, T. Manzoni, and A. Urbano, "Effects of fastiginal stimulation on thalamic neurones belonging to the diffuse projection system," *Brain research,* vol. 4, pp. 378-380, 1967.

[331] S. F. Sawyer, J. M. Tepper, and P. M. Groves, "Cerebellar-responsive neurons in the thalamic ventroanterior-ventrolateral complex of rats: light and electron microscopy," *Neuroscience,* vol. 63, pp. 725-745, 1994.

[332] S. Tokuda, B. J. Beyer, and W. N. Frankel, "Genetic complexity of absence seizures in substrains of C3H mice," *Genes Brain Behav.,* vol. 8, pp. 283-289, 2009.

[333] C. Marescaux, M. Vergnes, and A. Depaulis, "Genetic absence epilepsy in rats from Strasbourg - a review," *J. Neural Transm. Suppl.,* vol. 35, pp. 37-69, 1992.

[334] B. J. Kaplan, T. N. Seyfried, and G. H. Glaser, "Spontaneous polyspike discharges in an epileptic mutant mouse (tottering)," *Experimental Neurology,* vol. 66, pp. 577-586, 1979.

[335] M. Loureiro, T. Cholvin, J. Lopez, N. Merienne, A. Latreche, B. Cosquer*, et al.*, "The ventral midline thalamus (reuniens and rhomboid nuclei) contributes to the persistence of spatial memory in rats," *J. Neurosci.,* vol. 32, pp. 9947-9959, 2012.

[336] C. E. Rasmussen and C. K. I. Williams, "Gaussian processes for machine learning," ed. Cambridge, MA, U.S.A.: The MIT Press, 2006.

[337] C. Bandt and B. Pompe, "Permutation entropy: a natural complexity measure for time series," *Phys. Rev. Lett.,* vol. 88, p. 174102, 2002.

[338] I. Osorio, M. G. Frei, and S. B. Wilkinson, "Real-time automated detection and quantitative analysis of seizures and short-term prediction of clinical onset," *Epilepsia,* vol. 39, pp. 615-627, 1998.

[339] J. M. H. Karel, S. A. P. Haddad, S. Hiseni, R. L. Westra, W. A. Serdijn, and R. L. M. Peeters, "Implementing wavelets in continuous-time analog circuits with dynamic range optimization," *IEEE Transactions on Circuits and Systems - I,* vol. 59, pp. 229-242, 2012.

[340] G. van Luijtelaar, F. Y. Onat, and M. J. Gallagher, "Animal models of absence epilepsies: what do they model and do sex and sex hormones matter?," *Neurobiology of Disease,* vol. 72, pp. 167-179, 2014.

[341] G. van Luijtelaar and M. Zobeiri, "Progress and outlooks in a genetic absence epilepsy model (WAG/Rij)," *Current medicinal chemistry,* vol. 21, pp. 704-721, 2014.

[342] O. Akman, S. L. Moshé, and A. S. Galanopoulou, "Sex-specific consequences of early life seizures," *Neurobiology of Disease,* vol. 72, pp. 153-166, 2014.

[343] J. L. Nathanson, Y. Yanagawa, K. Obata, and E. M. Callaway, "Preferential labeling of inhibitory and excitatory cortical neurons by endogenous tropism of adeno-associated virus and lentivirus vectors," *Neuroscience,* vol. 161, pp. 441-450, 2009.

[344] J. A. Heckroth, "Quantitative morphological analysis of the cerebellar nuclei in normal and lurcher mutant mice. I. Morphology and cell number," *Journal of Comparative Neurology,* vol. 343, pp. 173-182, 1994.

[345] P. Alva, L. Kros, O. H. J. Eelkman Rooda, C. I. De Zeeuw, R. Adams, N. Davey, *et al.*, "Combining machine learning and simulations of a morphologically realistic model to study modulation of neuronal activity in cerebellar nuclei during absence epilepsy," *BMC Neuroscience,* vol. 15, p. 39, 2014.

[346] P. Alva, L. Kros, R. Maex, C. I. De Zeeuw, R. Adams, N. Davey, *et al.*, "A potential role for the cerebellar nuclei in absence seizures " *BMC Neuroscience,* vol. 14, p. 170, 2013.

[347] N. C. Rowland and D. Jaeger, "Coding of tactile response properties in the rat deep cerebellar nuclei," *Journal of Neurophysiology,* vol. 94, pp. 1236-1251, 2005.

[348] T. D. Aumann, J. A. Rawson, D. I. Finkelstein, and M. K. Horne, "Projections from the lateral and interposed cerebellar nuclei to the thalamus of the rat: a light and electron microscopic study using single and double anterograde labelling," *Journal of Comparative Neurology,* vol. 349, pp. 165-181, 1994.

[349] M. Steriade, "Two channels in the cerebellothalamocortical system," *Journal of Comparative Neurology,* vol. 354, pp. 57-70, 1995.

[350] P. Andersen, J. C. Eccles, and T. A. Sears, "The ventro-basal complex of the thalamus: types of cells, their responses and their functional organization," *J. Physiol.,* vol. 174, pp. 370-399, 1964.

[351] A. Destexhe, D. Contreras, and M. Steriade, "Mechanisms underlying the synchronizing action of corticothalamic feedback through inhibition of thalamic relay cells," *Journal of Neurophysiology,* vol. 79, pp. 999-1016, 1998.

[352] Y. Zhang, M. Mori, D. L. Burgess, and J. L. Noebels, "Mutations in high-voltage-activated calcium channel genes stimulate low-voltage-activated currents in mouse thalamic relay neurons," *Journal of Neuroscience,* vol. 22, pp. 6362-6371, 2002.

[353] V. Chan-Palay, *Cerebellar Dentate Nucleus: Organization, Cytology and Transmitters*. Heidelberg: Springer-Verlag, 1977.

[354] B. Y. Chow and E. S. Boyden, "Optogenetics and translational medicine," *Science Translational Medicine,* vol. 5, p. 177ps5, 2013.

[355] M. Creed, V. J. Pascoli, and C. Luscher, "Addiction therapy. Refining deep brain stimulation to emulate optogenetic treatment of synaptic pathology," *Science,* vol. 347, pp. 659-664, 2015.

[356] J. J. Engel, *Outcome with respect to epileptic seizures*. New York: Raven Press, 1987.

[357] R. S. Fisher, "Therapeutic devices for epilepsy," *Annals of Neurology,* vol. 71, pp. 157-168, 2012.

[358] K. M. Hartikainen, L. Sun, M. Polvivaara, M. Brause, K. Lehtimaki, J. Haapasalo*, et al.*, "Immediate effects of deep brain stimulation of anterior thalamic nuclei on executive functions and emotion-attention interaction in humans," *Journal of Clinical and experimental neuropsychology,* vol. 36, pp. 540-550, 2014.

[359] J. X. Brooks, J. Carriot, and K. E. Cullen, "Learning to expect the unexpected: rapid updating in primate cerebellum during voluntary self-motion," *Nature Neuroscience,* vol. 18, pp. 1310-1317, 2015.

[360] M. Manto, J. M. Bower, A. B. Conforto, J. M. Delgado-Garcia, S. N. da Guarda, M. Gerwig, *et al.*, "Consensus paper: roles of the cerebellum in motor control--the diversity of ideas on cerebellar involvement in movement," *Cerebellum,* vol. 11, pp. 457-487, 2012.

[361] P. Angaut, F. Cicirata, and M. R. Pantó, "An autoradiographic study of the cerebellopontine projections from the interposed and lateral cerebellar nuclei in the rat," *Journal fur Hirnforschung,* vol. 26, pp. 463-470, 1985.

[362] P. Angaut, F. Cicirata, and F. Serapide, "Topographic organization of the cerebellothalamic projections in the rat. An autoradiographic study," *Neuroscience,* vol. 15, pp. 389-401, 1985.

[363] M. Bentivoglio and H. G. Kuypers, "Divergent axon collaterals from rat cerebellar nuclei to diencephalon, mesencephalon, medulla oblongata and cervical cord. A fluorescent double retrograde labeling study," *Experimental Brain Research,* vol. 46, pp. 339-356, 1982.

[364] D. Cohen, W. W. Chambers, and J. M. Sprague, "Experimental study of the efferent projections from the cerebellar nuclei to the brainstem of the cat," *Journal of Comparative Neurology,* vol. 109, pp. 233-259, 1958.

[365] H. Daniel, J. M. Billard, P. Angaut, and C. Batini, "The interposito-rubrospinal system. Anatomical tracing of a motor control pathway in the rat," *Neuroscience Research,* vol. 5, pp. 87-112, 1987.

[366] A. J. Haroian, L. C. Massopust, and P. A. Young, "Cerebellothalamic projections in the rat: an autoradiographic and degeneration study," *Journal of Comparative Neurology,* vol. 197, pp. 217-236, 1981.

[367] E. Kuramoto, T. Furuta, K. C. Nakamura, T. Unzai, H. Hioki, and T. Kaneko, "Two types of thalamocortical projections from the motor thalamic nuclei of the rat: a single neuron-tracing study using viral vectors," *Cerebral Cortex,* vol. 19, pp. 2065-2077, 2009.

[368] E. Kuramoto, S. Ohno, T. Furuta, T. Unzai, Y. R. Tanaka, H. Hioki*, et al.*, "Ventral medial nucleus neurons send thalamocortical afferents more widely and more preferentially to layer 1 than neurons of the ventral anterior-ventral lateral nuclear complex in the rat," *Cerebral Cortex,* vol. 25, pp. 221-235, 2015.

[369] M. Deschenes, J. Bourassa, V. D. Douan, and A. Parent, "A single-cell study of the axonal projections arising from the posterior intralaminar thalamic nuclei in the rat," *European Journal of Neuroscience,* vol. 8, pp. 329-343, 1996.

[370] M. Deschenes, J. Bourassa, and A. Parent, "Striatal and cortical projections of single neurons from the central lateral thalamic nucleus in the rat," *Neuroscience,* vol. 72, pp. 679-687, 1996.

[371] M. Parent and A. Parent, "Single-axon tracing and three-dimensional reconstruction of centre median-parafascicular thalamic neurons in primates," *Journal of Comparative Neurology,* vol. 481, pp. 127-144, 2005.

[372] Y. B. Saalmann, " Intralaminar and medial thalamic influence on cortical synchrony, information transmission and cognition," *Frontiers in systems neuroscience,* vol. 8, 2014.

[373] F. Clascá, P. Rubio-Garrido, and D. Jabaudon, "Unveiling the diversity of thalamocortical neuron subtypes," *European Journal of Neuroscience,* vol. 35, pp. 1524-1532, 2012.

[374] L. Monconduit and L. Villanueva, "The lateral ventromedial thalamic nucleus spreads nociceptive signals from the whole body surface to layer I of the frontal cortex," *European Journal of Neuroscience,* vol. 21, pp. 3395-3402, 2005.

[375] Y. Yamamoto, T. Noda, A. Samejima, and H. Oka, "A morphological investigation of thalamic neurons by intracellular HRP staining in cats," *Journal of Comparative Neurology,* vol. 236, pp. 331-347, 1985.

[376] R. Arai, D. M. Jacobowitz, and S. Deura, "Distribution of calretinin, calbindin-D28k, and parvalbumin in the rat thalamus. Brain research bulletin," *Brain research bulletin,* vol. 33, pp. 595-614, 1994.

[377] A. L. Bodor, K. Giber, Z. Rovó, I. Ulbert, and L. Acsady, "Structural correlates of efficient GABAergic transmission in the basal ganglia-thalamus pathway," *Journal of Neuroscience,* vol. 28, pp. 3090-3102, 2008.

[378] E. G. Jones and S. H. Hendry, "Differential Calcium Binding Protein Immunoreactivity Distinguishes Classes of Relay Neurons in Monkey Thalamic Nuclei," *European Journal of Neuroscience,* vol. 1, pp. 222-246, 1989.

[379] E. Kuramoto, F. Fujiyama, K. C. Nakamura, Y. Tanaka, H. Hioki, and T. Kaneko, "Complementary distribution of glutamatergic cerebellar and GABAergic basal ganglia afferents to the rat motor thalamic nuclei," *European Journal of Neuroscience,* vol. 33, pp. 95-109, 2011.

[380] L. Rispal-Padel and A. Grangetto, "The cerebello-thalamo-cortical pathway. Topographical investigation at the unitary level in the cat," *Experimental Brain Research,* vol. 28, pp. 101-123, 1977.

[381] P. Rubio-Garrido, F. Perez-de-Manzo, C. Porrero, M. J. Galazo, and F. Clascá, "Thalamic input to distal apical dendrites in neocortical layer 1 is massive and highly convergent," *Cerebral Cortex,* vol. 19, pp. 2380-2395, 2009.

[382] J. D. Schmahmann and J. C. Sherman, "The cerebellar cognitive affective syndrome," *Brain,* vol. 121, pp. 561-579, 1998.

[383] C. J. Stoodley and C. Limperopoulos, "Structure-function relationships in the developing cerebellum: Evidence from early-life cerebellar injury and neurodevelopmental disorders," *Seminars in fetal & neonatal medicine,* vol. 21, pp. 356-364, 2016.

[384] S. S. Wang, A. D. Kloth, and A. Badura, "The cerebellum, sensitive periods, and autism," *Neuron,* vol. 83, pp. 518-532, 2014.

[385] S. Peter, M. M. Ten Brinke, J. Stedehouder, C. M. Reinelt, B. Wu, H. Zhou, *et al.*, "Dysfunctional cerebellar Purkinje cells contribute to autism-like behaviour in Shank2-deficient mice," *Nature Communications,* vol. 7, 2016.

[386] P. T. Tsai, C. Hull, Y. Chu, E. Greene-Colozzi, A. R. Sadowski, J. M. Leech, *et al.*, "Autistic-like behaviour and cerebellar dysfunction in Purkinje cell Tsc1 mutant mice," *Nature,* vol. 488, pp. 647-651, 2012.

[387] D. Popa, M. Spolidoro, R. D. Proville, N. Guyon, L. Belliveau, and C. Léna, "Functional role of the cerebellum in gamma-band synchronization of the sensory and motor cortices," *J. Neurosci.,* vol. 33, pp. 6552-6556, 2013.

[388] Z. V. Guo, H. K. Inagaki, K. Daie, S. Druckmann, C. R. Gerfen, and K. Svoboda, "Maintenance of persistent activity in a frontal thalamocortical loop," *Nature,* vol. 545, pp. 181-186, 2017.

[389] A. Bava, F. Cicirata, R. Giuffrida, S. Licciardello, and M. R. Pantó, "Electrophysiologic properties and nature of ventrolateral thalamic nucleus neurons reactive to converging inputs of paleo- and neocerebellar origin," *Experimental Neurology,* vol. 91, pp. 1-12, 1986.

[390] T. A. Ferreira, A. V. Blackman, J. Oyrer, S. Jayabal, A. J. Chung, A. J. Watt, *et al.*, "Neuronal morphometry directly from bitmap images," *Nature Methods,* vol. 11, pp. 982-984, 2014.

[391] P. Lavallée, N. Urbain, C. Dufresne, H. Bokor, L. Acsády, and M. Deschenes, "Feedforward inhibitory control of sensory information in higher-order thalamic nuclei," *Journal of Neuroscience,* vol. 25, pp. 7489-7498, 2005.

[392] Z. Rovó, I. Ulbert, and L. Acsády, "Drivers of the primate thalamus," *Journal of Neuroscience,* vol. 32, pp. 17894-17908, 2012.

[393] S. M. Sherman and R. W. Guillery, "On the actions that one nerve cell can have on another: distinguishing "drivers" from "modulators"," *Proc. Natl. Acad. Sci. U. S. A.,* vol. 95, pp. 7121-7126, 1998.

[394] A. Groh, C. P. de Kock, V. C. Wimmer, B. Sakmann, and T. Kuner, "Driver or coincidence detector: modal switch of a corticothalamic giant synapse controlled by spontaneous activity and short-term depression," *Journal of Neuroscience,* vol. 28, pp. 9652-9663, 2008.

[395] I. Reichova and S. M. Sherman, "Somatosensory corticothalamic projections: distinguishing drivers from modulators," *Journal of Neurophysiology,* vol. 92, pp. 2185-2197, 2004.

[396] M. Seol and T. Kuner, "Ionotropic glutamate receptor GluA4 and T-type calcium channel Cav 3.1 subunits control key aspects of synaptic transmission at the mouse L5B-POm giant synapse," *European Journal of Neuroscience,* vol. 42, pp. 3033-3044, 2015.

[397] X. B. Liu, A. Munoz, and E. G. Jones, "Changes in subcellular localization of metabotropic glutamate receptor subtypes during postnatal development of mouse thalamus," *Journal of Comparative Neurology,* vol. 395, pp. 450-465, 1998.

[398] S. Ohno, E. Kuramoto, T. Furuta, H. Hioki, Y. R. Tanaka, F. Fujiyama, *et al.*, "A morphological analysis of thalamocortical axon fibers of rat posterior thalamic nuclei: a single neuron tracing study with viral vectors," *Cerebral Cortex,* vol. 22, pp. 2840-2857, 2012.

[399] C. Asanuma, W. T. Thach, and E. G. Jones, "Distribution of cerebellar terminations and their relation to other afferent terminations in the ventral lateral thalamic region of the monkey," *Brain research,* vol. 286, pp. 237-265, 1983.

[400] T. D. Aumann and M. K. Horne, "A comparison of the ultrastructure of synapses in the cerebello-rubral and cerebello-thalamic pathways in the rat," *Neuroscience Letters,* vol. 211, pp. 175-178, 1996.

[401] M. Steriade, V. Apostol, and G. Oakson, "Control of Unitary Activities in Cerebellothalamic Pathway During Wakefulness and Synchronized Sleep," *Journal of Neurophysiology,* vol. 34, pp. 389-413, 1971.

[402] M. E. Bickford, N. Zhou, T. E. Krahe, G. Govindaiah, and W. Guido, "Retinal and Tectal "Driver-Like" Inputs Converge in the Shell of the Mouse Dorsal Lateral Geniculate Nucleus," *Journal of Neuroscience,* vol. 35, pp. 10523-10534, 2015.

[403] L. R. Kelly, J. Li, W. B. Carden, and M. E. Bickford, "Ultrastructure and synaptic targets of tectothalamic terminals in the cat lateral posterior nucleus," *Journal of Comparative Neurology,* vol. 464, pp. 472-486, 2003.

[404] S. P. Masterson, J. Li, and M. E. Bickford, "Synaptic organization of the tectorecipient zone of the rat lateral posterior nucleus," *Journal of Comparative Neurology,* vol. 515, pp. 647-663, 2009.

[405] A. Rollenhagen and J. H. Lubke, "The morphology of excitatory central synapses: from structure to function," *Cell and tissue research,* vol. 326, pp. 221-237, 2006.

[406] B. Zikopoulos and H. Barbas, "Parallel driving and modulatory pathways link the prefrontal cortex and thalamus," *PLoS One,* vol. 2, 2007.

[407] B. Zikopoulos and H. Barbas, "Pathways for emotions and attention converge on the thalamic reticular nucleus in primates," *Journal of Neuroscience,* vol. 32, pp. 5338-5350, 2012.

[408] Y. Geinisman, "Perforated axospinous synapses with multiple, completely partitioned transmission zones: probable structural intermediates in synaptic plasticity," *Hippocampus,* vol. 3, pp. 417-433, 1993.

[409] S. Chung, X. Li, and S. B. Nelson, "Short-term depression at thalamocortical synapses contributes to rapid adaptation of cortical sensory responses in vivo," *Neuron,* vol. 34, pp. 437-446, 2002.

[410] R. A. Mease, P. Krieger, and A. Groh, "Cortical control of adaptation and sensory relay mode in the thalamus," *Proc. Natl. Acad. Sci. U. S. A.,* vol. 111, pp. 6798-6803, 2014.

[411] A. N. Viaene, I. Petrof, and S. M. Sherman, "Activation requirements for metabotropic glutamate receptors," *Neuroscience Letters,* vol. 541, pp. 67-72, 2013.

[412] M. Herkenham, "Laminar organization of thalamic projections to the rat neocortex," *Science,* vol. 207, pp. 532-535, 1980.

[413] N. Yamawaki and G. M. Shepherd, "Synaptic circuit organization of motor corticothalamic neurons," *Journal of Neuroscience,* vol. 35, pp. 2293-2307, 2015.

[414] J. H. Goldberg, M. A. Farries, and M. S. Fee, "Basal ganglia output to the thalamus: still a paradox," *Trends in Neurosciences,* vol. 36, pp. 695-705, 2013.

[415] L. L. Glenn, J. Hada, J. P. Roy, M. Deschenes, and M. Steriade, "Anterograde tracer and field potential analysis of the neocortical layer I projection from nucleus ventralis medialis of the thalamus in cat," *Neuroscience,* vol. 7, pp. 1861-1877, 1982.

[416] H. W. Berendse and H. J. Groenewegen, "Restricted cortical termination fields of the midline and intralaminar thalamic nuclei in the rat," *Neuroscience,* vol. 42, pp. 73-102, 1991.

[417] A. Gummadavelli, J. E. Motelow, N. Smith, Q. Zhan, N. D. Schiff, and H. Blumenfeld, "Thalamic stimulation to improve level of consciousness after seizures: evaluation of electrophysiology and behavior," *Epilepsia,* vol. 56, pp. 114-124, 2015.

[418] D. A. McCormick and T. Bal, "Sleep and arousal: thalamocortical mechanisms," *Annual review of neuroscience,* vol. 20, pp. 185-215, 1997.

[419] K. Giber, M. A. Diana, V. Plattner, G. P. Dugué, H. Bokor, C. V. Rousseau, *et al.*, " A subcortical inhibitory signal for behavioral arrest in the thalamus," *Nature Neuroscience,* vol. 18, pp. 562-568, 2015.

[420] J. W. Miller, B. C. Gray, and M. E. Bardgett, " Characterization of cholinergic regulation of seizures by the midline thalamus," *Neuropharmacology,* vol. 31, pp. 349-356, 1992.

[421] J. Buee, J. M. Deniau, and G. Chevalier, "Nigral modulation of cerebello-thalamo-cortical transmission in the ventral medial thalamic nucleus," *Experimental Brain Research,* vol. 65, pp. 241-244, 1986.

[422] K. Franklin and G. Paxinos, *The mouse brain in stereotactic coordinates, Compact*, 2nd ed.: Academic Press, 2001.

[423] A. Aarabi, F. Wallois, and R. Grebe, "Does spatiotemporal synchronization of EEG change prior to absence seizures?," *Brain research,* vol. 1188, pp. 207-221, 2008.

[424] M. P. Beenhakker and J. R. Huguenard, "Neurons that fire together also conspire together: is normal sleep circuitry hijacked to generate epilepsy?," *Neuron,* vol. 62, pp. 612-632, 2009.

[425] J. R. Cressman, G. Ullah, J. Ziburkus, S. J. Schiff, and E. Barreto, "The influence of sodium and potassium dynamics on excitability, seizures, and the stability of persistent states," *Journal of Computational Neuroscience,* vol. 26, pp. 159-170, 2009.

[426] L. Danober, C. Deransart, A. Depaulis, M. Vergnes, and C. Marescaux, "Pathophsyiological mechanisms of genetic absence epilepsy in the rat," *Progress in neurobiology,* vol. 55, pp. 27-57, 1998.

[427] C. J. Stam, "Modern network science of neurological disorders," *Nature Reviews Neuroscience,* vol. 15, pp. 683-695, 2014.

[428] A. Adebimpe, A. Aarabi, E. Bourel-Ponchel, M. Mahmoudzadeh, and F. Wallois, "Functional Brain Dysfunction in Patients with Benign Childhood Epilepsy as Revealed by Graph Theory," *PLoS One,* vol. 10, 2015.

[429] E. Krook-Magnuson and I. Soltesz, "Beyond the hammer and the scalpel: selective circuit control for the epilepsies," *Nature Neuroscience,* vol. 18, pp. 331-338, 2015.

[430] C. B. Schafer and F. E. Hoebeek, "Convergence of primary sensory cortex and cerebellar nuclei pathways in the whisker system," *Neuroscience,* vol. 368, pp. 229-239, 2018.

[431] J. Mattis, K. M. Tye, E. A. Ferenczi, C. Ramakrishnan, D. J. O'Shea, R. Prakash, *et al.*, "Principles for applying optogenetic tools derived from direct comparative analysis of microbial opsins," *Nature Methods,* vol. 9, pp. 159-172, 2011.

[432] T. Houben, I. C. Loonen, S. M. Baca, M. Schenke, J. H. Meijer, M. D. Ferrari, *et al.*, "Optogenetic induction of cortical spreading depression in anesthetized and freely behaving mice. Journal of cerebral blood flow and metabolism," *Journal of Cerebral Blood Flow and metabolism,* vol. 37, pp. 1641-1655, 2017.

[433] A. J. Kundishora, A. Gummadavelli, C. Ma, M. Liu, C. McCafferty, N. D. Schiff, *et al.*, "Restoring conscious arousal during focal limbic seizures with deep brain stimulation," *Cerebral Cortex,* vol. 27, pp. 1964-1975, 2017.

[434] K. Franklin and G. Paxinos, *The mouse brain in stereotactic coordinates*, 2nd edition ed.: Academic Press, 2001.

[435] T. M. Teune, J. Van der Burg, J. Van der Moer, and T. J. Ruigrok, "Topography of cerebellar nuclear projections to the brain stem in the rat," *Prog. Brain Res.,* vol. 124, pp. 141-172, 2000.

[436] J. Chen and A. R. Kriegstein, "A GABAergic projection from the zona incerta to cortex promotes cortical neuron development," *Science,* vol. 350, pp. 554-558, 2015.

[437] I. Song, D. Kim, S. Choi, M. Sun, Y. Kim, and H. S. Shin, "Role of the A1G T-type calcium channel in spontaneous absence seizures in mutant mice," *Journal of Neuroscience,* vol. 24, pp. 5249-5257, 2004.

[438] A. Depaulis and S. Charpier, "Pathophysiology of absence epilepsy: Insights from genetic models," *Neuroscience Letters,* vol. 17, pp. 30141-30146, 2017.

[439] L. Kros, S. L. Lindeman, O. H. J. Eelkman Rooda, C. I. de Zeeuw, and F. E. Hoebeek, "Synchronicity and rhythmicity of Purkinje cell firing during generalized spike-and-wave discharges in a natural mouse model of absence epilepsy," *Frontiers in cellular neuroscience,* in press.

[440] L. Rispal-Padel and J. Latreille, "The organization of projections from the cerebellar nuclei to the contralateral motor cortex in the cat," *Experimental Brain Research,* vol. 19, pp. 36-60, 1974.

[441] M. Yoshida, K. Yajima, and M. Uno, "Different activation of the 2 types of the pyramidal tract neurones through the cerebello-thalamocortical pathway," *Experientia,* vol. 22, pp. 331-332, 1966.

[442] M. M. Halassa and L. Acsády, "Thalamic Inhibition: Diverse Sources, Diverse Scales," *Trends in Neurosciences,* vol. 39, pp. 680-693, 2016.

[443] J. T. Paz, M. Chavez, S. Saillet, J. M. Deniau, and S. Charpier, "Activity of ventral medial thalamic neurons during absence seizures and modulation of cortical paroxysms by the nigrothalamic pathway," *Journal of Neuroscience,* vol. 27, pp. 929-941, 2007.

[444] V. C. Bomben, I. Aiba, J. Qian, M. D. Mark, S. Herlitze, and J. L. Noebels, "Isolated P/Q Calcium Channel Deletion in Layer VI Corticothalamic Neurons Generates Absence Epilepsy," *Journal of Neuroscience,* vol. 36, pp. 405-418, 2016.

[445] C. Yu, D. Derdikman, S. Haidarliu, and E. Ahissar, "Parallel thalamic pathways for whisking and touch signals in the rat," *PLoS Biology,* vol. 4, p. e124, 2006.

[446] P. Marien, H. Ackermann, M. Adamaszek, C. H. Barwood, A. Beaton, J. Desmond*, et al.*, "Consensus paper: Language and the cerebellum: an ongoing enigma," *Cerebellum,* vol. 13, pp. 386-410, 2014.

[447] J. F. Poulet, L. M. Fernandez, S. Crochet, and C. C. Petersen, "Thalamic control of cortical states," *Nature Neuroscience,* vol. 15, pp. 370-372, 2012.

[448] E. van Diessen, S. J. Diederen, K. P. Braun, F. E. Jansen, and C. J. Stam, "Functional and structural brain networks in epilepsy:What have we learned?," *Epilepsia,* vol. 54, pp. 1855-1865, 2013.

[449] L. Claes, J. Del-Favero, B. Ceulemans, L. Lagae, C. Van Broeckhoven, and P. De Jonghe, "De Novo Mutations in the Sodium-Channel Gene SCN1A Cause Severe Myoclonic Epilepsy of Infancy," *American journal of human genetics,* vol. 68, pp. 1327-1332, 2001.

[450] L. R. Claes, L. Deprez, A. Suls, J. Baets, K. Smets, T. Van Dyck, *et al.*, "The SCN1A variant database: a novel research and diagnostic tool," *Human mutation,* vol. 30, pp. 904-920, 2009.

[451] C. S. Cheah, F. H. Yu, R. E. Westenbroek, F. K. Kalume, J. C. Oakley, G. B. Potter, *et al.*, "Specific deletion of NaV1.1 sodium channels in inhibitory interneurons causes seizures and premature death in a mouse model of Dravet syndrome," *Proc. Natl. Acad. Sci. U. S. A.,* vol. 109, pp. 14646-14651, 2012.

[452] I. Ogiwara, H. Miyamoto, N. Morita, N. Atapour, E. Mazaki, I. Inoue, *et al.*, "Nav1.1 localizes to axons of parvalbumin-positive inhibitory interneurons: a circuit basis for epileptic seizures in mice carrying an Scn1a gene mutation," *Journal of Neuroscience,* vol. 27, pp. 5903-5914, 2007.

[453] C. Tai, Y. Abe, R. E. Westenbroek, T. Scheuer, and W. A. Catterall, "Impaired excitability of somatostatin- and parvalbumin-expressing cortical interneurons in a mouse model of Dravet syndrome," *Proc. Natl. Acad. Sci. U. S. A.,* vol. 111, pp. 3139-3148, 2014.

[454] F. H. Yu, M. Mantegazza, R. E. Westenbroek, C. A. Robbins, F. K. Kalume, K. A. Burton, *et al.*, "Reduced sodium current in GABAergic interneurons in a mouse model of severe myoclonic epilepsy in infancy," *Nature Neuroscience,* vol. 9, pp. 1142-1149, 2006.

[455] M. Rubinstein, S. Han, C. Tai, R. E. Westenbroek, A. Hunker, T. Scheuer, *et al.*, "Dissecting the phenotypes of Dravet syndrome by gene deletion," *Brain,* vol. 138, pp. 2219-2233, 2015.

[456] L. A. Papale, C. D. Makinson, J. Christopher Ehlen, S. Tufik, M. J. Decker, K. N. Paul, *et al.*, "Altered sleep regulation in a mouse model of SCN1A-derived genetic epilepsy with febrile seizures plus (GEFS+)," *Epilepsia,* vol. 54, pp. 625-634, 2013.

[457] F. Crick, "Function of the thalamic reticular complex: the searchlight hypothesis," *Proc. Natl. Acad. Sci. U. S. A.,* vol. 81, pp. 4586-4590, 1984.

[458] L. J. Gentet and D. Ulrich, "Strong, reliable and precise synaptic connections between thalamic relay cells and neurones of the nucleus reticularis in juvenile rats," *Journal of Physiology,* vol. 546, pp. 801-811, 2003.

[459] C. R. Houser, J. E. Vaughn, R. P. Barber, and E. Roberts, "GABA neurons are the major cell type of the nucleus reticularis thalami," *Brain Research,* vol. 200, pp. 341-354, 1980.

[460] J. T. Paz, C. A. Christian, I. Parada, D. A. Prince, and J. R. Huguenard, "Focal Cortical Infarcts Alter Intrinsic Excitability and Synaptic Excitation in the Reticular Thalamic Nucleus," *Journal of Neuroscience,* vol. 30, pp. 5465-5479, 2010.

[461] S. J. Slaght, N. Leresche, J. M. Deniau, V. Crunelli, and S. Charpier, "Activity of Thalamic Reticular Neurons during Spontaneous Genetically Determined Spike and Wave Discharges," *Journal of Neuroscience,* vol. 22, pp. 2323-2334, 2002.

[462] F. Ferrarelli and G. Tononi, "The Thalamic Reticular Nucleus and Schizophrenia," *Schizophrenia Bulletin,* vol. 37, pp. 306-315, 2011.

[463] Z. W. Zhang, J. D. Zak, and H. Liu, "MeCP2 Is Required for Normal Development of GABAergic Circuits in the Thalamus," *Journal of Neurophysiology,* vol. 103, pp. 2470-2481, 2010.

[464] M. M. Huntsman, D. M. Porcello, G. E. Homanics, T. M. DeLorey, and J. R. Huguenard, "Reciprocal Inhibitory Connections and Network Synchrony in the Mammalian Thalamus," *Science,* vol. 283, 1999.

[465] P. Barthó, A. Slézia, F. Mátyás, L. Faradzs-Zade, I. Ulbert, K. D. Harris, *et al.*, "Ongoing Network State Controls the Length of Sleep Spindles via Inhibitory Activity," *Neuron,* vol. 82, pp. 1367-1379, 2014.

[466] F. K. Kalume, J. Oakley, R. E. Westenbroek, J. Gile, H. O. de la Iglesia, T. Scheuer, *et al.*, "Sleep impairment and reduced interneuron excitability in a mouse model of Dravet Syndrome," *Neurobiology of Disease,* vol. 77, pp. 141-154, 2015.

[467] H. Jahnsen and R. Llinás, "Electrophysiological properties of guinea-pig thalamic neurones: an in vitro study," *Journal of Physiology,* vol. 349, pp. 205-226, 1984.

[468] M. Bazhenov, I. Timofeev, M. Steriade, and T. Sejnowski, "Spiking-Bursting Activity in the Thalamic Reticular Nucleus Initiates Sequences of Spindle Oscillations in Thalamic Networks," *Journal of Neurophysiology,* vol. 84, pp. 1076-1087, 2000.

[469] M. Deschenes, M. Paradis, J. P. Roy, and M. Steriade, "Electrophysiology of neurons of lateral thalamic nuclei in cat: resting properties and burst discharges," *Journal of Neurophysiology,* vol. 51, pp. 1196-1219, 1984.

[470] M. Steriade, L. Domich, G. Oakson, and M. Deschenes, "The deafferented reticular thalamic nucleus generates spindle rhythmicity," *Journal of Neurophysiology,* vol. 57, pp. 260-273, 1987.

[471] S. M. Sherman, "A wake-up call from the thalamus," *Nature Neuroscience,* vol. 4, pp. 344-346, 2001.

[472] S. M. Sherman, "Tonic and burst firing: dual modes of thalamocortical relay," *Trends in Neurosciences,* vol. 24, pp. 122-126, 2001.

[473] L. Cueni, M. Canepari, R. Luján, Y. Emmenegger, H. Watanabe, C. T. Bond, *et al.*, "T-type Ca2+ channels, SK2 channels and SERCAs gate sleep-related oscillations in thalamic dendrites," *Nature Neuroscience,* vol. 11, pp. 683-692, 2008.

[474] R. D. Wimmer, S. Astori, C. T. Bond, Z. Rovó, J. Y. Chatton, J. P. Adelman, *et al.*, "Sustaining Sleep Spindles through Enhanced SK2-Channel Activity Consolidates Sleep and Elevates Arousal Threshold," *Journal of Neuroscience,* vol. 32, pp. 13917-13928, 2012.

[475] M. I. Botez, E. Attig, and J. L. Vezina, "Cerebellar atrophy in epileptic patients," *The Canadian Journal of neurological sciences,* vol. 15, pp. 299-303, 1988.

[476] J. Milton and P. Jung, in *Epilepsy as a dynamic disease*, ed Berlin-Heidelberg: Springer-Verlag, 2003, pp. 69-82.

[477] R. M. Kelly and P. L. Strick, "Cerebellar loops with motor cortex and prefrontal cortex of a nonhuman primate," *Journal of Neuroscience,* vol. 23, pp. 8432-8444, 2003.

[478] C. J. Stoodley, J. P. MacMore, N. Makris, J. C. Sherman, and J. D. Schmahmann, "Location of lesion determines motor vs. cognitive consequences in patients with cerebellar stroke," *NeuroImage. Clinical.,* vol. 12, pp. 765-775, 2016.

[479] G. Avanzini, F. Panzica, and M. de Curtis, "The role of the thalamus in vigilance and epileptogenic mechanisms," *Clinical Neurophysiology,* vol. 111, pp. S19-S26, 2000.

[480] G. K. Kostopoulos, "Spike-and-wave discharges of absence seizures as a transformation of sleep spindles: the continuing development of a hypothesis," *Clinical Neurophysiology,* vol. 111, pp. S27-S38, 2000.

[481] F. Picard, P. Mégevand, L. Minotti, P. Kahane, P. Ryvlin, M. Seeck, *et al.*, "Intracerebral recordings of nocturnal hyperkinetic seizures: demonstration of a longer duration of the pre-seizure sleep spindle," *Clinical Neurophysiology,* vol. 118, pp. 928-939, 2007.

[482] T. Futami, M. Kano, S. Sento, and Y. Shinoda, "Synaptic organization of the cerebello-thalamo-cerebral pathway in the cat. III. Cerebellar input to corticofugal neurons destined for different subcortical nuclei in areas 4 and 6," *Neuroscience Research,* vol. 3, pp. 321-344, 1986.

[483] H. Jorntell and C. F. Ekerot, "Topographical organization of projections to cat motor cortex from nucleus interpositus anterior and forelimb skin," *Journal of Physiology,* vol. 514, pp. 551-566, 1999.

[484] J. Na, S. Kakei, and Y. Shinoda, "Cerebellar input to corticothalamic neurons in layers V and VI in the motor cortex," *Neuroscience Research,* vol. 28, pp. 77-91, 1997.

[485] K. Sasaki, Y. Kawaguchi, H. Oka, M. Sakai, and N. Mizuno, "Electrophysiological studies on the cerebellocerebral projections in monkeys," *Experimental Brain Research,* vol. 24, pp. 495-507, 1976.

[486] L. F. Koziol, D. Budding, N. Andreasen, S. D'Arrigo, S. Bulgheroni, H. Imamizu, *et al.*, "Consensus paper: the cerebellum's role in movement and cognition.," *Cerebellum,* vol. 13, pp. 151-177, 2014.

[487] R. P. Dum, C. Li, and P. L. Strick, "Motor and nonmotor domains in the monkey dentate," *Annals of the New York Academy of Sciences,* vol. 978, pp. 289-301, 2002.

[488] R. P. Dum and P. L. Strick, "An unfolded map of the cerebellar dentate nucleus and its projections to the cerebral cortex," *Journal of Neurophysiology,* vol. 89, pp. 634-639, 2003.

[489] H. J. Park, H. Furmaga, J. Cooperrider, J. T. Gale, K. B. Baker, and A. G. Machado, "Modulation of Cortical Motor Evoked Potential After Stroke During Electrical Stimulation of the Lateral Cerebellar Nucleus," *Brain stimulation,* vol. 8, pp. 1043-1048, 2015.

[490] R. A. Badawy, J. M. Curatolo, M. Newton, S. F. Berkovic, and R. A. Macdonell, "Changes in cortical excitability differentiate generalized and focal epilepsy," *Annals of Neurology,* vol. 61, pp. 324-331, 2007.

[491] P. Manganotti, L. G. Bongiovanni, G. Fuggetta, G. Zanette, and A. Fiaschi, "Effects of sleep deprivation on cortical excitability in patients affected by juvenile myoclonic epilepsy: a combined transcranial magnetic stimulation and EEG study," *Journal of neurology, neurosurgery, and psychiatry,* vol. 77, pp. 56-60, 2006.

[492] D. Kraus, G. Naros, R. Bauer, F. Khademi, M. T. Leao, U. Ziemann, *et al.*, "Brain State-Dependent Transcranial Magnetic Closed-Loop Stimulation Controlled by Sensorimotor Desynchronization Induces Robust Increase of Corticospinal Excitability," *Brain stimulation,* vol. 9, pp. 415-424, 2016.

[493] H. Schulz, T. Ubelackter, J. Keil, N. Muller, and N. Weisz, "Now I am ready-now i am not: The influence of pre-TMS oscillations and corticomuscular coherence on motor-evoked potentials," *Cerebral Cortex,* vol. 24, pp. 1708-1719, 2014.

[494] M. Takemi, Y. Masakado, M. Liu, and J. Ushiba, "Event-related desynchronization reflects downregulation of intracortical inhibition in human primary motor cortex," *Journal of Neurophysiology,* vol. 110, pp. 1158-1166, 2013.

[495] D. Weiss, R. Klotz, R. B. Govindan, M. Scholten, G. Naros, A. Ramos-Murguialday, *et al.*, "Subthalamic stimulation modulates cortical motor network activity and synchronization in Parkinson's disease," *Brain,* vol. 138, pp. 679-693, 2015.

[496] C. S. Lin, M. A. Nicolelis, J. S. Schneider, and J. K. Chapin, "A Major Direct GABAergic Pathway from Zona Incerta to Neocortex," *Science,* vol. 248, pp. 1553-1556, 1990.

[497] N. Urbain and M. Deschenes, "Motor cortex gates vibrissal responses in a thalamocortical projection pathway," *Neuron,* vol. 56, pp. 714-725, 2007.

[498] P. Barthó, T. F. Freund, and L. Acsády, "Selective GABAergic innervation of thalamic nuclei from zona incerta," *European Journal of Neuroscience,* vol. 16, pp. 999-1014, 2002.

[499] P. L. Strick, R. P. Dum, and J. A. Fiez, "Cerebellum and nonmotor function," *Annual review of neuroscience,* vol. 32, pp. 413-434, 2009.

[500] A. T. Berg, J. T. Langfitt, F. M. Testa, S. R. Levy, F. DiMario, M. Westerveld, *et al.*, "Global cognitive function in children with epilepsy: A community-based study," *Epilepsia,* vol. 49, pp. 608-614, 2008.

[501] A. Austin, J. P. Lin, R. Selway, K. Ashkan, and T. Owen, "What parents think and feel about deep brain stimulation in paediatric secondary dystonia including cerebral palsy: A qualitative study of parental decision-making," *European Journal of Pediatric Neurology,* vol. 21, pp. 185-192, 2017.

[502] K. M. Fiest, T. T. Sajobi, and S. Wiebe, " Epilepsy surgery and meaningful improvements in quality of life: results from a randomized controlled trial," *Epilepsia,* vol. 55, pp. 886-892, 2014.

[503] L. Frings, A. Schulze-Bonhage, J. Spreer, and K. Wagner, "Remote effects of hippocampal damage on default network connectivity in the human brain," *Journal of neurology,* vol. 256, pp. 2021-2029, 2009.

[504] A. B. Waites, R. S. Briellmann, M. M. Saling, D. F. Abbott, and G. D. Jackson, " Functional connectivity networks are disrupted in left temporal lobe epilepsy," *Annals of Neurology,* vol. 59, pp. 335-343, 2006.

[505] S. Jiang, C. Luo, J. Gong, R. Peng, S. Ma, S. Tan, *et al.*, "Aberrant Thalamocortical Connectivity in Juvenile Myoclonic Epilepsy," *International journal of neural systems,* vol. epub ahead of print, 2017.

[506] K. B. Baker, D. Schuster, J. Cooperrider, and A. G. Machado, "Deep brain stimulation of the lateral cerebellar nucleus produces frequency-specific alterations in motor evoked potentials in the rat in vivo," *Experimental Neurology,* vol. 226, pp. 259-264, 2010.

[507] A. G. Machado, K. B. Baker, D. Schuster, R. S. Butler, and A. Rezai, "Chronic electrical stimulation of the contralesional lateral cerebellar nucleus enhances recovery of motor function after cerebral ischemia in rats," *Brain research,* vol. 1280, pp. 107-116, 2009.

[508] A. G. Machado, J. Cooperrider, H. Furmaga, K. B. Baker, H. J. Park, Z. Chen, *et al.*, "Chronic 30-Hz deep cerebellar stimulation coupled with training enhances post-ischemia motor recovery and peri-infarct synaptophysin expression in rodents," *Neurosurgery,* vol. 73, pp. 344-353, 2013.

[509] G. F. Molnar, A. Sailer, C. A. Gunraj, D. I. Cunic, R. A. Wennberg, A. M. Lozano, *et al.*, "Changes in motor cortex excitability with stimulation of anterior thalamus in epilepsy," *Neurology,* vol. 66, pp. 566-571, 2006.

[510] G. F. Molnar, A. Sailer, C. A. Gunraj, A. E. Lang, A. M. Lozano, and R. Chen, "Thalamic deep brain stimulation activates the cerebellothalamocortical pathway," *Neurology,* vol. 63, pp. 907-909, 2004.

[511] I. A. Prescott, J. O. Dostrovsky, E. Moro, M. Hodaie, A. M. Lozano, and W. D. Hutchison, "Levodopa enhances synaptic plasticity in the substantia nigra pars reticulata of Parkinson's disease patients," *Brain,* vol. 132, pp. 309-318, 2009.

[512] T. D. Aumann, S. J. Redman, and M. K. Horne, "Long-term potentiation across rat cerebello-thalamic synapses in vitro," *Neuroscience Letters,* vol. 287, pp. 151-155, 2000.

[513] P. Arcelli, C. Frassoni, M. C. Regondi, S. De Biasi, and R. Spreafico, "GABAergic neurons in mammalian thalamus: a marker of thalamic complexity?," *Brain research bulletin,* vol. 42, pp. 27-37, 1997.

[514] R. Spreafico, C. Frassoni, P. Arcelli, G. Battaglia, R. J. Wenthold, and S. De Biasi, "Distribution of AMPA selective glutamate receptors in the thalamus of adult rats and during postnatal development. A light and ultrastructural immunocytochemical study," *Brain research. Developmental brain research,* vol. 82, pp. 231-244, 1994.

[515] M. Steriade, E. G. Jones, and D. A. McCormick, *Thalamus*. Oxford: Elsevier, 1997.

[516] I. S. Cooper and A. R. Upton, "Use of chronic cerebellar stimulation for disorders of disinhibition," *Lancet,* vol. 1, pp. 595-600, 1978.

[517] I. S. Cooper, A. R. Upton, and I. Amin, "Chronic cerebellar stimulation (CCS) and deep brain stimulation (DBS) in involuntary movement disorders," *Applied neurophysiology,* vol. 45, pp. 209-217, 1982.

[518] A. R. Upton, I. S. Cooper, M. Springman, and I. Amin, "Suppression of seizures and psychosis of limbic system origin by chronic stimulation of anterior nucleus of the thalamus," *International journal of neurology,* vol. 19-20, pp. 223-230, 1985-1986.

[519] M. Lowenthal and V. Horsley, "On the relations between the cerebellar and other centers," *Proceedings of the Royal Society of London,* vol. 61, pp. 20-25, 1897.

[520] C. S. Sherrington, "Double (antidrome) conduction in the central nervous system," *Proceedings of the Royal Society of London,* vol. 61, pp. 243-246, 1897.

[521] J. C. Eccles, R. Llinás, and K. Sasaki, "The excitatory synaptic action of climbing fibres on the Purkinje cells of the cerebellum," *J. Physiol.,* vol. 182, pp. 268-296, 1966.

[522] R. Llinás, "The cortex of the cerebellum," *Scientific American,* vol. 232, pp. 56-71, 1975.

[523] C. G. Begley and L. M. Ellis, "Drug development: Raise standards for preclinical cancer research," *Nature,* vol. 483, pp. 531-533, 2012.

[524] O. S. Collaboration, "Estimating the reproducibility of psychological science," *Science,* vol. 349, 2015.

[525] J. P. Ioannidis, D. B. Allison, C. A. Ball, I. Coulibaly, X. Cui, A. C. Culhane*, et al.*, "Repeatability of published microarray gene expression analyses " *Nature Genetics,* vol. 41, pp. 149-155, 2009.

[526] D. M. Andrade, C. Hamani, A. M. Lozano, and R. A. Wennberg, "Dravet syndrome and deep brain stimulation: seizure control after 10 years of treatment," *Epilepsia,* vol. 51, pp. 1314-1316, 2010.

[527] S. Chabardés, P. Kahane, L. Minotti, A. Koudsie, E. Hirsch, and A. L. Benabid, "Deep brain stimulation in epilepsy with particular reference to the subthalamic nucleus," *Epileptic Disorders,* vol. 4, pp. S83-S93, 2002.

[528] J. Rosenow, K. Das, R. L. Rovit, and W. T. Couldwell, "Irving S. Cooper and His Role in Intracranial Stimulation for Movement Disorders and Epilepsy," *Stereotact. Funct. Neurosurg.,* vol. 78, pp. 95-112, 2002.

A

Appendix

Summary

Nederlandse Samenvatting

Curriculum Vitae

List of Publications

Terugblik

Summary

The primary goal of this dissertation was to further elucidate questions regarding the neural mechanism of cerebellar impact on thalamic nuclei and thalamus' primary output structure the cerebral cortex. To do so key experiments were performed using amongst others optogenetics in mice having an epileptic phenotype.

In **Chapter 2** we provide an overview of cell-specific markers usable for optogenetics in both cerebellar cortex and nuclei. This high-detail description of technical issues and solutions makes it an efficient guideline for starting and experienced researchers regarding cerebellar research.

Where chapter 2 ends, **Chapter 3** continues with a re-evaluation of the therapeutic potential of cerebellar stimulation in epilepsy. This chapter gives an introduction of the impact of cerebellum and its main output structure cerebellar nuclei on thalamocortical networks. Further we give directions on how to optimize the potential impact by adjusting stimulation parameters such as frequency, regularity and synchronicity.

In **Chapter 4** we show that a substantial portion of Purkinje cells show increase simple and complex spike activity combined with increased synchronicity for adjacent and remote Purkinje cells during GSWDs. Furthermore the activation of complex spike activity indirectly implicates widespread changes in olivary firing during seizures.

Chapter 5 embodies crucial evidence for this dissertation in which we show that CN neurons are potent modulators of GSWDs in thalamocortical networks. This is an evolution of the old idea that manipulation of cerebellar cortex activity intervenes with epileptic seizures into the fact that not cerebellar cortex but cerebellar nuclei seem easier to target and stronger in their manipulation of thalamocortical activity. An obvious next question is: How are CN neurons capable of suppressing seizures? In **Chapter 6 and 7** we test the hypothesis that CN neurons can cause desynchronization in the thalamus by first showing *in vitro* differences between post synaptic responses upon cerebellar terminal stimulation in different thalamic nuclei. Second we confirm this evidence *in vivo* where we find different response types in different thalamic cells recorded in different thalamic nuclei.

Finally we test in **Chapter 8** if CN manipulation can also dampen seizures in a much more severe mouse model of generalized epilepsy; i.e. the Dravet mouse. It turns out that either electrical CN stimulation or different thalamic nuclei stimulation sites are not capable of seriously controlling the generalized convulsive seizures. In the end our colleagues show that manipulation using a SK blocker is more capable.

Samenvatting

Deze dissertatie richt zich op het verder uitwerken van de vraag wat de achterliggende mechanisms zijn waarmee het cerebellum haar invloed uitoefent op thalamocorticale netwerken. Om dit te bereiken hebben we gebruik gemaakt van verschillende technieken, waaronder optogenetica, in muizen met en zonder epilepsie.

In **Hoofdstuk 2** wordt beschreven hoe verschillende cel-specifieke markers gebruikt kunnen worden in combinatie met optogenetica voor de manipulatie van cerebellaire schors en kernen. We bespreken technische moeilijkheden en oplossingen wat maakt dat het een mooi uitgangswerk is voor de beginnende en meer ervaren onderzoeker.

Hierop voortbordurend is **Hoofdstuk 3** ontstaan waarin de therapeutische (on) mogelijkheden van cerebellaire stimulatie bij epilepsie besproken worden. Een introductie als voorbereiding op het volgende hoofdstuk wordt gegeven over de impact van het cerebellum op thalamocorticale netwerken en we geven suggesties hoe deze impact gemaximaliseerd kan worden door middel van verschillende stimulatie parameters aan te passen.

In Hoofdstuk 4 laten we zien da teen substandieel deel van de Purkinje cellen een verhoogde simplex en complex spike activiteit heeft gedurende GSWDs. Dit gaat dan ook nog eens gepaard met een verhoogde synchroniciteit tussen aanliggende en op afstand zijnde collega Purkinje cellen. Indirect geeft dit aan dat de verhoogde complex spike activiteit gezien kan worden als veranderingen in het vuurgedrag van een andere belangrijke hersenstructuur; de inferieure olijf.

Hoofdstuk 5 gaat over de kern van deze dissertatie waarin we bewijs leveren dat CN neuronen krachtige modulatoren van pathologische thalamocorticale oscillaties kunnen zijn. Een verandering in denken tov het oude idee dat juist de cerebellaire schors hier goed in zou zijn. seem easier to target and stronger in their manipulation of thalamocortical activity. Een logische vervolgvraag op hoofdstuk 5 is: Wat is het achterliggende mechanisme waarmee CN neuronen de epilepsie kunnen stoppen? Met andere woorden, wat is het effect van hun vuurgedrag op de thalamus en via de thalamus op de cerebrale schors. In **Hoofdstuk 6 en 7** testen we de hypothese dat CN neuronen thalamische neuronen kunnen desynchroniseren in hun vuurgedrag. Dit laten we eerst *in vitro* zien waarbij we in verschillende thalamische kernen verschillende sterkte in post-synaptische respons zien. Vervolgens blijkt dit ook *in vivo* waarbij er verschillende respons types lijken te zijn tussen verschillende cellen maar dat binnen dezelfde cel de respons wel hetzelfde blijft.

Als laatste testen we in **Hoofdstuk 8** of CN manipulatie ook seizures kan stoppen in een muis model met een ernstiger epileptisch phenotype; de Dravet muis. Het blijkt dat

zowel CN stimulatie als stimulatie van verschillende thalamische kernen niet in staat is de convulsieve aanvallen te stoppen.

Curriculum Vitae

Personal information

Name:	Oscar Hubert Jan Eelkman Rooda
Date of birth:	03 October 1988
Place of birth:	Rotterdam
Nationality:	Dutch

Education

01/2017 – today	**Resident Neurosurgery, ErasmusMC, Rotterdam**
08/2013 – 12/2016	PhD Student, Department of Neuroscience, Erasmus MC, Rotterdam
09/2006 – 07/2013	Medicine, Erasmus University Rotterdam Passed 'Cum Laude' for the 'Artsexamen'
08/2009 – 08/2011	Master of Science in Neuroscience, Erasmus University Rotterdam
9/2000 – 9/2006	Gymnasium, Johan van Oldenbarnevelt Amersfoort, the Netherlands Profile: Physics & Health

Teaching experience

2014 – 2016:	Supervision of medicine students (1), Master of Science students (2)
2013 – 2015:	Practical anatomy courses 1st and 3 rd year medical students (Brain, Heart and vasculature (24 hr per year)

Additional achievements

- Line Honours Round Texel 2015
- Best Poster Award ILAE Istanbul 2015

List of journal publications

M.L. van Veelen, **O.H.J. Eelkman Rooda**, T. De Jong, R. Dammers, L.N. van Adrichem, I.M. Mathijssen (2013) Results of early surgery for sagittal suture synostosis: long-term follow-up and the occurrence of raised intracranial pressure. *Child's Nervous System 29(6): 997-1005*

L. Kros, **O.H.J. Eelkman Rooda**, J.K. Spanke, P. Alva, M.N. van Dongen, A. Karapatis, E.A. Tolner, C. Strydis, N. Davey, B.H. Winkelman, M. Negrello, W.A. Serdijn, V. Steuber, A.M. van den Maagdenberg, C.I. de Zeeuw, F.E. Hoebeek (2015) Cerebellar output controls generalized spike-and-wave discharge occurrence. *Annals of Neurology 77(6): 1027-1049*

L. Kros, **O.H.J Eelkman Rooda**, C.I. de Zeeuw, F.E. Hoebeek (2015) Controlling cerebellar output to treat refractory epilepsy. *Trends in Neurosciences 38(12): 787-799*

L. Kros*, S. Lindeman*, **O.H.J. Eelkman Rooda***, P. Murugesan, L. Bina, L.W.J. Bosman, C.I. De Zeeuw* and F.E. Hoebeek* (*in press, Frontiers in Cellular Neuroscience*) Synchronicity and rhythmicity of Purkinje cell complex spike firing during GSWDs

S.V. Gornati*, C.B. Schäfer*, **O.H.J. Eelkman Rooda**, A. Nigg, C.I. De Zeeuw and F.E. Hoebeek (submitted for publication) Diversifying the cerebellar impact on thalamic nuclei

O.H.J. Eelkman Rooda*, L. Kros*, S.J. Faneyte, P.J. Holland, S.V. Gornati, T.B. Houben, H.J. Poelman, N.A. Jansen, E.A. Tolner, A.M.J.M. van den Maagdenberg, C.I. De Zeeuw and F.E. Hoebeek (Submitted) Single-pulse stimulation of cerebellar nuclei desynchronizes epileptic thalamus and cerebral cortex

S. Ritter-Makinson, A. Clemente-Perez, B. Higashikubo, A. Chkaidze, **O.H.J. Eelkman Rooda**, M.-C. Cornet, F.E. Hoebeek, M. Roberta Cilio, B. Delord, J.T. Paz (submitted for publication) Potassium current deficit in reticular thalamic cells causes epilepsy in SCN1A-deficient Dravet Syndrome

List of poster presentations

O.H.J Eelkman Rooda, L. Kros, C.I. de Zeeuw, F.E. Hoebeek (2013). Epileptic signatures in cerebello-thalamic activity of the Cacna1a^{tottering} mutant mouse. Federation of European Neurosciences (FENS) Winter School, Obergurgl, Austria.

O.H.J Eelkman Rooda, L. Kros, C.M.F. Dirven, C.I. de Zeeuw, F.E. Hoebeek (2014). Epileptic signatures in cerebello-thalamic activity of the Cacna1a^{tottering} mutant mouse. International Congress of Clinical Neurophysiology (ICCN), Berlin, Deutschland.

O.H.J Eelkman Rooda, L. Kros, C.I. de Zeeuw, F.E. Hoebeek (2014). Cerebellar output potently increases thalamic activity, disrupts oscillatory thalamo-cortical activity and stops epileptic absence seizures. FENS, Milan, Italy.

O.H.J Eelkman Rooda, L. Kros, N.A. Jansen, C.I. de Zeeuw, F.E. Hoebeek (2015). Cerebellar nuclei stimulation stops epileptic absence seizures in Cacna1a^{tottering} mouse mutants by overruling oscillatory activity in thalamic nuclei. 31st International Epilepsy Congress, Istanbul, Turkey.

O.H.J Eelkman Rooda, L. Kros, N.A. Jansen, C.I. de Zeeuw, F.E. Hoebeek (2016). Pharmacologic and optogenetic increase of cerebellar output prevents and overrules corticothalamic oscillations in epileptic mice. Gordon Research conference (GRC) 'Thalamocortical Interactions'. Ventura, California, USA.

Terugblik

Af!! Klaar! Dat was het dan. Nog een paar woorden en het is definitief af. Een raar moment? Ja zeker, maar daarom niet minder waardevol om deze terugblik op papier te zetten. Het geploeter in het lab, muizen die wel of niet meewerken, de trots van het eerste optogenetica experiment, het vinden van cerebellaire en thalamische kerncellen en de directe confrontaties met Matlab gecombineerd met het geroddel en de gezelligheid van koffie om 8u 's morgens met de bekende vroege vogels was in 1 woord geweldig. Maar of ik het weer zou doen? Het afmaken en de bijbehorende mentale pijn, al helemaal als je vervolgens in de kliniek werkt, staat ook vrij helder op m'n netvlies. En zoals elke promovendus to be weet, dit boek (behalve inleiding en discussie) was er echt nooit gekomen zonder de volgende mensen.

Met stipt op 1 en schier oneindig onoverbrugbare afstand tot de rest:

Prof. Dr. Freek Hoebeek, ik weet nog goed hoe ik in september 2009 jouw kamer binnenkwam en jij me vertelde over de toevalsbevinding die je had gedaan betreffende de vuurpatronen van cerebellaire kernen bij 'epilepsie-muizen'. Een en ander was snel beklonken en nu zijn we jaren verder waarin jij professor (verdiend!) bent geworden en ik deze promotie tot een eind heb gebracht. Trots en met veel plezier denk ik terug aan de afgelopen jaren. De werkbesprekingen, die met grote regelmaat diep in de nacht plaatsvonden, de congressen en het bier drinken om ook eens niet over werk te praten heeft de afgelopen jaren niet alleen maar een mentor-student karakter gegeven. **Veel dank**.

Prof. Dr. Clemens Dirven, als afdeling neurochirurgie zijn we aan een spannend traject (Deep Brain Stimulation) begonnen. Dat komt niet in de laatste plaats door jouw inzet tijdens mijn promotie traject. Veel dank dat ik binnen de neurochirurgie een kans heb gekregen.

Prof. Dr. Chris de Zeeuw, we hebben elkaar niet veel gesproken over het onderzoek zelf. Het vertrouwen wat daar vanuit ging en de wetenschap dat je er altijd staat op de momenten dat het nodig is, is heel veel waard voor een promovendus. Hopelijk gaan we ooit nog eens samen naar een wedstrijd van Ajax!

Erika & Mandy, jullie staan achterop, zoals afgesproken. Jullie grote mond en nog groter hart (altijd op de tong, man wat moet dat zwaar zijn) is zeldzaam. Mijn dank is oneindig.

Vanuit het lab is er nog een aantal mensen belangrijk geweest. In particular I would like to mention Elisa Galliano, Boeke van Beugen, Zhenyu Gao and Petra Plak. All of you are intelligent, meticulous and persistent which have had a profound impact on my academic rookie years. Thanks for hosting me in the warm Freek cake lab. Lieke Kros, de gemiddelde angry bird verbleekt bij de discussies die wij kunnen hebben. Desalniettemin heb ik bewondering voor de passie voor het onderzoek die je hebt en was dit boek zonder jou zeker een paar pagina's dunner of 1-2 jaar later pas uitgekomen. Dear Simo, ciao S, we started together in 2013 (Obergurugllg, still don't know how to pronounce this) not knowing the ~~pain~~ fun ahead of us. We shared many up's and down's these years but one thing is for sure; it would have been a lot more boring without you. Sade (nu jij nog!), Bibi (be ready voor het einde), Negah, Dick (namen blijven lastig), Tom, Gerard, Carmen, Nico, Hanna, Bas, Sverrir, Daniel, Huub, Henk Jan, Ilya, Sasa, Leonoor, Bastiaan, Sander, Elize (je hulp met EM is cruciaal geweest); dank voor het taart eten, tafelvoetballen en de (soms lastige) vragen over het onderzoek. Elise Buitenhuis en Loes Nijs; zonder jullie dondert de hele boel in elkaar. Het georganiseer voor al die Phd's en masterstudenten op de afdeling neurowetenschappen is een geruisloze maar absolute prestatie.

Dear Jeanne Paz, Stefanie Makinson and all lab members at the Gladstone Neurological Institute (San Francisco). Thanks for hosting me at your wonderful lab. Somewhere I hope we can collaborate again in the future, although I realize this will be a challenge ☺

Staf en assistenten van de afdeling neurochirurgie; met jullie samenwerken maakt dat ik elke dag met veel plezier kom.

Alex, Frans en Xavier. Jullie karakter eigenschappen vormen een waar kleurenpalet. Verschillend in alle opzichten en daardoor zulke goede vrienden. We hebben schitterende dingen (Texel 2015, WK 2010, En een reus als paranymf which says it all) meegemaakt en wat mij betreft nog veel meer. Voor jullie de wereld en nog een stuk!

Mannen van Huize Zeezicht, oneindige potjes fifa spelen, controllers tegen het plafond en naakt door de straat (10-0!); Samen in een pand wonen was schitterend. Ik had er een apart boek over kunnen schrijven.

Koen en Quirine, we go way back. Als basisschool rookies elke dag naar school gefietst. De wereld bleek zo veel groter te zijn dan het toen leek, maar wisten wij veel. Van school naar huis was al een avontuur op zich (5min). Een vriendschap die zo groen als gras begonnen is, maar door de jaren alleen maar groeit.

Mannen van JC Hoef, met Rotterdam als onze bakermat is het allemaal begonnen. Ondertussen kennen we elkaar al jaren en zitten we verspreid over de wereld. Dank voor alle avonden waardoor ik de boel de boel kon laten.

Lieve Em, Over en uit, Roger. Dat geldt nooit voor ons.

Lieve opa's en oma's, altijd zijn jullie geinteresseerd hoe het gaat. Dat het bijna onmogelijk was om uit te leggen weerhield jullie daar niet van. Het dreigement, dat als de verdediging niet voor kerst 2017 zou plaatsvinden mogelijk niet iedereen erbij zou zijn, leek mij bluf. Ik vind het schitterend dat jullie erbij zijn op deze dag.

Lieve Merlyn, René, Mees en Berber. Familie kan je niet kiezen zeggen ze. Wat als dat wel zo was? Ik zou jullie hebben gekozen.

Lieve Sebo Jan en Anky, dank voor jullie onvoorwaardelijke en jarenlange steun, liefde en interesse voor alles wat ik doe. Geen woorden voor de mazzel die ik met jullie heb... Lieve Steven, waar we jarenlang het kleine water 'de Potten' onveilig maakten in ons zeilbootje, waarvan we overigens dachten dat dat een heus Skutsje was, blijken kleine jongens echt groot te worden. Al jarenlang woon je in het buitenland, maar m'n kleine broertje zul je altijd blijven.

Vaak heb ik me afgevraagd of het er zou komen.

Het is er gekomen.